# Characterization of cell type-specific endocannabinoid signaling at biochemical level

Dissertation

zur Erlangung des Grades

„Doktor der Naturwissenschaften“

am Fachbereich Biologie der


vorgelegt von

Tobias Mattheus

Mainz, September 2016

# Table of contents

# 1 Summary / Zusammenfassung

## 1.1 Summary

The cannabinoid receptor type 1 (CB1) is one of the most abundant G protein-coupled receptors (GPCRs) in the brain and mediates a wide range of behavioral and physiological responses. It is differentially expressed in various neuronal subtypes and moreover, exerts distinct signaling in the respective cell types. Whereas its physiological functions have been well studied, the highly complex intracellular signaling at the molecular level, which leads to differential CB1 signaling, has not been well understood.

The present study aimed at the purification of cell type-specific CB1 protein complexes and identification of CB1-interacting proteins. By combining adeno-associated virus (AAV)-mediated transgene transfer, conditionally Cre-recombinase expressing mouse lines, and tandem affinity purification (TAP) of hippocampal synaptosome preparations, an experimental set up was established, which allowed the purification of CB1 multiprotein complexes in mouse hippocampal glutamatergic neurons and GABAergic interneurons under native conditions. The composition of these protein complexes was then revealed by deep-coverage mass spectrometry (MS).

In the MS approach, 951 proteins were identified in the TAP samples of glutamatergic and GABAergic CB1 protein complexes, with 41 being specific for glutamatergic neurons and 83 specific for GABAergic interneurons. The high number of co-purified proteins suggests that not only directly interacting proteins were purified, but higher order structures including cytoskeletal elements and scaffolding proteins. The whole dataset of purified proteins reflects known functions of CB1 and depicts the complex biosynthesis and trafficking of this membrane receptor, which acts in different subcellular compartments. Together with a number of identified already known CB1-interacting proteins, the dataset can be judged as coherent and meaningful, with a plethora of yet unknown distinctly interesting potential interactors. A number of cell type-specific co-purified proteins may hold the potential to contribute to differential signaling in the respective hippocampal neuronal subtype, but further functional studies need to be performed to reveal the functional relevance of interesting target proteins. Thus, an extensive basis for new hypotheses and further studies on differential CB1 signaling was generated.

To further test a yet unknown identified potential interactor of CB1, functional studies on G protein subunit alpha z ($G\alpha_z$) were carried out. CB1 and $G\alpha_z$ are coexpressed in glutamatergic principal cells as well as GABAergic interneurons in the hippocampus of wildtype mice. A functional interaction of $G\alpha_z$ after activation of CB1 could be shown in an *in vitro* model using stably CB1 expressing HEK293 cells with transiently overexpressed inhibitory G proteins $G\alpha_z$ or $G\alpha_o$. A kinetic assay to measure cyclic adenosine monophosphate (cAMP) turnover upon adenylyl cyclase (AC) stimulation with forskolin showed a CB1-mediated inhibition of cAMP synthesis upon CB1 agonist treatment of the cells. An additional treatment with pertussis toxin (PTX) led to an inhibition of cAMP synthesis only in the $G\alpha_z$, but not in the $G\alpha_o$ overexpressing cells, since $G\alpha_z$ is the only PTX-insensitive inhibitory G protein. Thus, a functional interaction with one identified candidate interactor of CB1 could be verified.

## 1.2 Zusammenfassung

Der Cannabinoidrezeptor Typ 1 (CB1) ist einer der häufigsten Rezeptoren im Gehirn und vermittelt ein breites Spektrum an Verhaltens- und physiologischen Reaktionen. Er ist in verschiedenen Neuronentypen unterschiedlich stark exprimiert und zeigt darüber hinaus unterschiedlich ausgeprägte Signalübertragungseigenschaften in den jeweiligen Zelltypen. Seine Rolle in der Regulation physiologischer Funktionen ist gut untersucht, wohingegen die hochkomplexe intrazelluläre Signalübertragung auf molekularer Ebene, die Grundlage seines differenziellen Signalverhaltens, noch nicht gut erforscht ist.

Die vorliegende Arbeit zielte auf eine Aufreinigung von zelltyp-spezifischen CB1 Proteinkomplexen und anschließender Identifikation CB1-interagierender Proteine ab. Mit einer Kombination aus adeno-assoziierten Virus (AAV)-vermitteltem Transgentransfer, konditional Cre Rekombinase-exprimierenden Mauslinien und Tandem Affinity Purification (TAP) von hippocampalen Synaptosomenpräparationen wurde ein Experimentalaufbau geschaffen, der eine Isolation von CB1 Multiproteinkomplexen aus hippocampalen glutamatergen Neuronen und GABAergen Interneuronen von Mäusen unter nativen Bedingungen ermöglicht. Die Zusammensetzung dieser Proteinkomplexe wurde daraufhin mittels hochsensitiver Massenspektrometrie (MS) entschlüsselt.

Mittels dieses experimentellen Ansatzes konnten 951 Proteine in den TAP Proben glutamaterger und GABAerger CB1 Proteinkomplexe identifiziert werden, von denen 41 spezifisch für glutamaterge Neurone und 83 spezifisch für GABAerge Interneurone sind. Die hohe Zahl

identifizierter Proteine deutet auf eine Aufreinigung nicht nur direkt CB1-interagierender Proteine hin, sondern Strukturen höherer Ordnung, inklusive Zytoskelettproteinen und Strukturproteinen. Der gesamte Datensatz aufgereinigter Proteine reflektiert bekannte Funktionen von CB1 und stellt die komplexe Biosynthese und den Transport dieses Membranrezeptors in verschiedenen subzellulären Bereichen dar. Zusammen mit der Identifikation einiger bereits bekannter CB1-interagierender Proteine kann der Datensatz als kohärent und aussagekräftig betrachtet werden, mit einer Vielzahl bisher unbekannter, potentiell interessanter Interaktoren. Eine Anzahl von zelltyp-spezifisch gereinigten Proteinen könnte das Potential haben zum differentiellen Signalverhalten in den jeweiligen Neuronentypen beizutragen, jedoch müssen weitere funktionelle Studien durchgeführt werden, um die funktionelle Bedeutung interessanter Proteine zu entschlüsseln. Somit wurde eine umfangreiche Basis für neue Hypothesen und weitere Studien für differentielle CB1 Signalübertragung generiert.

Um darüber hinaus ein bisher unbekanntes, potentiell mit CB1 interagierendes Protein zu testen, wurden funktionale Studien mit G protein subunit alpha z ($G\alpha_z$), welches in den TAP Proben identifiziert wurde, durchgeführt. CB1 und $G\alpha_z$ sind in glutamatergen Neuronen und GABAergen Interneuronen im Hippocampus von Wildtyp-Mäusen ko-exprimiert. Eine funktionelle Interaktion von $G\alpha_z$ nach Aktivierung von CB1 konnte in einem *in vitro*-Modell mit stabil CB1-exprimierenden HEK293 Zellen und transient überexprimierten inhibitorischen G Proteinen $G\alpha_o$ oder $G\alpha_z$ gezeigt werden. Eine kinetische Untersuchung des Umsatzes von zyklischem Adenosinmonophosphat (cAMP) nach Stimulierung der Adenylatzyklase (AC) mit Forskolin zeigte eine CB1-vermittelte Inhibition der cAMP Synthese nach CB1 Agonist-Behandlung der Zellen. Eine zusätzliche Behandlung mit Pertussistoxin (PTX) führte zu einer Inhibition der cAMP Synthese nur in den $G\alpha_z$-, jedoch nicht in den $G\alpha_o$-überexprimierenden Zellen, da $G\alpha_z$ das einzige Pertussistoxin-insensitive inhibitorische G Protein ist. Somit konnte eine funktionelle Interaktion mit einem der identifizierten Interaktionskandidaten von CB1 verifiziert werden.

# 2 Introduction

Throughout history, interdisciplinary attempts have been made to propose a definition for life, and it is still an elusive task for scientists and philosophers today (Tsokolov, 2009). Classic definitions of life, overlapping to a significant extent, include the maintenance of internal homeostasis within a functionally and structurally integrated entity, or dissipative structure, against changes in the environment with the ability to adapt in response to external stimuli, as well as feedback mechanisms allowing for a regulation of various responses (Schrödinger, 1945; Muller, 1955; Prigogine, 1980; Koshland, 2002).

In the interdisciplinary study of cybernetics, negative feedback was defined as the main regulatory mechanism within a system, in which any deviation from an assigned parameter leads to a counteraction of this system and subsequently to the stabilization of this parameter and maintenance on a constant level (Wiener, 1948).

This theory led to an approach to define life as a set of living individuals, which in turn are unique networks of negative feedbacks subordinated to a superior positive feedback, which is self-sustaining and reproducing of the living individual. These negative feedbacks act as regulatory mechanisms on different hierarchical levels in order to sustain the positive feedback. Even the simplest unicellular organisms exhibit a high degree of complexity within a structure of complex and hierarchical sets of functions. Higher order organisms, such as mammals, have an even greater amount of hierarchically organized negative feedbacks, controlling fundamental reactions on the biochemical level, such as keeping the concentration of a metabolite or enzyme on an optimal level, up to the behavioral level of the whole organism, which finds expression for instance in the control of movements in order to acquire food. Furthermore, the whole complex of negative feedback mechanisms that constitute the identity of a living individual is directly or indirectly interconnected, thus, the assigned values of parameters that function as elements of a negative feedback can be mutually changed by other negative feedbacks on other levels of hierarchy (Korzeniewski, 2001).

The endocannabinoid system (ECS) is a lipid signaling system that appeared early in evolution and is present in all vertebrates and several invertebrate phyla (Elphick and Egertova, 2005; McPartland et al., 2006). It can be considered as one of these negative feedback mechanisms regulating important parameters on a physiological level with the purpose being determined by the context

of the whole complex of negative feedbacks, and thus, the function of the organism. The ECS with its components and functional properties will be described in detail in the following paragraphs.

## 2.1 The endocannabinoid system

### 2.1.1 Discovery of the components of the endocannabinoid system

Discoveries that indicate the earliest use of the plant *Cannabis sativa* for psychoactive or pharmacological purposes date back to 2200-2400 BP (Russo et al., 2008). Widely used in the Middle East for centuries, Napoleonic soldiers introduced the psychoactive variety of *Cannabis sativa* in Europe after returning from the Egyptian campaign (Mechoulam and Parker, 2013). First scientific approaches to isolate the psychoactive constituents of the plant and to determine its behavioral effects were performed in the nineteenth century (Scripture, 1893), but it took until the 1960s that the development of chromatographic techniques advanced enough to isolate and identify the chemical structure of the main psychoactive compound $\Delta^9$-tetrahydrocannabinol (THC) among over 100 phytocannabinoids with closely related structures (Gaoni and Mechoulam, 1964; Mechoulam et al., 2014). In subsequent years, until the late 1980s, a considerable amount of pharmacological work was performed and animal behavioral tests established (Pertwee, 1972; Dewey, 1986) until the mechanism of action of this compound was elucidated. The first indication of a receptor-mediated action of cannabinoids was found by showing that cannabinoids inhibit adenylyl cyclase (AC) via an inhibitory guanine nucleotide-binding protein-dependent mechanism (Howlett et al., 1986). Shortly thereafter, the existence of specific binding sites in rat brain were validated with a distribution that was found to be consistent with already described cannabinoid-related psychotropic properties (Devane et al., 1988; Herkenham et al., 1990). Finally, a corresponding classical seven-transmembrane G protein coupled receptor (GPCR) was identified and cloned, consequently named cannabinoid receptor type 1 (CB1) (Matsuda et al., 1990), thereby marking the identification of the first component of the ECS.

The discovery of a specific receptor mediating the effects of plant cannabinoids suggested the presence of endogenous cannabinoids produced by the organism itself. By purifying and fractionating lipid fractions of porcine brain synaptosomal membranes, arachidonylethanolamide (AEA), an arachidonic acid derivate that was termed anandamide (coined from the Sanskrit word “ananda”, meaning bliss, and from the chemical nature of the compound), was identified as the

first endogenous ligand for the cannabinoid receptor with an inhibitory activity that was equivalent to THC (Devane et al., 1992). Using the same methodological approach, a second compound, 2-arachidonyl glycerol (2-AG), an ester of arachidonic acid, was isolated from canine gut and its structure deciphered, acting as another endogenous ligand with a potency similar to THC (Mechoulam et al., 1995). In the meantime also a second, peripheral cannabinoid receptor (CB2) was cloned and the expression first localized in macrophages in the marginal zone of the spleen (Munro et al., 1993). Later, 2-AG was characterized as a full agonist of CB1 and CB2, whereas AEA has a higher affinity at both receptors, but only acts as a low-efficacy partial CB1 agonist, and with an even lower efficacy at CB2 (Gonsiorek et al., 2000).

After the discovery of the endocannabinoids, research focused on the metabolism of these lipid compounds and the underlying fundamental biochemical processes. Due to their hydrophobic nature, it seemed unlikely that AEA and 2-AG were stored in synaptic vesicles, and it could be shown that these two endocannabinoids are synthesized and acting on demand from membrane phospholipid precursors or storage sites in an activity-dependent manner (Marsicano et al., 2003; Piomelli, 2003).

The biosynthesis of 2-AG is catalyzed from arachidonoyl-containing diacyglycerol (DAG) precursors by *sn*-1-specific diacylglycerol lipase-α and -β (DAGL-α/β), with the former playing a primary role in the brain and the latter in peripheral tissues (Bisogno et al., 2003). The synthesis of AEA, on the contrary, is not completely understood. The AEA-precursor *N*-arachidonoyl phosphatidylethanolamine (NArPE) is produced by a calcium ($Ca^{2+}$)-dependent transfer of arachidonic acid from the *sn*-1 position of membrane phospholipids to the primary amine of phosphatidylethanolamine (PE) by a molecularly for a long time not identified $Ca^{2+}$-dependent transacylase enzyme (Di Marzo et al., 1994; Cadas et al., 1996). Recently, the yet poorly characterized serine hydrolase phospholipase A2 group IVE (PLA2G4E) was identified as a mouse brain $Ca^{2+}$-dependent transacylase that generates NArPE in mammalian cells (Ogura et al., 2016). Multiple mechanisms were suggested by which the NArPE is converted into AEA, including direct synthesis by the enzyme *N*-acyl phosphatidylethanolamine-selective phospholipase D (NAPE-PLD), sequential deacylation by lyso-*N*-acyl phosphatidylethanolamine-lipase α-β hydrolase 4 (ABHD4) and cleavage of the phosphodiester bond by the glycerophosphodiesterase 1 (GDE1), sequential deacylation by phospholipase A2 (PLA2) and hydrolysis of the phosphodiester bond by a lyso-phospholipase D (lyso-PLD) enzyme, and lastly, conversion to phosphor-AEA by a phospholipase C (PLC)-like enzyme and subsequent dephosphorylation by the protein tyrosine phosphatase, non-receptor type 22 (PTPN22) or the SH2 domain-containing inositol 5'-phosphatase (SHIP) (Alger and Kim, 2011; Blankman and Cravatt, 2013). Following their release, both AEA and 2-AG are degraded

to arachidonic acid. AEA is degraded by the enzyme fatty acid amide hydrolase (FAAH) (Cravatt et al., 1996), whereas the majority of 2-AG is hydrolyzed by the enzyme monoacylglycerol lipase (MAGL) (Dinh et al., 2002). Additionally, the degradation of a minor part of 2-AG can be attributed to the enzymes α-β hydrolase 6 (ABHD6) and α-β hydrolase 12 (ABHD12) in a compartment-selective manner due to their distinct subcellular distributions, thereby potentially controlling different pools of 2-AG in *in vivo* (Blankman et al., 2007). Another part of 2-AG was shown to be degraded by cyclooxygenase-2 (COX-2) (Kozak et al., 2000; Hermanson et al., 2013). Taken together, the entirety of receptors, ligands and their synthesizing and degrading enzymes constitutes the ECS.

### 2.1.2 The endocannabinoid system (ECS) in the brain

The sites of action of a system are determined by the localization of its components. Since the ECS is widely distributed throughout the central nervous system (CNS), it is involved in numerous behavioral and physiological responses. Beyond that, CB1 is the most abundant GPCR in the brain, with the highest expression levels in various neuronal subtypes in the basal ganglia, substantia nigra, globus pallidus, cerebellum and hippocampus (Marsicano and Kuner, 2008). Consistent with the high abundance in the limbic system, numerous effects in learning and memory, anxiety and depression, and the reward system have been described (Mechoulam and Parker, 2013; Lutz et al., 2015; Parsons and Hurd, 2015). Furthermore, the ECS plays important roles in the developing brain in axonal outgrowth and guidance, and in the adult brain in modulating synaptic strength and adult neurogenesis (Maccarrone et al., 2014; Prenderville et al., 2015).

The aforementioned effects, contributing to the general behavioral expression of an organism, underlie the flow of information in the brain, which in turn is controlled by the synaptic transmission between neurons. Anterograde synaptic transmission has been well studied in the last decades and is characterized by the $Ca^{2+}$-triggered release of amino acid or amino acid derivative monoamine neurotransmitters from the presynaptic active zone of a neuron to the postsynaptic density of another neuron (Sudhof and Malenka, 2008). In order to dynamically regulate the flow of information between neurons, feedback mechanisms are necessary, as in all biological systems (Katona and Freund, 2012). Messengers, released from the cell body or dendritic compartment that travel retrogradely from the postsynapse to the presynapse to modulate the activity and strength of synapses neurons receive, include peptides, growth factors, gases, and also conventional neurotransmitters, but the best characterized and most widespread are the lipid-

derived endocannabinoids (Regehr et al., 2009). The first evidence of retrograde endocannabinoid signaling was the discovery that endocannabinoids mediate a form of short term plasticity in the hippocampus and cerebellum in excitatory glutamatergic synapses and γ-aminobutyric acid (GABA)ergic inhibitory synapses, referred to as depolarization-induced suppression of excitation (DSE) and depolarization-induced suppression of inhibition (DSI), respectively (Kreitzer and Regehr, 2001; Maejima et al., 2001; Ohno-Shosaku et al., 2001; Wilson and Nicoll, 2001; Ohno-Shosaku et al., 2002). The underlying mechanism for both DSE and DSI is based on $Ca^{2+}$-influx via the opening of voltage-gated $Ca^{2+}$-channels (VGCCs) in the postsynaptic membrane after depolarization (Castillo et al., 2012). The rise in intracellular $Ca^{2+}$ concentration leads to the activation of DAGL-α, presumably via activation of $Ca^{2+}$-sensitive enzymes and in turn production of 2-AG, the principal endocannabinoid required for activity-dependent retrograde signaling (Gao et al., 2010; Tanimura et al., 2010). In addition, after the release of glutamate, the activation of postsynaptic group I metabotropic glutamate receptors (mGluRs) and subsequent activation of guanine nucleotide-binding protein G(q) subunit alpha ($G\alpha_q$), leads to the activation of phospholipase Cβ (PLCβ), which produces the 2-AG precursor DAG from phosphatidylinositol (PI) (Castillo et al., 2012). Ultimately, both pathways converge in order to produce 2-AG, that is released into the synaptic cleft (Katona and Freund, 2012). How these highly lipophilic molecules are transported through the extracellular space to the presynaptic site is still unsolved, but finally leads to the activation of presynaptically located CB1 and subsequent inhibition of neurotransmitter release via G protein-dependent inhibition of presynaptic VGCCs, most likely directly through the βγ subunits and activation of G protein-activated inwardly rectifying potassium ($K^+$) channels (GIRKs) (Kano et al., 2009; Castillo et al., 2012) (Fig. 2.1).

The role of AEA, the second major endocannabinoid, is less clear. As stated above, the synthesis of AEA is not completely characterized yet, but like 2-AG, AEA can be produced postsynaptically by NAPE-PLD and act in a retrograde manner. Nevertheless, as NAPE-PLD is also presynaptically located, it was shown that AEA can be produced in the presynapse and then may act anterogradely on postsynaptic transient receptor potential cation channel subfamily V member 1 (TRPV1) (Chavez et al., 2010), before getting inactivated by FAAH, which is located primarily in the postsynapse as well (Gulyas et al., 2004) (Fig. 2.1). In contrast to the phasic modulation of transient neurotransmitter release, generally attributed to 2-AG, there was also a tonic endocannabinoid-mediated modulation observed (Losonczy et al., 2004). A blockade of FAAH, which causes continuously elevated levels of AEA, sustained activity of CB1 without any changes in receptor expression, therefore indicating a role for AEA as a tonic signal (Ohno-Shosaku and Kano, 2014). However, as it was shown that a combined action of 2-AG and AEA at specific synapses is necessary

to fully engage CB1, a model was proposed with CB1 operating as a coincidence detector, integrating different physiological signals, which are required to modulate synaptic plasticity (Katona and Freund, 2012).

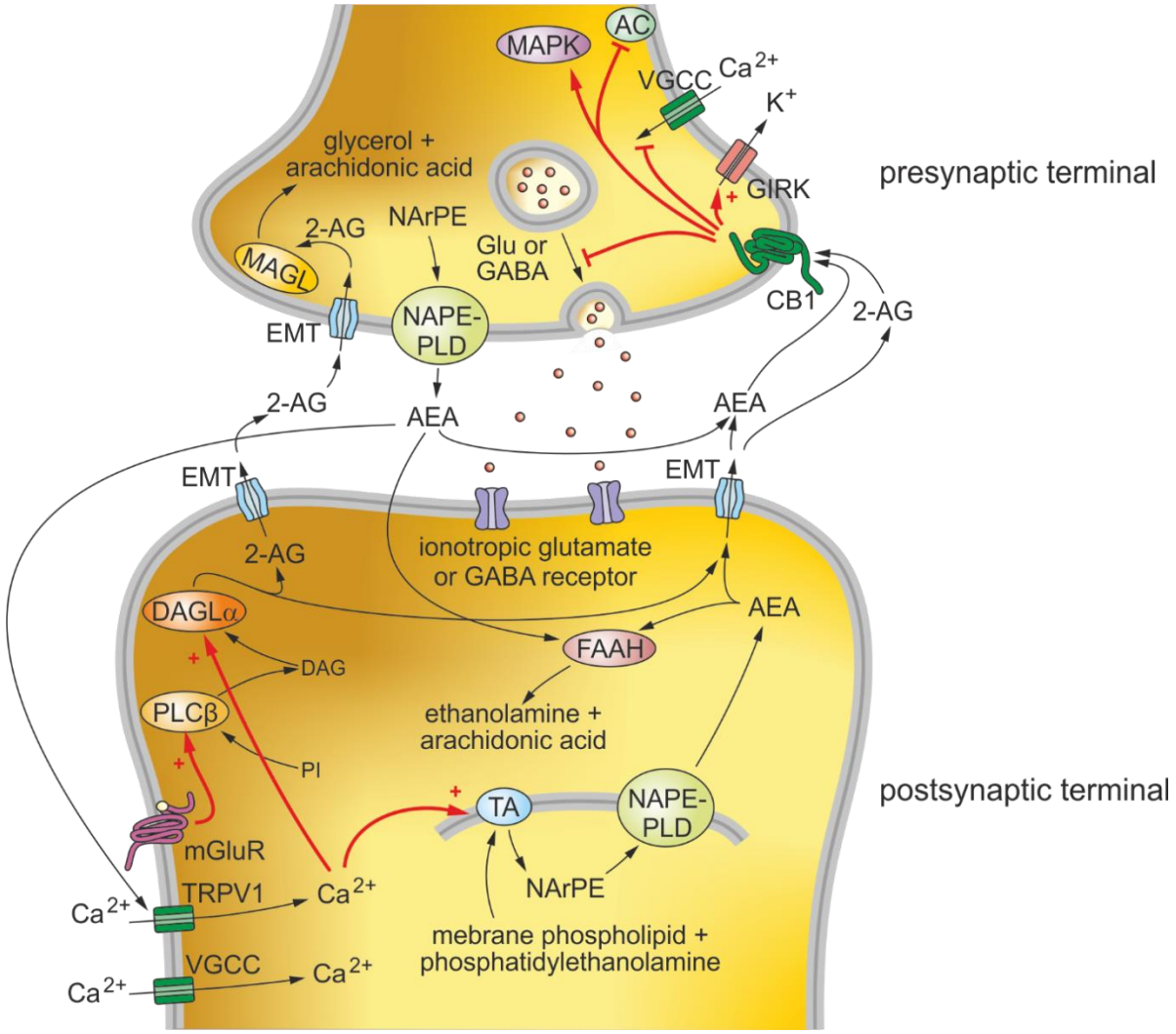


**Fig. 2.1 Components of the endocannabinoid system in the neuronal synapse**

Depolarization of the postsynapse leads to an influx of $Ca^{2+}$ via voltage-gated $Ca^{2+}$ channels (VGCCs). A rise in intracellular $Ca^{2+}$ activates sn-1-specific diacylglycerol lipase-α (DAGLα), presumably via $Ca^{2+}$-sensitive enzymes and production of 2-arachidonyl glycerol (2-AG). After release of glutamate, a simultaneous activation of postsynaptic group I metabotropic glutamate receptors (mGluRs) leads to the activation of phospholipase Cβ (PLCβ), which produces the 2-AG precursor diacylglycerol (DAG) from phosphatidylinositol (PI), and thus, further promotes the production of 2-AG, which is then released into the synaptic cleft via a yet not characterized endocannabinoid membrane transporter (EMT). 2-AG activates cannabinoid receptor type 1 (CB1) and initiates downstream signaling cascades, which lead to opening of G protein-activated inwardly rectifying K+ channels (GIRKs), inhibition of VGCCs, inhibition of adenylyl cyclase (AC) and inhibition of neurotransmitter release (Glu or GABA) until 2-AG gets hydrolyzed by its degrading enzyme monoacylglycerol lipase (MAGL). The second major endocannabinoid arachidonylethanolamide (AEA) is produced postsynaptically, as well as presynaptically by the enzyme *N*-acyl phosphatidylethanolamine-selective phospholipase D (NAPE-PLD) from the precursor *N*-arachidonoyl phosphatidylethanolamine (NArPE), which in turn is produced by a not yet identified $Ca^{2+}$-dependent transacylase enzyme (TA). AEA therefore can act on CB1 in a retrograde manner according to 2-AG or anterogradely on postsynaptic

transient receptor potential cation channel subfamily V member 1 (TRPV1), before getting inactivated by fatty acid amide hydrolase (FAAH), which is located primarily in the postsynapse.

Extending beyond transient suppression of neurotransmitter release in endocannabinoid-mediated short term depression (eCB-STD), stimulation of CB1 inhibits AC via activation of Gα proteins of the $G_{i/o}$-family ($G\alpha_{i/o}$), consequently affecting the activity state of downstream targets, which forms the molecular basis for endocannabinoid-mediated long term depression (eCB-LTD), and thereby suppressing neurotransmitter release persistently. The mechanisms of endocannabinoid release from the postsynapse in the induction process of eCB-LTD vary depending on the brain region and experimental conditions, and also whether the activation of CB1 alone for several minutes is sufficient is not consistent among studies (Kano et al., 2009). The induction of long term changes in neurotransmitter release by a short activation of CB1, however, requires presynaptic cAMP/protein kinase A (PKA) signaling, the downstream target of $G\alpha_{i/o}$, in order to forward the signal from CB1 to the release machinery (Chevaleyre et al., 2007; Mato et al., 2008).

Due to the complexity, and as a consequence thereof, the great potential of the ECS in modulating neuronal activity, its role as a neuroprotective system has been investigated. Endocannabinoid signaling in effect can act as a dampener of over-active circuits in the brain, which is essential to protect it from harmful processes, but dysregulation of this system on the other hand, can also lead to pathological conditions. Excessive glutamate release from axon terminals of excitatory neurons, in particular during epileptic seizures, can lead to neuronal death, a process known as excitotoxicity, which is counteracted by an increase in 2-AG levels via the mGluR - PLCβ - DAGL-α pathway (Soltesz et al., 2015). Mice lacking CB1 in glutamatergic principal forebrain neurons and hippocampal neurons show less protection against chemically induced seizures as a result of impaired CB1-mediated inhibition of glutamatergic transmission and increased neuronal damage (Marsicano et al., 2003; Monory et al., 2006). Furthermore, CB1 does not only mediate an acute response to neurotransmitter release, but it also induces intracellular signaling cascades, including extracellular signal-regulated kinase (ERK) phosphorylation and the expression of immediate early genes that code for transcription factors and neurotrophins, which lead to long term adaptation processes in neurons (Marsicano et al., 2003). Hippocampal CB1 expression itself was shown to underlie temporal changes in epilepsy, with a downregulation in the acute phase, and as a response of that, an upregulation in the chronic phase afterwards (Falenski et al., 2009). Whereas the actions of CB1 in epilepsy could be pinned down to hippocampal glutamatergic CB1, other neuronal subtype-specific actions of CB1 were shown, such as the ECS-mediated stimulation on food intake via CB1 signaling in ventrostriatal GABAergic neurons (Bellocchio et al., 2010), thereby

proving the general principle of highly specific actions of this receptor on different neuronal populations. The neuroprotective properties attributed to CB1 in the aforementioned epilepsy models can be extended to the regulation of cell survival and proliferation after brain injury or anti-neuroinflammatory effects (Zogopoulos et al., 2013). The plethora of ECS-mediated modulations of physiological responses is eventually proving its role as an important feedback system maintaining a state of homeostasis within an organism.

## 2.2 G protein-coupled receptor signaling

The synergy of cells, or cell populations, within an organism requires a fine-tuned communication between the cells and the ability of single cells to integrate vast amounts of information conveyed to them by extracellular signals, such as hormones, growth factors or neurotransmitters. These signals mostly do not pass the membrane, but act on the cell surface on specific receptors (Gudermann et al., 1997). The largest and most versatile group of cell surface receptors involved in signal transduction is constituted by the superfamily of G protein-coupled receptors (GPCRs). Approximately 800 genes, which make up more than 1% of the human genome, encode for approximately 1000 - 2000 functional receptors considering all splice variants (Luttrell, 2008). GPCRs in human form five main families, as determined by phylogenetic analysis, which are termed adhesion (family, secretin, glutamate, frizzled/taste2, and the rhodopsin family with by far the largest number of receptors. This family is therefore subdivided into four main groups and includes the huge cluster of 460 unique functional olfactory receptors, leaving 342 identified unique functional non-olfactory receptors throughout the human genome (Fredriksson et al., 2003). About 90% of GPCRs are expressed in the CNS (Brugarolas et al., 2014), where they function primarily as mediators of slowly modulating biologically active molecules, rather than fast acting neurotransmitters, with a critical role in maintaining a normal brain function (Gainetdinov et al., 2004). After activation of the receptor by a ligand, it acts as a ligand-activated guanine nucleotide exchange factor (GEF) for intracellular heterotrimeric guanine nucleotide-binding proteins (G proteins), which dissociate from the receptor upon activation (Luttrell, 2008). In consequence, the α-subunit binds and hydrolyzes guanosine-5'-triphosphate (GTP), activating downstream effectors in its GTP-bound state, whereas the βγ subunit serves as another functional monomer affecting other downstream targets (Hamm and Gilchrist, 1996).

### 2.2.1 G protein-coupled receptor (GPCR) structure and functional properties

GPCRs are heptahelical (7TM) receptors and share similar primary amino acid sequences that lead to common structural patterns (Gudermann et al., 1997). The N-terminus of the protein is located extracellularly and the C-terminus at the cytosolic side, with seven membrane-spanning α-helices (TM1 - TM7) in between, which are linked by three alternating intracellular and extracellular loops (i1 - i3, e1 - e3), respectively. While the transmembrane helices are highly conserved throughout the GPCR variants, the intra- and extracellular loops vary extensively in size and composition, in order to fulfill the demands of specific ligand-binding domains on the extracellular side and differential signal transduction and feedback modulation capabilities on the intracellular side. In addition, GPCRs are targets of a variety of post-translational modifications. The N-terminus and less often the extracellular loops are targets for *N*-glycosylation. Two cysteine residues, which are common in most GPCRs, form a disulfide bridge between e1 and e2, which is crucial for normal protein folding. The C-terminus contains another cysteine residue, which serves as a target for palmitoylation, which in turn leads to the formation of a putative fourth intracellular loop. Further intracellular amino acid residues can serve as sites for G protein-coupled receptor kinase (GRK)-mediated phosphorylation or PKA-mediated phosphorylation, in order to modulate downstream signaling events (Luttrell, 2008) (Fig. 2.2).

The two-state model illustrates how GPCRs exist in equilibrium between an active (R*) state, in which the receptor can couple to and activate G proteins, and an inactive (R) state, in which it is uncoupled from G proteins. Depending on ligand-binding, GPCRs undergo conformational changes, associated with bidirectional R to R* isomerization (Seifert and Wenzel-Seifert, 2002). The transmission of the extracellular signal to the cytosolic compartment is achieved by ligand-binding-induced conformational changes of the GPCR, which depend on the transmembrane helices acting as communication links between the extracellular and partly membranous ligand-binding pocket and the intracellular G protein binding site. Binding of a ligand leads to a rearrangement of the transmembrane helices, as it was shown in detail for the $\beta_2$ adrenergic receptor ($\beta_2$AR), in particular TM3, TM5 and TM6, which eventually change the conformation of the intracellular G protein-interacting sites. On the contrary, binding of G proteins to the GPCR can stabilize a conformation that increases the affinity of the receptor to its ligand, suggesting that the allosteric coupling between G-protein- and ligand-binding sites is bidirectional (Rasmussen et al., 2011; Venkatakrishnan et al., 2013).

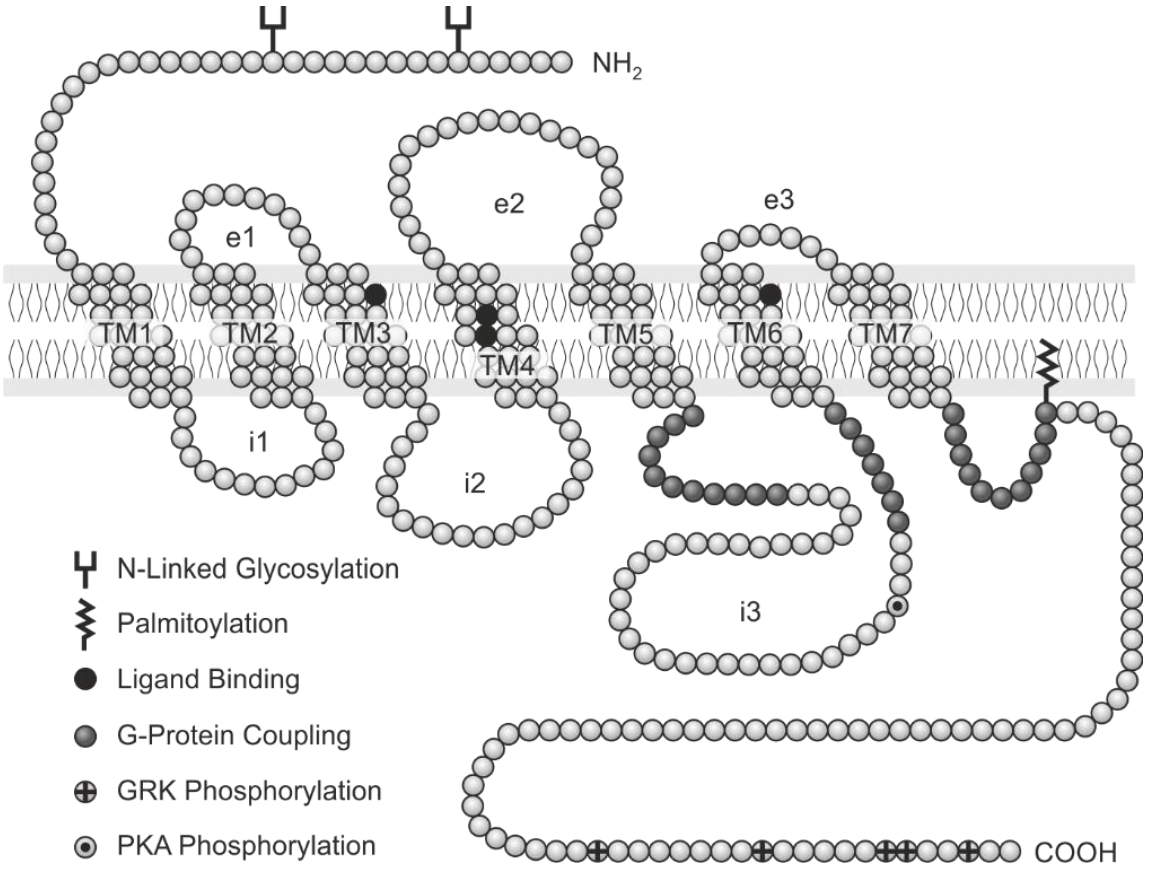


**Fig. 2.2 Structure of GPCRs**

Schematic diagramm of a GPCR. Seven transmembrane helices (TM1 - TM7) are connected by three extracellular loops (e1 - e3) and three intracellular loops (i1 - i3). Extracellular residues at the N-terminus are often targets for glycosylation, whereas intracellular residues are often targets for modulation of intracellular protein-protein interactions, which include phosphorylation by G protein-coupled receptor kinases (GRKs) or protein kinase A (PKA). The approximate positions of residues involved in G protein-binding are colored in darker grey and residues involved in ligand binding in black. A cysteine residue at the C-terminus can serve as a target for palmitoylation, which leads to the formation of a putative fourth intracellular loop (modified from Luttrell, 2008).

In the absence of a ligand, given receptors show a distinct amount of basal activity or constitutive activity, which can be shifted into the direction of either the R- or R*-state depending on the characteristics of the ligand upon binding. Based on these characteristics, ligands are classified into full agonists, partial agonists, neutral antagonists, partial inverse agonists and full inverse agonists. Full agonists and full inverse agonists stabilize the GPCR in the R*- or R-state, respectively, whereas a neutral antagonist does not affect the R/R* equilibrium but inhibits binding of other ligands. Partial agonists and partial inverse agonists exert the same actions than full agonists and full inverse agonists but have lower efficacies, thus, they do not shift the R/R* equilibrium entirely in one direction (Seifert and Wenzel-Seifert, 2002) (Fig. 2.3).

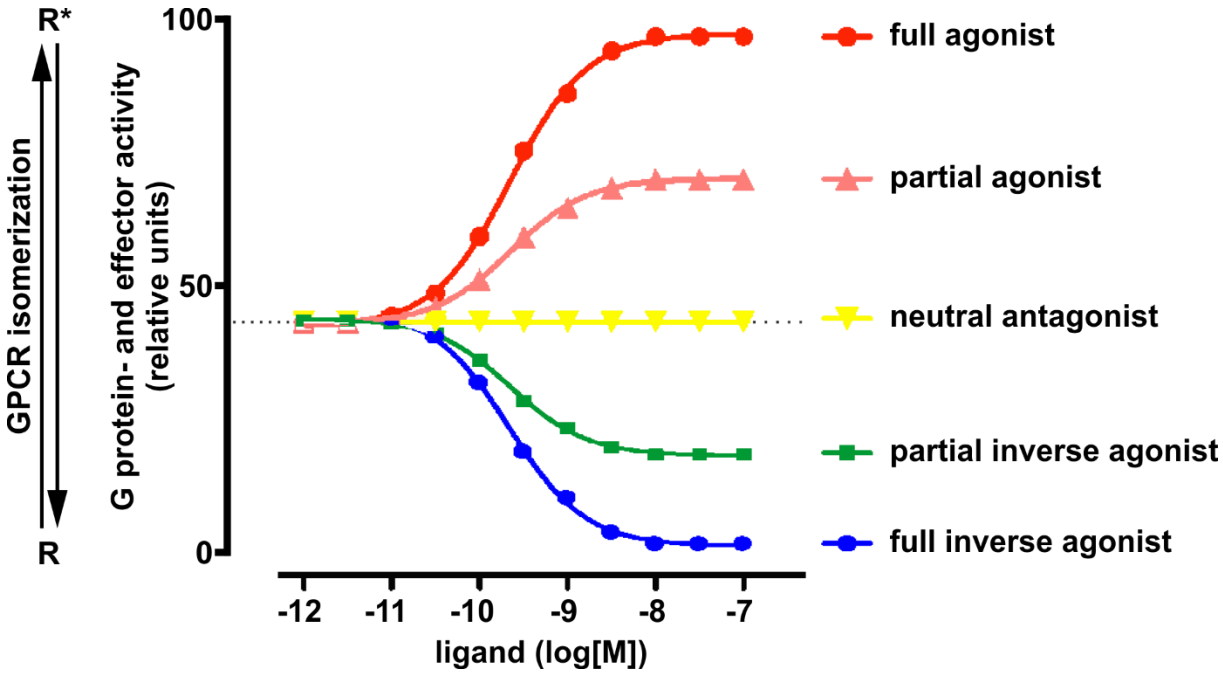


**Fig. 2.3 Two-state model of GPCR activation**

Bidirectional isomerization from the active (R*) to the inactive (R) state occurs in GPCRs in the absence of any ligands and is referred to as constitutive or baseline activity (as indicated by dashed line). Binding of a ligand can lead to concentration-dependent shifts in the R/R* equilibrium as shown by theoretical dose-response curves for different classes of ligands, which in turn leads to changes in downstream GDP/GTP exchange at G proteins and effector activation. Full agonists (red) maximally stabilize the receptor in the R*-state, whereas full inverse agonists (blue) maximally stabilize the R state. Partial agonists (pink) and inverse agonists (green) exhibit less efficacy, whereas neutral antagonists (yellow) do not change the R/R* equilibrium, but inhibit other agonists or inverse agonists from binding (modified from Low, 2011).

Extending beyond the two-state model of GPCR activation, agonists were characterized as being biased or functionally selective towards certain response pathways by stabilizing different receptor conformations. Thus, binding of an agonist can lead to the activation of multiple G proteins or arrestins and induce other effects, such as receptor phosphorylation or receptor internalization. The different efficacies of one ligand to induce one or the other pathway is referred to as pluridimensional efficacy of the ligand (Kenakin, 2011). This concept requires the existence of multiple active conformations of a given receptor that do not only depend on the conformational changes induced by the ligand itself, but involve the actions of GRKs as well (Reiter et al., 2012) (Fig. 2.4).

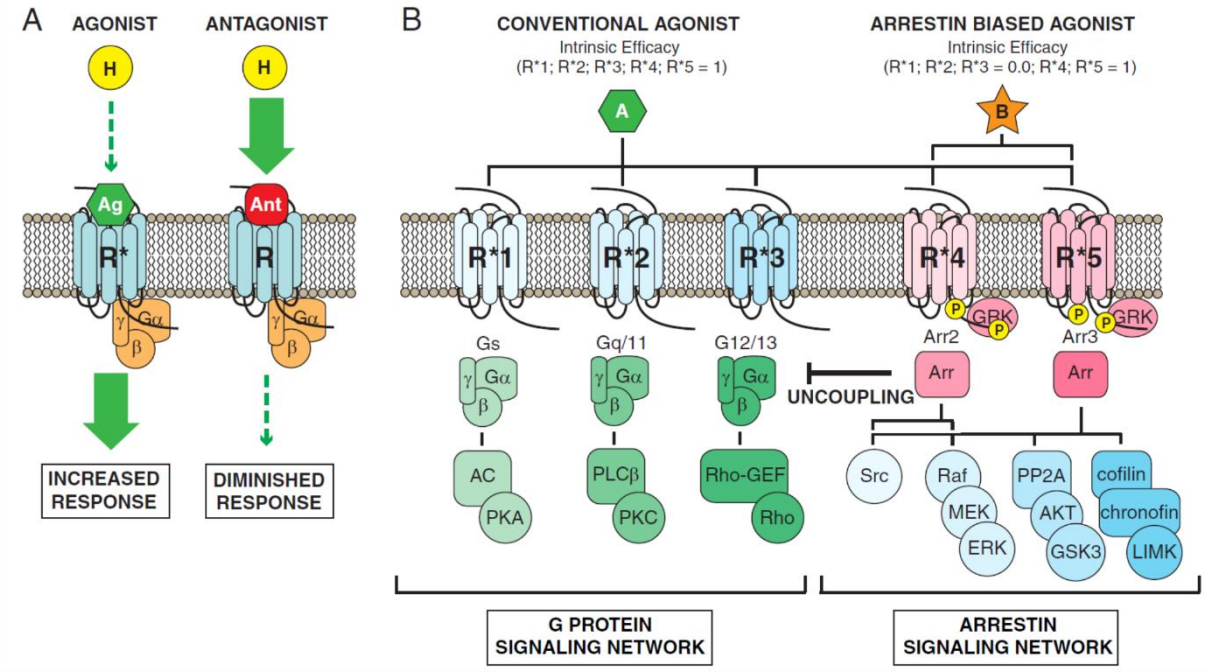


**Fig. 2.4 Multiple active conformational states of a GPCR**

**A**: Classical view of ligand-binding-mediated activation or inhibition of a GPCR. Binding of an agonist (Ag) leads to an increase in receptor activity (R*), consequently promoting the "on"-state of the receptor, whereas binding of an antagonist (Ant) leads to a decrease in receptor activity (R), thus stabilization of the conformational "off"-state. All downstream signaling events arise from one single active state. **B**: Hypothetical GPCR with five distinct active states (R*1 - R*5) depending on ligand and GPCR phosphorylation state. Ligands A and B promote different hypothetical "on" states of the GPCR, coupling the receptor to downstream G protein (Gs, Gq/11, G12/13) and non-G protein β-arrestin1/2 (Arr2, Arr3) effectors with different efficacies, referred to as pluridimensional efficacy. Ligand A shows a full agonist response, promoting activation of all downstream effectors, whereas Ligand B shows a biased agonist response, activating only a subset of hypothetical active receptor states (R*4, R*5) and antagonizing the others (R*1 - R*3). AC: adenylyl cyclase. GEF: guanine nucleotide exchange factor. PKA: protein kinase A. PKC: protein kinase C. PLC: phospholipase C. MEK: MAPK kinase. ERK: extracellular signal-regulated kinase. PP2A: protein phosphatase 2A. Akt: protein kinase B. GSK3: glycogen synthase kinase 3. LIMK: lim domain-containing kinase (Luttrell, 2014).

### 2.2.2 Heterotrimeric G proteins and effectors

Heterotrimeric G proteins share a common structure consisting of a 39 - 52 kDa GTP-binding Gα subunit that possesses an intrinsic GTPase activity and a tightly linked dimeric Gβγ subunit which is non-covalently bound to the Gα subunit in its inactive GDP-bound state. Gα subunits share approximately 40% amino acid sequence homology. Similarities are principally attributable to the guanine nucleotide-binding pocket, whereas the N-terminus and C-terminus are more divergent, corresponding to the requirements of Gβγ subunit-binding at the N-terminus and association with receptors and effectors at the C-terminus. Gβ subunits are all approximately 36 kDa in size and

associate with 7 - 8 kDa Gγ subunits which are tightly embedded in Gβ and do not make contact with Gα. Gα and Gγ are both post-translationally modified by the addition of lipids that are essential for membrane localization. The Gβ subunit contacts the Gα subunit and occludes access to the GDP/GTP-binding pocket of Gα in the heterotrimeric state. Upon isomerization of a GPCR to an active state, it catalyzes the exchange of GDP to GTP in the Gα subunit, consequently leading to the dissociation of the Gα subunit from the receptor and displacement of the Gβγ dimer (Luttrell, 2008).

The activated and separated G protein subunits interact with various downstream effectors until they go back to the resting state by hydrolyzing a phosphate group from GTP, converting it to GDP. 21 Gα, 6 Gβ, and 12 Gγ subunits were identified in human and create various distinct combinations of heterotrimeric G protein complexes. Depending on sequence similarity, Gα proteins are grouped into four main classes ($G\alpha_s$, $G\alpha_{i/o}$, $G\alpha_{q/11}$, and $G\alpha_{12/13}$) (Duc et al., 2015). The effectors and most widely studied enzymes regulated by G proteins of the $G\alpha_s$- and $G\alpha_{i/o}$-family are the ACs which catalyze the turnover of adenosine triphosphate (ATP) to the second messenger cAMP. All of the ten cloned AC isoforms are stimulated by $G\alpha_s$, some also by Gβγ or calmodulin but only in the presence of $G\alpha_s$. The family of $G\alpha_{i/o}$ proteins, on the contrary, mediates the inhibition of some but not all AC isoforms, just as intracellular $Ca^{2+}$ (Luttrell, 2008). Furthermore, $G\alpha_o$ was shown to inhibit N-type VGCCs, and $G\alpha_s$ to stimulate L-type VGCCs (Wickman and Clapham, 1995). The $G\alpha_{q/11}$-family of G proteins, as well as Gβγ, activate PLCβ isoforms 1 - 3, whereby PLCβ1 shows a bias for $G\alpha_{q/11}$ activation, and PLCβ2 and PLCβ3 are more sensitive to Gβγ regulation. The latter usually accounts for the activation of PLCβ by $G\alpha_{i/o}$-coupled GPCRs (Luttrell, 2008). Rho GTPases, which are a family of small G proteins and belong to the superfamily of Ras proteins, are regulated by the family of $G\alpha_{12/13}$ proteins, which bind to the regulator of G protein signaling (RGS) domain of p115RhoGEF, a nucleotide exchange factor for Rho. Binding of $G\alpha_{13}$ but not $G\alpha_{12}$ stimulates GEF activity, thus, $G\alpha_{12}$ activates Rho by binding of RhoGEF, and serves as a link between heterotrimeric G protein and small GTPase pathways. In addition, $G\alpha_{12/13}$ proteins interact with other proteins, such as heat shock protein 90 (HSP90), which is modulating cytoskeletal actin organization or the activity of cadherin, which is implicated in cell - cell interactions (Kurose, 2003). Beyond Gα subunit-mediated modulations of downstream effectors, the Gβγ dimer also directly activates GIRKs, regulates GRK2 and GRK3, and may regulate PLA2 (Luttrell, 2008).

### 2.2.3 Regulation of G protein-coupled receptor signaling by protein-protein interactions and cross-talk with other signaling pathways

Activation of GPCRs and subsequent recruitment of heterotrimeric G proteins leading to the activation or inhibition of downstream effectors, is subject to modulation of its components on multiple levels. Since this study aims at the identification of yet unknown interacting proteins of CB1, already described interactions of GPCRs with other proteins in general are presented in the next paragraphs.

#### *2.2.3.1 GPCR oligomerization*

Many GPCRs can exist as homodimers, heterodimers with other receptors, and higher order multimers in many variations. In some cases, assembly occurs already during translation and is a prerequisite for the trafficking of the receptors from the endoplasmic reticulum (ER) to the plasma membrane. Receptor oligomerization holds a huge potential in order to further increase the diversity of G protein-coupling, signaling, and internalization (Luttrell, 2008). Most GPCR dimers or oligomers are formed through non-covalent interactions of the transmembrane helices of the single protomers, although dimerization also occurs including the formation of covalent disulfide bridges. Although oligomerization is often necessary to obtain full functionality, GPCRs exist in a dynamic equilibrium between monomeric and oligomeric states (Gonzalez-Maeso, 2011). Heteromerization of receptors may have different effects. The mutual allosteric modulation can lead to a change of signaling properties as compared to the single units, based on alterations of intracellular binding domains, and thus, changes in G protein selectivity or β-arrestin binding. Ligand-binding properties can be changed and the ligand-induced activation of one GPCR protomer can also lead to transactivation or blockade of the other within a complex. The presence of a protomer can also change the localization of the partner protomer. The possibility to form heteromers placed at specific neuronal subsets and at specific locations (pre-, post- or perisynaptically) illustrates the versatility underlying nervous system anatomy, and contributes to the attainment of unique neuronal functions. The dynamics of GPCR heteromerization expressed in a distinct manner in different brain regions and neuronal localizations are a fundamental property for neural transmission and plasticity (Brugarolas et al., 2014). Many GPCR dimers and oligomers were reported, also for CB1, which will be presented in the later sections, but for many of them the functional relevance *in vivo* still has to be established (Gomes et al., 2016).

### *2.2.3.2 GPCR modification, functional selectivity and trafficking*

Phosphorylation of intracellular serine and threonine residues of a GPCR by second messenger-dependent protein kinases upon agonist exposure can lead to direct impairment of further G protein coupling, referred to as heterologous desensitization of the receptor (Luttrell, 2008). Alternatively, instead of inhibiting G protein coupling, phosphorylation can also lead to a switch in G protein selectivity, as it was shown for $\beta_2$AR, which upon phosphorylation of PKA leads to preferential coupling of $G\alpha_i$, instead of $G\alpha_s$, and eventually initiates a new set of signaling events (Daaka et al., 1997). Homologous desensitization, on the other hand, involves phosphorylation of the receptor by GRKs followed by binding of β-arrestin. In mammals, there are seven isoforms of GRKs and four of arrestin with distinct expression patterns and functions (Magalhaes et al., 2012). In contrast to GPCR phosphorylation by PKA or PKC, GRKs preferentially phosphorylate agonist-occupied receptors and have little direct effect but are increasing the affinity of the receptor to arrestin-binding. Upon binding, β-arrestin acts as an adapter protein targeting GPCRs to clathrin-coated pits for endocytosis, also referred to as internalization or sequestration (Luttrell and Lefkowitz, 2002). In addition to that, β-arrestin itself is a target of post-translational modifications, such as phosphorylation and ubiquitination, which indirectly affects GPCR endocytosis and trafficking (Shenoy et al., 2001; Lin et al., 2002), and interacts with a variety of protein complexes implicated in endocytic processes, such as E3 ubiquitin ligases (Magalhaes et al., 2012). It has to be noted that under certain circumstances endocytosis occurs also under control of β-arrestin-independent mechanisms (Luttrell, 2008). Initially, the role of GRKs and β-arrestins were limited to control desensitization, internalization and recycling of GPCRs, but it was shown that β-arrestin also induces G protein-independent signaling via the non-receptor tyrosine kinase c-Src, and downstream activation of mitogen-activated protein kinase (MAPK) (Luttrell et al., 1999). Generally, phosphorylation of agonist-occupied receptors by various GRKs and other second messenger-dependent protein kinases can lead to recruitment of β-arrestin and initiation of signaling cascades in the absence of G protein interactions, which depend on distinct GRK phosphorylation patterns (Luttrell, 2014; Rankovic et al., 2016). Hence, GRKs play a central role in regulating desensitization of GPCR-G protein signaling, endocytosis of GPCRs to endosomes, and GPCR signaling via G protein-independent mechanisms (Magalhaes et al., 2012). Furthermore, β-arrestin is able to recruit specific isoforms of phosphodiesterase (PDE) to the receptor, and consequently promotes degradation of cAMP, which in turn leads to accelerated termination of membrane-associated PKA activity (Perry et al., 2002; Baillie et al., 2003). For CB1, interactions with the respective proteins mentioned in this paragraph were described as well and will be presented in the later sections.

Upon internalization, the GPCR enters either a recycling pathway, leading to its return to the plasma membrane, or a degradation pathway, which is under control of the stability of the receptor-β-arrestin complex, and further regulated by the Rab family of small Ras-like GTPases. Rab proteins are generally involved in budding, transport, docking and fusion of intracellular vesicles and hence, in sorting and trafficking of internalized GPCRs (Seachrist and Ferguson, 2003). Beyond that, a multitude of members of the whole superfamily of small GTP-binding proteins, which contains over 100 members and is divided into the Ras, Rho, Arf, Ran, and Rab families by structural similarity, is involved in the regulation of GPCR functions by direct or indirect interactions (Magalhaes et al., 2012).

Receptor resensitization of many GPCRs is dependent upon dephosphorylation in endosomes. Protein phosphatases, such as protein phosphatase 2A (PP2A), were shown to co-precipitate with specific GPCRs, and mediate the dephosphorylation of the receptors. The functional consequences, however, remain to be determined (Magalhaes et al., 2012).

#### *2.2.3.3 GPCR-interacting proteins and cross-talk between signaling pathways*

A multitude of other interacting proteins were identified for specific subsets of GPCRs and with a wide range of functions. They play important roles in regulating receptor-ligand specificity, endocytosis, cell surface trafficking, receptor recycling, and are mediating signaling cross-talk between different pathways.

Receptor activity modifying proteins (RAMPs) are a family of single membrane-spanning glycoproteins that interact with a number GPCRs, in particular calcitonin family receptors, and influence the trafficking and pharmacological properties of the receptor by acting as pharmacological switches and chaperones (Hay and Pioszak, 2016). In addition, they may also influence receptor trafficking and post-translational modifications via protein interactions mediated by postsynaptic density protein 95 (PSD95)-disc large-zona occludens (PDZ) domain binding motifs (Magalhaes et al., 2012).

The C-terminal tail of several GPCRs contains a PDZ domain which is involved in binding of PDZ domain-containing peptides. These, in turn, usually possess other protein interaction domains and consequently serve as scaffolds in order to integrate GPCRs with other proteins, which modulate the receptor function and localization (Dunn and Ferguson, 2015). A single GPCR has the capacity to bind multiple different PDZ proteins with varying and often opposing effects with regards to

trafficking and signaling and conformational states of the GPCR affect the regulation of PDZ protein interactions (Magalhaes et al., 2012).

The family of GPCR-associated sorting proteins (GASPs) is comprised of ten different proteins with high sequence similarity. By interacting with GPCRs, they function as regulators of post-endocytic sorting. Beyond that, they interact with other proteins, but the physiological relevance of these interactions still has to be determined (Magalhaes et al., 2012). They regulate sorting of a selected subset of GPCRs after homologous desensitization and contribute to the remarkable diversity necessary for the regulation of receptor signaling in multicellular organisms. It was shown for the δ-opioid receptor (δ-OR) to bind to the receptor C-terminus and preferentially targeting the receptor to lysosomes for proteolytic degradation (Whistler et al., 2002).

Homer proteins function primarily as scaffolds in the post-synaptic density in neurons by forming tetrameric structures (Hayashi et al., 2006), are implicated in the regulation of actin filament dynamics, and have also been shown to interact with several GPCRs, other signaling and scaffolding proteins, and ion channels. They also promote dimerization of receptors, regulate trafficking from the ER to the plasma membrane, and promote or inhibit activation of receptors (Fagni et al., 2002).

14-3-3 proteins are a family of proteins which are widely expressed throughout the brain and interact with a multitude of signaling proteins, as well as GPCRs. They assemble as dimers and bind to phosphorylated serine/threonine residues, where they modulate signal transduction by regulating in particular the localization of RGS proteins, cytoskeletal proteins, and also dimerization of receptors (Luttrell, 2008).

Calmodulin is a $Ca^{2+}$-binding protein and was shown to interact with several GPCRs. It was shown to reduce constitutive and agonist-stimulated G protein coupling, antagonize PKC binding, stabilize GPCR-β-arrestin complexes, or prevent receptor phosphorylation. Thus, it affects G protein-dependent and -independent signaling and trafficking of the receptors (Magalhaes et al., 2012).

The aforementioned protein-protein interactions and possibilities of GPCR modifications imply that the impact of GPCR activation extends the classical canonical GPCR-G protein-effector signaling model. GPCR-mediated activation of the MAPK pathway, for instance, involves the activation of Gβγ subunits, Src family non-receptor tyrosine kinases, and small G protein Ras, which intermediates signaling by receptor tyrosine kinase (RTK) growth factor receptors (van Biesen et al., 1995; Luttrell et al., 1996). The assembly of GPCRs and RTKs in a multireceptor complex and

transactivation of both could be shown for the $\beta_2$AR and epidermal growth factor receptor (EGFR) (Maudsley et al., 2000). Involvement of the a disintegrin and metalloproteinase (ADAM) family of matrix metalloproteases, which are activated upon GPCR-ligand interaction and process epidermal growth factor (EGF) by cleaving its precursor molecule, adds further complexity in understanding the regulation of cross-talk between these signaling pathways (Prenzel et al., 1999).

#### *2.2.3.4 Regulation of G protein activity*

Intrinsic GTP-turnover rates of Gα subunits vary to a significant extent and are also modulated by protein-protein interactions that increase GTPase activity. This GTPase activating protein (GAP) activity can be exerted by the effector of the GTP-bound Gα subunit itself or by a large family of RGS proteins, that bind to and stabilize the G protein in a conformational transition state for GTP hydrolysis (Ross and Wilkie, 2000). 20 distinct genes for RGS proteins were identified in mammals, some producing different protein isoforms in consequence of alternative splicing, which are grouped into four subfamilies based on sequence homology (R4/B, RZ/A, R7/C and R12/D). Beyond their role as GTPase activating proteins for activated Gα subunits, they contain a variety of domains that allow for complex tasks. Based on the composition of their domains, RGS proteins can interact with GPCRs, Gβγ subunits, inactive $G\alpha_i$ subunits, thereby preventing their activation, ACs, GIRK channels, PDEs, PLCβ, $Ca^{2+}$-channels, 14-3-3 proteins, or calmodulin, thereby capable of modulating the functional properties of their interactors, acting as scaffolding proteins, and being regulated by a complex web of intracellular factors (Abramow-Newerly et al., 2006).

Ultimately, GPCRs, G proteins, and effectors are organized in multi-protein complexes, referred to as signalosomes, which modulate the response to receptor activation and downstream signaling. These protein-protein interactions influence ligand binding, coupling of G proteins and effectors, trafficking to distinct subcellular compartments, dimerization of GPCRs, and involve the actions of scaffolding proteins. Protein-protein interactions that were described in particular for CB1 are summarized in the following sections.

## 2.3 The cannabinoid receptor type 1

CB1 is a member of the rhodopsin receptors, which constitute the largest group of GPCRs. It is classified into subfamily A13 (A corresponds to the rhodopsin receptor-like family), based on phylogenetic analyses, together with CB2, the adrenocorticotropic hormone receptor, sphingosine-1-phosphate receptors 1 - 8, melanocortin receptor 1 and 3 - 5, and G-protein coupled receptor 3, 6, and 12 (Joost and Methner, 2002). It is classically considered to be located in neurons and to act predominantly in the presynaptic compartment, thereby decreasing neurotransmitter release after being activated by endocannabinoids, which are produced at the postsynaptic site (Castillo et al., 2012). The first cannabinoid agonist-stimulated CB1-mediated response discovered was the inhibition of AC and subsequently PKA, which could be blocked by PTX, and therefore indicating that it was mediated by G proteins of the $G\alpha_{i/o}$ family (Howlett et al., 1986). Later, co-expression of AC isoforms 1, 3, 5, 6 and 8 were shown to result in CB1-mediated inhibition, indicating that these isoforms are regulated by the activated $G\alpha_{i/o}$ proteins (Rhee et al., 1998). The discovery of inhibition of AC was followed by uncovering the PTX-sensitive inhibition of N-type VGCCs and activation of GIRKs (Mackie and Hille, 1992; Henry and Chavkin, 1995; Guo and Ikeda, 2004), and functional coupling to the MAPK cascade (Bouaboula et al., 1995).

Nonetheless, besides its actions in the presynaptic compartment of neurons, where CB1 represents a pivotal point in the mechanism of feedback inhibition of synaptic activity, it has to be pointed out that other populations of CB1 were identified.

Compartment-selective actions of CB1 in polarized cells were shown, in which the receptor stably accumulates in the axonal plasma membrane after going through cycles of endocytosis and recycling in the somatodendritic compartment, involving specific intracellular pathways before being delivered to axons, and thus, indicating a somatodendritic or postsynaptic fraction of CB1 (Leterrier et al., 2006). Whereas a CB1-dependent strong decrease of PKA activity can be observed in the nerve terminals, somatodendritic CB1 is constitutively activated by locally produced 2-AG, thereby constitutively inhibiting the cAMP/PKA pathway and eventually leading to its relocation to the axonal compartment (Ladarre et al., 2014). In hippocamapal neurons, somatodendritic CB1 plays a role in the modulation of the neural actomyosin cytoskeleton by inducing rapid neuronal remodeling, such as retraction of neurites and axonal growth cones, elevated neuronal rigidity, and reshaping of somatodendritic morphology (Roland et al., 2014).

CB1 is also present in mitochondrial membranes of neurons, where it controls cellular respiration and energy production by decreasing the cAMP concentration, and consequently protein kinase A activity and respiratory electron transport chain complex I enzymatic activity. Furthermore, it was shown to regulate short-term synaptic plasticity and directly contributing to DSI in the mouse hippocampus (Benard et al., 2012; Fisar et al., 2014; Hebert-Chatelain et al., 2014).

Besides its fundamental roles in neurons, CB1 is expressed as well in astrocytes, where it gets activated upon release of endocannabinoids released by surrounding neurons in consequence of their depolarization. In the hippocampus, activation of astrocytic CB1 leads to a PLC-mediated increase in astrocytic $Ca^{2+}$ levels, which indirectly potentiate synaptic transmission in relatively more distant neurons in contrast to the role of CB1 in direct synaptic depression. Thus, astrocytes serve as a bridge for non-synaptic interneuronal communication, which is mediated by CB1 (Navarrete and Araque, 2008; Navarrete and Araque, 2010).

### 2.3.1 Multiple active conformations of CB1

Upon binding of distinct and sometimes structurally diverse agonists, CB1 mediates disparate behavioral effects suggesting fundamental differences in the mechanisms of action. Eventually, CB1 was shown to adopt different active conformations depending on binding of two structurally different agonists, CP55,940 (CP) and WIN55,212-2 (WIN), consistent with the concept of multiple active conformational states of GPCRs (Georgieva et al., 2008). Furthermore, WIN treatment of CB1-transfected HEK293 cells, as well as cultured hippocampal neurons, can induce ligand-specific coupling of CB1 to $G\alpha_{q/11}$ instead of $G\alpha_{i/o}$, thus leading to a PLC-dependent increase in inositol trisphosphate ($IP_3$), DAG and release of intracellular $Ca^{2+}$ stores. The release of $Ca^{2+}$ with concomitant synthesis of DAG in turn may activate PKC, which phosphorylates other effectors, eventually leading to altered cellular activity. This effect occurs depending on high receptor occupancy or an increase in the ratio of available $G\alpha_{q/11}$ as compared to $G\alpha_{i/o}$, which was shown by pretreatment of the cells with PTX (Lauckner et al., 2005).

Likewise, opposing actions of the agonists CP and HU-210 on the regulation of tyrosine hydroxylase (TH) transcription in neuroblastoma N1E-115 cells were observed. Transcription of TH is regulated by activator protein 1 (AP-1) and cAMP response element (CRE) binding sites in the TH gene promoter region. Upon cAMP/PKA-mediated phosphorylation, the cAMP response element-binding protein (CREB) serves as the major transcription factor inducing the transcription of TH. HU-210 treatment leads to a decrease in TH expression, with PKC signaling constituting the

principal pathway and PKA activity amplifying the response. CP treatment, on the other hand, leads to an increase in TH expression. This effect can be inhibited by pharmacologically blocking PKC, which leads to a switch in the response, and eventually a decrease of TH mRNA in the cells. Both effects are strictly dependent on $G\alpha_{i/o}$ activity and on the basal levels of cAMP, since an artificial increase of cAMP levels by a stimulation of AC with forskolin leads to a decrease in TH mRNA levels upon stimulation with either agonists. The dependency on the basal level of cAMP suggests that any concomitant stimulus that modulates cellular cAMP levels, for instance through activation of other GPCRs, could influence the modulating effects of CB1 ligand binding, thus adding further complexity to specific actions of a given GPCR (Bosier et al., 2009). These findings support the principle of multiple active conformations of CB1 and how distinct agonists differentially influence intracellular signalling cascades.

### 2.3.2 CB1 heterodimerization and oligomerization

The ability of a ligand acting at a specific receptor to induce a range of signaling events also depends on oligomerization or dimerization of GPCRs. Whereas activation of CB1 or the dopamine D2 receptor (D2) per se leads to a decrease of cAMP levels as a result of AC inhibition, it was shown that co-stimulation of both leads to an increase in cAMP levels. A switch from $G\alpha_{i/o}$ to $G\alpha_s$ was also observed in CB1 agonist-stimulated chinese hamster ovary (CHO) cells after PTX treatment, indicating that blocking one type of G protein can lead to a change in G protein coupling preference (Glass and Felder, 1997). Ultimately, co-activation of CB1 and D2 in co-transfected HEK293 cells leads to a physical interaction of both GPCRs with the consequence of a differential preference for signaling through $G\alpha_s$ instead of the expected $G\alpha_{i/o}$ proteins and PTX-insensitive ERK phosphorylation (Kearn et al., 2005).

In the basal ganglia the interaction of CB1 and adenosine $A_{2A}$ receptor ($A_{2A}$) strongly influences basic synaptic functions with $A_{2A}$ exerting complex permissive or inhibitory influence on CB1-mediated synaptic effects, with additional modulatory inputs by interacting with D2 or mGluRs (Tebano et al., 2012). A direct physical interaction was shown in striatal indirect pathway medium spiny neurons (MSNs), but not corticostriatal projections, which leads to a switch in preferential G protein coupling from $G\alpha_i$ or $G\alpha_s$ to $G\alpha_q$. Furthermore, a loss in this receptor heterodimerization occurs in late stages of Huntington's disease, eventually proving a role in in motor function and neurodegenerative diseases (Moreno et al., 2016).

Using fluorescent complementation techniques, CB1-D2-$A_{2A}$ heterotrimers were identified in transfected HEK293 cells, suggesting a possible formation of a part of a molecular network, which depends on the co-expression and -distribution of the respective GPCRs. The presence of all these receptors in the plasma membrane of striatal neurons indicates a possible interplay and reciprocal regulation of associated signaling pathways depending on the receptors present, their degree of activation and coexpressed G proteins and other interacting proteins *in vivo* (Navarro et al., 2008).

Heteromerization of CB1 with the 5-$HT_{2A}$ receptor (5-$HT_{2A}$) occurs brain region-specifically in the hippocampus, striatum, and cortex and mediates some specific behavioral effects of THC, such as amnesia, anxiolytic-like effects, and social interaction. In 5-$HT_{2A}$-knockout mice, these effects are abolished, whereas hypolocomotion, hypothermia, anxiety, and antinociception are not. On the biochemical level, antagonist treatment of one of the receptors blocks signaling of the other receptor, and heterodimerization leads to a switch in preferential G-protein coupling for 5-$HT_{2A}$ from $G\alpha_q$ to $G\alpha_i$ (Vinals et al., 2015).

In HEK293 cells, a physical and functional interaction between CB1 and $\beta_2$AR decreases the constitutive activity and increases the cell surface trafficking of CB1. The signaling properties are altered, resulting in $G\alpha_{i/o}$-dependent phosphorylation of ERK and decreased $G\alpha_{i/o}$-independent phosphorylation of the transcription factor CREB, which is likely to occur via $G\alpha_s$ (Hudson et al., 2010).

CB1 and the μ-opioid receptor (μ-OR) co-localize in neuronal cells and activity of μ-OR is attenuated by CB1 agonist treatment and vice versa. Co-activation of both receptors leads to an attenuated phosphorylation of downstream Src tyrosine kinase as compared to the activation of the individual receptors and decreased neuritogenesis, but without changes in the subcellular localization of the receptors (Ellis et al., 2006; Rios et al., 2006).

Heterodimerization of CB1 with the δ-OR in rodent neurons affects localization of the receptors, increases CB1-mediated ERK signaling, initiates recruitment of β-arrestin2, and finally activates signaling pathways that lead to decreased apoptosis and enhanced cell survival upon CB1 agonist-binding (Rozenfeld et al., 2012).

CB1 and the orexin receptor type 1 ($Ox_1R$) form heteromers, and co-expression in HEK293 cells leads to spontaneous internalization of both receptors. Treatment with an antagonist specific for either receptor was shown to induce re-localization of both receptors to the cell surface and concurrent decreased potency of the other receptor to phosphorylate ERK. Whereas CB1 recycles constitutively, $Ox_1R$ is predominantly maintained at the cell surface until it gets stimulated. In the

presence of CB1, $Ox_1R$ adopts the dominant recycling phenotype of CB1, thereby demonstrating another mechanism of GPCR interaction and how a range of ligands may modulate GPCRs to which they have been considered to have no affinity (Ellis et al., 2006).

### 2.3.3 CB1 signaling pathways and uncovered protein interactions

A number of CB1-interacting proteins that regulate its signaling properties were discovered and underpin the concept of this GPCR to exist in, and signal through, a complex of macromolecules, a CB1 signalosome.

CB1 desensitization and down-regulation is enhanced by the actions of GRK2 and GRK3, which phosphorylate CB1 at the C-terminus, and β-arrestin2 in *Xenopus* oocytes and hippocampal neurons (Jin et al., 1999; Kouznetsova et al., 2002). Agonist treatment of CB1 can lead to degradation after endocytosis, whereby GASP1 was shown to play a major role in the process of sorting and targeting of CB1 to lysosomes in HEK293 cells, as well as primary striatal cultures (Martini et al., 2007). While β-arrestin2 is suggested to be more critical for receptor internalization, β-arrestin1 is more likely to be involved in $G\alpha_{i/o}$-independent activation of downstream effectors, thus inducing the formation of a β-arrestin signalosome (Ahn et al., 2013). In a β-arrestin signaling-biased CB1 mutant expressed in HEK293 cells, activation of CB1 has led to recruitment of β-arrestin1 and subsequent phosphorylation of 43 different kinases, including ERK and CREB, and validation of previously described pathways, in which the involvement of β-arrestins was unknown. Furthermore, phosphorylation by GRK4, GRK5 and GRK6 controls β-arrestin-mediated signaling, whereas GRK3 is suggested to play a key role in CB1 internalization (Delgado-Peraza et al., 2016).

By introducing a knockin mutation of a highly conserved aspartate in TM2 of CB1 to asparagine in AtT20 cells, it was shown that this aspartate residue is necessary for the coupling to GIRKs and for the internalization for the receptor. However, agonist binding affinity, coupling to VGCCs and inhibition of forskolin-induced cAMP production was not affected and activation of the MAPK cascade still functional. Although the exact mechanism of how the loss of coupling to specific effectors is not clear, the most likely explanation may be a change in receptor localization with respect to certain effectors (Roche et al., 1999).

Depending on the cell culture system and experimental conditions, CB1 also regulates the utilization of glucose in the cell by inducing the activation of protein kinase B (PKB/Akt) via Gβγ-activated phosphoinositide 3 kinase (PI3K). PKB consequently phosphorylates and inhibits

glycogen synthase kinase 3 (GSK3), which is directly involved in glycogenesis (Gomez del Pulgar et al., 2000). Acute administration of THC increases the CB1-mediated phosphorylation of PKB in mouse hippocampus, striatum and cerebellum, thereby activating the PI3K/PKB pathway and negatively regulating GSK3β, thus showing cannabinoid-induced activation of survival signaling pathways and demonstrating a neuroprotective role for THC *in vivo* (Ozaita et al., 2007). GABAergic CB1 activation with THC has furthermore been shown to transiently modulate the important downstream effector of PI3K/PKB, the mammalian target of rapamycin (mTOR) pathway and associated protein synthesis machinery in the hippocampus, which eventually leads to THC-induced amnesia (Puighermanal et al., 2009).

Another mechanism explaining THC-mediated memory impairment could be pinned down to a small subpopulation of somatodendritic CB1 on superficial pyramidal cells in the CA1 region of the hippocampus. These are mediating an impairment of LTP and spatial memory formation by a modulation of somatic and distal dendritic h-currents ($I_h$), which are a key regulator of dendritic excitability. Although somatodendritic CB1 shows a higher constitutive activity, due to locally produced 2-AG, it can still induce signaling cascades upon activation. The underlying mechanism involves activation of the MAPK signaling cascade, leading to the activation of c-Jun N-terminal kinase (JNK), which in turn activates nitric oxide synthase (NOS). The increase in nitric oxide activates guanylyl cyclase (GC) and thus, increases cyclic guanosine monophosphate (cGMP) levels. The interaction of cGMP and hyperpolarization-activated cyclic nucleotide-gated (HCN) channels causes the causes the depolarizing shift in $I_h$ activation in this small subset of pyramidal cells, which is sufficient to induce the actions of cannabinoids on LTP and spatial memory formation (Maroso et al., 2016).

CB1 activation leads to inhibition of AC and PKA, which is the fundamental molecular mechanism underlying long term synaptic changes. In addition, eCB-LTD in the hippocampus depends on the actions of the active zone protein RIM1α, which gets directly or indirectly phosphorylated via PKA and acts as a scaffolding protein regulating neurotransmitter release (Chevaleyre et al., 2007). Furthermore, induction of eCB-LTD in inhibitory synapses and reversal learning specifically requires the interaction of RIM1α with the synaptic vesicle protein Rab3B which is a RIM1α effector in a GTP-dependent manner (Tsetsenis et al., 2011).

Cannabinoid receptor interacting protein 1a (Crip1a) binds to the distal C-terminal tail of CB1 and was initially shown to functionally interact by suppressing CB1-mediated tonic inhibition of VGCCs. It furthermore contains a PDZ class I ligand at its C-terminus, which could potentially interact with other PDZ domain-containing proteins, thus acting as a scaffolding protein (Niehaus et al., 2007).

Co-expression of CB1 and Crip1a in HEK293 cells decreased CB1-mediated G protein activation, and Crip1a inhibits constitutive and agonist-stimulated CB1 activity in cultured autaptic hippocampal neurons (Smith et al., 2015). Furthermore, Crip1a overexpression in N18TG2 cells reduced basal ERK phosphorylation levels, whereas a depletion augmented basal phosphorylated ERK levels. Stimulation of ERK phosphorylation by CB1 agonists was unaltered in Crip1a overexpressing clones as compared to wildtype controls. Reduction in Crip1a protein levels increased coupling of CB1 to $G\alpha_{i3}$ and $G\alpha_{o}$, suggesting a role for endogenous Crip1a to promote coupling of CB1 to $G\alpha_{i1}$ and $G\alpha_{i2}$, thereby demonstrating a mechanism for a fine-tuning of CB1 function by accessory proteins (Blume et al., 2015). In another study, Crip1a was shown to co-localize with CB1 in presynaptic terminals of glutamatergic neurons and GABAergic interneurons in the hippocampus, and enhance cannabinoid-induced G protein signaling *in vivo* (Guggenhuber et al., 2016), which taken together indicates how the signaling properties of a receptor-protein complex can vary depending on the composition of the signalosome and subcellular environment.

In a yeast two-hybrid system approach, 14-3-3β was identified as another interactor of CB1 and confirmed by affinity-binding assays. 14-3-3β mediates the effect of cannabinoids on cell cycle progression by integrating and binding further proteins and inducing a significant cell cycle delay at the $G_2$/M phase, a mechanism which may account for cannabinoid effects on tumor cell growth (Jung et al., 2014).

A pull-down of overexpressed green fluorescent protein (GFP)-tagged CB1 in mouse cortex and subsequent proteomics leads to the identification of CB1-interacting members of the Wiskott-Aldrich syndrome protein-family verprolin-homologous protein 1 (WAVE1) complex, Nck-associated protein 1 (NCKAP1), cytoplasmic FMR1-interacting protein 2 (CYFP2), Ras-related C3 botulinum toxin substrate 1 (Rac1) and Abl interactor 2 (ABI2). This protein complex mediates the actions of cannabinoids on the actin cytoskeleton in growth cones of cortical neurons by directly acting on actin polymerization and stability in developing neurons as well as mature neurons (Njoo et al., 2015).

While coupling to the MAPK cascade was initially thought to be mediated by Gβγ subunits, later a Gβγ-independent mechanism was uncovered, involving the actions of Src family non-receptor tyrosine kinase Fyn with a possible involvement of PKA activity in the hippocampus (Derkinderen et al., 2003). In N18TG2 neuroblastoma cells, the time course of CB1-mediated ERK activation was investigated. A first phase of maximal ERK phosphorylation was mediated by CB1 receptor-stimulated ligand-independent transactivation of multiple RTKs, which involved the actions of Gβγ-stimulated PI3K activation and Src kinase activation, and is modulated by inhibition of PKA. This

was followed by a second phase of a rapid decline in ERK phosphorylation, involving PKA inhibition and PP2A activation. Eventually, a plateau of ERK phosphorylation is reached in a third phase, again mediated by transactivation of multiple RTKs (Dalton and Howlett, 2012).

Cross-talk between CB1 and the brain-derived neurotropic factor (BDNF)-specific receptor TrkB was suggested to play an important role in neuronal migration and differentiation. Both are expressed on terminal axon segments of developing cholecystokinin-positive (CCK+) GABAergic interneurons, which show CB1-dependent AEA-induced chemotaxis, which is dependent on CB1 transactivation of TrkB. CB1-TrkB receptor complex formation and phosphorylation of TrkB could be shown for AEA-treated pheochromocytoma (PC12) cells with a probable involvement of Src kinases (Berghuis et al., 2005).

### 2.3.4 Cell type-specific CB1 signaling

Another striking feature of CB1 is the cell type-specific signaling. In the hippocampus, CB1 is expressed in glutamatergic principal and GABAergic interneurons, which exert antagonizing effects on the overall neuronal circuitry output (Lutz et al., 2015). Despite the fact that in the hippocampus CB1 density is remarkably higher in GABAergic interneurons than in glutamatergic neurons, studies using conditional CB1-KO mice have shown that coupling to G protein signaling is several fold stronger in glutamatergic neurons as compared to GABAergic interneurons (Steindel et al., 2013). The more efficient coupling of CB1 to G proteins in glutamatergic neurons is in accordance with glutamatergic CB1 being engaged in the majority of CB1-mediated physiological effects and further supported by behavioral studies, which have shown that low doses of cannabinoids activate glutamatergic CB1, whereas high doses are necessary to activate CB1 on GABAergic terminals (Rey et al., 2012). Moreover, electrophysiological measurements have shown that in the lateral amygdala cannabinoid actions on glutamatergic synaptic transmission override those on GABAergic synaptic transmission (Azad et al., 2003) and CB1 in glutamatergic neurons exerts a low constitutive activity (Roberto et al., 2010), which is pronouncedly higher in GABAergic interneurons (Slanina and Schweitzer, 2005).

Despite coupling preferentially to G proteins of the $G\alpha_{i/o}$ family, CB1 signaling exceeds the classical view on GPCR signaling, which was initially described as receptors being simple on and off switches. CB1 can couple with distinct G proteins and shows a great versatility in inducing various signaling cascades, which requires various conformational active states and distinct agonists

inducing different responses (Fig. 2.5). In addition, interacting proteins and the cellular environment play important regulatory roles (Bosier et al., 2010).

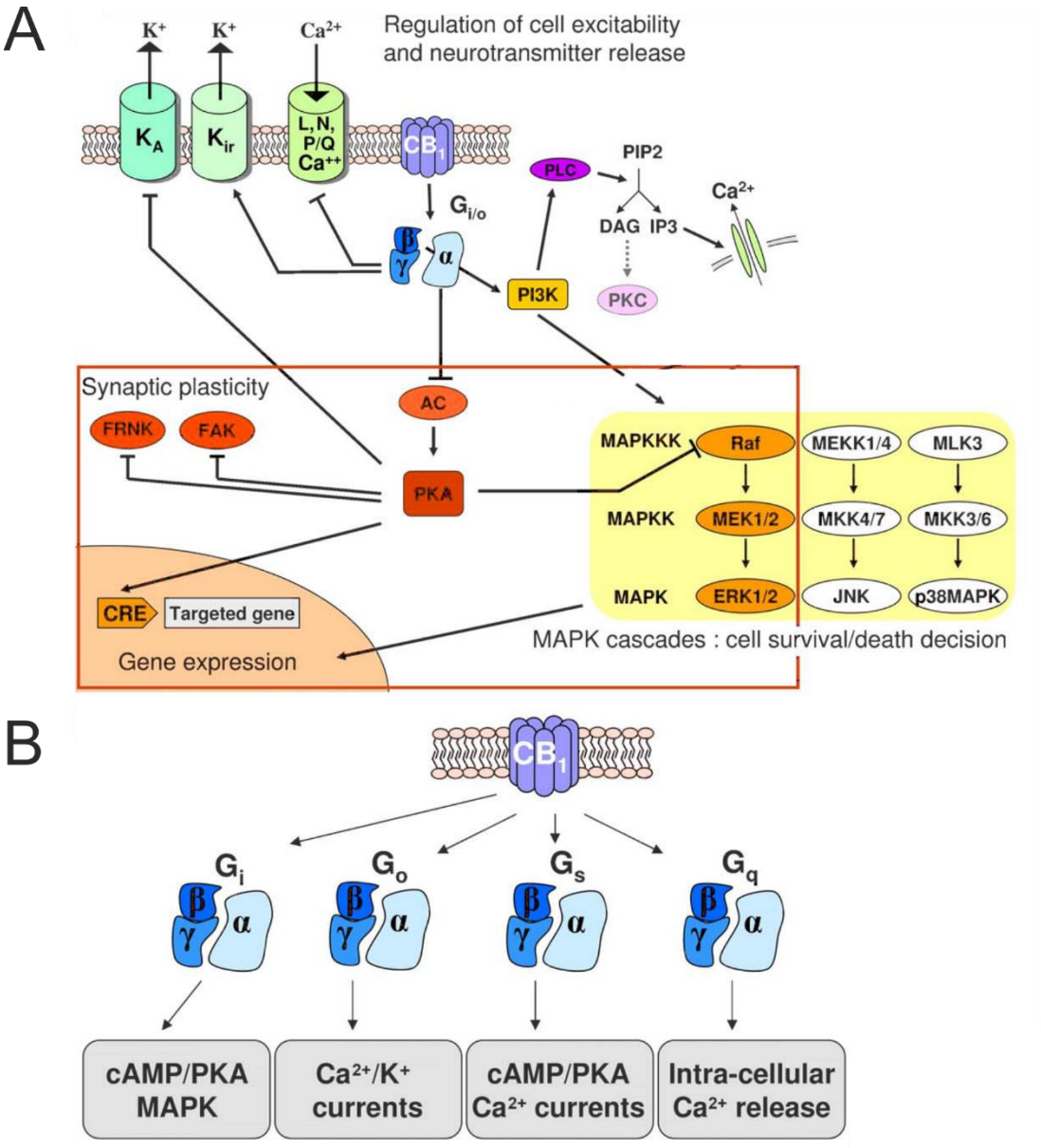


**Fig. 2.5 CB1 signaling cascades**

**A**: CB1 couples preferentially to $G\alpha_{i/o}$ proteins. Upon activation, it positively regulates the activity of inwardly rectifying $K^+$ channels and negatively regulates the activity of voltage-gated $Ca^{2+}$ channels, and thus cell excitability and neurotransmitter release. Activation of $G\alpha_{i/o}$ leads to inhibition of AC and increases intracellular $Ca^{2+}$ via a Gβγ-mediated activation of PLC. The reduction of PKA activity subsequently leads to activation of voltage-gated $K^+$ channels, changes in gene expression through a decrease in CRE activity, and a decrease in constitutive inhibitory phosphorylation of Raf, and therefore activation of the MAPK pathway. **B**: CB1 has been shown to be capable of activating $G\alpha_s$ and $G\alpha_q$ proteins, and subsequently inducing other downstream signaling pathways, which contributes to the diversity of responses induced by cannabinoids (modified from Bosier et al., 2010).

## 2.4 Aim of the thesis

The involvement of the ECS in a plethora of physiological functions and behavioral manifestations is well studied and certain ECS-mediated effects could be assigned to CB1 populations on specific neuronal subtypes. But our understanding of the impact of this system regulating important parameters on a macroscopic scale still faces a substantial lack of insights into the highly complex intracellular signaling at the molecular level. In the hippocampus, CB1 differentially modulates glutamatergic and GABAergic neurotransmission, two neurotransmitter systems with opposing functions. A number of CB1-interacting proteins, which could set the foundation for differences in signaling properties of distinct subsets of CB1, were described using different methodological approaches, but the majority of proteins assembling with CB1 in a multiprotein complex are most likely still unknown.

The present study aimed at revealing differences between hippocampal CB1 protein complex compositions in synaptosomes from glutamatergic neurons versus GABAergic interneurons. GPCR function and its signaling properties are dependent on the cellular environment and the cellular proteome. Furthermore, GPCR conformation mutually affects binding of interacting proteins. Therefore, a combination of conditionally Cre recombinase-expressing mouse lines, adeno-associated viral vectors for transgene expression, and tandem affinity purification is intended to eventually obtain a model system as close as possible to the *in vivo* situation in order to reveal CB1 protein interactions that are more likely of significance in the physiological context of the organism.

# 3 Materials and methods

## 3.1 Molecular biology

### 3.1.1 DNA constructs

All deoxyribonucleic acid (DNA) constructs in this study, used for the expression of proteins via transfection of cells or in order to produce AAV vectors, are based on pAM AAV expression cassette plasmids. pAM vectors contain a CAG promoter (CMV early enhancer element, promoter, first exon and the first intron of the chicken beta-actin gene and the splice acceptor of the rabbit beta-globin gene), woodchuck hepatitis virus posttranscriptional regulatory element (WPRE), AAV2 inverted terminal repeats (ITRs) and a bovine growth hormone polyadenylation signal (bGHpA).

Transfection of HEK293 cells was performed using pAM/CAG-N-SF-CB1-WPRE-bGHpA (pAM-N-SF-CB1) and pAM/CAG-CB1-SF-C-WPRE-bGHpA (pAM-CB1-SF-C) plasmids (kindly provided by Katharina Kukla from our lab). For the generation of AAVs used for the Cre recombinase (Cre)-mediated cell type-specific expression of StrepII/FLAG (SF)-tagged CB1, which was performed in the diploma thesis of Katharina Kukla in our lab, N-terminal SF-tag (N-SF) and C-terminal SF-tag (SF-C) (Gloeckner et al., 2007) coding sequences (CDSs) were synthesized into pCR2.1 vector backbones by Eurofins Genomics, Ebersberg (Germany), taking into account the codon usage of *Mus musculus*.

In a first step in order to obtain an AAV expression vector including the N-terminal SF-tagged CB1 (N-SF-CB1), N-SF was cut out of the pCR2.1 plasmid, using the restriction enzyme AgeI and subcloned in frame into a linearized pcDNA3 plasmid (Invitrogen, Carlsbad, USA) containing the CB1 CDS, obtained by our lab. The insertion of N-SF at the AgeI insertion site occurred 129 bp downstream of the 5′ end of the CB1 CDS to prevent disturbances in membrane localization and trafficking of the expressed fusion protein. Additionally, the open reading frame (ORF) of this vector contained sequentially a preprolactin signal sequence for ER trafficking and human influenza hemagglutinin (HA)-tag upstream the N-SF-CB1 CDS. In a second step, a PacI restriction site was added at the 5′ end of the preprolactin-HA-N-SF-CB1 ORF by polymerase chain reaction (PCR), and the amplificates eventually subcloned into a pAM vector containing a 340 bp transcriptional stop cassette composed of a herpes simplex virus thymidin kinase pA signal sequence and a pA terminator from pGL3 (Promega, Madison, USA) flanked by loxP sites

(Guggenhuber et al., 2010) to obtain a pAM/CAG-Stop-N-SF-CB1-WPRE-bGHpA (pAM-Stop-N-SF-CB1) (Fig. 3.1A).

For the generation of the AAV expression vector including the C-terminal SF-tagged CB1 (CB1-SF-C), the SF-C sequence in the pCR2.1 vector was amplified in a PCR, adding sequential BamHI and AgeI restriction sites at the 5' end of the CDS (FWD: 5'-CTC AGG ATC CAC CGG TCT CCG CTT GGA GCC ACC-3'; REV: 5'-GGA TGA CGA CGA TAA GTG AGC GGC CGC ATA TAA G-3'). The amplificates were then subcloned in frame into a CB1 CDS containing pcDNA3 expression plasmid at the 3' end of the CB1 ORF using AgeI and NotI insertion sites. For the generation of the AAV expression plasmid, the CB1-SF-C CDS was amplified in a PCR adding a PacI restriction site at the 5' end and an EcoRI restriction site at the 3' end, and finally subcloned into a linearized pAM AAV plasmid containing a floxed stop cassette, as described above, to generate a pAM/CAG-Stop-CB1-SF-C-WPRE-bGHpA (pAM-Stop-CB1-SF-C) (Fig. 3.1B).

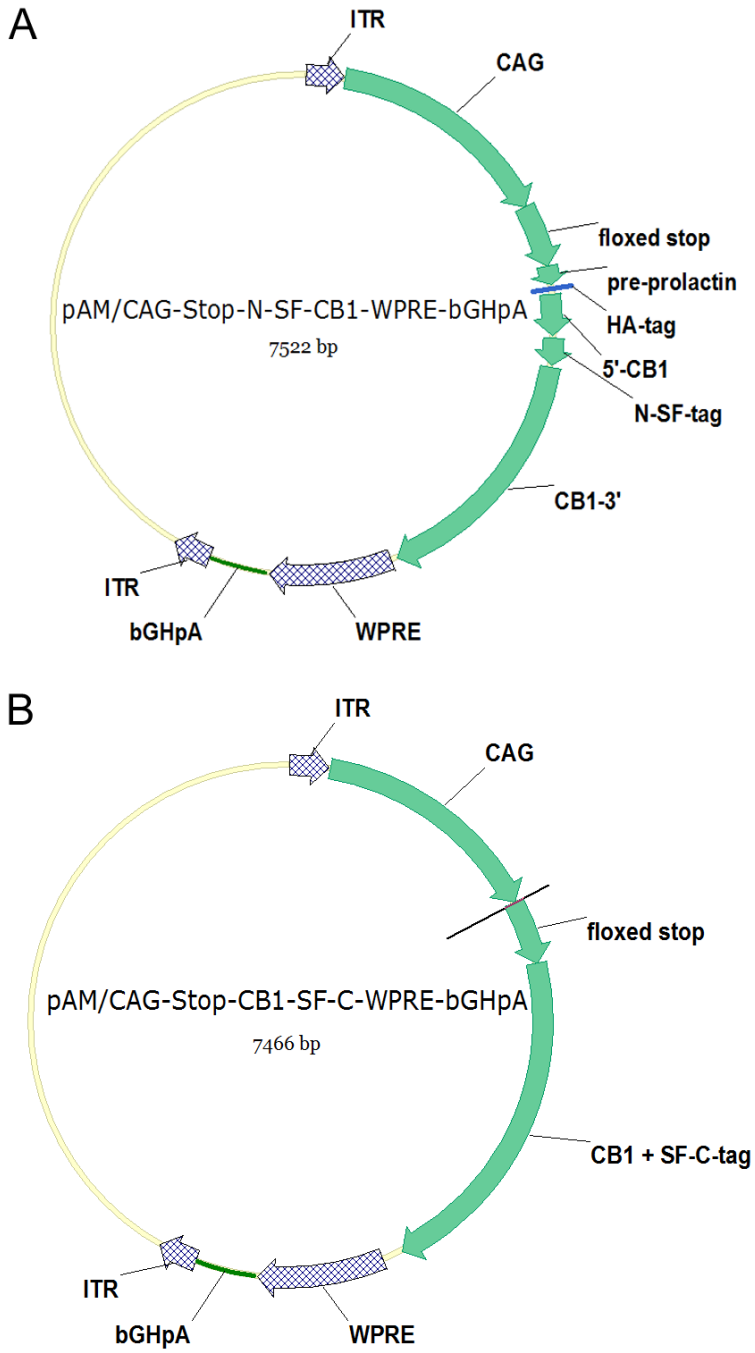


**Fig. 3.1 Plasmid maps of pAM/CAG-Stop-N-SF-CB1-WPRE-bGHpA and pAM/CAG-Stop-CB1-SF-C-WPRE-bGHpA**

pAM AAV expression plasmids used for the expression of SF-tagged CB1 (previous work of Katharina Kukla for her diploma thesis in our lab). **A**: pAM/CAG-Stop-N-SF-CB1-WPRE-bGHpA (pAM-Stop-N-SF-CB1), used for the expression of N-terminally SF-tagged CB1, contains an additional pre-prolactin sequence for targeting the translated protein to the ER and an additional HA-tag. The SF-tag sequence was inserted 66 amino acids downstream the start of the CB1 ORF, in order not to interfere with potentially important localization sequences at the N-terminus. **B**: pAM/CAG-Stop-CB1-SF-C-WPRE-bGHpA (pAM-Stop-CB1-SF-C) used for the expression of C-terminally SF-tagged CB1. ITR: inverted terminal repeat. CAG: CAG promoter (CMV early enhancer element, promoter, first exon and the first intron of the chicken beta-actin gene and the splice acceptor of the rabbit beta-globin gene). WPRE: woodchuck hepatitis virus posttranscriptional regulatory element. bGHpA: bovine growth hormone polyadenylation signal.

Two AAV expression vectors for an expression of HA-tagged G proteins $G\alpha_o$ and $G\alpha_z$ were cloned by adding an EcoRI restriction site at the 5′ end and a HindIII restriction site at the 3′ end of the complementary DNAs (cDNAs) of $G\alpha_o$ and $G\alpha_z$ in a PCR amplification using KOD Hot Start DNA polymerase (EMC Chemicals, San Diego, USA), respectively ($G\alpha_o$ FWD: 5′-TTTT GAA TTC ATG GGA TGT ACG CTG AGC-3′; $G\alpha_o$ REV: 5′-TTTT AAG CTT TCA GTA CAA GCC GCA GCC-3′; $G\alpha_z$ FWD: 5′-TTTT GAA TTC ATG GGA TGT CGG CAA AGC TC-3′; $G\alpha_z$ REV: 5′-TTTT AAG CTT CTC GAG GTT TCA CCA CAG GCG AGC AG-3′). Whereas the cDNA of $G\alpha_o$ was amplified by using a $G\alpha_o$ cDNA-containing pCIS mammalian expression vector (kindly provided by Prof. Dr. Nina Wettschureck, Max-Planck-Institute for Heart and Lung Research, Bad Nauheim, Germany), the cDNA of $G\alpha_z$ was obtained by isolating total ribonucleic acid (RNA) from mouse cortex using the RNeasy Lipid Tissue Mini Kit (Qiagen, Hilden, Germany), followed by reverse transcription of mRNA with oligo d(T) primers using the SuperScript II Reverse Transcriptase (Invitrogen, Carlsbad, USA). The amplificates were finally subcloned into an EcoRI/HindIII-linearized pAM AAV plasmid containing an HA-tag, generated by our lab, to generate pAM/CAG-HA-G_alpha(z)-WPRE-bGHpA (pAM-HA-$G\alpha_z$) and pAM/CAG-HA-G_alpha(o)-WPRE-bGHpA (pAM-HA-$G\alpha_o$), respectively.

For the generation of riboprobes used for fluorescent *in situ* hybridization, the obtained $G\alpha_z$ cDNA with its additional EcoRI/HindIII restriction sites was used for directed cloning into a pBluescript II KS plasmid (pBSIIKS) containing promoters for T3 and T7 RNA polymerases.

### 3.1.2 Double fluorescent *in situ* hybridization

Single-stranded labeled RNA-riboprobes used for targeting and detecting CB1- and $G\alpha_z$-specific mRNAs in tissue slices, were obtained by using pBSIIKS vectors containing the cDNA sequences of CB1 and $G\alpha_z$, respectively. 5µg of linearized vector DNA were used for the transcription of a CB1 or $G\alpha_z$ riboprobe, using T3 RNA polymerase (Roche, Basel, Switzerland) for generating the antisense probe and T7 RNA polymerase (Roche, Basel, Switzerland) for generation of the sense probe. For the transcription step, fluorescin (FITC) was added for the labeling of the CB1 riboprobe (CB1-FITC) and digoxigenin (DIG) for labeling the $G\alpha_z$ riboprobe ($G\alpha_z$-DIG). After transcription of CB1-FITC and $G\alpha_z$-DIG, both underwent column-based purification using the RNeasy Mini Kit (Qiagen, Hilden, Germany).

Double fluorescent *in situ* hybridization targeted against CB1 and $G\alpha_z$ mRNA was performed on 20 µm cryosections of fresh frozen C57BL/6N mouse brain on SuperFrost Plus glass slides (Thermo Scientific, Waltham, USA). Slices were first fixed in 4% paraformaldehyde (PFA) at 0°C for 20 min

and afterwards the endogenous peroxidase enzyme activity inactivated with 1% $H_2O_2$ in methanol for 15 min at room temperature (RT). Permeabilization of the tissue by incubation with proteinase K (Roche, Basel, Switzerland) in 50 mM tris(hydroxymethyl)aminomethane (Tris)/5 mM ethylenediaminetetraacetic acid (EDTA) was followed by a postfixation step in 4% PFA at 0°C for 20 min and incubation in 0.1 M triethanolamine with acetic anhydride as an acetylation step in order to reduce non-specific binding of the negative probe to the positively charged glass slides and tissue. The slices then underwent dehydration by passing through successive concentrations of ethanol (30%, 50%, 70%, 80%, 95%, 100%), before incubation with 30 ng of CB1-FITC and $G\alpha_z$-DIG riboprobe, respectively, in 100 µl hybridization mix (20 mM Tris-HCl pH 8.0, 50% formamide, 0.3 M NaCl, 5 mM EDTA pH 8.0, 10% dextran sulphate (Sigma Aldrich, St. Louis, USA), 0.02% Ficoll 400, 0.02% polyvinylpyrrolidone, 0.02% bovine serum albumin (BSA), 0.5 mg/ml tRNA (Roche, Basel, Switzerland); 0.2 mg/ml carrier DNA acid cleaved; 200 mM dithiothreitol (DTT))/glass slide in a hybridization chamber prepared with chamberfluid (50% formamide, 2X saline-sodium citrate (SSC) (300 mM NaCl, 30 mM trisodium citrate, pH 7.4)) to keep slides moist in the oven at 54°C for 17h overnight. The next day, the glass slides were prepared for antibody administration by washing with decreasing concentrations of SSC buffer with or without 50% formamide at 62°C to decrease background signals by removing unspecific binding of riboprobes and a subsequent blocking step using 4% sheep serum (Sigma Aldrich, St. Louis, USA) in Tris-NaCl-Tween (TNT) buffer (0.05% Tween 20, 100 mM Tris pH 7.6, 150 mM NaCl) for 1 h at 30°C. After transferring the slides to shandon cassettes, peroxidase (POD)-coupled anti FITC antibody (Roche, Basel, Switzerland) [1:1000] was applied and slides incubated for 2 h at 30°C, followed by another incubation in TSA Fluorescein Tyramide signaling enhancer (Perkin Elmer, Waltham, USA) [1:50] for 15 min at 30°C. POD activity was then quenched by successive washing steps in 3% $H_2O_2$, before incubation with POD-coupled anti DIG antibody (Roche, Basel, Switzerland) [1:2000] at 4°C overnight. The next day, slides were incubated in TSA Cy3 Tyramide signaling enhancer (Perkin Elmer, Waltham, USA) [1:75] for 15 min at 30°C and eventually counterstained with the nuclear dye 4',6-diamidino-2-phenylindole (DAPI). Fluorescent signals were visualized using a Leica DM5500 fluorescence microscope (Leica microsystems, Wetzlar, Germany).

## 3.2 Cell culture

### 3.2.1 Maintenance of HEK293 cells

Human embryonic kidney (HEK293) cells were grown in 150 $cm^2$ flasks in Dulbecco's modified Eagle's medium (DMEM) (Gibco by life technologies, Carlsbad, USA), supplemented with 10% fetal bovine serum (FBS) (Gibco by life technologies, Carlsbad, USA) (growth medium), and maintained in a Heracell 150i $CO_2$ Incubator (Thermo Scientific, Waltham, USA) at 37°C and 5% $CO_2$. Cells were passaged twice a week in order to prevent high cell densities that lead to cell death by removing the growth medium, washing with phosphate-buffered saline (PBS) (Gibco by life technologies, Carlsbad, USA), and treatment with prewarmed trypsin-EDTA (Gibco by life technologies, Carlsbad, USA) to detach the adherent cells from the flask. The enzymatic reaction was stopped by adding prewarmed growth medium, followed by centrifugation for 5 min at 100 x g. Afterwards, the cell pellet was resuspended and the appropriate amount reseeded in a new flask or cell culture plates.

### 3.2.2 Transfection of HEK293 cells

Transient transfection of HEK293 cells was performed using calcium phosphate (CalPhos) precipitation (Chen and Okayama, 1987). 2 h before transfection, growth medium was discarded and replaced by Iscove's modified Dulbecco's medium (IMEM) (Gibco by life technologies, Carlsbad, USA), supplemented with 5% FBS (Gibco by life technologies, Carlsbad, USA) (transfection medium). For one 14 cm plate, 12.5 µg plasmid DNA was added to 2.4 ml sterile $H_2O$ (Gibco by life technologies, Carlsbad, USA) and 320 µl 2.5 M $CaCl_2$. After sterile filtration through 0.22 µm syringe sterile filters (Hartenstein, Würzburg, Germany), 2.6 ml HEBS buffer (50 mM HEPES, 28 mM NaCl, 1.5 mM $Na_2HPO_4$, pH 7.05) was added while vortexing and the solution left for 5 min until white precipitate was formed. The solution was then carefully dripped on the cells in transfection medium while gently swirling and put back in the incubator until 16 h later the transfection medium was removed and substituted again with growth medium. Another 24 h later, the cells were used for further experiments.

## 3.3 cAMP assay

A kinetic assay to investigate GPCR-induced cAMP turnover was performed using the cAMP-Glo Assay (Promega, Madison, USA), according to the manufacturer's protocol. Transfected or untransfected HEK293 cells were seeded in white, clear-bottom, poly-D-lysine-coated 96 well plates (Thermo Scientific, Waltham, USA) in growth medium at a number of 30,000 cells/well. The next day, cell-free cAMP standards of various concentrations and a cAMP-free negative control were prepared and added to empty wells in the 96 well plate before starting the treatment of the HEK293 cells. Growth medium was removed and cells treated with 20 µl of induction buffer (serum-free DMEM (Gibco by life technologies, Carlsbad, USA), 500 µM isobutyl-1-methylxanthine (IBMX) (Thermo Scientific, Waltham, USA), 100 µM 4-(3-butoxy-4-methoxy-benzyl)imidazolidone (Ro 20-1724) (Thermo Scientific, Waltham, USA)), containing 5 µM forskolin and additionally either 1 µM WIN, prediluted in dimethyl sulfoxide (DMSO), 1 µM WIN + 100 ng/ml PTX or vehicle (DMSO). In order to terminate the induction process, 20 µl of cAMP-Glo lysis buffer was added and the plate incubated on a plate shaker for 30 min at RT. Afterwards, 40 µl of cAMP detection solution was added to all wells and incubated on a plate shaker for 1 min and further 20 min without shaking at RT. Finally, 80 µl of Kinase-Glo reagent was added to all wells, mixed on a plate shaker for 1 min and incubated on the bench for 10 min at RT. Luminescence intensity was measured with the Fluostar Galaxy (BMG Labtech, Ortenberg, Germany).

## 3.4 Adeno-associated virus

### 3.4.1 Production of AAVs

AAV pseudotyped vectors were produced as described (Hauck et al., 2003), generating virions with a 1:1 ratio of AAV1 and AAV2 capsid proteins with AAV2 ITRs. Briefly, HEK293 cells were transfected using the CalPhos precipitation method as described (3.2.2) with the pAM AAV expression *cis* plasmid, the AAV1 (pH21) and AAV2 (pRV1) helper plasmids and the adenovirus helper plasmid (pFΔ6). 48 h after transfection, the cells were harvested, underwent benzonase endonuclease (Sigma Aldrich, St. Louis, USA) digestion and were afterwards frozen at -20°C. After thawing, the vector was then purified using heparin affinity columns (Sigma Aldrich, St. Louis, USA) and concentrated using Amicon Ultra-4 columns (Merck Millipore, Billerica, USA). Vector packaging and

purity was assessed on a Coomassie gel and the genomic titer evaluated by quantitative PCR (qPCR) using the ABI 7700 real time PCR cycler (Applied Biosystems, Foster City, USA) with primers designed to bind the AAV WPRE (WPRE FWD: 5'-GGC TGT TGG GCA CTG ACA AT-3'; WPRE REV: 5'-CCG AAG GGA CGT AGC AGA AG-3').

### 3.4.2 AAV delivery

AAVs were delivered to anaesthetized adult mice of at least 8 weeks, bilaterally into the dorsal (-3.1 mm anteroposterior (AP), -3.0 mm mediolateral (ML), -3.5 mm dorsoventral (DV) from bregma) and ventral (-2.0 mm AP, -2.0 mm ML, -2.0 mm DV from bregma) hippocampus after fixing the mice in a stereotaxic frame (Kopf Instruments, Tujunga, USA) on heating pads dynamically regulated by the ATC2000 animal temperature controller (World Precision Instruments, Sarasota, USA). The scalp was cut in rostrocaudal direction and holes were drilled in the skull at the respective coordinates. Injections were performed using a microprocessor controlled mini-pump (World Precision Instruments, Sarasota, USA) with 34 x G beveled needles (World Precision Instruments, Sarasota, USA), injecting 1 µl per injection site at a rate of 200 nl/min. Anesthesia was performed by intraperitoneal (i.p.) injection of a mix of 0.05 mg/kg fentanyl (opioid receptor agonist), 5 mg/kg midazolam (benzodiazepine) and 0.5 mg/kg medetomidin ($\alpha_2$ adrenergic receptor ($\alpha_2$AR) agonist) 45 min before surgery and another subcutaneous (s.c.) injection of 0.025 mg/kg fentanyl, 2.5 mg/kg midazolam and 0.25 mg/kg medetomidin 15 min before surgery. The nociception of anesthetized mice was tested by pinching the hind paw with a forceps. After delivery of the AAV, the scalp was sewed, followed by s.c. injection of 1.2 mg/kg naloxone (opioid receptor antagonist), 0.5 mg/kg flumazenil (benzodiazepine antagonist) and 2.5 mg/kg atipamezol ($\alpha_2$AR antagonist) in order to antagonize anesthesia. After additional s.c. injection of 0.05 mg/kg buprenorphine (analgetic agent) and 700 µl saline to restore the fluid balance, mice were kept under an infrared heat lamp or on a heat plate at 37°C until they recovered.

## 3.5 Animals

Male and female mice at an age of 2 - 10 months were used in this study and maintained under standard conditions (group-housed in a temperature- and humidity-controlled room with a 12 h light-dark cycle and food and water *ad libitum*). All experimental procedures were approved by the

Committee on Animal Health and Care of the local government. Conditional glutamatergic CB1-KO-mice and GABAergic CB1-KO-mice, bred in the C57BL/6N background, were obtained as described previously. NEX-Cre mice, which show a restricted expression of Cre in dorsal telencephalic glutamatergic neurons (Goebbels et al., 2006) or Dlx5/6-Cre mice, which express Cre only in forebrain GABAergic interneurons, were crossed to $CB1^{f/f}$ mice, in which the genomic CB1 locus was modified by flanking the CB1 ORF with loxP sites (Marsicano et al., 2002). This led to the generation of conditional NEX-Cre x $CB1^{f/f}$ (Glu-CB1-KO) mice and Dlx5/6-Cre x $CB1^{f/f}$ (GABA-CB1-KO) mice (Monory et al., 2006).

## 3.6 Preparation of hippocampal lysates

The hippocampi of one mouse were dissected and homogenized in 500 µl RIPA buffer (10 mM Tris pH 7.4, 140 mM NaCl, 1 mM EDTA, 0.5 mM EGTA, 0.1% Triton X-100, 0.1% sodium dodecyl sulfate (SDS), 2.4 mM sodium deoxycholate, Halt Protease/Phosphatase inhibitor (Thermo Scientific, Waltham, USA)) using the TissueLyser II (Qiagen, Hilden, Germany) for 30 sec at 30 Hz. All steps were performed at 4°C. The lysate was then transferred to new Eppendorf tubes (Eppendorf, Hamburg, Germany) and centrifuged for 30 min with 20,000 x g at 4°C. The supernatant was then transferred to fresh tubes and centrifuged again for 30 min with 20,000 x g at 4°C. The protein concentration in the supernatant was then analyzed using the Pierce BCA Protein Assay Kit (Thermo Scientific, Waltham, USA) and kept at -80°C until use.

## 3.7 Synaptosome preparation

Hippocampi of five mice were dissected and homogenized in 4 ml buffer A (0.32 M sucrose, 5 mM HEPES pH 7.4, 1 mM EGTA, Halt Protease/Phosphatase inhibitor (Thermo Scientific, Waltham, USA)) using a glass Potter-Elvehjem homogenizer. After centrifugation for 10 min with 1000 x g at 4°C, the supernatant was transferred to a Falcon tube (Greiner Bio-One, Kremsmünster, Austria), and the pellet resuspended and homogenized again. The supernatant after centrifugation of the second homogenate was then combined with the first one and then centrifuged for 15 min with 12,000 x g at 4°C. After discarding the supernatant, the pellet was resuspended in 2 ml buffer A and centrifuged again for 20 min with 12,000 x g at 4°C. The supernatant was then discarded and the

pellet resuspended in 400 µl buffer B (0.32 M sucrose, 5 mM Tris pH 8.1, 1 mM EGTA, Halt Protease/Phosphatase inhibitor (Thermo Scientific, Waltham, USA)). After loading the resuspended pellet onto a sucrose gradient (1.2 M, 1 M, 0.85 M in buffer B) it was centrifuged for 2 h with 85,000 x g at 4°C and the synaptosome containing phase between 1.2 M and 1 M sucrose collected (Carlin et al., 1980).

## 3.8 Protein biochemistry

### 3.8.1 Co-immunoprecipitation

After removal of growth medium and two washing steps with PBS, 14 cm cell culture plates of transfected HEK293 cells were harvested in ice-cold lysis buffer (30 mM Tris pH 7.4, 150 mM NaCl, 0.3% Brij O10, Halt Protease/Phosphatase inhibitor (Thermo Scientific, Waltham, USA)) on ice using a cell scraper, transferred to an Eppendorf tube (Eppendorf, Hamburg, Germany), and incubated in an overhead rotor at 4°C overnight. The next day, the lysate was centrifuged for 30 min with 20,000 x g at 4°C and the supernatant afterwards transferred to a fresh tube and taken as input material for the co-immunoprecipitation (CoIP). Alternatively, hippocampal lysates of mice were prepared and used as source material. 50 µl of antibody-coupled agarose beads or Dynabeads (Thermo Scientific, Waltham, USA) were washed 3x with wash buffer (30 mM Tris pH 7.4, 150 mM NaCl, detergent as described in the results section, Halt Protease/Phosphatase inhibitor (Thermo Scientific, Waltham, USA)) and afterwards added to the cell lysates or hippocampal lysates. The lysate bead mix was then incubated for 2 h in an overhead rotor at 4°C. Afterwards, the beads were washed in varying procedures with wash buffer in Eppendorf tubes (Eppendorf, Hamburg, Germany) or Illustra MicroSpin columns (GE Healthcare, Little Chalfont, United Kingdom), before elution of the proteins.

### 3.8.2 Tandem Affinity Purification (TAP)

The Tandem Affinity Purification (TAP) procedure was adapted from the original publication (Gloeckner et al., 2007) and step-by-step optimized for the SF-tagged CB1 (Fig. 3.2) in the expression systems in the current study. The final protocol was performed as described in this section. All steps were performed on ice or at 4°C.

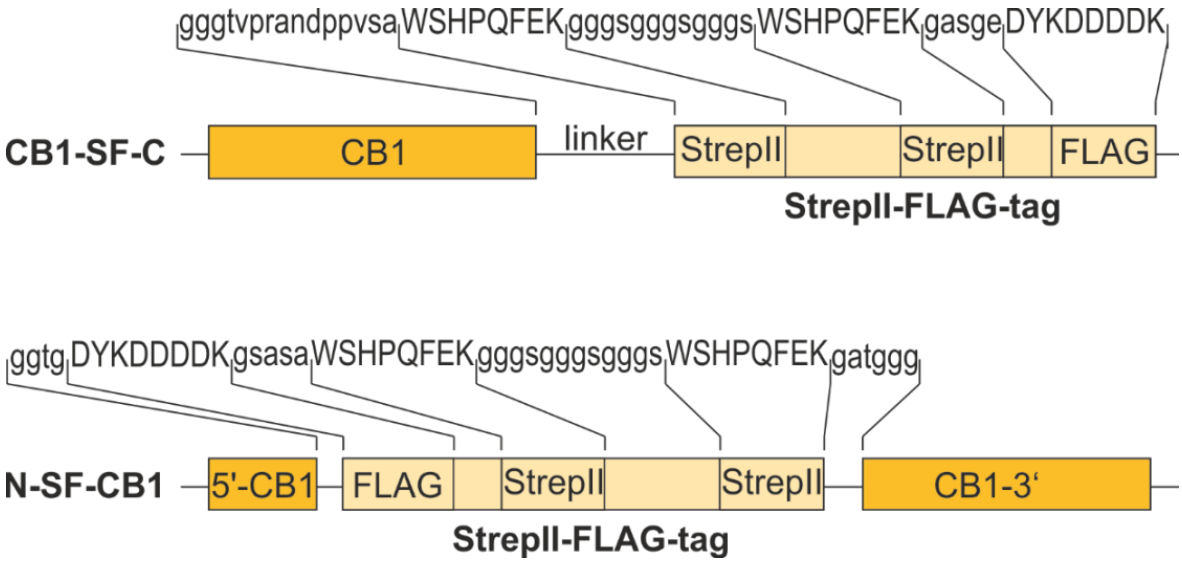


**Fig. 3.2 SF-tagged CB1 constructs**

Schematic view of CB1-SF-C and N-SF-CB1 constructs including the amino acid sequence of the tag used for the TAP of CB1. The SF-tag of the C-terminally tagged CB1 is separated by a short additional linker sequence of 15 amino acids. The SF-tag of the N-terminally tagged CB1 is inserted 66 amino acids downstream the start of the CB1 ORF, in order not to interfere with potentially important localization sequences at the N-terminus of the translated protein.

5x 14 cm plates of HEK293 cells or the synaptosome preparations of five mice were used, respectively as input material for one TAP. Transfected HEK293 cells were washed 2x with PBS and then harvested on ice using a cell scraper in 1 ml lysis buffer (30 mM Tris pH 7.4, 150 mM NaCl, detergent as described in the results section, Halt Protease/Phosphatase inhibitor (Thermo Scientific, Waltham, USA)), followed by transferring the cells to a Falcon tube (Greiner Bio-One, Kremsmünster, Austria), and resuspension of cells by pipetting up and down a few times. Synaptosome preparations were transferred to 5 ml of ice-cold lysis buffer. HEK293 cells or synaptosome preparations in the lysis buffer were then incubated on a rocker at 4°C overnight. The next day, HEK293 cell lysates were centrifuged for 1 h with 20,000 x g at 4°C, whereas the synaptosome lysates were centrifuged for 10 min with 5,000 x g at 4°C. The supernatants were then filtered through a 0.22 µm syringe sterile filter (Hartenstein, Würzburg, Germany) and incubated with 150 µl of Streptactin Superflow beads (IBA lifesciences, Göttingen, Germany) on a rocker for 1 h at 4°C. After centrifugation for 30 sec with 1,000 x g at 4°C, the supernatant was discarded and the bead mixture transferred to Illustra MicroSpin columns (GE Healthcare, Little Chalfont, United Kingdom). The beads were then washed 3x with 500 µl wash buffer (30 mM Tris pH 7.4, 150 mM NaCl, detergent as described in the results section, Halt Protease/Phosphatase inhibitor (Thermo Scientific, Waltham, USA)), and the proteins were eluted with 700 µl of 3X desthiobiotin (IBA

lifesciences, Göttingen, Germany) in wash buffer by incubating for 10 min in an overhead rotor at 4°C. The eluate was transferred to fresh MicroSpin columns together with 50 µl of anti FLAG M2 agarose beads (Sigma Aldrich, St. Louis, USA) and incubated for 1 h at 4°C in an overhead rotor. The column was then washed 3x with 500 µl wash Buffer, and afterwards the protein complexes eluted from the beads by incubation with 250 µl of 2X FLAG Peptide (Sigma Aldrich, St. Louis, USA) for 20 min in an overhead rotor at 4°C. The final samples were then collected by centrifugation of the eluate for 5 sec with 2,000 x g at 4°C into fresh Eppendorf tubes (Eppendorf, Hamburg, Germany).

### 3.8.3 Western blot

The protein content of samples was determined using the Pierce BCA Protein Assay Kit (Thermo Scientific, Waltham, USA). Samples were heated to 95°C for 5 min or 65°C for 10 min in Laemmli reducing sample buffer. The proteins were resolved by 10% or 12% sodium dodecyl sulfate polyacrylamide gel electrophoresis (SDS-PAGE) and electroblotted onto a nitrocellulose membrane. After blocking in 5% non-fat dry milk or 5% BSA in TBS-T (Tris-buffered saline (TBS), 0.1% Tween 20) for 45 min at room temperature, the membrane was incubated with primary antibodies: rabbit anti Actin [1:10,000] (Merck Millipore, Billerica, USA), rabbit anti CB1 [1:500] (Frontier Sciences, Hokkaido, Japan), mouse anti CoxIV [1:1,000] (Abcam, Cambridge, United Kingdom), rabbit anti FLAG [1:500] (Sigma Aldrich, St. Louis, USA), mouse anti $G\alpha_o$ [1:500] (Santa Cruz Biotechnology, Dallas, USA), rabbit anti $G\alpha_z$ [1:250] (Santa Cruz Biotechnology, Dallas, USA), mouse anti PSD95 [1:500] (BD Biosciences, Franklin Lakes, USA), mouse anti PTPRS [1:500] (Sigma Aldrich, St. Louis, USA), mouse anti Syntaxin [1:500] (Abcam, Cambridge, United Kingdom), and rabbit anti VGAT [1:500] (Merck Millipore, Billerica, USA) at 4°C overnight. After washing with TBS-T, the membranes were incubated in horseradish peroxidase-conjugated anti rabbit or anti mouse IgG secondary antibodies [1:5,000] (Dianova, Hamburg, Germany) in 5% non-fat dry milk in TBS-T for 1 h at room temperature. After washing with TBS-T, western blot (WB) was performed by incubating the membrane with the Amersham ECL Prime Western Blotting Detection Reagent (GE Healthcare, Little Chalfont, United Kingdom) for 5 min, followed by an analysis with the FUSION-SL chemiluminescence imaging system (Peqlab, Erlangen, Germany).

### 3.8.4 Silver staining

Silver stainings of proteins separated SDS-PAGE were performed with the Silver Stain Plus Kit (Bio-Rad, Hercules, USA), according to the manufacturer's protocol. Gels with a thickness of 1.5 mm were placed in the fixative enhancer solution (50% methanol, 10% acetic acid, 10% fixative enhancer concentrate, 30% deionized distilled $H_2O$) and incubated for 30 min. The solution was then discarded and the gels first rinsed with $H_2O$, and then washed 2x for 20 min, before staining and development was performed in the staining solution (5 ml silver complex solution, 5 ml reduction moderator solution, 5 ml image development reagent, 35 ml $H_2O$, 50 ml development accelerator solution), until desired staining intensity was reached. In order to stop the staining reaction, the gels were finally placed in a 5% acetic acid solution for 15 min and pictures were taken on an illuminated table.

### 3.8.5 Immunohistochemistry

Mice were anesthetized using 160 mg/kg pentobarbital (barbiturate) and perfused with 4% PFA in PBS. Brains were then removed, postfixated in 4% PFA overnight and incubated in 30% sucrose for cryoprotection before 40 µm free-floating coronal cryosections were cut. Free-floating sections were then permeabilized in PBS containing 0.2% Triton X-100 (PBS-TX) and afterwards blocked in 4% normal goat serum (NGS) in PBS-TX for 15 min at room temperature. Primary antibody incubation was performed at 4°C overnight in 4% NGS using the following primary antibodies: mouse anti FLAG [1:500] (Sigma Aldrich, St. Louis, USA), guinea pig anti VGlut1 [1:500] (Merck Millipore, Billerica, USA), and guinea pig anti VGAT [1:100] (Merck Millipore, Billerica, USA). The next day, sections were washed with PBS-TX and incubated with Alexa488- or Alexa546-conjugated secondary antibodies goat IgG [1:1,000] (Invitrogen, Carlsbad, USA) in 4% NGS for 1 h in the dark. After washing with PBS-TX, the slices were counterstained with DAPI for 5 min and washed in PBS. Sections were transferred onto glass slides and coverslipped with Mowiol mounting medium. Fluorescence was visualized with a Leica TCS SP5 Confocal Microscope (Leica microsystems, Wetzlar, Germany).

## 3.9 Proteomics

### 3.9.1 Identification of proteins in the TAP samples

The experiments described in this paragraph were carried out by Stefan Tenzer, Institute for Immunology, University Medical Center of the Johannes Gutenberg-University Mainz.

TAP Eluates were frozen at -80°, lyophilized to dryness and solubilized in 200 µl 7 M urea, 2 M thiourea and 2% CHAPS. Proteins were digested with sequencing grade Trypsin Gold (Promega, Madison, USA) using a modified filter-aided sample preparation (FASP) (Distler et al., 2014). After FASP digest, resulting tryptic peptides were concentrated to 20 µl by lyophilization and 5 µl of 100 fmol/µl MassPrep Enolase Digestion Standard (Waters, Milford, USA) were added to each sample and transferred into an autosampler vial. For nano ultra performance liquid chromatography-mass spectrometry (nanoUPLC-MS) analysis, 2 µl were used per injection. Samples were analyzed in three technical replicates. Tryptic peptides were separated by reversed-phase nanoUPLC in direct injection mode on a nanoAcquity System (Waters, Milford, USA) equipped with a C18 HSS-T3 75 µm x 250 mm column using a gradient from 4% to 40% B over 90 min (Distler et al., 2014). Buffer A was 0.1% formic acid in water and 3% DMSO. Buffer B was 0.1% formic acid in acetonitrile and 3% DMSO. The column was coupled to a nanoelectrospray source on a Synapt G2-S mass spectrometer (Waters, Milford, USA) operated in ion-mobility enhanced, data-independent acquisition mode (Distler et al., 2014). Resulting raw data files were processed by ProteinLynxGlobalServer v3.0.2 and database search was performed against the mouse UniProt Reference Proteome database supplemented with common contaminants (trypsin, bovine serum albumin, human keratins, etc). Data post-processing and TOP3-based label-free quantification were performed in the ISOQuant software (Distler et al., 2014).

### 3.9.2 Bioinformatic analysis of proteomics data

A network of all identified proteins with a molar ratio of at least 1% relative to the bait protein was generated using the STRING database for known and predicted protein-protein interactions (string-db.org) (Jensen et al., 2009) with required medium confidence scores (0.400). Clustering analysis of the network based on the confidence scores of protein interactions was performed using Cytoscape (Cline et al., 2007) with the ClusterMaker2 plugin (Morris et al., 2011) using the

Markov Cluster Algorithm (MCL). Gene Ontology (GO) annotation analysis was performed using DAVID (https://david.ncifcrf.gov) (Huang da et al., 2009) or the BiNGO Cytoscape plugin (Maere et al., 2005).

## 3.10 Software

WB image acquisition was performed using Fusion (Vilber Lourmat, Eberhardzell, Germany) and densitometric measurements of band intensities on WB images with Bio1D (Vilber Lourmat, Eberhardzell, Germany). Image acquisition of immunohistochemistry was performed using the Leica Application Suite Advanced Fluorescence v3.1.0 (Leica microsystems, Wetzlar, Germany). DNA plasmid design and management were carried out using Vector NTI software (Invitrogen, Carlsbad, USA). Graphs and statistics were generated with GraphPad Prism 4.0 (GraphPad Software, La Jolla, USA), whereas two-way ANOVA followed by Bonferroni's post-hoc test in the analysis of the cAMP assay was performed using SPSS Statistics (IBM, Armonk, North Castle, USA). Image processing was performed using Corel Draw X7 (Corel Corporation, Ottawa, Canada).

# 4 Cell type-specific TAP of CB1 receptor complexes

## 4.1 Introduction

Several techniques are available for the identification of protein interactions. CoIP, using antibodies against a bait protein, and subsequent screening for co-purified interacting proteins by western blot, is the standard assay in this field, but only allows for directed screening towards expected proteins. Proximity Ligation Assay (PLA) or Fluorescence Resonance Energy Transfer (FRET)/Bioluminescence Resonance Energy Transfer (BRET) represent alternative methods, but like performing CoIP, only candidate proteins can be tested. Yeast two-hybrid assays, however, allow for high throughput screens, but are performed within a highly artificial cellular environment. TAP is a method that allows for unbiased high throughput screening, whereby interactions are detected within a natural cellular environment (Rigaut et al., 1999). The two step purification process furthermore minimizes false positive results. This method was applied for other GPCRs using StrepII/FLAG (SF)-tagged receptors (Gloeckner et al., 2007), such as the $MT_1$ and $MT_2$ melatonin receptors ($MT_1$, $MT_2$) (Daulat et al., 2007) and $A_{2A}$ (Bergmayr et al., 2013). Importantly, SF-tagged receptors were shown to be functionally indistinguishable from wildtype receptors (Bergmayr et al., 2013).

In previous work of Katharina Kukla for her diploma thesis in our lab, N- and C-terminally SF-tagged CB1 cDNA-containing pcDNA3 mammalian expression plasmids were generated. Expression, correct subcellular distribution in response to agonist and antagonist treatment, and correct functionality of the CB1 fusion protein was verified in HEK293 cells, HT22 cells, and N2a cells. A first approach of the TAP method, purifying the recombinant CB1 receptor from transfected HEK293 cells, could be successfully performed for both the N- and C-terminal tagged CB1 (N-SF-CB1, CB1-SF-C), but the protein complex integrity and identification of co-purified proteins were still to be investigated. In order to address this, the TAP procedure was applied again on N-SF-CB1- and CB1-SF-C-transfected HEK293 cells, and the eluates then analyzed using WBs, silver stainings, and MS, with a concomitant optimization of the TAP method.

Eventually, SF-tagged CB1 was expressed cell type-specifically in mouse hippocampus using a combination of AAV vectors and Cre-expressing mouse lines, which allows the purification of neuronal subtype-specific CB1 protein complexes, and identification of CB1-interacting proteins *in*

*vivo*. AAVs were shown to be a valuable tool for transgene expression in the central nervous system by occupying features such as neurotropism, lack of pathogenicity, and sustained transgene expression (During et al., 2003). Based on reports of robust expression in the hippocampus (Richichi et al., 2004; Klugmann et al., 2005; Guggenhuber et al., 2010), mosaic AAV1/2 serotypes were used in this study to target hippocampal neurons.

Cloning of SF-tagged CB1 cDNA in pAM AAV expression plasmids, packaging of the single-stranded DNA genome in AAV1/2 capsids, and successful expression of SF-tagged CB1 after stereotaxic delivery of recombinant AAV1/2 into the hippocampus of CB1-KO mice could be accomplished. Furthermore, the foundation for a Cre-dependent cell type-specific expression was laid by subcloning a floxed stop-cassette (Guggenhuber et al., 2010) upstream the SF-tagged CB1 sequence in the respective pAM AAV expression plasmids.

After verifying neuron type-specific expression and localization of SF-tagged CB1 in mouse hippocampus and further optimization of the TAP protocol for hippocampal synaptosome preparations, co-purified proteins were identified using a deep coverage proteomics approach (Distler et al., 2014). Differences between glutamatergic and GABAergic CB1 protein complexes were detected and the entirety of these proteins analyzed regarding their biological function using bioinformatic tools.

## 4.2 Results

### 4.2.1 Optimization of the SF-TAP method using N-SF-CB1- and CB1-SF-C-transfected HEK293 cells

The original TAP method was described with a successful isolation of a cytosolic protein complex under native conditions in yeast (Rigaut et al., 1999). For the purification of membrane-bound GPCRs and their associated proteins, the TAP method was optimized with focus on solubilization and purification conditions with special emphasis on the use of detergents in lysis and wash buffers, as they are essential for the solubilization process, but at the same time critical regarding the maintenance of protein-protein interactions. Digitonin, a saraponin obtained from the plant *Digitalis purpurea*, and Brij O10 (old tradename Brij 96V), a polyethylene glycol ether, were proven effective as non-ionic detergents, when used in low concentrations and prolonged solubilization

steps (Daulat et al., 2007). Therefore, these detergents were also used in the optimization process of the TAP method specifically for the SF-tagged CB1 in this study.

As a first step towards a successful implementation of the StrepII/FLAG-TAP method, TAP eluates of pAM-N-SF-CB1- and pAM-CB1-SF-C-transfected HEK293 cells were initially analyzed in regard to the presence of the SF-tagged CB1 protein itself. In order to optimize the TAP protocol, it was crucial to analyze samples obtained during the purification process. Therefore, five samples were collected throughout the procedure and kept for western blot analysis of the target fusion protein (Fig. 4.1). The first sample was taken after the initial lysis step of the cells in detergent-containing lysis buffer and spinning down of the cell debris, showing the entirety of all proteins in the source material. The second sample shows the remaining proteins in the supernatant after CB1 protein complexes binding to Streptavidin beads, whereas the third sample represents the purified proteins after elution from the Streptavidin beads. After the following incubation of the eluate with M2 anti FLAG agarose beads, the supernatant was taken as fourth sample, showing the remaining proteins apart from the anti FLAG-bound CB1 protein complexes. The fifth sample is the final TAP eluate, after using FLAG protein containing buffer to competitively elute the protein complexes from the M2 anti FLAG beads.

Various concentrations of digitonin or Brij O10 were tested in lysis and wash buffers used in the TAP method, aiming at maximum reduction of the detergent concentration to avoid disruption, but at the same time sufficient solubilization of the membranous protein complexes. In HEK293 cells, purification of N-SF-CB1 and CB1-SF-C were successful at concentrations of 0.3% (lysis buffer)/0.05% (wash buffer) Brij O10 and, at least for CB1-SF-C, using 0.5% (lysis buffer)/0.1% (wash buffer) digitonin as shown by western blot analysis of the final TAP eluates and intermediate steps using a polyclonal antibody directed against the C-terminus of CB1 (Fig. 4.2). To enable a comparison of the amount of SF-tagged CB1 in the single steps of the TAP process, the same volume of each sample was loaded onto the lanes of the gel in order to get a rough estimation of the concentration of the target protein in the respective samples.

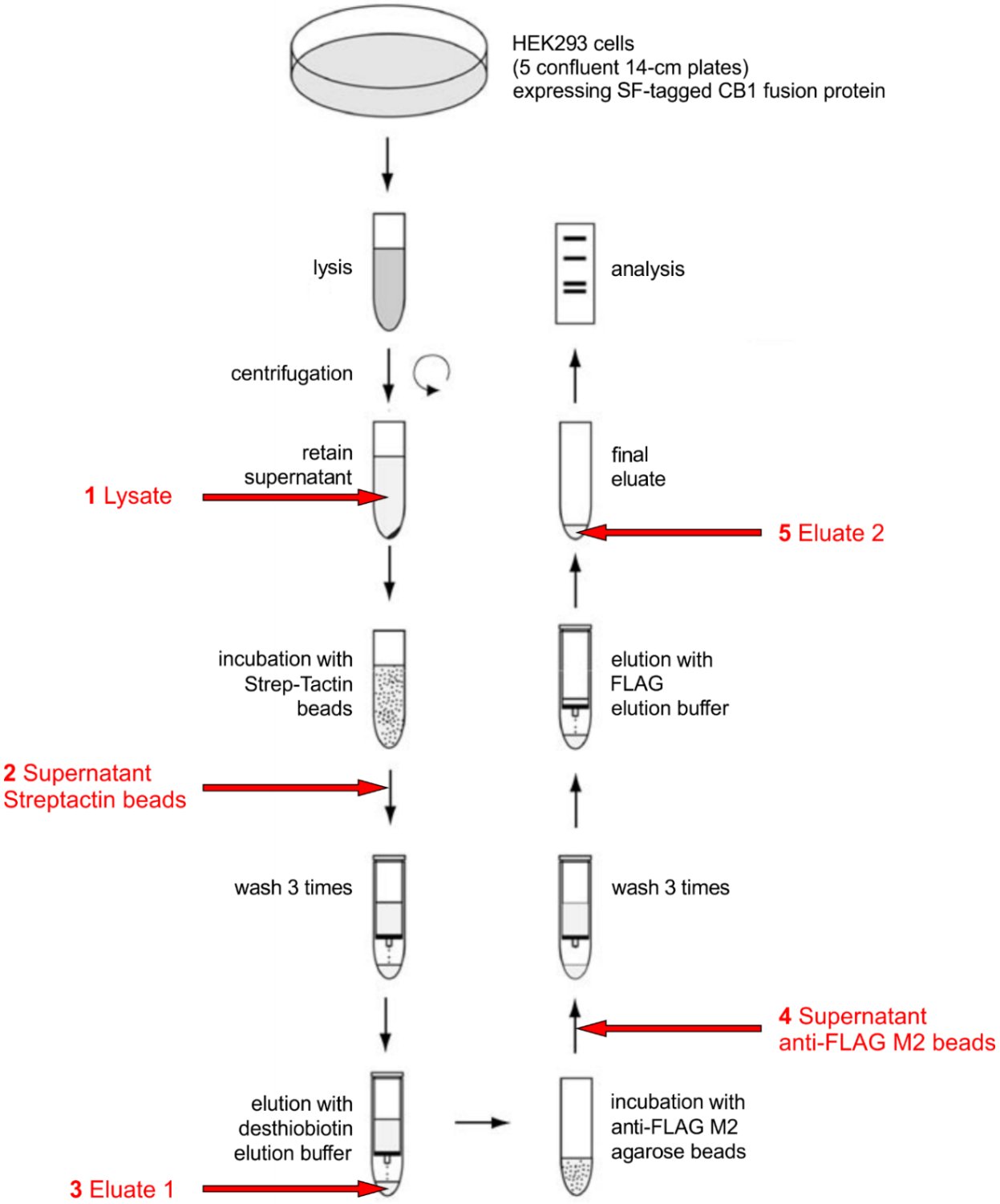


**Fig. 4.1 Schematic diagram of the TAP protocol**

Samples were taken at various steps throughout the TAP procedure as indicated by red arrows, and kept for western blot analysis of the target SF-tagged CB1 fusion protein (modified from Gloeckner et al., 2009).

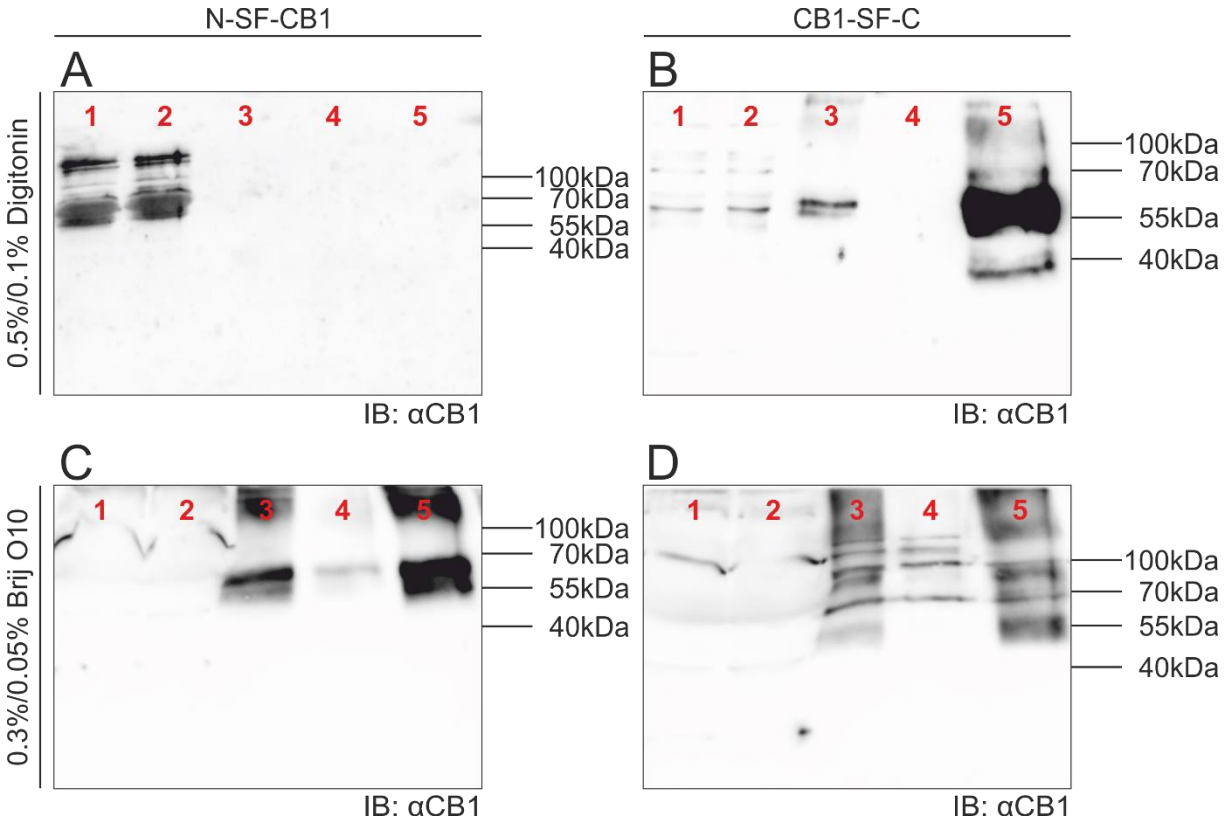


**Fig. 4.2 Western blot analysis of samples taken during various steps of individual TAP procedures for N-SF-CB1- and CB1-SF-C-transfected HEK293 cells**

TAPs of HEK293 cells transfected with N-SF-CB1 (**A**, **C**) or CB1-SF-C (**B**, **D**) using 0.5% (lysis buffer)/0.1% (wash buffer) digitonin (**A**, **B**) or 0.3% (lysis buffer)/0.05% (wash buffer) Brij O10 (**C**, **D**). 1: Lysate of HEK293 cells. 2: Supernatant after Streptavidin bead incubation. 3: Eluate from Streptavidin beads. 4: Supernatant after M2 anti FLAG bead incubation. 5: Eluate from M2 anti FLAG beads. **A**: Expression of N-SF-CB1 in HEK293 cells was successful as indicated by CB1-specific bands in the cell lysate (1) and in the supernatant after Streptavidin bead incubation (2), but purification did not work using digitonin as there is no band visible after the elution step of the fusion protein from the Streptavidin beads (3). **B**: The purification of CB1-SF-C was successful as indicated by CB1-specific bands in the cell lysate (1), after the first elution from the Streptavidin beads (3), and the second elution from the M2 anti FLAG beads (5). The concentration of the purified CB1 fusion protein increases from step to step as indicated by increasing band intensities pointing out an efficient purification process particularly for the M2 anti FLAG beads as there is no band visible in the supernatant (4) compared to the supernatant after the Streptavidin bead incubation (2). **C**: Purification of N-SF-CB1 was successful using Brij O10 comparable to **B** with little less increase in band intensities from the first eluate (3) to the second eluate (5), and a weak band visible in the supernatant after M2 anti FLAG bead incubation (4) indicating a less efficient purification. **D**: Purification of CB1-SF-C using Brij O10 was successful with CB1-specific bands in the cell lysate (1) and both eluates (3, 5). The bands are more blurry indicating an increased aggregation of proteins in the samples. kDa: Kilodalton. IB: Immunoblot.

The choice of detergent and location of the SF-tag up- or downstream the CB1 sequence both have an influence on the outcome of the TAP process. Although N-CB1-SF was expressed in HEK293 cells, the TAP did not work when using digitonin in the solubilization and purification process (Fig. 4.2A). In contrast, the C-terminal SF-tagged CB1 protein showed a strong increase in the

concentration of the fusion protein in the final TAP eluate, indicating an efficient binding and elution from the Streptavidin and, in particular, the M2 anti FLAG beads (Fig. 4.2B). The use of Brij O10 allowed for a purification of both, the N- and C-terminal SF-tagged CB1, again with an increase of the target protein concentration after each purification step, although the bands in the CB1-SF-C blot appeared more blurry, indicating an increased aggregation of proteins compared to the N-SF-CB1 samples.

Afterwards the final TAP eluates were analyzed focusing on the visualization of co-purified proteins by using silver stainings of proteins in the TAP samples, which were separated by SDS-PAGE. Since N-SF-CB1 could not be purified using digitonin, only CB1-SF-C was analyzed and compared for both detergents tested, and furthermore, the TAPs in which Brij O10 was used, compared regarding differences between N-SF-CB1 and CB1-SF-C (Fig. 4.3).

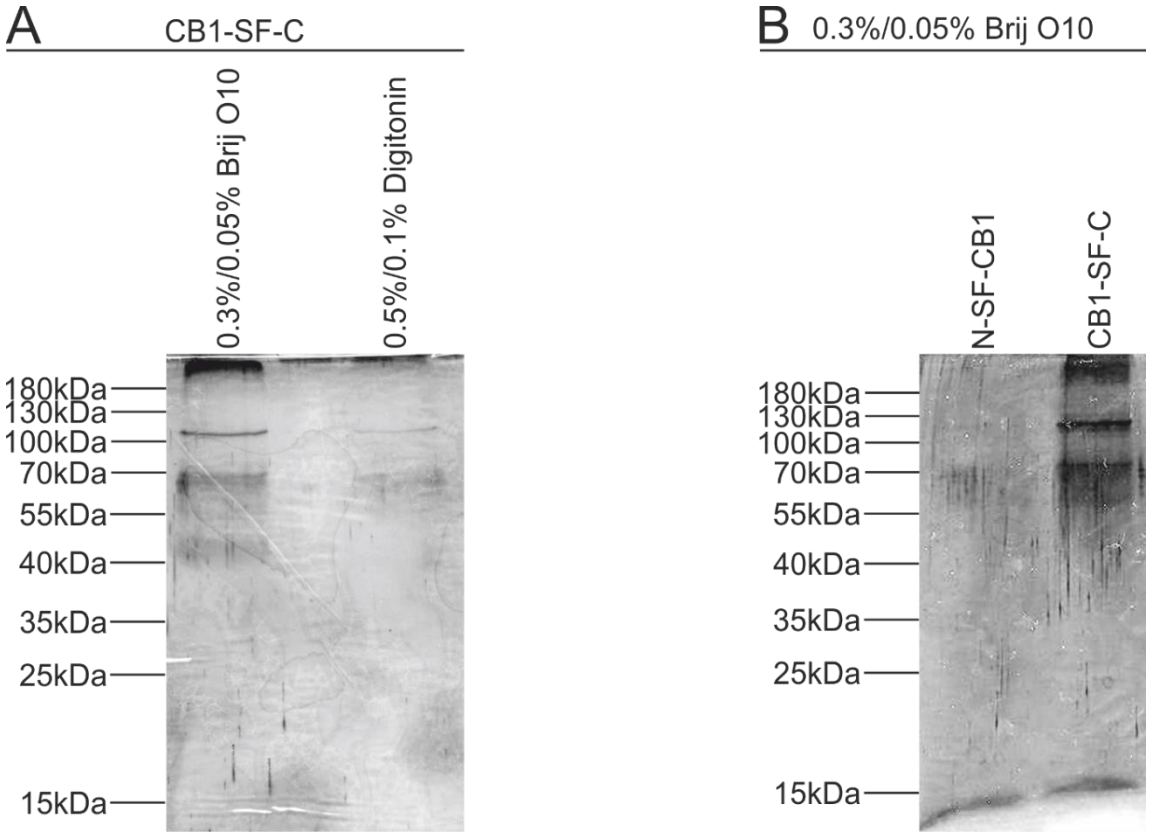


**Fig. 4.3 Silver stainings of individual TAP eluates of N-SF-CB1- and CB1-SF-C-transfected HEK293 cells**

**A**: TAP eluates of CB1-SF-C-transfected HEK293 cells processed with 0.3% (lysis buffer)/0.05% (wash buffer) Brij O10 or 0.5% (lysis buffer)/0.1% (wash buffer) digitonin. In both samples, a band at 64 kDa is visible in accordance to the molecular weight of the SF-tagged CB1 detected by western blot analysis and another not specified band at ~110 kDa. The staining intensity is stronger and additional bands and smear visible in the Brij O10-treated TAP sample indicating an increased amount and variety of co-purified proteins. **B**: TAP eluates of N-SF-CB1- and CB1-SF-C-transfected HEK293 cells processed with 0.3% (lysis buffer)/0.05% (wash buffer) Brij O10. The CB1-SF-C sample shows a pattern of bands and smear comparable to the sample in A in

contrast to the N-SF-CB1 sample, which shows only a very weak band probably related to the target SF-tagged CB1 at 64 kDa. kDa: kilodalton.

The purification of CB1-SF-C using Brij O10, in contrast to digitonin, led to an increased amount and variety of purified proteins as indicated by the stronger staining intensity, variety of bands, and smear in the silver staining (Fig. 4.3A). A clear band was visible in both samples with a molecular weight according to the specific SF-tagged CB1 band shown in the western blot analysis of the respective samples (Fig. 4.2B, D) Furthermore, a substantial difference could be observed when comparing the purification of the N- and C-terminally tagged CB1 when using Brij O10 in the TAP. Whereas the silver staining of the TAP eluate of the CB1-SF-C sample showed diverse bands with a strong staining intensity as described before, there was hardly any staining observable in the N-SF-CB1 sample (Fig. 4.3B).

In order to gain insight into the composition of the TAP eluates of N-SF-CB1- and CB1-SF-C-transfected HEK293 cells, we used a proteomics approach for the identification of proteins in the TAP samples in which Brij O10 was used in the purification process. For a direct comparison of the TAP eluates, the abundance of proteins was determined using the Top3 label-free quantification method, as it was demonstrated to allow for a meaningful comparison for absolute abundance values and direct proportionality of proteins (Ahrne et al., 2013, Fabre et al., 2014).

In accordance with the silver stainings of the respective samples (Fig. 4.3), the abundance of the CB1 target protein in the TAP samples of CB1-SF-C-transfested HEK293 cells (n = 2) was several fold higher as compared to the TAP samples of N-SF-CB1-transfected HEK293 cells. Furthermore, 21 other co-purified proteins were identified in the CB1-SF-C-TAPs, whereas only low amounts of Tubulin alpha 1b, mitochondrial Propionyl-CoA carboxylase beta and mitochondrial Pyruvate carboxylase were detectable in the N-SF-CB1-TAPs apart from CB1. A TAP of non-transfected HEK293 cells served as negative control to determine unspecific binding of proteins in the absence of SF-tagged CB1, and none of the proteins identified in the other TAP-samples were detectable (Fig. 4.4, Tab. 8.1).

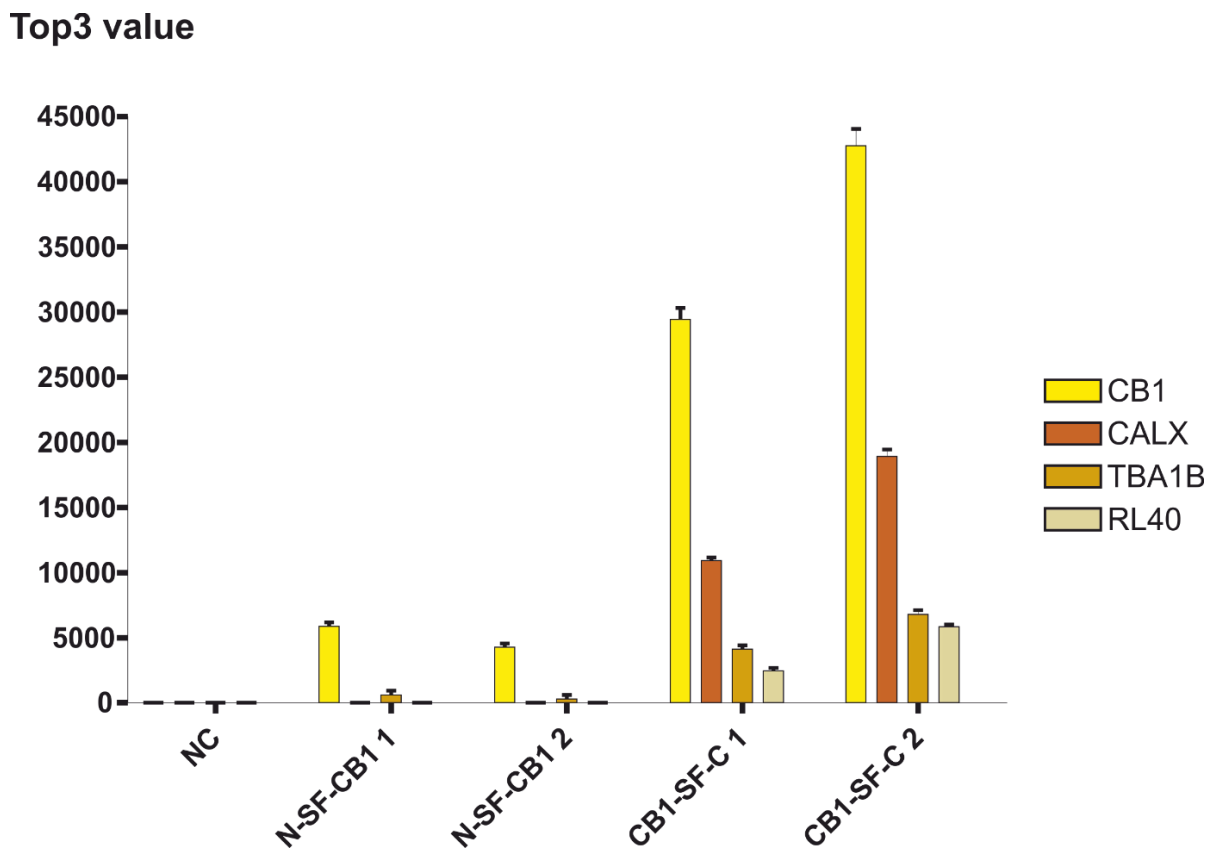


**Fig. 4.4 Label-free quantification of the most abundant proteins in the TAP samples of N-SF-CB1- and CB1-SF-C-transfected HEK293 cells**

Comparison of TAPs of two N-SF-CB1- and CB1-SF-C-transfected HEK293 cells, respectively, evaluating the composition of the final TAP eluates. The target protein CB1 (yellow) was identified in CB1-SF-C TAP samples (CB1-SF-C 1, CB1-SF-C 2) with a several fold higher abundance as compared to N-SF-CB1 TAP samples (N-SF-CB1 1, N-SF-CB1 2), as determined by the Top3 label-free quantification method (Ahrne et al., 2013). 21 Co-purified proteins were identified in the CB1-SF-C TAP samples (Tab. 8.1) (3 with highest abundancy shown; Calnexin (CALX, red-brown), Tubulin alpha 1b (TBA1B, brown), Ubiquitin-60S ribosomal protein L40 (RL40, beige)), but not in the N-SF-CB1 TAP samples, except for Tubulin alpha 1b (TBA1B, brown). TAP of non-transfected HEK293 cells served as negative control (NC) for the determination of non-specific binding of proteins and with none of the identified proteins in the other samples detected. n=4.

Taken together, these findings show that using Brij O10, instead of digitonin, in the solubilization process of the membranous CB1 protein complexes and succeeding washing steps led to an increased amount of purified proteins with digitonin not being able to solubilize N-SF-CB1 at all. Comparing the results for CB1-SF-C to N-SF-CB1 with the use of Brij O10 throughout the TAP process, expressing CB1-SF-C led to an increased amount of purified proteins and at the same time an apparently better maintenance of protein-protein interactions.

### 4.2.2 Optimization of the SF-TAP method for the purification of SF-tagged CB1 after cell type-specific *in vivo* overexpression

The findings that the use of Brij O10 is superior over digitonin and expressing CB1-SF-C led to better results as compared to N-SF-CB1 in the SF-TAP method using HEK293 cells had to be tested for the *in vivo* approach when using a cell type-specific AAV-mediated expression of SF-tagged CB1 in mouse hippocampal neurons.

In order to target only glutamatergic or GABAergic subtypes of neurons in the hippocampus, we combined an AAV vector containing a transcriptional stop sequence flanked by loxP sites (floxed stop cassette) (Guggenhuber et al., 2010) between the CAG promoter region and the coding sequence of N-SF-CB1 (AAV-Stop-N-SF-CB1) or CB1-SF-C (AAV-Stop-CB1-SF-C) and neuronal subtype-specific Cre-expressing mouse lines. The AAV was delivered via bilateral stereotactic injection into the hippocampi of either Glu-CB1-KO mice, which show a restricted expression of Cre in dorsal telencephalic glutamatergic neurons, or GABA-CB1-KO mice, which express Cre only in forebrain GABAergic interneurons. Furthermore, in both mouse lines, the genomic CB1 locus was modified, whereby the CB1 ORF was flanked by loxP sites (Monory et al., 2006) (3.5). The expression of Cre finally leads to the concomitant excision of the endogenous floxed CB1 sequence and the expression of the AAV-mediated recombinant SF-tagged CB1 in the respective neuronal subtype (Fig. 4.5). We used this strategy in order to express N-SF-CB1 or CB1-SF-C in neurons which lacked the endogenous CB1, avoiding that putative interactions of proteins with the recombinant CB1 are competed by the endogenous CB1.

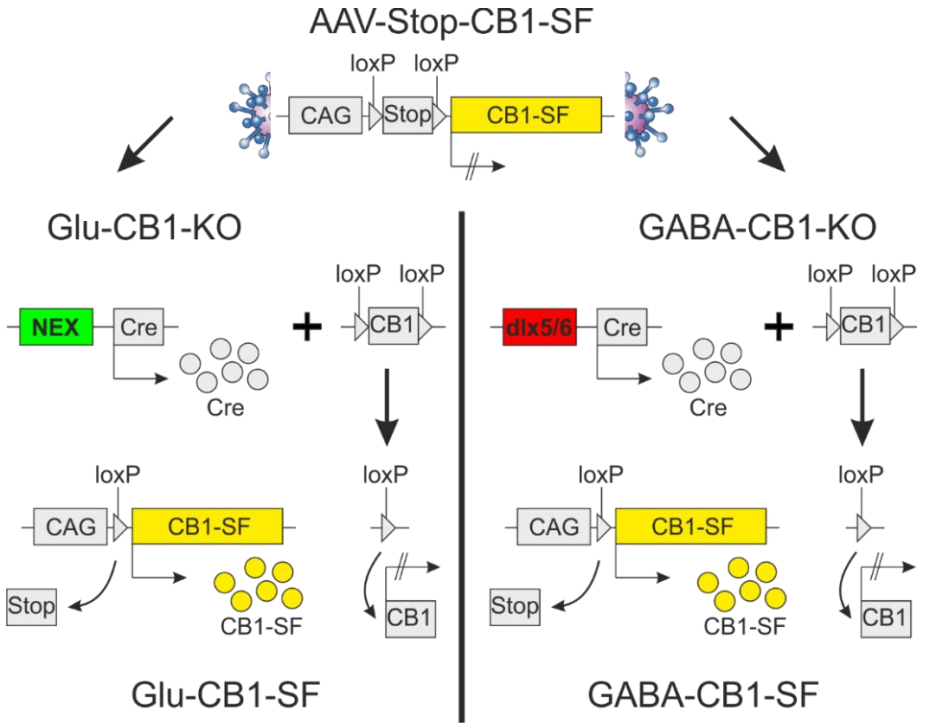


**Fig. 4.5 Cell type-specific AAV-mediated overexpression of SF-tagged CB1**

Cell type-specific knockout of endogenous CB1 and simultaneous expression of recombinant SF-tagged CB1 (CB1-SF). Glu-CB1-KO mice express Cre recombinase under control of the NEX promoter and GABA-CB1-KO mice under control of the dlx5/6 promoter, respectively. Expression of Cre recombinase leads to the excision of the genomic floxed CB1 CDS and, after stereotactic delivery of the AAV, the floxed Stop cassette of AAV-Stop-CB1-SF (AAV-Stop-N-SF-CB1 or AAV-Stop-CB1-SF-C) in glutamatergic neurons or GABAergic interneurons, respectively. Thus, a concomitant expression of recombinant CB1-SF and knockout of endogenous CB1 is obtained specifically in the respective cell type.

#### *4.2.2.1 Expression analysis of N-SF-CB1 and CB1-SF-C in glutamatergic neurons and GABAergic interneurons in mouse hippocampus*

In order to evaluate the correct expression of N-SF-CB1 and CB1-SF-C in glutamatergic neurons and GABAergic interneurons, Glu-CB1-KO mice and GABA-CB1-KO mice were injected with AAV-Stop-N-SF-CB1 and AAV-Stop-CB1-SF-C, respectively, to obtain a restricted expression of one of the SF-tagged CB1 proteins in either glutamatergic neurons (Glu-N-SF-CB1 or Glu-CB1-SF-C) or GABAergic interneurons (GABA-N-SF-CB1 or GABA-CB1-SF-C). Three weeks after stereotactic delivery of the AAVs, the injected mice were perfused, brains isolated, and coronal cryosections cut as described (3.8.5). Immunohistochemistry was performed to determine FLAG immunoreactivity together with co-stainings for the vesicular glutamate transporter 1 (VGlut1) as a presynaptic marker for glutamatergic neurons in Glu-N-SF-CB1 and Glu-CB1-SF-C mice (Fig. 4.6), and with vesicular GABA transporter (VGAT) as a presynaptic marker for GABAergic neurons in GABA-N-SF-CB1 and GABA-CB1-SF-C mice, respectively (Fig. 4.7).

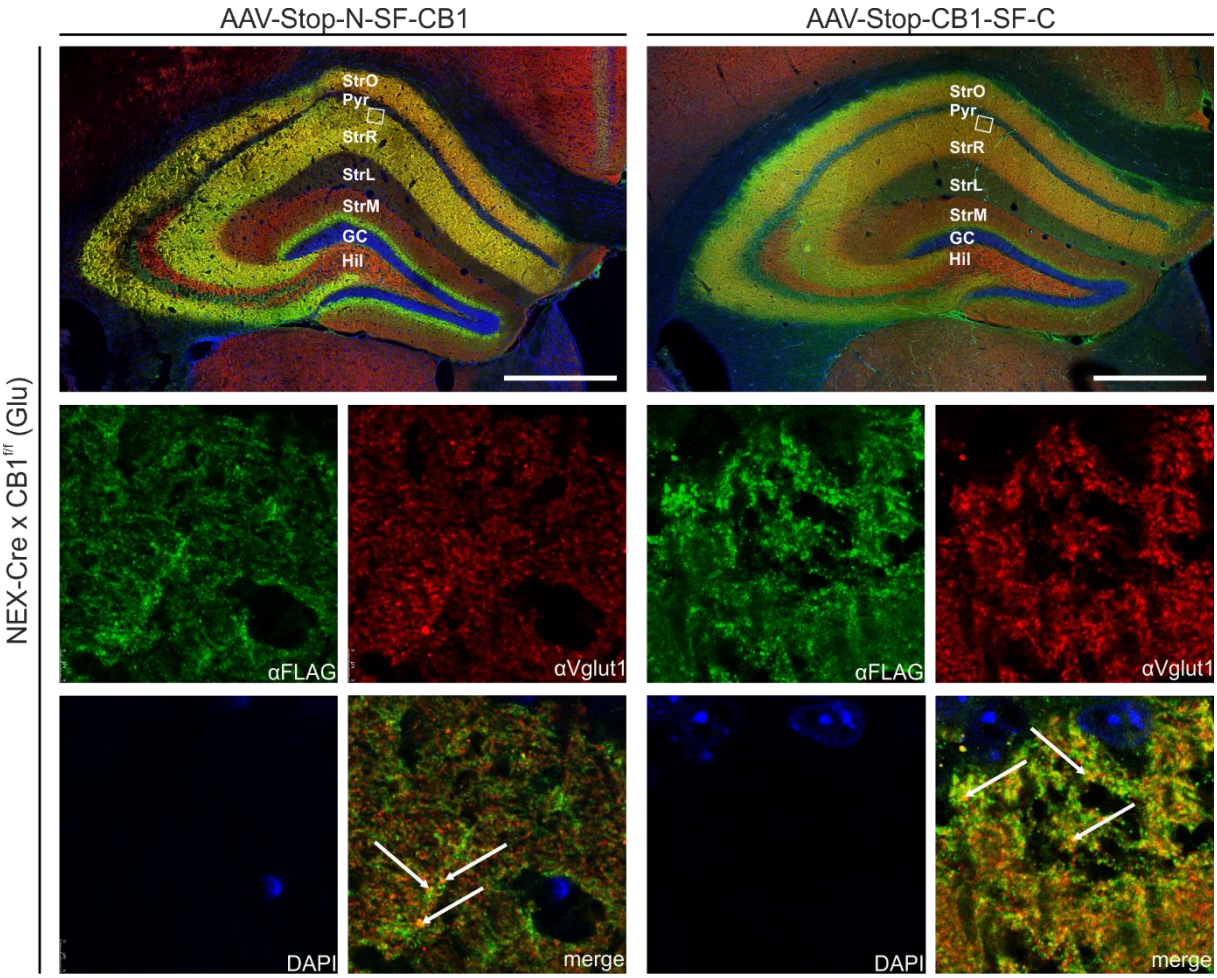


**Fig. 4.6 AAV-mediated expression of N-SF-CB1 and CB1-SF-C in glutamatergic neurons in the hippocampus**

AAV-Stop-N-SF-CB1 and AAV-Stop-CB1-SF-C were bilaterally injected in the hippocampus of NEX-Cre x CB1$^{f/f}$ mice, respectively, to obtain cell type-specific expression of N-SF-CB1 or CB1-SF-C in glutamatergic neurons. **Upper Box**: Overview of the whole hippocampus. FLAG immunoreactivity and presynaptic location was determined together with anti VGlut1 antibody as a presynaptic marker for glutamatergic neurons. Glu-N-SF-CB1 and Glu-CB1-SF-C mice show a strong FLAG immunostaining in the glutamatergic neurons of the stratum oriens and stratum radiatum of the CA1 – CA3 region and in the mossy fibers, which project from the dentate gyrus (DG) to CA3. FLAG staining in the inner third of the stratum moleculare of the dentate gyrus, where the mossy cells are synapsing on granule cell dendrites, validates the presynaptic location of both N-SF-CB1 and CB1-SF-C. StrO: Stratum oriens. Pyr: Pyramidal cell layer. StrR: stratum radiatum. StrL: Stratum lacunosum. StrM: Stratum moleculare. GC: Granule cell layer. Hil: Hilus. Green: FLAG. Red: Vglut1. Blue: DAPI-stained cell nuclei. Scale bar: 500 µm. **Lower Boxes**: Higher magnification of the CA1 regions of Glu-N-SF-CB1 and Glu-CB1-SF-C (areas indicated by white boxes in overview illustration) showing co-expression of FLAG and VGlut1 as indicated by white arrows. Green: FLAG. Red: Vglut1. Blue: DAPI-stained cell nuclei.

In Glu-N-SF-CB1 and Glu-CB1-SF-C mice, we observed a strong FLAG antibody signal in the pyramidal neurons of the stratum oriens and stratum radiatum of the CA1 - CA3 region and in the mossy fibers, which project from the dentate gyrus (DG) to CA3, but not in the granule cells of the DG. This is in accordance with the description of NEX gene activity, the Cre expression-driving

promoter in this mouse line, in adult mice after P10 (Goebbels et al., 2006). The overlap of FLAG and Vglut1 staining and the strong FLAG staining in the inner third of the molecular layer of the dentate gyrus, where the mossy cells are synapsing on granule cell dendrites, validate the presynaptic location of N-SF-CB1 as well as CB1-SF-C on glutamatergic neurons.

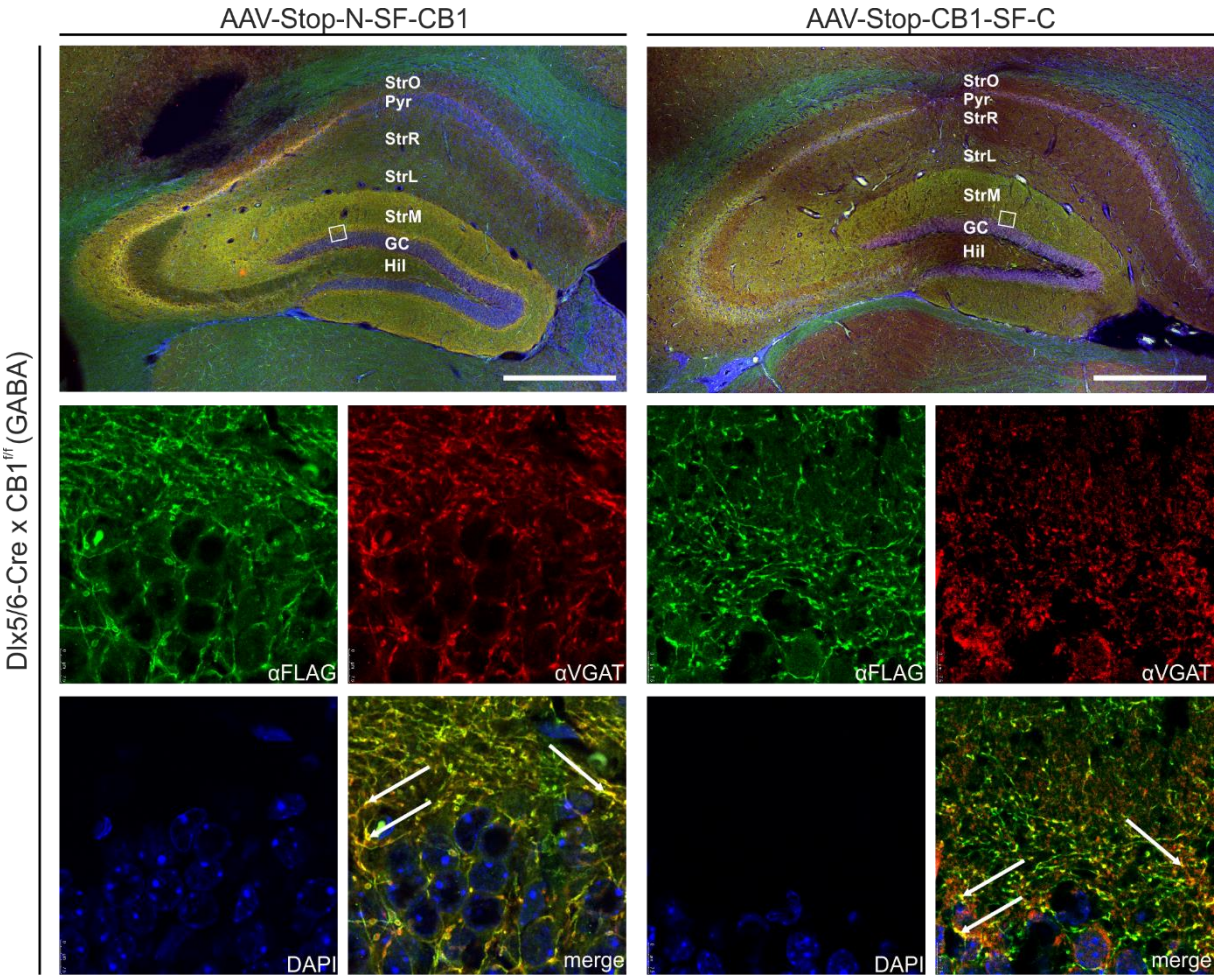


**Fig. 4.7 AAV-mediated expression of N-SF-CB1 and CB1-SF-C in GABAergic interneurons in the hippocampus**

AAV-Stop-N-SF-CB1 and AAV-Stop-CB1-SF-C were bilaterally injected in the hippocampus of Dlx5/6-Cre x $CB1^{f/f}$ mice, respectively, to obtain a cell type-specific expression of N-SF-CB1 or CB1-SF-C in GABAergic interneurons. **Upper Box**: Overview of whole hippocampus. FLAG immunoreactivity and presynaptic location was determined together with an anti VGAT antibody as a presynaptic marker for GABAergic interneurons. GABA-N-SF-CB1 and GABA-CB1-SF-C FLAG staining is less intense as compared to Glu-N-SF-CB1 and Glu-CB1-SF-C (Fig. 4.6) due to the lower amount of GABAergic interneurons as compared to glutamatergic neurons in the hippocampus. The strongest immunoreactivity is visible in the stratum moleculare and the stratum pyramidale of CA3, CA2 and lateral CA1. StrO: Stratum oriens. Pyr: Pyramidal cell layer. StrR: stratum radiatum. StrL: Stratum lacunosum. StrM: Stratum moleculare. GC: Granule cell layer. Hil: Hilus. Green: FLAG. Red: Vglut1. Blue: DAPI-stained cell nuclei. Scale bar: 500 µm. **Lower Boxes**: Higher magnification of the stratum moleculare in the dentate gyrus of GABA-N-SF-CB1 and GABA-CB1-SF-C (areas indicated by white boxes in overview illustration) showing co-expression of FLAG and VGAT as indicated by white arrows. Green: FLAG. Red: VGAT. Blue: DAPI-stained cell nuclei.

In GABA-N-SF-CB1 and GABA-CB1-SF-C mice, FLAG staining was generally less intense as compared to Glu-N-SF-CB1 and Glu-CB1-SF-C. The strongest immunoreactivity was observed in the stratum moleculare and the stratum pyramidale of CA3, CA2 and lateral CA1. Consistent with this observation, the Cre expression-driving promoter Dlx5/6 was shown to be active in neocortical parvalbumin positive interneurons, which in the hippocampus can be subdivided into basket, axo-axonic, bistratified and oriens-lacunosum moleculare cells, which innervate pyramidal cells on different subcellular regions, respectively (Klausberger et al., 2005). The overlap with VGAT immunoreactivity confirms the presynaptic localization of CB1-SF on GABAergic interneurons.

#### *4.2.2.2 Preparation of subcellular fractions of hippocampal tissue*

CB1 exerts its main actions at neuronal synapses. To obtain an enriched fraction of synaptic proteins in the source material used for the TAP of CB1 protein complexes, synaptosomes were prepared as described (Carlin et al., 1980) (3.7). Throughout the preparation procedure samples were collected as shown in Fig. 4.8 for western blot analysis to validate the presence of the postsynaptic density protein 95 (PSD95), which served as a marker for the synaptosomal compartment.

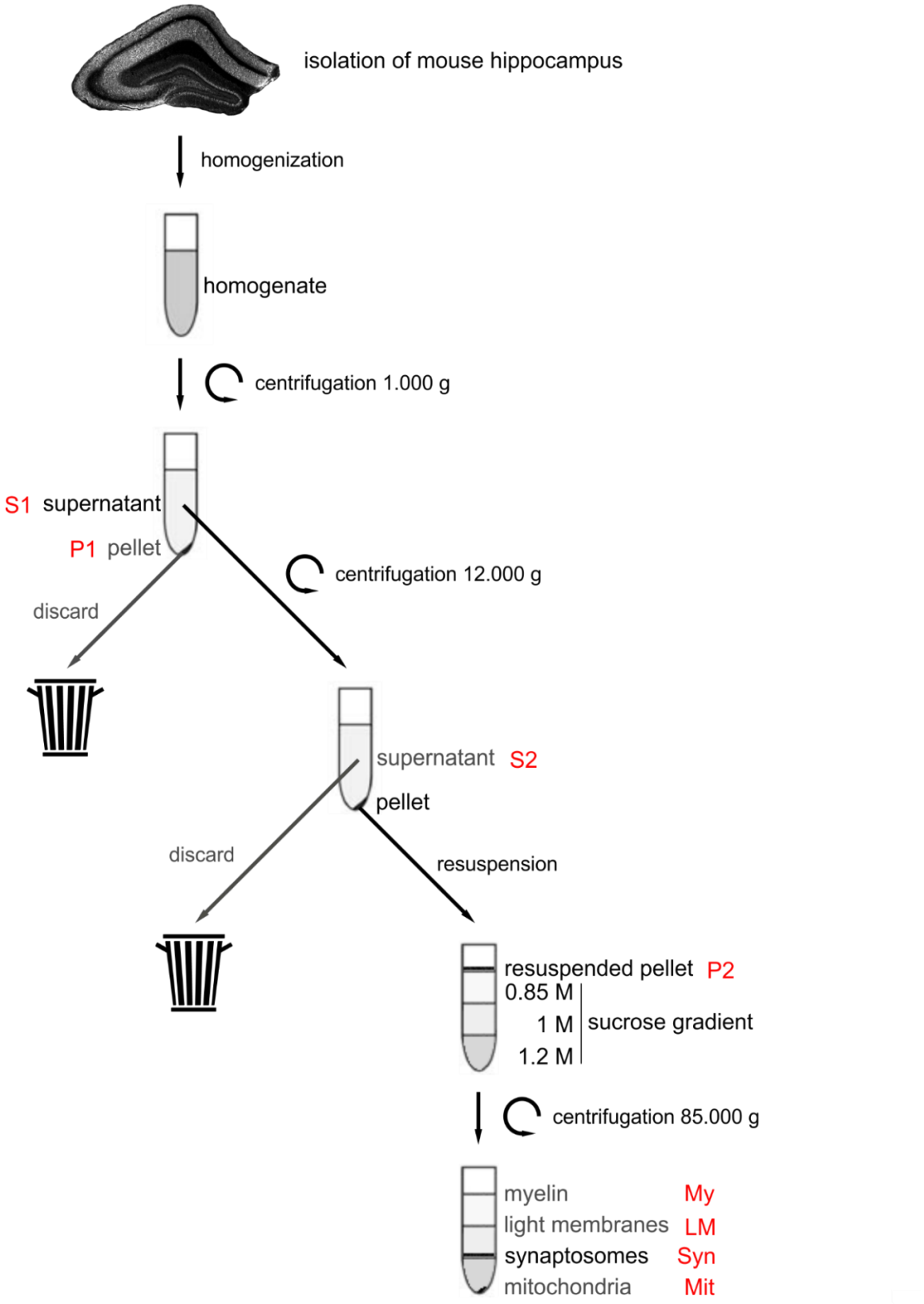


**Fig. 4.8 Schematic diagram of the synaptosome preparation protocol**

Samples were taken at various steps throughout the synaptosome preparation procedure as indicated by red abbreviations and kept for western blot analysis of the synaptosome marker protein PDS95.

Western blot analysis of the samples, using a PSD95 antibody, showed an enrichment of PSD95 protein in every step throughout the preparation procedure, finally showing clear evidence of the synaptosomal marker protein in the final sample (Fig. 4.9; Syn). Only after the first centrifugation step, there is a loss of a part of the synaptosomal fraction in the pellet (Fig. 4.9; P1). After centrifuging the sample through the sucrose gradient, no PSD95 signal can be observed in the subcellular fractions of myelin (Fig. 4.9; My), light membranes (Fig. 4.9; LM) or mitochondria (Fig. 4.9; Mit).

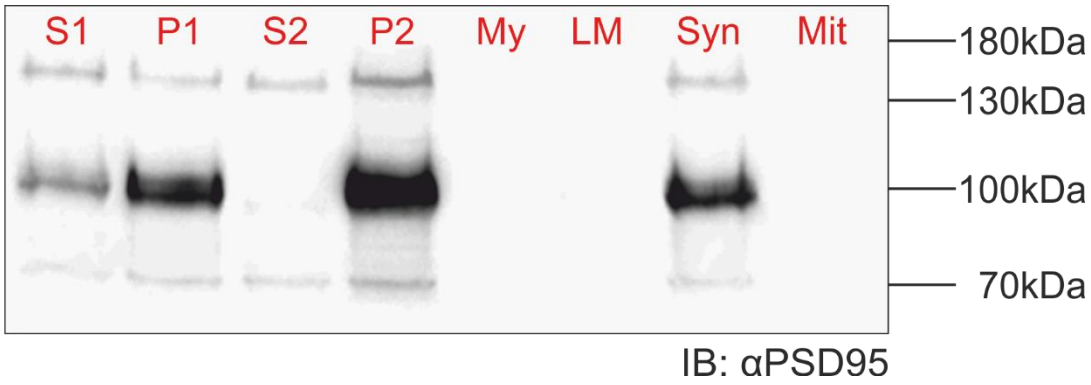


**Fig. 4.9 Western blot analysis of individual steps of the synaptosome preparation procedure**

Western Blot analysis of samples as shown in Fig. 4.8 taken throughout the synaptosome preparation using an anti PSD95 antibody as a marker for the synaptosomal compartment. Loss of a part of PSD95 is visible in the pellet after the first centrifugation step (P1). No loss is visible after the second centrifugation as indicated by the lack of a signal in the supernatant (S2) with an increase in the PSD95 concentration in the pellet (P2) as compared to the previous step. After centrifugation of the resuspended pellet P2 through the sucrose gradient, PSD95 is only visible in the synaptosomal compartment (Syn), but not in the myelin, light membrane, or mitochondrial fraction. kDa: kilodalton. IB: immunoblot.

The subcellular fractionation of the synaptosomal compartment could successfully be performed, but as there is also a mitochondrial location of CB1, which could be analyzed separately in regard to protein-protein interactions using the TAP technique, the purity of the synaptosomal and mitochondrial fraction was further investigated. Samples of synaptosomes and mitochondria were taken after centrifugation through the sucrose gradient in the synaptosome preparation procedure, as shown in Fig. 4.8, and both analyzed using an anti PSD95 antibody as a marker for the synaptosomal compartment and an antibody directed towards cytochrome c oxidase subunit IV (CoxIV) as a marker for the mitochondrial compartment (Fig. 4.10).

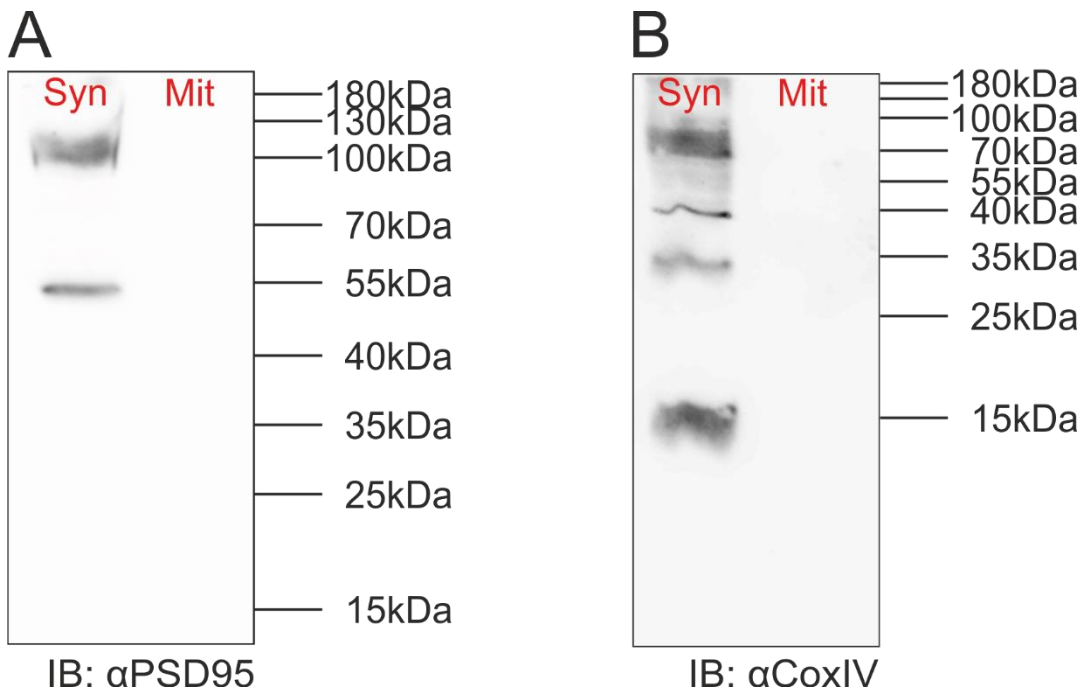


**Fig. 4.10 Western blot analysis of synaptosomal and mitochondrial fractions after synaptosome preparation**

Western blot analyses of synaptosomal fraction (Syn) and mitochondrial fraction (Mit) after synaptosome preparation. **A**: PSD95 is detected only in the synaptosomal fraction as indicated by the 100kDa band. An additional band is visible at 54kDa. **B**: CoxIV is detected only in the synaptosomal fraction and not in the mitochondrial fraction as indicated by the specific 15kDa band and additional bands. No signal is visible in the mitochondrial fraction indicating the localization of mitochondria in the synaptosomal compartment after the synaptosome preparation process. kDa: kilodalton. IB: immunoblot.

PSD95 and CoxIV were detected only in the synaptosomal, but not in the mitochondrial fraction after the purification procedure indicating that the majority of mitochondria remains localized in the synaptosomal compartment. Therefore, the TAP method was applied on a combined sample of purified synaptosomes including mitochondria.

#### *4.2.2.3 Optimization of the SF-TAP method for synaptosome preparations after AAV-mediated neuron type-specific expression of N-SF-CB1 and CB1-SF-C in mouse hippocampal tissue*

In order to optimize the SF-TAP method itself, initially only Glu-CB1-KO mice were used to express SF-tagged CB1 in glutamatergic neurons as the method itself should work independently from the site of expression within the same brain region, and therefore should be feasible afterwards for the expression of the same target protein in other types of neurons, such as GABAergic interneurons.

Three weeks after stereotactic delivery of the AAV, hippocampi from five mice per TAP were isolated and synaptosome preparations performed as source material for subsequent TAPs. In accordance with the optimization process using HEK293 cells, the final eluates were analyzed in regard to the presence of the SF-tagged CB1 protein and additional samples collected throughout the procedure, which were kept for western blot analysis (Fig. 4.1). Lysis of the synaptosome preparations was performed overnight as it was shown that the amount of solubilized receptors reach a maximum after approximately 15h with the use of the respective detergents (Daulat et al., 2007).

TAPs of both Glu-N-SF-CB1 and Glu-CB1-SF-C were successfully performed at concentrations of 0.3% (lysis buffer/wash buffer) Brij O10 and 0.5% (lysis buffer)/0.1% (wash buffer) digitonin of hippocampal synaptosome preparations as shown by western blot analysis using an anti CB1 antibody (Fig. 4.11). Using the same concentration of Brij O10 in the lysis and wash buffer did not lead to any observable changes in the outcome of the TAP. The same volume of each sample was loaded onto the lanes of the gel to allow for a relative comparison of the concentration of the target protein in the respective samples. In contrast to the TAPs of transfected HEK293 cells, purifications of Glu-N-SF-CB1 and Glu-CB1-SF-C from synaptosome preparations worked for both detergents tested.

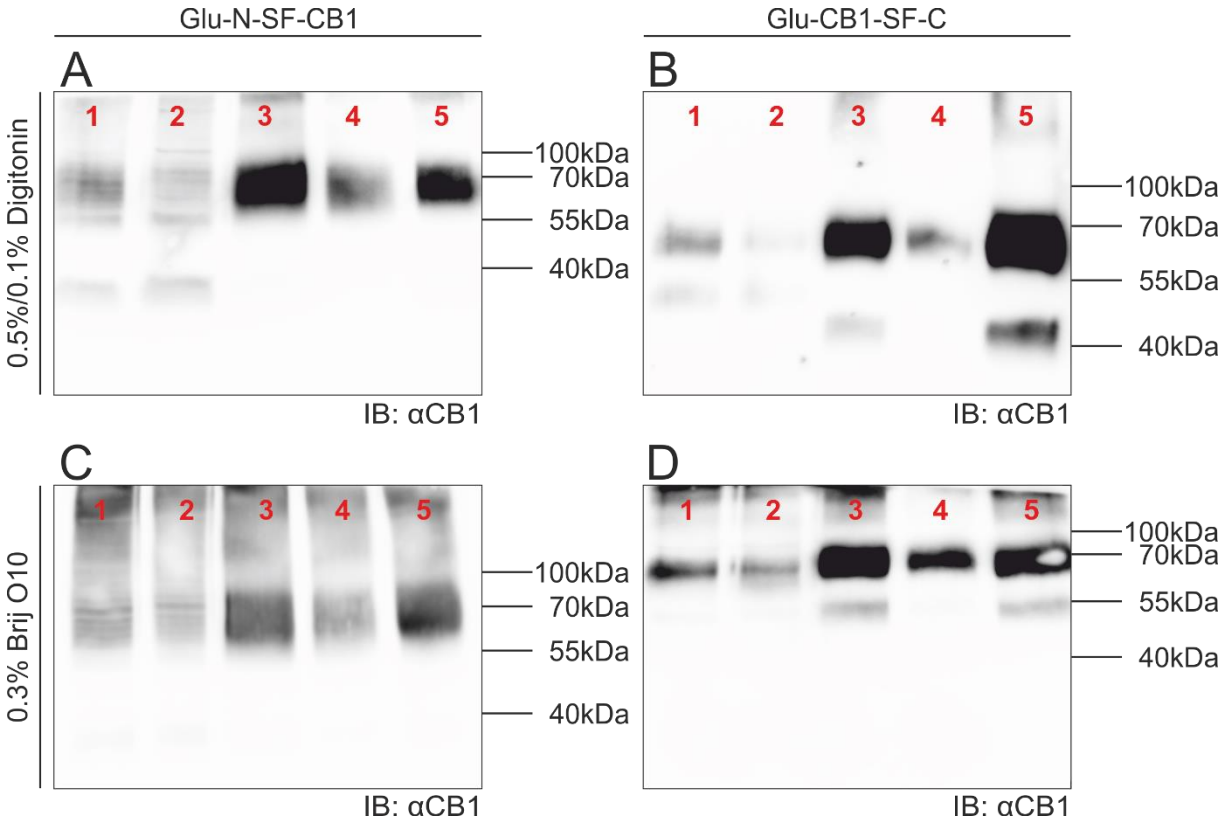


**Fig. 4.11 Western blot analysis of samples taken during various steps of individual TAP procedures for Glu-N-SF-CB1 and Glu-CB1-SF-C**

TAPs of synaptosomal preparations of mice expressing N-SF-CB1 (**A**, **C**) or CB1-SF-C (**B**, **D**) in hippocampal glutamatergic neurons using 0.5% (lysis buffer)/0.1% (wash buffer) digitonin (**A**, **B**) or 0.3% (lysis buffer/wash buffer) Brij O10 (**C**, **D**). 1: Lysate of synaptosome preparations. 2: Supernatant after Streptavidin bead incubation. 3: Eluate from Streptavidin beads. 4: Supernatant after M2 anti FLAG bead incubation. 5: Eluate from M2 anti FLAG beads. **A, B, C, D**: Successful expression and purification of Glu-N-SF-CB1 and Glu-CB1-SF-C as indicated by CB1-specific bands in the synaptosome lysate (1), in the first eluate from Streptavidin beads (3) and in the final eluate after binding and elution from M2 anti FLAG beads (5). kDa: Kilodalton. IB: Immunoblot.

AAV-Stop-CB1-SF-C was then injected into the hippocampi of GABA-CB1-KO mice (Monory et al., 2006) via bilateral stereotactic injection. These mice show a restricted expression of Cre in forebrain GABAergic interneurons leading to a knockout of endogenous CB1 and expression of SF-tagged CB1 in hippocampal GABAergic interneurons (GABA-CB1-SF-C), according to the cell type-specific expression of SF-tagged CB1 in glutamatergic neurons. Synaptosome preparations of five AAV-injected mice underwent TAP procedures using digitonin and Brij O10, respectively. This time only the final eluates were analyzed with regard to the presence of SF-tagged CB1 with western blots using CB1-specific antibody (Fig. 4.12).

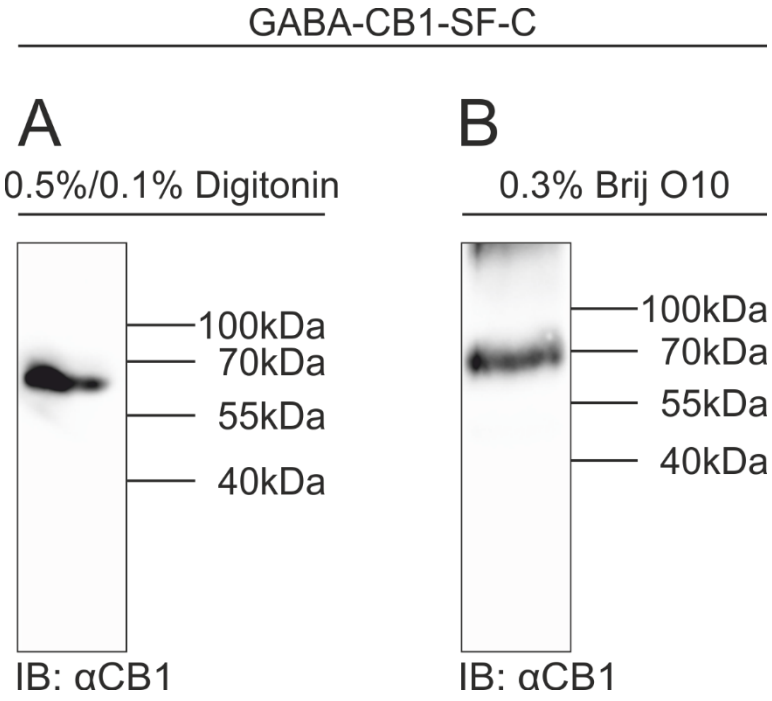


**Fig. 4.12 Western Blot analysis of final TAP eluates of GABA-CB1-SF-C**

Final eluates of TAPs of synaptosomal preparations of mice expressing CB1-SF-C in hippocampal GABAergic interneurons using 0.5% (lysis buffer)/0.1% (wash buffer) digitonin (**A**) or 0.3% (lysis buffer/wash buffer) Brij O10 (**B**). Purification of CB1-SF-C was successfully performed for both detergents tested as indicated by CB1-specific bands in the final eluates after the TAP procedure. kDa: Kilodalton. IB: Immunoblot.

The purification of CB1-SF-C was successfully performed when expressed in GABAergic interneurons with weaker band intensities in western blot analysis as compared to the TAP of Glu-CB1-SF-C. This indicated a lower amount of CB1-SF-C protein expressed in the hippocampus due to a smaller number of GABAergic interneurons as compared to glutamatergic principal cells.

In the next step, the samples had to be analyzed in regard to co-purified proteins, therefore silver stainings of final TAP eluates of Glu-N-SF-CB1, Glu-CB1-SF-C, and GABA-CB1-SF-C were performed (Fig. 4.13).

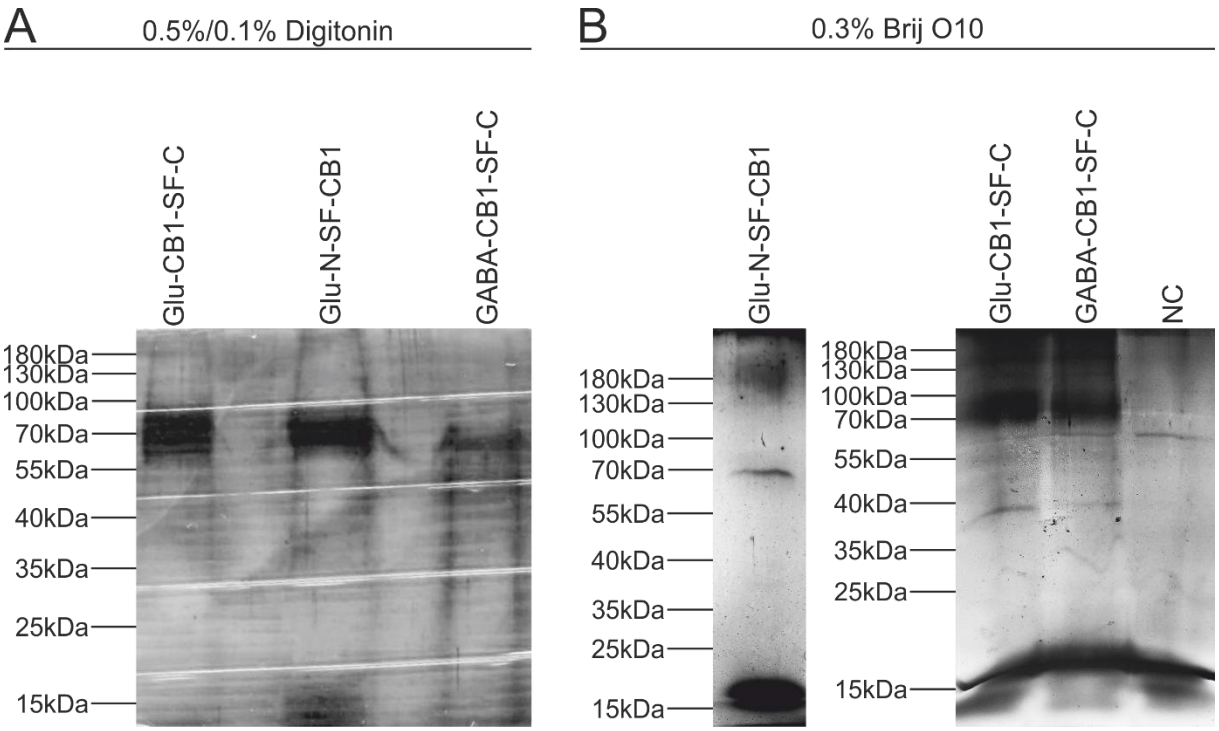


**Fig. 4.13 Silver stainings of TAP eluates of Glu-N-SF-CB1, Glu-CB1-SF-C and GABA-CB1-SF-C**

**A**: TAP eluates of Glu-N-SF-CB1, Glu-CB1-SF-C, and GABA-CB1-SF-C when 0.5% (lysis buffer)/0.1% (wash buffer) digitonin was used in the purification process. In all three samples a band at 64 kDa is visible in accordance to the molecular weight of the SF-tagged CB1 detected by western blot analysis. In the GABA-CB1-SF-C sample, the staining intensity is not as strong as compared to the TAPs of Glu-N-SF-CB1 and Glu-CB1-SF-C indicating for a decreased amount of CB1-SF-C in the hippocampus due to the expression in a smaller number of GABAergic interneurons as compared to glutamatergic neurons. No additional bands are visible. **B**: TAP eluates of Glu-N-SF-CB1, Glu-CB1-SF-C, GABA-CB1-SF-C, and non-injected animals as a negative control (NC) processed with 0.3% (lysis buffer/wash buffer) Brij O10. Glu-N-SF-CB1 again shows a band at 64kDa as expected for SF-tagged CB1, but no further bands are visible except smear in the high molecular weight area around 180kDa. Glu-CB1-SF-C and GABA-CB1-SF-C also show a strong band at 64 kDa with additional bands and smear throughout the respective lanes as compared with the NC indicating for further co-purified proteins. kDa: kilodalton.

The use of digitonin in the TAP process led to a successful purification of SF-tagged CB1 when expressed in glutamatergic neurons, as well as GABAergic interneurons, but silver stainings show no additional bands, indicating no co-purification of further interacting proteins. With the use of Brij O10, however, the silver stainings of Glu-CB1-SF-C, as well as GABA-CB1-SF-C, clearly indicated a variety of purified proteins in addition to the SF-tagged CB1. The TAP of Glu-N-SF-CB1 again showed only a band at the expected molecular weight for the SF-tagged CB1 without any further bands, in accordance with results obtained from TAPs of N-SF-CB1-transfected HEK293 cells (Fig. 4.3). Due to the lack of evidence for N-terminal tagged CB1 working out properly as a bait protein for the co-purification of interacting proteins of CB1, all following experiments were performed using C-terminally SF-tagged CB1.

#### 4.2.2.4 *AAV-mediated cell type-specific expression of CB1-SF-C in mouse hippocampus occurs at levels comparable to endogenous CB1*

Preceding results showed that TAPs of hippocampal synaptosome preparations expressing CB1-SF-C could be performed with a concomitant purification of additional proteins, whereas there was no evidence of co-purified proteins associated with N-SF-CB1 in a protein complex. In order to evaluate the AAV-mediated expression levels of CB1-SF-C *in vivo*, stereotactic injections of AAV-Stop-CB1-SF-C in the hippocampi of adult Glu-CB1-KO and GABA-CB1-KO mice were performed. Three weeks after injection, a western blot analysis of hippocampal lysates was performed in order to compare the expression levels of endogenous CB1 and recombinant CB1-SF-C in AAV-Stop-CB1-SF-C-injected Glu-CB1-KO mice (Glu-CB1-SF-C) and GABA-CB1-KO mice (GABA-CB1-SF-C), non-injected Glu-CB1-KO mice and GABA-CB1-KO mice, CB1-KO mice, and C57BL/6N mice (Fig. 4.14).

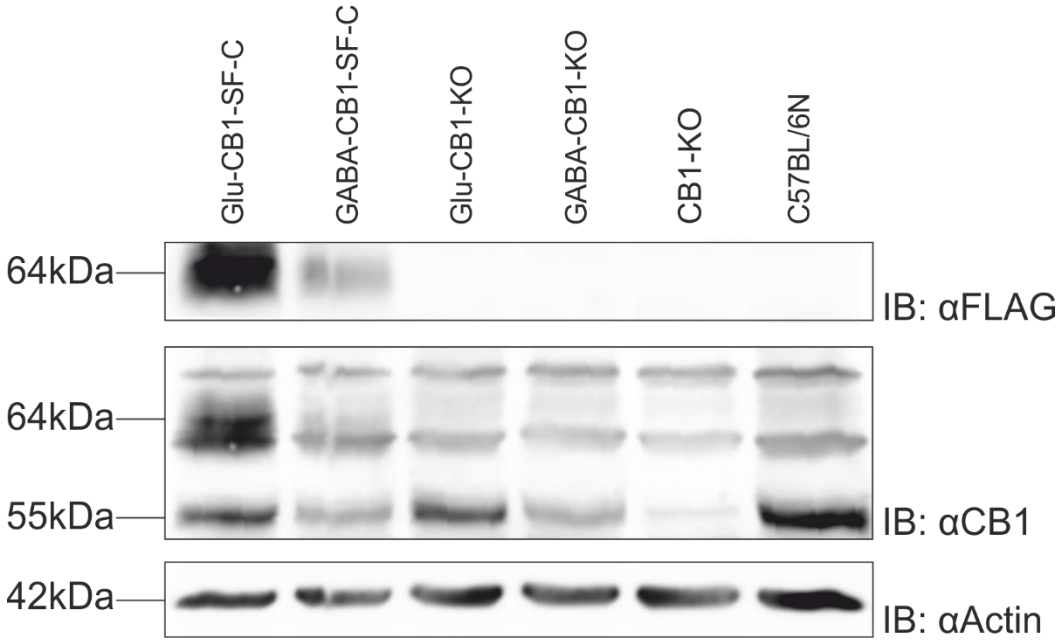


**Fig. 4.14 Western blot analysis of endogenous CB1 and recombinant CB1-SF-C expression in mouse hippocampus**

Glu-CB1-SF-C and GABA-CB1-SF-C show expression of recombinant CB1-SF-C protein detected with anti FLAG antibody at 64 kDa. The same bands are visible using anti CB1 antibody showing CB1-SF-C together with endogenous CB1 expressed at varying levels in the different mouse lines at 55 kDa. CB1-SF-C-specific signals at 64 kDa using anti CB1 antibody are close to unspecific background bands in every sample. Highest band intensity of endogenous CB1 was visible in wild-type C57BL/6N mice. Decreased CB1 expression was observed in the Glu-CB1-KO mice and even less in the GABA-CB1-KO mice due to the significantly higher loss of CB1 in GABAergic interneurons as compared to glutamatergic neurons. In contrast to the endogenous CB1 expression levels, the recombinant AAV-mediated CB1-SF-C levels are inverted because of the higher number of glutamatergic principal cells compared to GABAergic interneurons and AAV-mediated CB1-SF-C expression under control of the same CAG promoter in both neuronal subtypes. Actin is shown for comparison of total protein amount used for each sample. kDa: Kilodalton. IB: Immunoblot.

Using a CB1-specific antibody, we could clearly distinguish between the endogenously expressed CB1 (55 kDa) and the recombinant CB1-SF-C (64 kDa). The highest band intensity of endogenous CB1 was visible in the C57BL/6N mice. Decreased CB1 expression was observed in the Glu-CB1-KO mice and even less in the GABA-CB1-KO mice, in accordance with a significantly higher amount of CB1 in GABAergic interneurons, although the higher number of glutamatergic principal neurons in the hippocampus (Marsicano and Lutz, 1999). Densitometric quantification of western blot band intensities showed an approximately 3x higher expression of CB1-SF in glutamatergic neurons as compared to endogenous CB1, and vice versa a slightly lower, but not significant, expression of CB1-SF as compared to endogenous CB1 in GABAergic neurons (Fig. 4.15).

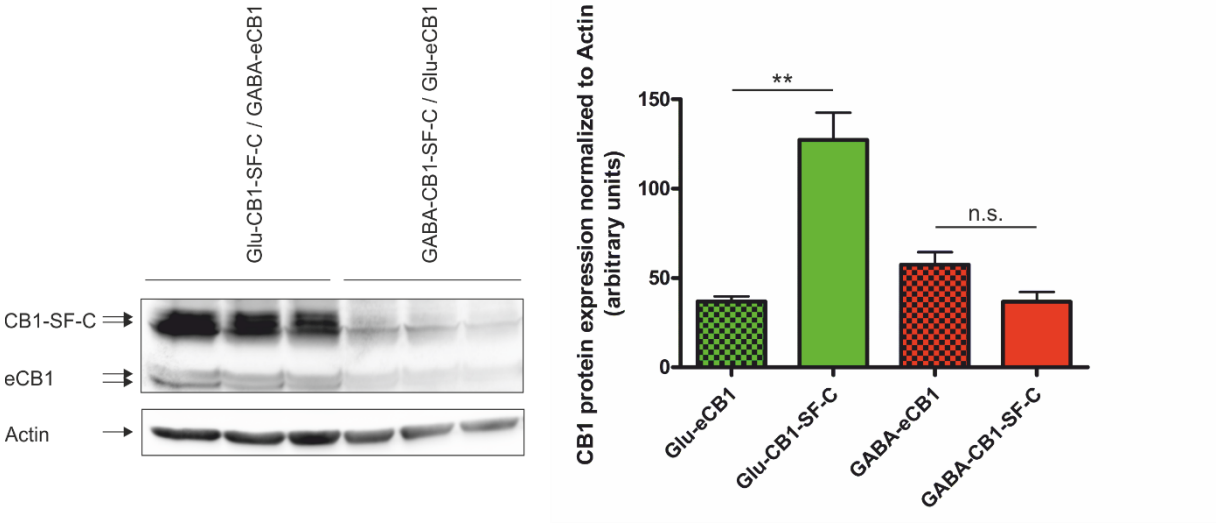


**Fig. 4.15 Densitometric quantification of the expression of recombinant SF-tagged CB1 as compared to endogenous CB1 (eCB1).**

Densitometric quantification of western blot band intensities of AAV-Stop-CB1-SF-C-injected Glu-CB1-KO mice (Glu-CB1-SF-C + GABA-eCB1) and AAV-Stop-CB1-SF-C-injected GABA-CB1-KO mice (GABA-CB1-SF-C + Glu-eCB1) (n = 3). Expression of CB1-SF-C is approximately 3x higher as compared to eCB1 in glutamatergic neurons, whereas in GABAergic interneurons the expression of CB1-SF-C is only slightly lower than eCB1. Importantly, the overall expression levels of the recombinant CB1 are comparable to those of the endogenous CB1 without a pronounced overexpression that might occur using AAV vectors. ** = $p < 0.01$; unpaired t-test analysis, two-tailed.

It has to be considered that the transgenic CAG promoter is driving expression with the same intensity in both neuronal populations, whereas the endogenous CB1 expression in glutamatergic and GABAergic neurons differs to a very high degree (Steindel et al., 2013). Therefore, the CB1-SF-C band intensity is higher in the Glu-CB1-SF-C mice as compared to the GABA-CB1-SF-C mice because of the higher number of glutamatergic neurons relative to GABAergic interneurons. Most importantly, the overall band intensities of the recombinant CB1 are comparable to those of the

endogenous CB1 without vast differences that might occur using AAV-mediated overexpression under the CAG promoter. After stripping the membrane and re-incubating with a FLAG-specific antibody, we confirmed the 64 kDa band as the recombinant CB1-SF-C, again showing a stronger signal in the Glu-CB1-SF-C mice as compared to the GABA-CB1-SF-C mice (Fig. 4.14).

### 4.2.3 Analysis and comparison of mouse hippocampal glutamatergic and GABAergic CB1 receptor complexes

Based on the results of the optimization process, TAPs of CB1-SF-C following AAV-mediated overexpression in mouse hippocampal glutamatergic neurons or GABAergic interneurons were performed using Brij O10 throughout the TAP procedure. To obtain a sufficient amount of total protein in the final samples for the MS analysis, four TAPs of Glu-CB1-SF-C mice were pooled and eight TAPs of GABA-CB1-SF-C mice, respectively. Additionally, four pooled TAPs of non-AAV-injected mice served as a negative control (control-TAP).

#### *4.2.3.1 Identification of proteins in the TAP samples of glutamatergic and GABAergic CB1 protein complexes*

A deep-coverage proteomics approach (Distler et al., 2014) led to the identification of 951 specifically enriched proteins in the Glu-CB1-SF-C-TAP and GABA-CB1-SF-C-TAP as compared to the control-TAP sample (Tab. 8.2). Although all proteins in the dataset were detected as high confidence interactors, a STRING network analysis was performed with only the proteins with a relative molar ratio of at least 1% as compared to the bait CB1-SF protein for the following reason. STRING does not consider the abundance of the detected proteins, and CRIP1a, a previously described interactor of CB1 was identified in our dataset as a CB1 interactor with a relative molar ratio of close to 1% in both neuronal subtypes (Glu: 0.009, GABA: 0.008). Among these 571 proteins, the majority showed no enrichment in glutamatergic or GABAergic CB1 complexes. Specificity was determined as a $\geq$ 2x enrichment of a protein in one cell type as compared to the other one. 33 proteins in the AAV-Glu-CB1-SF-TAP and 56 proteins in the AAV-GABA-CB1-SF-TAP fulfilled this criterion (Fig. 4.16; Tab. 4.1).

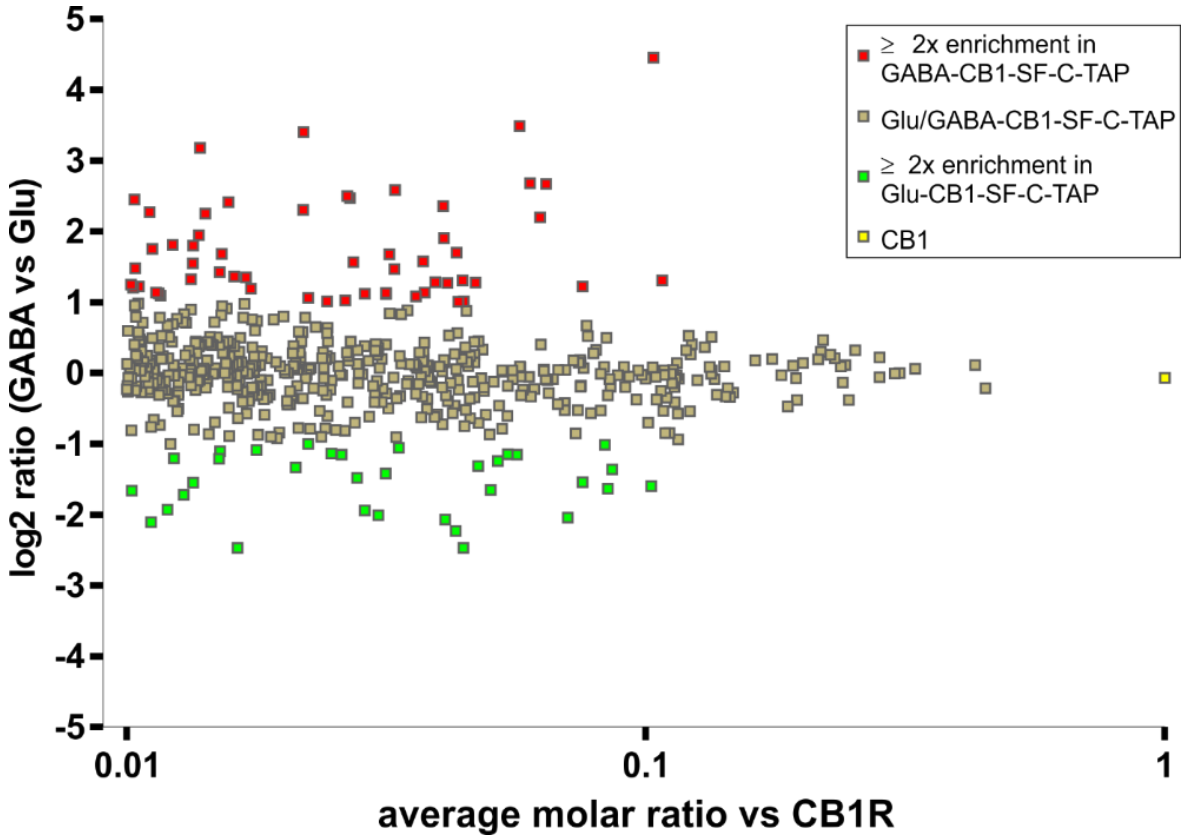


**Fig. 4.16 Dotplot of identified proteins in TAP samples with a molar ratio of at least 1% to CB1**

Dotplot diagram of proteins identified in the TAP samples of Glu-CB1-SF-C and GABA-CB1-SF-C with a molar ratio of at least 1% to CB1. Specificity for one cell type was determined as a ≥ 2x enrichment of a protein in one neuronal subtype as compared to the other, and indicated with green color for glutamatergic neurons and red color for GABAergic neurons. Brown color indicates no specificity for one or the other cell type. X-axis: logarithmic scale of molar ratio of the protein to CB1 (yellow). For non-specific proteins (brown), the average molar ratio to CB1 in glutamatergic and GABAergic CB1-SF-C-TAP samples is shown. For Glu- or GABA-specific proteins (green and red, respectively) the molar ratio of the protein in the respective sample as compared to CB1 is shown. Y-axis: $\log_2$ ratio of the abundance of the identified protein relative to CB1 in Glu-CB1-SF-C to the abundance of the identified protein relative to CB1 in GABA-CB1-SF-C.

## Tab. 4.1 Glu-CB1-SF-C-TAP- and GABA-CB1-SF-C-TAP-specific proteins

All cell type-specific proteins identified in the Glu-CB1-SF-C-TAP and GABA-CB1-SF-C-TAP with a relative molar ratio of at least 1% to CB1. Specificity was determined as a ≥ 2x enrichment of the abundance of a protein in one cell type as compared to the other. gene name: official gene symbol of the respective protein; molar ratio to CB1: molar ratio of the protein relative to CB1 either in the Glu-CB1-SF-C-TAP or GABA-CB1-SF-C-TAP, respectively; UniProt entry: UniProtKB/Swiss-Prot entry name of the protein; description: detailed description of the identified protein. **A**: Glu-CB1-SF-C-TAP-specific proteins. **B**: GABA-CB1-SF-C-TAP-specific proteins.

**A** Glu-CB1-SF-C-TAP-specific proteins

| gene name | molar ratio to CB1 | UniProt entry | description |
|---|---|---|---|
| Epha4 | 0.1024 | EPHA4_MOUSE | Ephrin type-A receptor 4 |
| Adcy9 | 0.0861 | ADCY9_MOUSE | Adenylate cyclase type 9 |
| Prkcg | 0.0846 | KPCG_MOUSE | Protein kinase C gamma type |
| Fxyd7 | 0.0833 | FXYD7_MOUSE | FXYD domain-containing ion transport regulator 7 |
| Hpca | 0.0755 | HPCA_MOUSE | Neuron-specific calcium-binding protein hippocalcin |
| Krt81 | 0.0707 | KRT81_MOUSE | Keratin, type II cuticular Hb1 |
| Sept7 | 0.0564 | SEPT7_MOUSE | Septin-7 |
| Sema4b | 0.0542 | SEM4B_MOUSE | Semaphorin-4B |
| Krt34 | 0.0518 | KRT34_MOUSE | Keratin, type I cuticular Ha4 |
| Lztr1 | 0.0502 | LZTR1_MOUSE | Leucine-zipper-like transcriptional regulator 1 |
| Krt85 | 0.0475 | KRT85_MOUSE | Keratin, type II cuticular Hb5 |
| Krt35 | 0.0445 | KRT35_MOUSE | Keratin, type I cuticular Ha5 |
| Napa | 0.043 | SNAA_MOUSE | Alpha-soluble NSF attachment protein |
| Krt4 | 0.0411 | K2C4_MOUSE | Keratin, type II cytoskeletal 4 |
| Grm2 | 0.0334 | GRM2_MOUSE | Metabotropic glutamate receptor 2 |
| Krt33a | 0.0315 | KT33A_MOUSE | Keratin, type I cuticular Ha3-I |
| Krt31 | 0.0305 | K1H1_MOUSE | Keratin, type I cuticular Ha1 |
| Pde2a | 0.0287 | PDE2A_MOUSE | cGMP-dependent 3',5'-cyclic phosphodiesterase |
| - | 0.0278 | CA095_MOUSE | Uncharacterized membrane protein C1orf95 homolog |
| Npy2r | 0.0259 | NPY2R_MOUSE | Neuropeptide Y receptor type 2 |
| Kcnma1 | 0.0248 | KCMA1_MOUSE | Calcium-activated potassium channel subunit alpha-1 |
| Plxna1 | 0.0224 | PLXA1_MOUSE | Plexin-A1 |
| Abca7 | 0.0211 | ABCA7_MOUSE | ATP-binding cassette sub-family A member 7 |
| C1ql3 | 0.0178 | C1QL3_MOUSE | Complement C1q-like protein 3 |
| Islr2 | 0.0163 | ISLR2_MOUSE | Immunoglobulin superfamily containing leucine-rich repeat protein 2 |
| Unc5a | 0.0151 | UNC5A_MOUSE | Netrin receptor UNC5A |
| Acvr1b | 0.0151 | ACV1B_MOUSE | Activin receptor type-1B |
| Sept3 | 0.0134 | SEPT3_MOUSE | Neuronal-specific septin-3 |
| Fam189a1 | 0.0129 | F1891_MOUSE | Protein FAM189A1 |
| Bbs7 | 0.0123 | BBS7_MOUSE | Bardet-Biedl syndrome 7 protein homolog |
| Kdr | 0.012 | VGFR2_MOUSE | Vascular endothelial growth factor receptor 2 |
| Tspan18 | 0.0111 | TSN18_MOUSE | Tetraspanin-18 |
| Plxnd1 | 0.0102 | PLXD1_MOUSE | Plexin-D1 |

**B** GABA-CB1-SF-C-TAP-specific proteins

| gene name | molar ratio to CB1 | UniProt entry | description |
|---|---|---|---|
| Slc32a1 | 0.1074 | VIAAT_MOUSE | Vesicular inhibitory amino acid transporter |
| Hspa5 | 0.1034 | GRP78_MOUSE | 78 kDa glucose-regulated protein |
| Gad1 | 0.0755 | DCE1_MOUSE | Glutamate decarboxylase 1 |
| Mgll | 0.0643 | MGLL_MOUSE | Monoglyceride lipase |
| Kcnc2 | 0.0626 | KCNC2_MOUSE | Potassium voltage-gated channel subfamily C member 2 |
| Slc6a1 | 0.0599 | SC6A1_MOUSE | Sodium- and chloride-dependent GABA transporter 1 |
| Gad2 | 0.057 | DCE2_MOUSE | Glutamate decarboxylase 2 |
| Hcn1 | 0.0469 | HCN1_MOUSE | Potassium/sodium hyperpol.-activated cyclic nucleotide-gated channel 1 |
| Prkar2a | 0.0446 | KAP2_MOUSE | cAMP-dependent protein kinase type II-alpha regulatory subunit |
| Lamp5 | 0.0444 | LAMP5_MOUSE | Lysosome-associated membrane glycoprotein 5 |
| Prkar2b | 0.0436 | KAP3_MOUSE | cAMP-dependent protein kinase type II-beta regulatory subunit |
| Eef2 | 0.0432 | EF2_MOUSE | Elongation factor 2 |
| Epb41l1 | 0.0414 | E41L1_MOUSE | Band 4.1-like protein 1 |
| C1qbp | 0.0408 | C1QBP_MOUSE | Complement component 1 Q subcomponent-binding protein, mitochondrial |
| Kcnc1 | 0.0407 | KCNC1_MOUSE | Potassium voltage-gated channel subfamily C member 1 |
| Kiaa1033 | 0.0393 | WASH7_MOUSE | WASH complex subunit 7 |
| Ndrg4 | 0.0374 | NDRG4_MOUSE | Protein NDRG4 |
| Ptprn | 0.0372 | PTPRN_MOUSE | Receptor-type tyrosine-protein phosphatase-like N |
| Ncam2 | 0.0361 | NCAM2_MOUSE | Neural cell adhesion molecule 2 |
| Ldhb | 0.0329 | LDHB_MOUSE | L-lactate dehydrogenase B chain |
| Cd99l2 | 0.0328 | C99L2_MOUSE | CD99 antigen-like protein 2 |
| Gnal | 0.0321 | GNAL_MOUSE | Guanine nucleotide-binding protein G(olf) subunit alpha |
| Syt2 | 0.0316 | SYT2_MOUSE | Synaptotagmin-2 |
| Erp44 | 0.0315 | ERP44_MOUSE | Endoplasmic reticulum resident protein 44 |
| Dhrs1 | 0.0287 | DHRS1_MOUSE | Dehydrogenase/reductase SDR family member 1 |
| Cd81 | 0.0273 | CD81_MOUSE | CD81 antigen |
| Kcna3 | 0.0269 | KCNA3_MOUSE | Potassium voltage-gated channel subfamily A member 3 |
| Kcnk1 | 0.0266 | KCNK1_MOUSE | Potassium channel subfamily K member 1 |
| Hist2h3c1 | 0.0264 | H32_MOUSE | Histone H3.2 |
| Hist1h3f | 0.0264 | H32_MOUSE | Histone H3.2 |
| Hist2h3c2 | 0.0264 | H32_MOUSE | Histone H3.2 |
| Hist1h3b | 0.0264 | H32_MOUSE | Histone H3.2 |
| Hist1h3d | 0.0264 | H32_MOUSE | Histone H3.2 |
| Hist2h3b | 0.0264 | H32_MOUSE | Histone H3.2 |
| Hist1h3e | 0.0264 | H32_MOUSE | Histone H3.2 |
| Hist1h3c | 0.0264 | H32_MOUSE | Histone H3.2 |
| Kcnc3 | 0.0243 | KCNC3_MOUSE | Potassium voltage-gated channel subfamily C member 3 |
| Hist1h3g | 0.0224 | H31_MOUSE | Histone H3.1 |
| Hist1h3h | 0.0224 | H31_MOUSE | Histone H3.1 |
| Hist1h3a | 0.0224 | H31_MOUSE | Histone H3.1 |
| Hist1h3i | 0.0224 | H31_MOUSE | Histone H3.1 |
| Irgm1 | 0.0219 | IRGM1_MOUSE | Immunity-related GTPase family M protein 1 |
| Clu | 0.0219 | CLUS_MOUSE | Clusterin |
| Myh14 | 0.0173 | MYH14_MOUSE | Myosin-14 |
| Asph | 0.017 | ASPH_MOUSE | Aspartyl/asparaginyl beta-hydroxylase |
| Prkaca | 0.0161 | KAPCA_MOUSE | cAMP-dependent protein kinase catalytic subunit alpha |
| H2-D1 | 0.0157 | HA11_MOUSE | H-2 class I histocompatibility antigen, D-B alpha chain |
| Sfn | 0.0152 | 1433S_MOUSE | 14-3-3 protein sigma |

| | | | |
|---|---|---|---|
| Krt18 | 0.0151 | K1C18_MOUSE | Keratin, type I cytoskeletal 18 |
| Pdia3 | 0.0142 | PDIA3_MOUSE | Protein disulfide-isomerase A3 |

**B** GABA-CB1-SF-C-TAP-specific proteins (continued)

| gene name | molar ratio to CB1 | UniProt entry | description |
|---|---|---|---|
| Hnrnpk | 0.0138 | HNRPK_MOUSE | Heterogeneous nuclear ribonucleoprotein K |
| Ptprt | 0.0138 | PTPRT_MOUSE | Receptor-type tyrosine-protein phosphatase T |
| Cntnap5a | 0.0134 | CTP5A_MOUSE | Contactin-associated protein like 5-1 |
| Neto1 | 0.0134 | NETO1_MOUSE | Neuropilin and tolloid-like protein 1 |
| Cnnm1 | 0.0133 | CNNM1_MOUSE | Metal transporter CNNM1 |
| Anxa1 | 0.0123 | ANXA1_MOUSE | Annexin A1 |
| Clstn3 | 0.0116 | CSTN3_MOUSE | Calsyntenin-3 |
| Slc38a1 | 0.0115 | S38A1_MOUSE | Sodium-coupled neutral amino acid transporter 1 |
| Kiaa0513 | 0.0114 | K0513_MOUSE | Uncharacterized protein KIAA0513 |
| Rps13 | 0.0112 | RS13_MOUSE | 40S ribosomal protein S13 |
| Oas1a | 0.0111 | OAS1A_MOUSE | 2'-5'-oligoadenylate synthase 1A |
| Hprt1 | 0.0105 | HPRT_MOUSE | Hypoxanthine-guanine phosphoribosyltransferase |
| Crip2 | 0.0104 | CRIP2_MOUSE | Cysteine-rich protein 2 |
| P4hb | 0.0103 | PDIA1_MOUSE | Protein disulfide-isomerase |
| Pccb | 0.0103 | PCCB_MOUSE | Propionyl-CoA carboxylase beta chain, mitochondrial |
| Csrp1 | 0.0102 | CSRP1_MOUSE | Cysteine and glycine-rich protein 1 |

Western Blot analyses of another three independent TAP samples of Glu-CB1-SF-C, GABA-CB1-SF-C, and control hippocampal synaptosome preparations confirmed the presence of a few selected proteins in the synaptosome input material, as well as in the respective TAP samples, whereas no bands were visible in the control-TAP (Fig. 4.17). The ratio of the band intensity of an identified protein to the band intensity of CB1 in one sample can be considered as the equivalent of the calculated relative abundance of the protein in the label-free quantification MS approach. Although using different antibodies for each protein in the WB analysis, the ratio of this ratio of band intensities for a protein in the Glu-CB1-SF-C-TAP to the GABA-CB1-SF-C-TAP can be compared to the ratio of the calculated abundances of the same protein in the Glu-CB1-SF-C-TAP and GABA-CB1-SF-C-TAP in the label-free quantification MS in order to confirm the MS results by WB densitometry. This Glu vs GABA ratio of ratios of the band intensities of one protein to the band intensity of CB1 in the same sample shows good correlation ($r^2 = 0.9809$) to the Glu vs GABA ratio of abundances of the same protein calculated in the label-free quantification MS approach (Fig. 4.18).

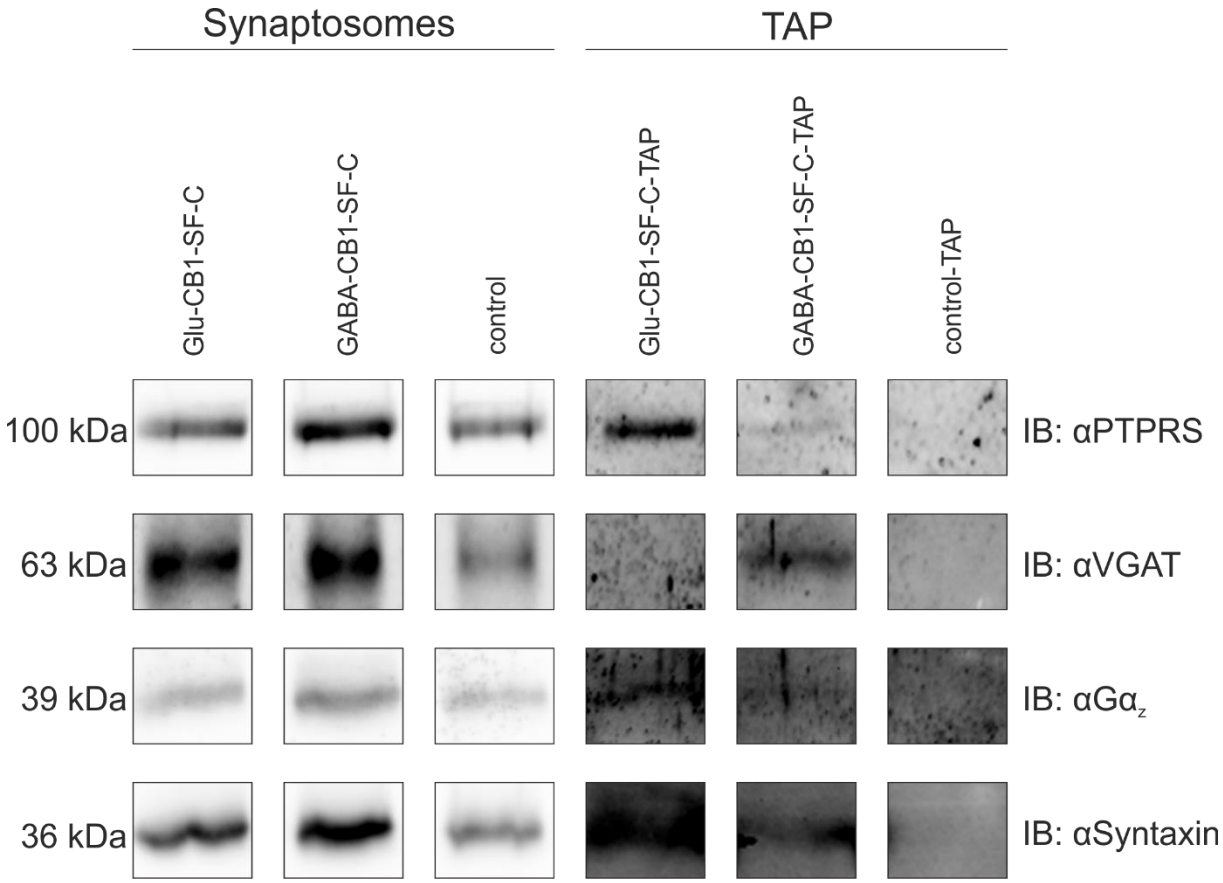


**Fig. 4.17 Western blot analysis of hippocampal synaptosomal TAP samples from Glu-CB1-SF-C, GABA-CB1-SF-C, and non-AAV-injected control mice**

Western blot analysis of TAPs of Glu-CB1-SF-C, GABA-CB1-SF-C, and control synaptosomal preparations confirming the presence of four selected proteins, which were identified in the MS approach. Syntaxin, guanine nucleotide-binding protein G(z) subunit alpha ($G\alpha_z$), vesicular inhibitory amino acid transporter (VGAT), and receptor-type tyrosine-protein phosphatase σ (PTPRS) were confirmed using specific antibodies against the respective proteins. Synaptosomal preparations, taken as input controls, showed specific bands for each protein at the respective molecular weights in all samples. TAP eluates showed specific bands only in the Glu-CB1-SF-C-TAP and GABA-CB1-SF-C-TAP, but not in the control-TAP for the respective proteins. kDa: kilodalton. IB: immunoblot.

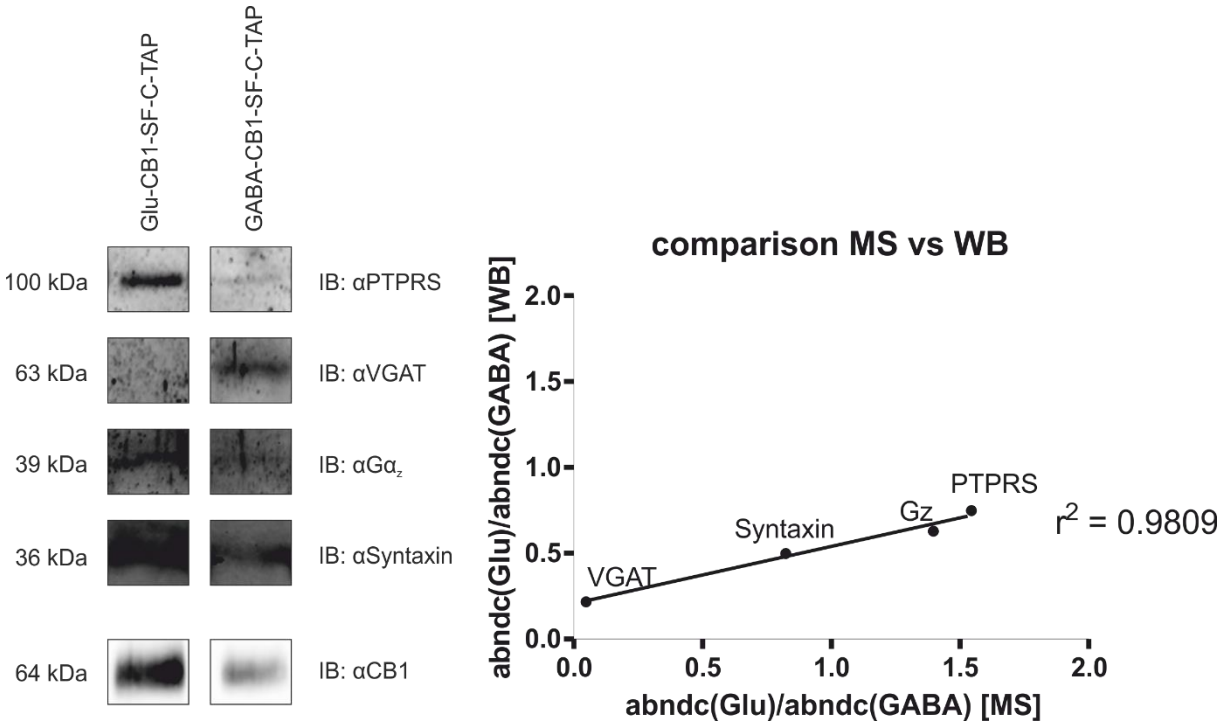


**Fig. 4.18 Comparison of the abundance of proteins obtained by MS and band intensities of proteins in the WB analysis**

Glu vs GABA ratio of the ratio of the WB band intensities of a protein to CB1 is compared to the Glu vs GABA ratio of abundance of the protein calculated in the label-free quantification MS approach. Despite the strong background in the WB samples, densitometry could be performed successfully and the ratio of a protein in the Glu-CB1-SF-C-TAP to the same protein in the GABA-CB1-SF-C-TAP as compared to the ratio of abundances of the same protein in the MS approach showed a good linear correlation ($r^2 = 0.9809$), thereby confirming the quantitative MS data. Differences in the ratio of the proteins in Glu vs GABA in the WB analysis are generally lower than in the MS approach, due to the strong background staining in the WB, and the use of different antibodies for each protein, which directly affects the calculated ratios for the protein to CB1. abndc (abundance): amount of protein in the respective TAP sample relative to CB1. $G\alpha_z$: guanine nucleotide-binding protein G(z) subunit alpha. VGAT: vesicular inhibitory amino acid transporter. PTPRS: receptor-type tyrosine-protein phosphatase σ. kDa: kilodalton. IB: immunoblot.

#### *4.2.3.2 Network analysis of the identified proteins in the Glu-CB1-SF-C-TAP and GABA-CB1-SF-C-TAP samples*

To gain insight into the functional properties of the identified proteins, a functional protein network analysis was performed considering all proteins with a molar ratio of at least 1% to CB1 using the STRING online tool. This tool generates protein association networks of the proteins by calculating confidence values based on known and predicted protein-protein interactions (Jensen et al., 2009). The resulting network was exported to the network data analysis software Cytoscape with every node representing a protein and confidence values of the protein interactions as edges. Using the ClusterMaker2 plugin, proteins were clustered into functional groups based on the interaction confidence values using the Markov Cluster Algorithm (MCL) and an inflation value of 1.8. Proteins that could not be embedded in the network by the STRING algorithm were discarded and left a network containing 483 proteins in 7 main clusters containing at least 15 proteins. Neuron type-specifically isolated proteins within these were colored in green (Glu-specific) or red (GABA-specific) to highlight neuron type-specific enrichment of proteins within the clusters (Tab. 4.2) together with an additional adjustment of color saturation to visualize their abundance. Furthermore, protein interactions calculated by the STRING algorithm are illustrated by solid lines for proteins grouped within a cluster and dashed lines for intercluster protein interactions. The associated confidence values are depicted with a transparency gradient of the lines ranging from light grey (low interaction confidence value) to dark grey (high interaction confidence value) (Fig. 4.19).

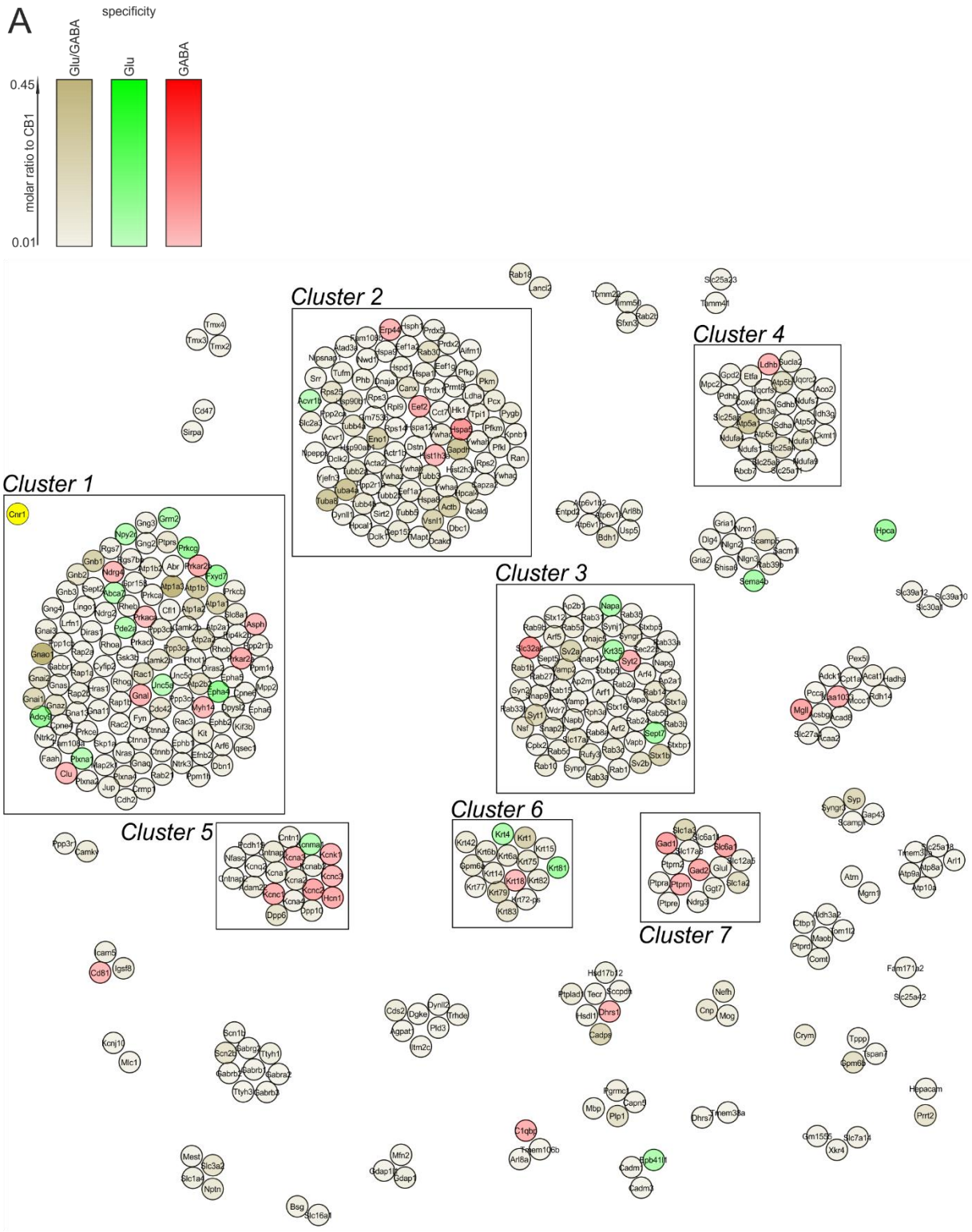
A
specificity
Glu/GABA
Glu
GABA
0.45
molar ratio to CB1
0.01
Cluster 1
Cluster 2
Cluster 3
Cluster 4
Cluster 5
Cluster 6
Cluster 7

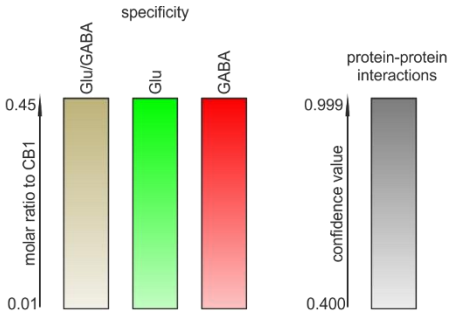
specificity
Glu/GABA
Glu
GABA
0.45
molar ratio to CB1
0.01
protein-protein interactions
0.999
confidence value
0.400

*Cluster 1*

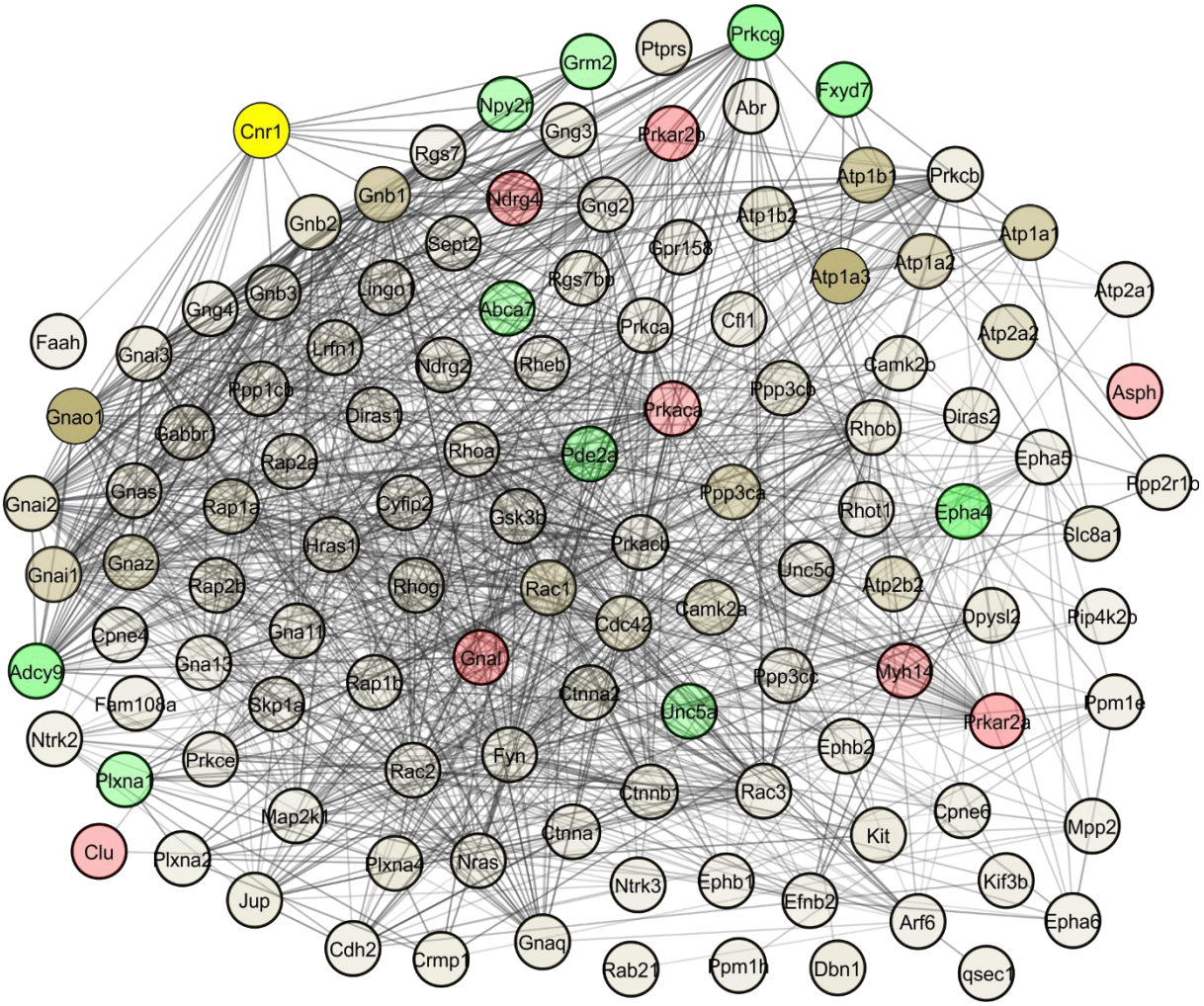
Prkcg
Ptprs
Grm2
Fxyd7
Npy2r
Abr
Cnr1
Gng3
Prkar2b
Rgs7
Atp1b1
Prkcb
Gnb1
Ndrg4
Gng2
Atp1b2
Atp1a1
Gnb2
Sept2
Gpr158
Atp1a3
Atp1a2
Atp2a1
Rgs7bp
Gng4
Gnb3
Lingo1
Abca7
Prkca
Cfl1
Atp2a2
Faah
Gnai3
Lrfn1
Ndrg2
Rheb
Camk2b
Ppp1cb
Ppp3cb
Asph
Gnao1
Diras1
Prkaca
Rhob
Diras2
Gabbr1
Rhoa
Pde2a
Epha5
Rap2a
Ppp2r1b
Gnai2
Gnas
Rap1a
Cyfip2
Ppp3ca
Rhot1
Epha4
Slc8a1
Gsk3b
Hras1
Prkacb
Gnai1
Gnaz
Unc5c
Atp2b2
Rap2b
Rhog
Rac1
Camk2a
Dpysl2
Pip4k2b
Cpne4
Gna11
Cdc42
Gna13
Gnal
Myh14
Adcy9
Ppp3cc
Ppm1e
Fam108a
Rap1b
Ctnna2
Unc5a
Skp1a
Prkar2a
Ntrk2
Ephb2
Prkce
Fyn
Plxna1
Rac2
Ctnnb1
Rac3
Cpne6
Map2k1
Kit
Mpp2
Ctnna1
Clu
Plxna2
Plxna4
Nras
Ntrk3
Ephb1
Kif3b
Jup
Efnb2
Arf6
Epha6
Cdh2
Crmp1
Gnaq
Rab21
Ppm1h
Dbn1
qsec1

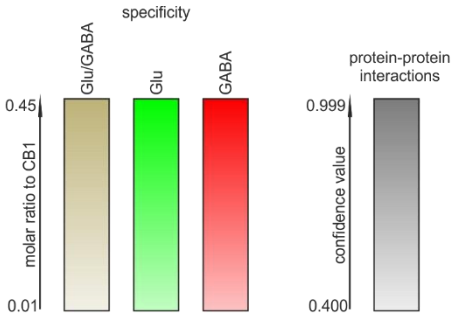
specificity
Glu/GABA
Glu
GABA
0.45
molar ratio to CB1
0.01
protein-protein interactions
0.999
confidence value
0.400

*Cluster 2*

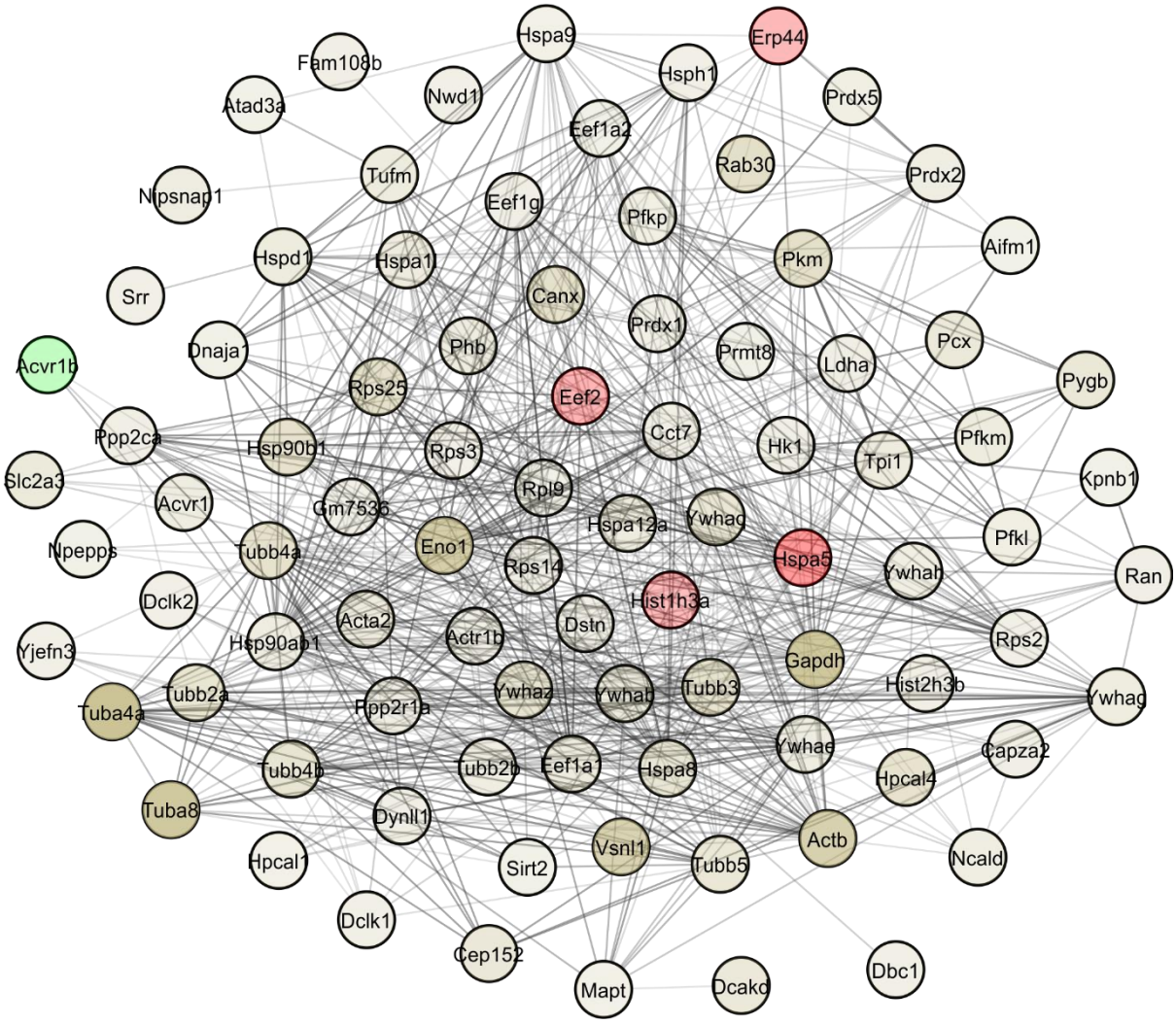
Hspa9
Erp44
Fam108b
Hsph1
Nwd1
Prdx5
Atad3a
Eef1a2
Rab30
Tufm
Prdx2
Nipsnap1
Eef1g
Pfkp
Aifm1
Hspd1
Hspa1
Pkm
Srr
Canx
Prdx1
Pcx
Dnaja1
Phb
Prmt8
Ldha
Acvr1b
Rps25
Eef2
Pygb
Ppp2ca
Hsp90b1
Rps3
Cct7
Hk1
Pfkm
Tpi1
Slc2a3
Rpl9
Kpnb1
Acvr1
Gm7536
Hspa12a
Ywhaq
Pfkl
Npepps
Tubb4a
Eno1
Rps14
Hspa5
Ywhah
Ran
Dclk2
Hist1h3a
Acta2
Dstn
Rps2
Yjefn3
Hsp90ab1
Actr1b
Gapdh
Hist2h3b
Tubb2a
Ywhaz
Ywhab
Tubb3
Ywhag
Tuba4a
Ppp2r1a
Ywhae
Capza2
Tubb4b
Tubb2b
Eef1a1
Hspa8
Hpcal4
Tuba8
Dynll1
Actb
Vsnl1
Ncald
Hpcal1
Sirt2
Tubb5
Dclk1
Cep152
Dbc1
Mapt
Dcakd

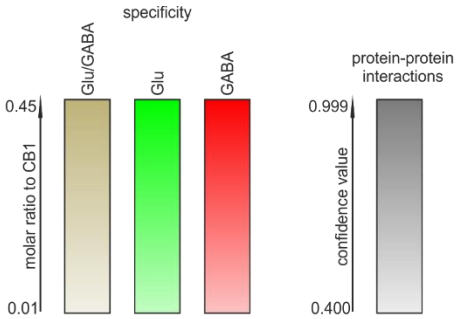
specificity
Glu/GABA
Glu
GABA
0.45
molar ratio to CB1
0.01
protein-protein interactions
0.999
confidence value
0.400

*Cluster 3*

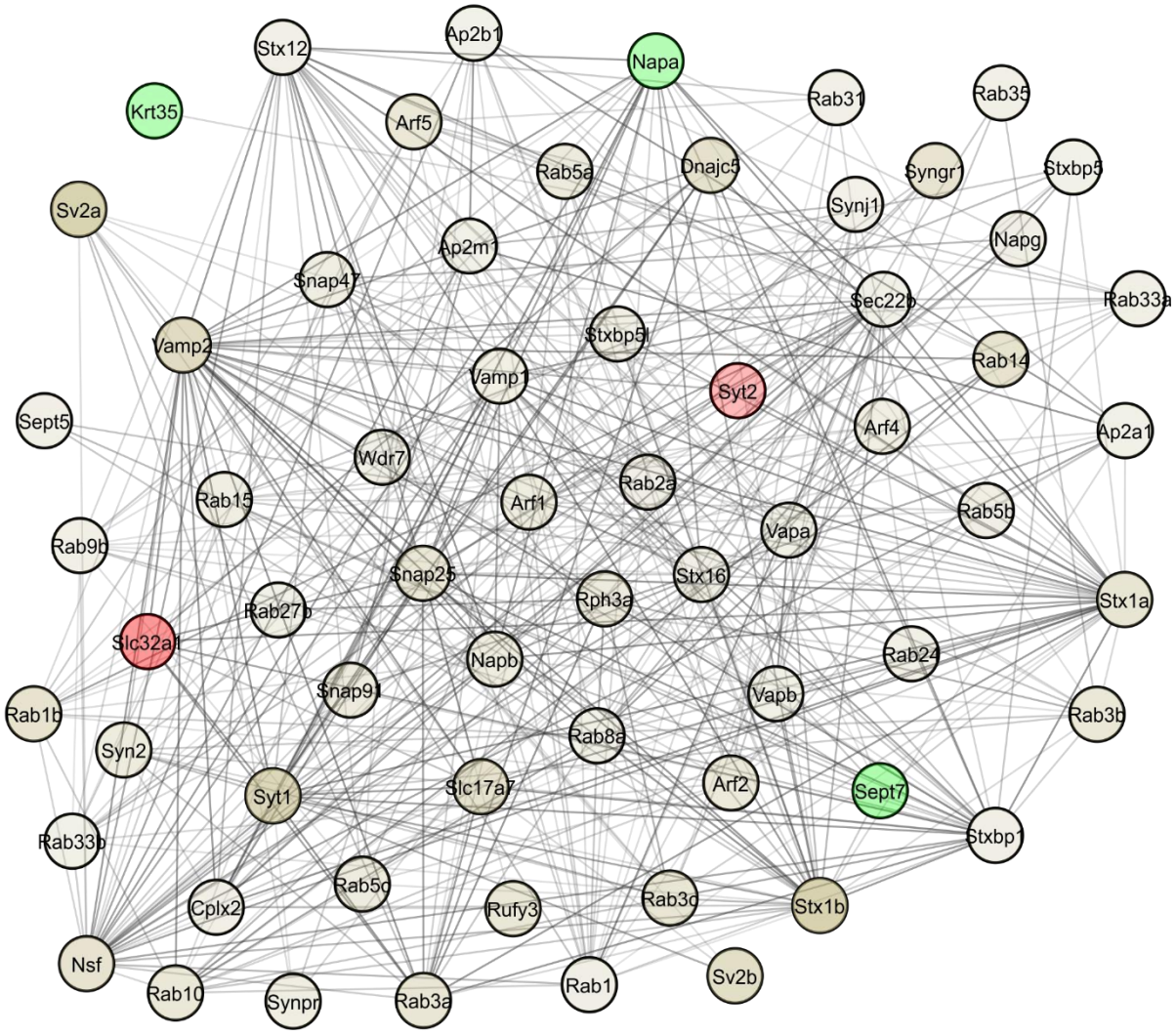
Stx12
Ap2b1
Napa
Krt35
Arf5
Rab31
Rab35
Rab5a
Dnajc5
Syngr1
Stxbp5
Sv2a
Synj1
Ap2m1
Napg
Snap47
Sec22b
Rab33a
Vamp2
Stxbp5l
Rab14
Vamp1
Syt2
Sept5
Arf4
Ap2a1
Wdr7
Rab2a
Rab15
Arf1
Rab5b
Vapa
Rab9b
Snap25
Stx16
Stx1a
Rph3a
Rab27b
Slc32a1
Napb
Rab24
Snap91
Vapb
Rab1b
Rab3b
Rab8a
Syn2
Arf2
Slc17a7
Sept7
Syt1
Stxbp1
Rab33b
Rab5c
Cplx2
Rufy3
Rab3d
Stx1b
Nsf
Sv2b
Rab10
Rab1
Synpr
Rab3a

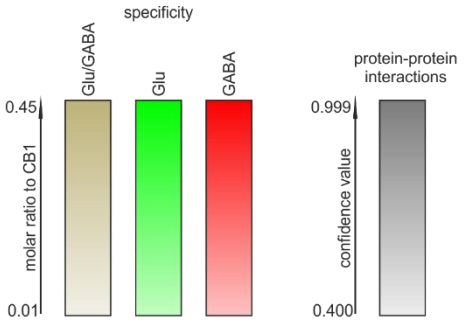
specificity
Glu/GABA
Glu
GABA
0.45
molar ratio to CB1
0.01
protein-protein interactions
0.999
confidence value
0.400

*Cluster 4*

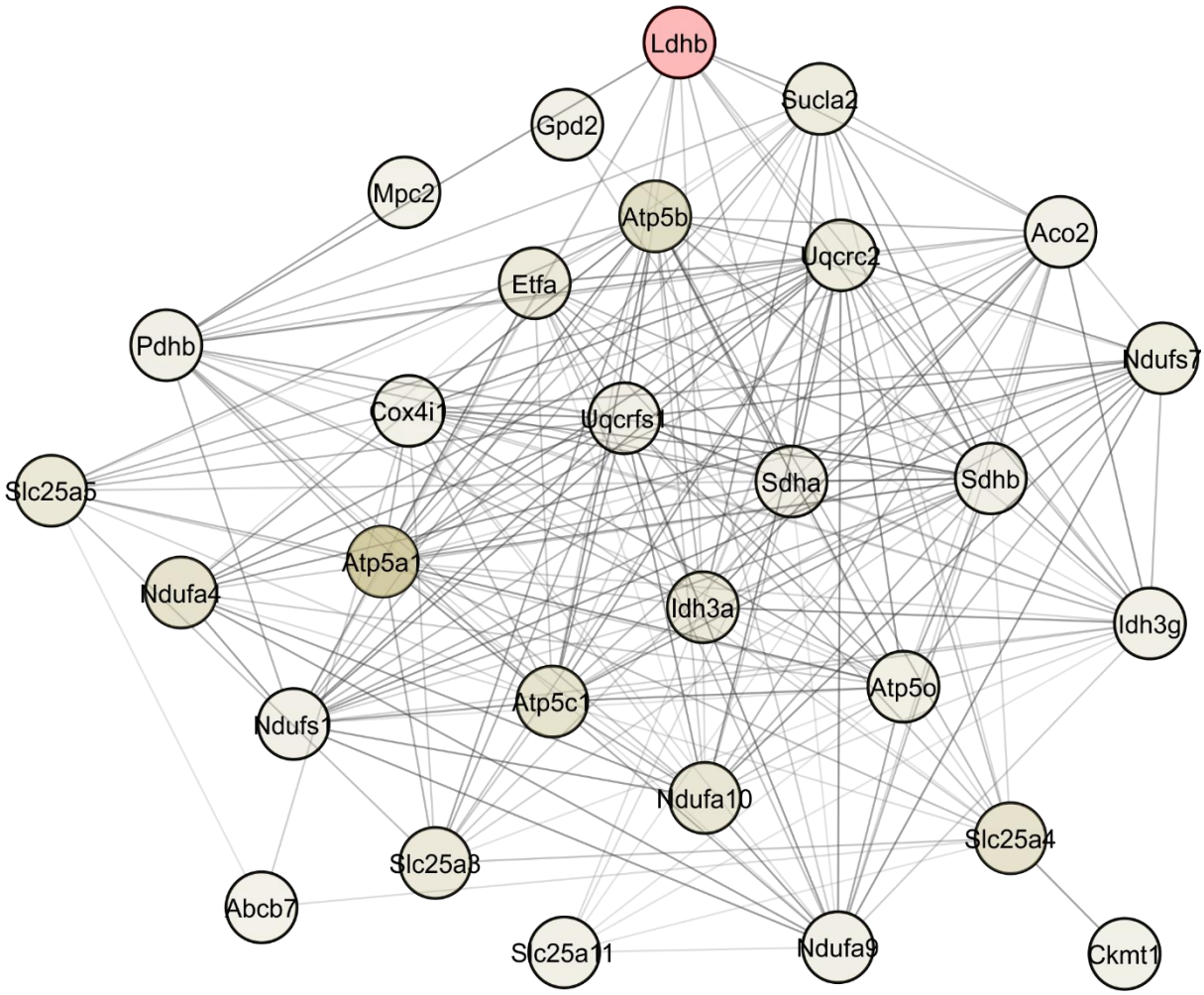
Ldhb
Sucla2
Gpd2
Mpc2
Atp5b
Aco2
Uqcrc2
Etfa
Pdhb
Ndufs7
Cox4i1
Uqcrfs1
Slc25a5
Sdha
Sdhb
Atp5a1
Ndufa4
Idh3a
Idh3g
Atp5o
Atp5c1
Ndufs1
Ndufa10
Slc25a4
Slc25a3
Abcb7
Slc25a11
Ndufa9
Ckmt1

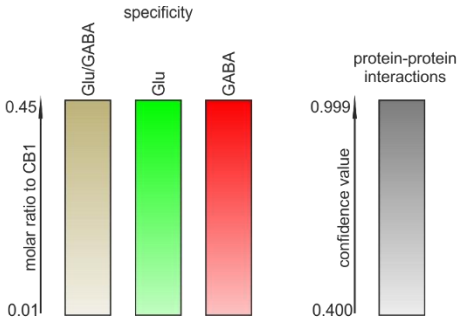
specificity
Glu/GABA
Glu
GABA
0.45
molar ratio to CB1
0.01
protein-protein interactions
0.999
confidence value
0.400

*Cluster 5*

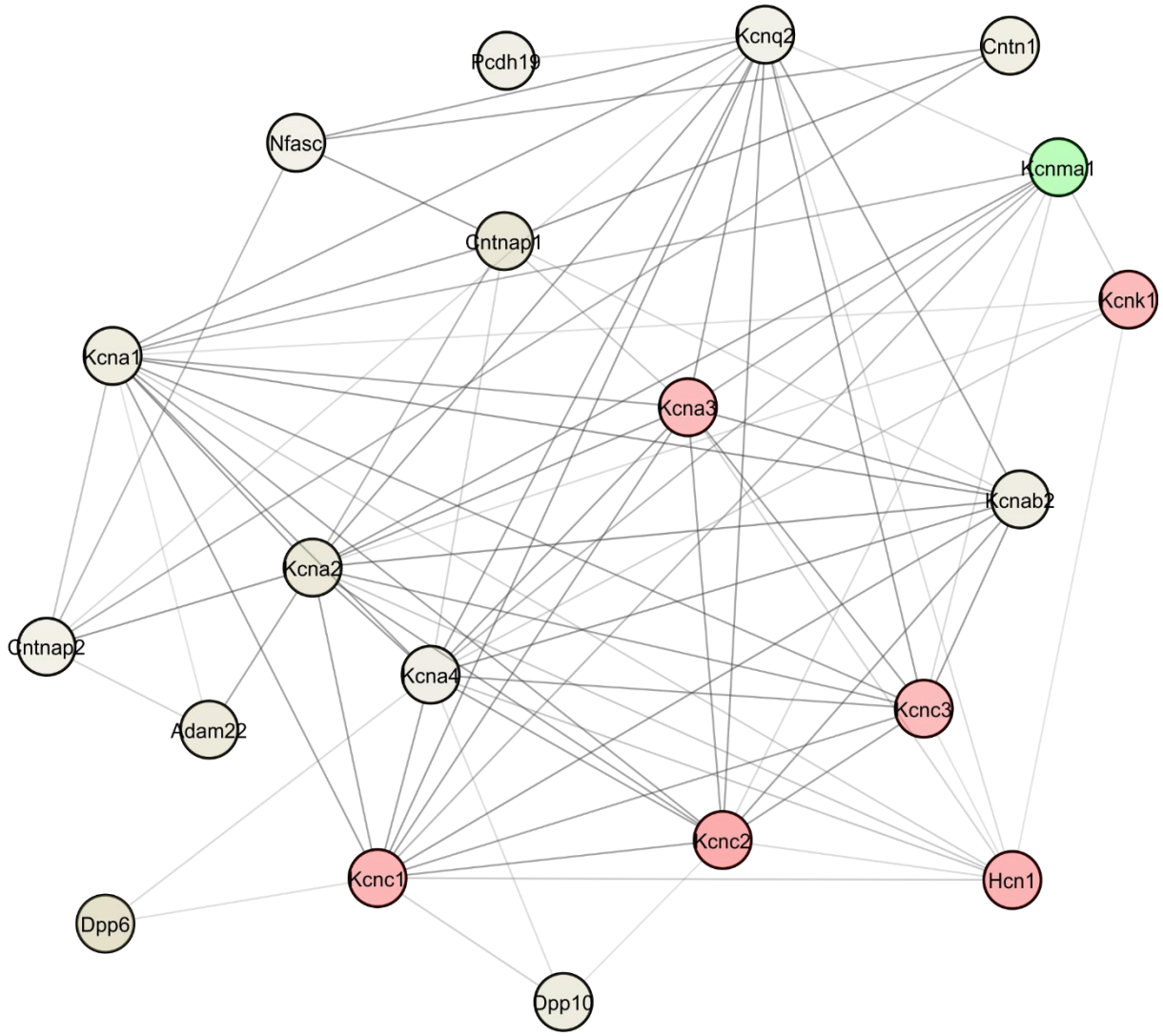
Kcnq2
Cntn1
Pcdh19
Nfasc
Kcnma1
Cntnap1
Kcnk1
Kcna1
Kcna3
Kcnab2
Kcna2
Cntnap2
Kcna4
Kcnc3
Adam22
Kcnc2
Kcnc1
Hcn1
Dpp6
Dpp10

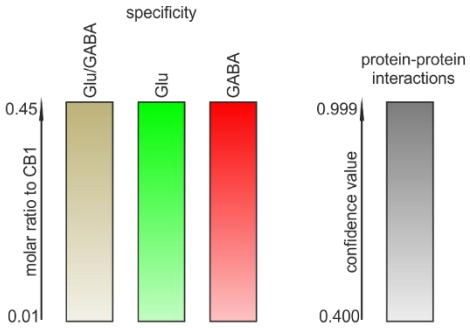
specificity
Glu/GABA
Glu
GABA
0.45
molar ratio to CB1
0.01
protein-protein interactions
0.999
confidence value
0.400

*Cluster 6*

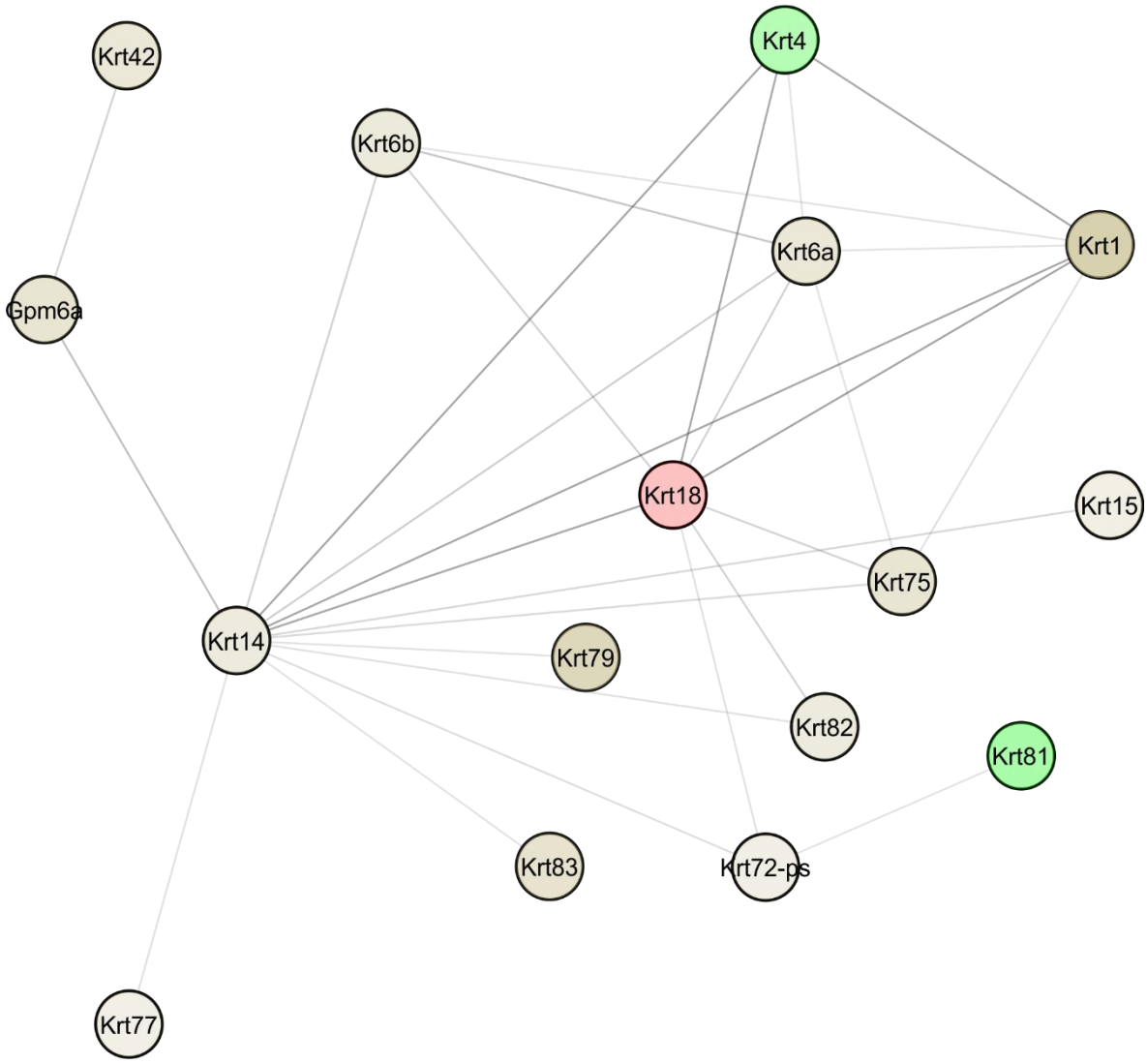
Krt42
Krt4
Krt6b
Krt6a
Krt1
Gpm6a
Krt18
Krt15
Krt75
Krt14
Krt79
Krt82
Krt81
Krt83
Krt72-ps
Krt77

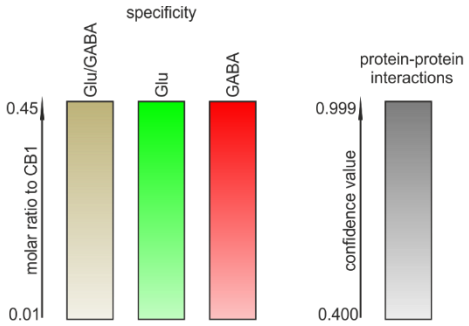
specificity
Glu/GABA
Glu
GABA
0.45
molar ratio to CB1
0.01
protein-protein
interactions
0.999
confidence value
0.400

*Cluster 7*

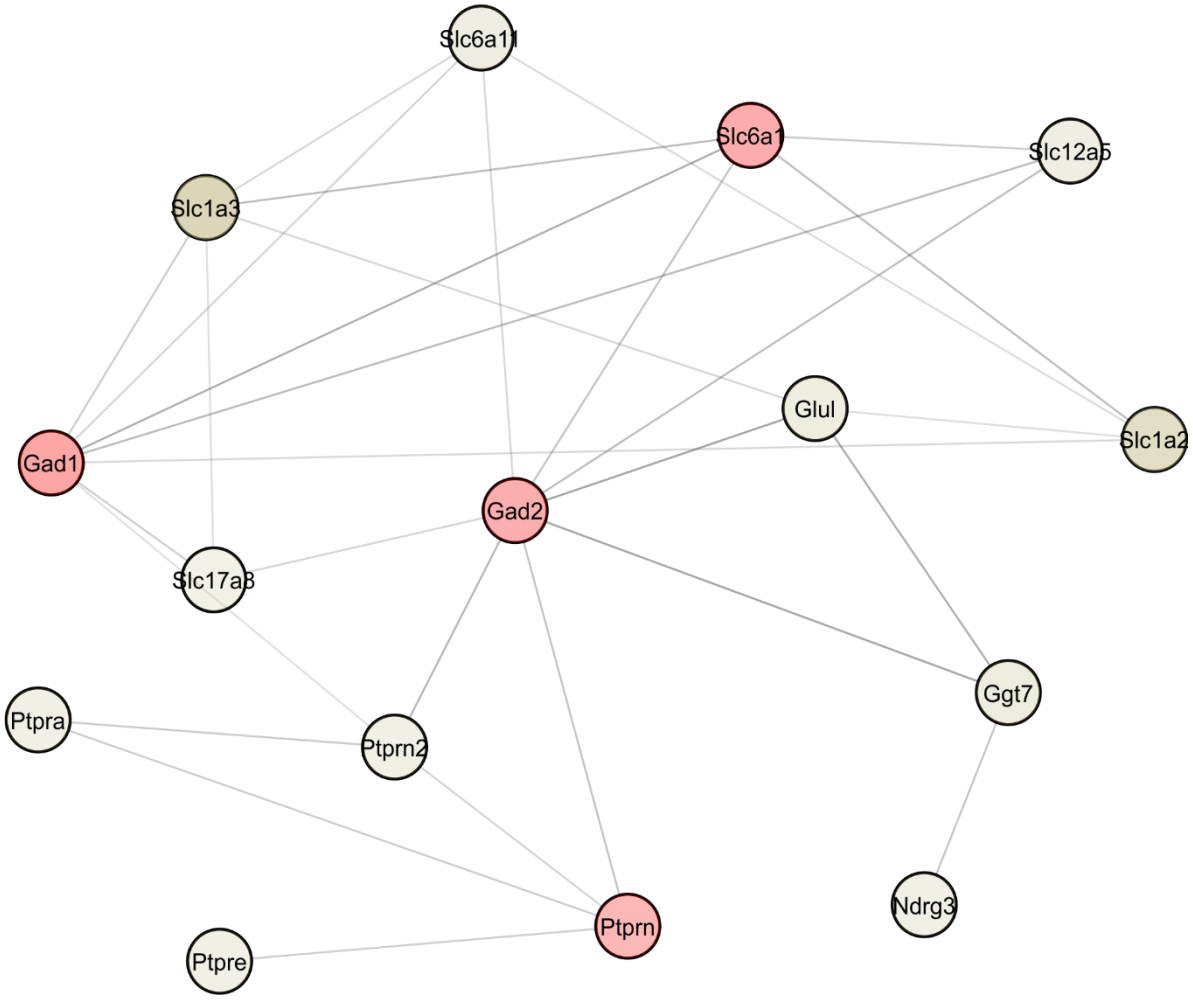
Slc6a11
Slc6a1
Slc12a5
Slc1a3
Glul
Slc1a2
Gad1
Gad2
Slc17a8
Ggt7
Ptpra
Ptprn2
Ndrg3
Ptprn
Ptpre

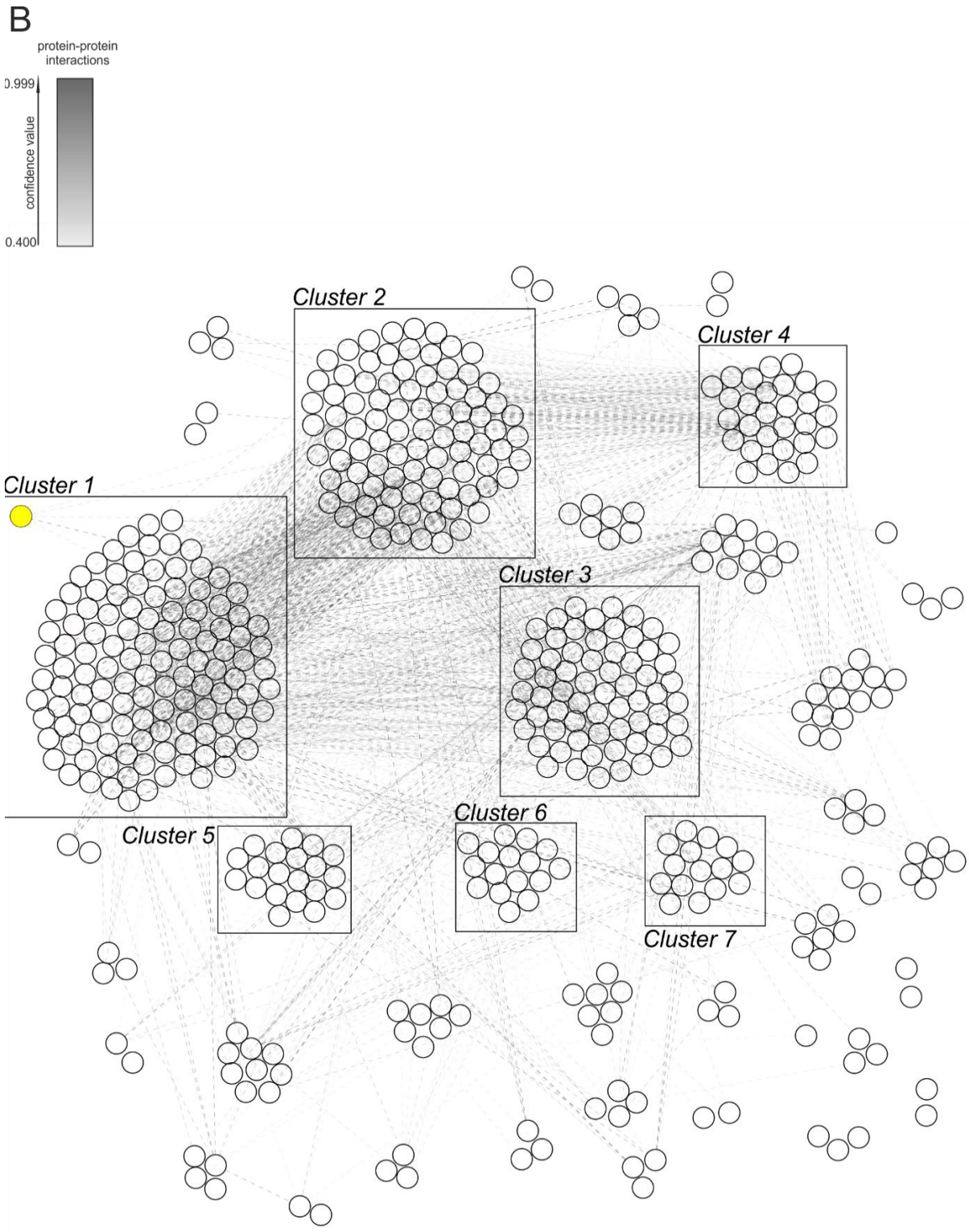
B
protein-protein interactions
0.999
confidence value
0.400
Cluster 1
Cluster 2
Cluster 3
Cluster 4
Cluster 5
Cluster 6
Cluster 7

### Fig. 4.19 Network analysis of proteins identified in the TAP samples

Functional protein network analysis based on all proteins identified in the TAP samples with a molar ratio of at least 1% to CB1 using STRING. Including 571 proteins, the analysis of protein-protein interactions derived from the STRING database generated a network containing 483 embedded proteins, displayed with their official gene symbol, using a medium threshold for protein-protein interaction confidence value (0.400). Proteins were clustered based on the interaction confidence values using Markov Cluster Algorithm (MCL) with an inflation value of 1.8. 7 main clusters containing at least 15 proteins were obtained. **A**: Overview of whole network with functionally related proteins embedded in clusters including cell type specificity of single proteins illustrated with color code (yellow: CB1; brown: no specificity for either cell type; green: specific for Glu-CB1-SF-C; red: specific for GABA-CB1-SF-C). Abundance of single proteins by their relative molar ratio to CB1 is illustrated with a color saturation gradient. Close-ups of single clusters include confidence values for protein-protein interactions calculated by STRING depicted with a transparency gradient of lines between the proteins ranging from light grey (low interaction confidence value) to dark grey (high interaction confidence value). **B**: Network overview with functionally related proteins embedded in clusters including intercluster protein-protein interaction confidence values calculated by the STRING algorithm illustrated with dashed lines between the proteins and a transparency gradient representing the confidence values.

**Tab. 4.2 Glu-CB1-SF-C-TAP- and GABA-CB1-SF-C-TAP-specific proteins in the 7 main clusters after network analysis of the identified proteins in the TAP samples**

For each of the main clusters, Glu-CB1-SF-C-TAP-specific proteins are highlighted in green and sorted from top to bottom based on their relative molar ratios to CB1. GABA-CB1-SF-C-TAP-specific proteins are highlighted in red, again with the respective molar ratios to CB1 in the column to their right.

| Cluster | Glu-spec. | molar ratio to CB1 | GABA-spec. | molar ratio to CB1 |
|---|---|---|---|---|
| *Cluster 1* | Epha4 | 0.1024 | Prkar2a | 0.0446 |
| | Adcy9 | 0.0861 | Prkar2b | 0.0436 |
| | Prkcg | 0.0846 | Ndrg4 | 0.0374 |
| | Fxyd7 | 0.0833 | Gnal | 0.0321 |
| | Grm2 | 0.0334 | Clu | 0.0219 |
| | Pde2a | 0.0287 | Myh14 | 0.0173 |
| | Npy2r | 0.0259 | Asph | 0.017 |
| | Plxna | 0.0224 | Prkaca | 0.0161 |
| | Abca7 | 0.0211 | | |
| | Unc5a | 0.0151 | | |
| *Cluster 2* | Acvr1b | 0.0151 | Hspa5 | 0.1034 |
| | | | Eef2 | 0.0432 |
| | | | Erp44 | 0.0315 |
| | | | Hist1h3a | 0.0224 |
| *Cluster 3* | Sept7 | 0.0564 | Slc32a1 | 0.1074 |
| | Krt35 | 0.0445 | Syt2 | 0.0316 |
| | Napa | 0.043 | | |
| *Cluster 4* | | | Ldhb | 0.0329 |
| *Cluster 5* | Kcnma1 | 0.0248 | Kcnc2 | 0.0626 |
| | | | Hcnc1 | 0.0469 |
| | | | Kcnc1 | 0.0407 |
| | | | Kcna3 | 0.0269 |
| | | | Kcnk1 | 0.0266 |
| | | | Kcnc3 | 0.0243 |
| *Cluster 6* | Krt81 | 0.0707 | Krt18 | 0.0151 |
| | Krt4 | 0.0411 | | |
| *Cluster 7* | | | Gad1 | 0.0755 |
| | | | Slc6a1 | 0.0599 |
| | | | Gad2 | 0.057 |
| | | | Ptprn | 0.0372 |

The proteins embedded in the network as a whole and proteins within the main clusters were analyzed in respect of Gene Ontology (GO) term enrichment. A visualized gene annotation of the entirety of all proteins within the network using the BiNGO plugin for Cytoscape and reduced GOSlim_GOA subset of GO terms was performed against the whole mouse genome as background set to gain comprehensive insight into the functional properties of the purified proteins (Fig. 4.20).

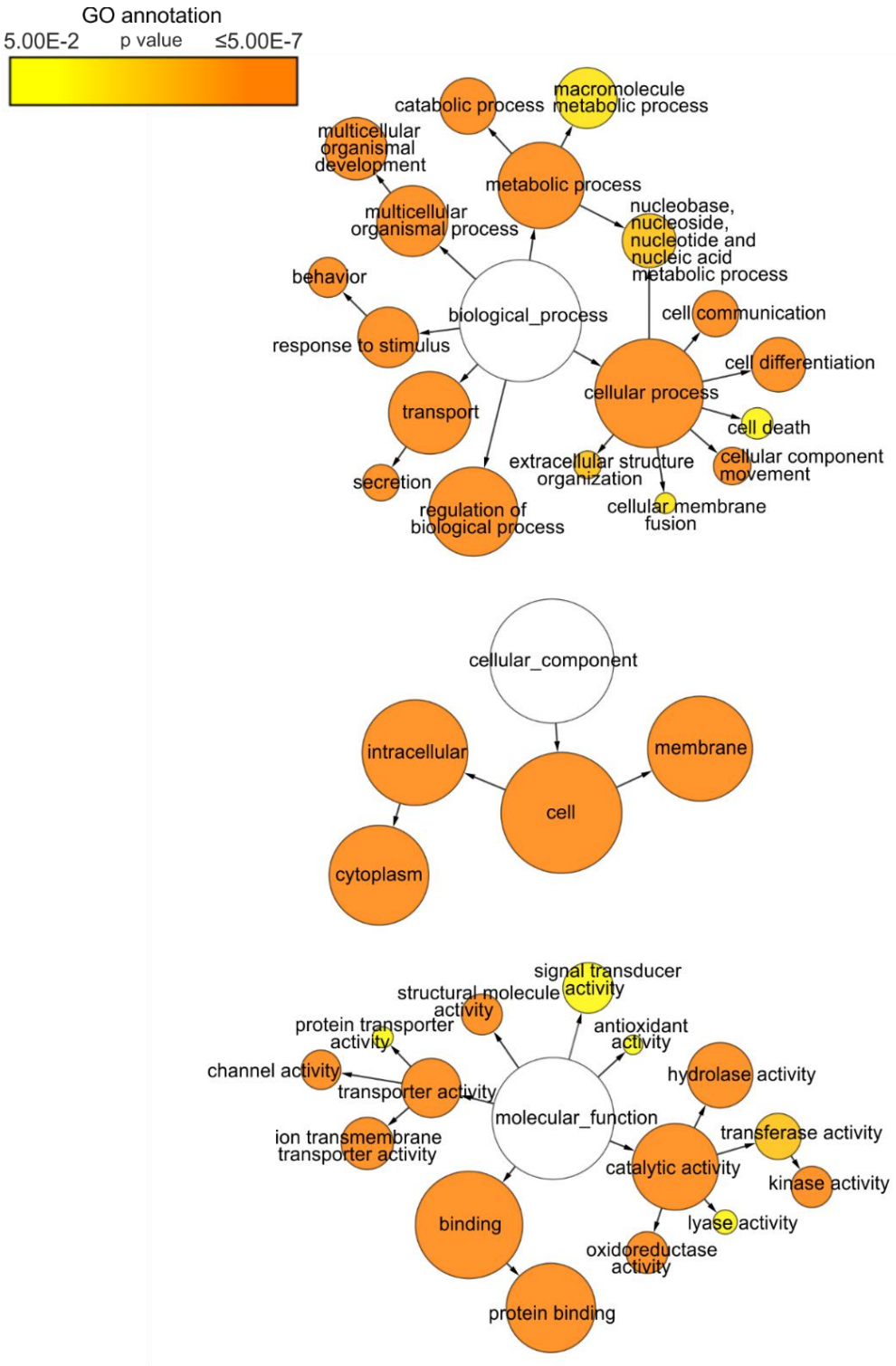


**Fig. 4.20 Gene Ontology (GO) analysis of proteins identified in the TAP samples**

GO term enrichment using the reduced GOSlim_GOA subset of GO terms based on all proteins identified in the TAP samples with a molar ratio of at least 1% to CB1 against the whole mouse genome as background set using the BiNGO plugin for Cytoscape. Visualization of enrichment of GO terms is based on the amount of proteins annotated in a GO term illustrated with the size of the circles and significance of the GO term enrichment visualized with a color gradient ranging from yellow ($p = 0.05$) to orange ($p \leq 5 \times 10^{-7}$). Analysis was separately performed for biological process (top), cellular component (middle) and biological function (bottom).

For the biological process (BP) ontology, proteins are significantly enriched in several cellular and metabolic processes, and furthermore, in multicellular organismal development, behavior, secretion, and regulation of biological processes in general. The cellular compartment (CC) ontology shows a significant enrichment of proteins annotated in membrane as well as cytoplasma. The molecular function (MF) ontology shows enrichment for proteins involved in ion channel and transporter activity, protein binding, structural molecule activity, signal transducer activity, catalytic activity of hydrolases, kinases, oxidoreductases and lyases, and also antioxidant activity.

Aiming for a better understanding of how the identified single Glu- or GABA-specific proteins could affect the overall output of CB1 signaling in the neuronal subtypes, GO analyses using GO_FAT categories of the single main clusters were performed using the DAVID Functional Annotation Tool, and compared to the GO_FAT term enrichment analysis of the whole network. The two annotations with the highest significance for each category (CC, BP, MF) of the single clusters were compared with the p-values of the same annotations for the whole network and, if significant for the whole network, summarized for each cluster (Tab. 4.3).

**Tab. 4.3 Gene Ontology (GO) term enrichment analysis of the 7 main clusters obtained by the network analysis of the identified proteins in the TAP samples using the STRING database and MCL clustering**

GO analyses using GO_FAT categories for molecular function (MF), cellular compartment (CC), and biological process (BP) of all proteins embedded in the network and for its single main clusters were performed using the DAVID Functional Annotation Tool. If existing, the two GO term annotations with the highest significance for each category (CC, BP, MF) of the single clusters were summarized for each cluster if the GO terms were also significant for the whole network GO analysis. Cluster/Category: analyzed cluster and category for MF, CC, or BP; GO term: enrichment of proteins in the respective cluster and category for GO term; p value: significance for GO term displayed by p value (Benjamini corrected) calculated for GO analysis of all proteins in the network.

| Cluster/Category | GO Term | p value |
|---|---|---|
| *Cluster 1* | | |
| GOTERM_MF_FAT | GTPase activity | 2.60E-27 |
| GOTERM_MF_FAT | ribonucleotide binding | 6.00E-26 |
| GOTERM_CC_FAT | heterotrimeric G-protein complex | 4.50E-11 |
| GOTERM_CC_FAT | plasma membrane | 7.50E-19 |
| GOTERM_BP_FAT | intracellular signaling cascade | 1.00E-15 |
| GOTERM_BP_FAT | small GTPase mediated signal transduction | 6.50E-26 |
| *Cluster 2* | | |
| GOTERM_MF_FAT | purine nucleotide binding | 9.50E-35 |
| GOTERM_MF_FAT | ribonucleotide binding | 1.70E-34 |
| GOTERM_CC_FAT | pigment granule | 1.30E-14 |
| GOTERM_CC_FAT | melanosome | 1.30E-14 |
| GOTERM_BP_FAT | glycolysis | 1.60E-04 |

| | | |
|---|---|---|
| GOTERM_BP_FAT | hexose catabolic process | 5.90E-04 |
| *Cluster 3* | | |
| GOTERM_MF_FAT | GTP binding | 7.40E-37 |
| GOTERM_MF_FAT | guanyl nucleotide binding | 2.20E-36 |
| GOTERM_CC_FAT | cytoplasmic vesicle | 4.90E-15 |
| GOTERM_CC_FAT | vesicle | 1.50E-14 |
| GOTERM_BP_FAT | protein transport | 1.10E-16 |
| GOTERM_BP_FAT | establishment of protein localization | 5.30E-17 |
| *Cluster 4* | | |
| GOTERM_MF_FAT | hydrogen ion transmembrane transporter activity | 2.60E-02 |
| GOTERM_MF_FAT | monovalent inorganic cation transmembrane transporter activity | 2.60E-02 |
| GOTERM_CC_FAT | mitochondrion | 5.30E-10 |
| GOTERM_CC_FAT | mitochondrial part | 3.40E-10 |
| GOTERM_BP_FAT | generation of precursor metabolites and energy | 3.30E-11 |
| GOTERM_BP_FAT | electron transport chain | 3.00E-02 |
| *Cluster 5* | | |
| GOTERM_MF_FAT | potassium ion binding | 1.40E-08 |
| GOTERM_MF_FAT | potassium channel activity | 1.70E-03 |
| GOTERM_CC_FAT | voltage-gated potassium channel complex | 1.20E-02 |
| GOTERM_CC_FAT | potassium channel complex | 1.20E-02 |
| GOTERM_BP_FAT | potassium ion transport | 2.10E-06 |
| GOTERM_BP_FAT | monovalent inorganic cation transport | 2.80E-08 |
| *Cluster 6* | | |
| GOTERM_MF_FAT | structural molecule activity | 8.10E-05 |
| GOTERM_CC_FAT | intermediate filament | 1.20E-04 |
| GOTERM_CC_FAT | intermediate filament cytoskeleton | 1.50E-04 |
| *Cluster 7* | | |
| GOTERM_MF_FAT | L-amino acid transmembrane transporter activity | 1.50E-02 |
| GOTERM_MF_FAT | symporter activity | 6.30E-03 |
| GOTERM_CC_FAT | neuron projection | 1.00E-08 |
| GOTERM_CC_FAT | axon | 7.00E-10 |

All clusters show internally consistent enrichment of GO terms, which are depicting single clusters as distinct functional groups. Therefore, an accumulation of Glu- or GABA-specific proteins in one cluster might increase the possibility that these cell type-specifically acting proteins could be responsible for an overall change in CB1 signaling output in one specific cell type by acting through these functional clusters.

## 4.3 Discussion

### 4.3.1 The impact of the use of detergents and location of the CB1-linked SF-tag in the TAP

In the optimization process of the TAP procedure in HEK293 cells and hippocampal synaptosome preparations, qualitative differences regarding the purification success could be observed, which depended primarily on the use of detergents and the N- or C-terminal location of the SF-tag.

The physical properties of detergents in solution are leading initially, at very low concentrations, to a partly dissolution of the molecules as monomers, and another part which forms a monolayer at the air/water interphase. When the monomer concentration reaches a critical value, the amphiphile begins to associate and forms micelles, which vary in size depending on the physical properties of the respective molecule. This critical value is referred to as critical micellar concentration (CMC). The underlying mechanism when used in the solubilization of cell membranes, is first the binding and integration of the surfactant molecules into the lipid bilayer. Second, a lamellar-micellar phase transition occurs when the bilayers are saturated with detergent and mixed micelles begin to form. Upon further increase in detergent concentration, the size of mixed micelles decreases with a concomitant increase in the detergent/phospholipid ratio. As the physical properties are furthermore influenced by temperature, pH value, and ionic strength, and biological membranes constitute extremely complex mixtures of lipids, proteins, and ions, the actions of distinct detergents and their influence on the outcome of biochemical experiments can hardly be predicted but rather have to be empirically tested (Helenius and Simons, 1975).

As the majority of protein-protein interactions are non-covalent hydrophobic interactions, the use of detergents by nature can disrupt these interactions which are to maintain in order to purify a protein with its interacting proteins and protein complexes, which occur under native conditions *in vivo*. On the other hand, the use of detergents or other soluble amphiphile reagents is necessary in order to solubilize membrane proteins and allow for an affinity chromatography-based purification. Before the final optimization steps of the TAP procedure described in the results section (4.2.1), in which Brij O10 and digitonin were used, other common non-ionic surfactants were tested as well, such as Triton X-100, Nonidet P40, and CHAPS, all in low concentrations, but their use did not lead to a successful purification of the target SF-tagged CB1-bait protein as evaluated by western blot. The TAP of N-SF-CB1 could not be accomplished with the use of

digitonin when HEK293 cells were used as expression system, but nonetheless for CB1-SF-C (Fig. 4.2), which rather indicates issues due to the localization of the SF-tag. In the TAPs of hippocampal synaptosome preparations, N-SF-CB1 and CB1-SF-C both could be successfully purified (Fig. 4.11), but the use of digitonin did not lead to any indication of co-purified proteins in the silver staining analysis (Fig. 4.13). In this case, digitonin apparently disrupts the CB1 protein complex, which still allows for a successful purification of the bait protein, but without maintaining the integrity of CB1 with its interacting proteins.

Digitonin was shown to be intricate to use, because of its toxicity and low solubility, which can only be achieved by heating up the aqueous carrier solution and often precipitates when the buffer is cooled down to 4°C. Moreover, commercially available digitonin preparations are contaminated up to 50% with compounds of unknown chemical nature, and even batches of the same company vary to a high degree regarding their quality (Rehm and Rehm, 2006).

Eventually, the use of Brij O10 turned out to enable a successful purification of CB1 and maintaining the protein complex with interacting proteins at the same time. Brij O10 is a polyethylene glycol oleyl ether with a low CMC (< 0.04 mM), therefore it can be used in low concentrations, and has been successfully used in order to solubilize a number of integral membrane proteins without loss of their biological activities (Helenius and Simons, 1975).

Furthermore, differences in the purification of N- and C-terminally SF-tagged CB1 could be observed. Whereas the N-terminus of a GPCR is mainly involved in ligand binding and serves as a target for *N*-glycosylation, the C-terminus fulfills the demands of differential signal transduction and feedback modulation capabilities on the intracellular side (Luttrell, 2008). Adding an additional amino acid chain in form of a tag sequence to one or the other site, may lead to disturbances or alterations in the respective GPCR functions, therefore it is recommended to use both N- and C-terminal SF-tagged fusion proteins for a direct comparison (Gloeckner et al., 2009). Although the C-terminus of a GPCR is crucial for the interaction with other interacting membrane and cytosolic signaling proteins, the TAP of CB1-SF-C in hippocampal glutamatergic neurons and GABAergic interneurons led to the identification of a plethora of potential interactors (Tab. 8.2), including directly interacting G proteins, and therefore indicating no disturbance of protein interactions by the C-terminal SF-tag. Applying the same TAP protocol using Brij O10 on N-SF-CB1, on the other hand, enabled the purification of N-SF-CB1 itself, but apparently at lower amounts as compared to CB1-SF-C and without any indication of other purified proteins (Fig. 4.13B). Interestingly, the amount of purified SF-tagged CB1 from the same amount of input material appeared to be the same when digitonin was used in the purification process of hippocampal synaptosomes (Fig.

4.13A), indicating a more efficient solubilization using this detergent, but with a concomitant disruption of protein interactions. Decreasing the concentration of digitonin, even only slightly, could not solve this issue, as this led to a complete failure of the TAP (data not shown). It has to be noted that the differences in the amount of purified SF-tagged CB1 appeared for digitonin, as well as Brij O10, when the TAP eluates of transfected HEK293 cells were analyzed using silver stainings (Fig. 4.3B) and MS (Fig. 4.4). A speculative explanation for this might be potential post-translational modifications based on the N-terminal location of the SF-tag, which is more likely a target for these modifications than the C-terminus in GPCR biosynthesis (2.2.1). The FLAG sequence was shown to be target of various potential modifications, such as phosphorylation, sulfation, and glycosylation leading to a decreased accessibility of the tag for purification (Schmidt et al., 2012). These modifications might as well affect the physical properties of detergent-protein interactions, in particular when used in low concentrations, as described before. One hint to this speculative mechanism is provided by the ladder pattern in western blots of the lysates of hippocampal synaptosome preparations when detected with the CB1 antibody, which only occurs in the N-SF-CB1 samples (Fig. 4.11A, C). This might indicate various post-translational modifications of the SF-tag, leading to changes in accessibility or even changes in protein folding or trafficking, which is mostly ascribed to N-terminal sequences of membrane proteins. A higher concentration of Brij O10 in order to compensate for the potential changes in physical properties of N-SF-CB1 still allowed for a purification of N-SF-CB1 itself, but again, no interacting proteins could be detected in silver stainings, as expected, due to the disruption of protein-protein interactions upon increase of the concentration of detergent (data not shown).

Taken together, these findings illustrate the complexity in membrane protein-detergent interactions and the intricacy of executing biochemical experiments in this field. In this work, only the use of one specific detergent within a very low concentration tolerance allowed for the purification of CB1 protein complexes, which was furthermore dependent on the N- or C-terminal location of the tag. The question remains, however, why no further proteins could be purified when N-SF-CB1 was solubilized with the lowest possible concentration of Brij O10, which was able to maintain the protein complex integrity for CB1-SF-C. Although the overall amount of purified N-SF-CB1 appeared to be reduced, it can be argued that at least a number of interacting proteins should be co-purified. This question could not be solved in this study. Possible speculative reasons could be that the N-terminal tag or its modifications change protein folding and subsequently prevent interactions with other proteins, or only a population of receptors remains accessible for purification, which are not stabilized by other interacting or anchoring proteins in their environment upon a given concentration of a detergent. This would finally lead to the purification

of a majority of N-SF-CB1 only, without interactors. A necessary increase of detergent concentration in order to compensate for this phenomenon would then immediately disrupt the sensitive protein-protein interactions as stated before.

Another issue that could not be solved is whether the C-terminally located SF-tag led to false positive binding of interacting proteins to the SF-tag that naturally do not interact with endogenous CB1. This question can only be solved by a direct comparison of successfully performed TAPs of N-SF-CB1 and CB1-SF-C, which could not be achieved in this study, and which would need empirical testing of further amphiphile reagents in different concentrations and other purification optimizations. Nevertheless, meta-analyses of the obtained data by the TAP of CB1-SF-C only, which are discussed in the next paragraph, help in order to address this question and understand the relevance of the detected co-purified proteins.

### 4.3.2 Analysis of proteins in the TAP samples of glutamatergic and GABAergic CB1 protein complexes

The mere number of 951 proteins identified in the TAP samples of glutamatergic and GABAergic CB1-SF-C is intriguing. Co-purified scaffolding and cytoskeletal elements suggest the purification of not only directly interacting proteins but higher order multiprotein structures. However, it has been shown that membrane proteins undergo more complicated biogenesis then soluble proteins, and thus, have more interactors (Pankow et al., 2015). In addition, it has to be pointed out that the expression levels of the SF-tagged CB1 generally occurs at levels comparable to endogenous CB1 (Fig. 4.14), in contrast to other studies in which the use of AAV vectors led to a strong overexpression (Guggenhuber et al., 2016). This is important in order not to overrun the AAV-infected cell with a recombinant protein, thus triggering severe compensatory mechanisms, which might lead to artificial protein interactions. The reliability of the relative abundances of proteins calculated by label-free quantification MS could be confirmed by densitometric quantification of WB band intensities of a few proteins as well (Fig. 4.18).

In order to assess the relevance of the proteins identified in the TAP samples, in a first step already known CB1-interacting proteins were screened. In both TAP samples of Glu-CB1-SF-C and GABA-CB1-SF-C, CB1 is the most abundant protein, followed by the G protein subunit $G\alpha_o$ with a relative molar ratio of 0.428 (Glu) and 0.474 (GABA) (from here, molar ratios of a protein to CB1 are presented in brackets after the respective protein), respectively. Since CB1 is a $G\alpha_{i/o}$-coupled GPCR

(Howlett et al., 1986), with the G protein as a directly interacting protein, this depicts a first and very important proof of a reasonable dataset.

Furthermore, various Gβ and Gγ subunits could be identified as well, with $G\beta_1$ (Glu: 0.272, GABA: 0.219) and $G\gamma_3$ (Glu: 0.033, GABA: 0.021) being the most abundant variants. Other G proteins that were shown to couple to CB1, could also be identified. These are the inhibitory G protein subunits $G\alpha_{i1}$ (Glu: 0.216, GABA: 0.174), $G\alpha_{i2}$ (Glu: 0.127, GABA: 0.124), and $G\alpha_{i3/k}$ (Glu: 0.050, GABA: 0.035), and members of other G protein classes, which are $G\alpha_s$ (Glu: 0.019, GABA: 0.018) (Glass and Felder, 1997), $G\alpha_q$ (Glu: 0.054, GABA: 0.037), and $G\alpha_{11}$ (Glu: 0.020, GABA: 0.017) (Lauckner et al., 2005).

Consequently, also downstream effectors of CB1-G protein-mediated activation were identified, namely AC1 (Glu: 0.008, GABA: 0.011) (Rhee et al., 1998) and several PKA subunits, with type II subunit α being the most abundant (Glu: 0.013, GABA: 0.045). The identification of VGCC subunits β4 (Glu: 0.004, GABA: 0.006) and γ8 (Glu: 0.085, GABA: 0.062) is consistent with the description of CB1-mediated inhibition of neurotransmitter release via G protein-dependent inhibition of presynaptic VGCCs. Furthermore, the CB1-mediated activation of the ERK signaling cascade is reflected by the identification of MAPK1 (Glu: 0.007, GABA: 0.006) and MAPK3 (Glu: 0.003, GABA: 0.003) (Kano et al., 2009).

Other identified proteins in the TAP samples that have already been shown to be functionally involved in CB1-mediated actions are GSK3β (Glu: 0.010, GABA: 0.012) (Gomez del Pulgar et al., 2000; Ozaita et al., 2007), Rab3B (Glu: 0.072, GABA: 0.080) (Tsetsenis et al., 2011), Crip1a (Glu: 0.009, GABA: 0.008) (Niehaus et al., 2007; Blume et al., 2015; Guggenhuber et al., 2016), 14-3-3β (Glu: 0.046, GABA: 0.037) (Jung et al., 2014), PP2A (Glu: 0.017, GABA: 0.027) (Dalton and Howlett, 2012), and Src family non-receptor tyrosine kinase Fyn (Glu: 0.024, GABA: 0.022) (Derkinderen et al., 2003). Further CB1-interacting proteins WAVE1, NCKAP1, CYFP2, Rac1 and ABI2 were shown to mediate the actions of cannabinoids on the actin cytoskeleton in growth cones of cortical neurons (Njoo et al., 2015). Of these proteins, only CYFP2 (Glu: 0.014, GABA: 0.011) and Rac1 (Glu: 0.158, GABA: 0.137) were co-purified in the TAP, but not WAVE1, NCKAP1 and ABI2. This may be a result of the preceding synaptosome preparations, which served as input for the TAPs, since in the work of Njoo et al. whole cell extracts were used. Another discrepancy between both studies are the investigated brain areas. The interactions of proteins with CB1 in the work of Njoo et al. occurred in the mouse cortex, and therefore do not necessarily need to interact with CB1 in other brain areas, such as the hippocampus, which was investigated in this work.

Interestingly, proteins that were shown to be involved in desensitization and endocytosis of CB1, such as β-arrestin2, GRK2, GRK3 (Jin et al., 1999; Kouznetsova et al., 2002), and GASP1 (Martini et al.,

2007), or β-arrestin1, which leads to the formation of a β-arrestin signalosome with other GRK isoforms (Ahn et al., 2013) (Delgado-Peraza et al., 2016), could not be identified in the TAP samples. In a similar approach of purifying $MT_1$ and $MT_2$, β-arrestins, which are known to interact with these GPCRs, could not be co-purified as well, probably because this interaction is agonist-stimulated and transient and may need to be stabilized for instance by chemical cross-linking (Daulat et al., 2007). In order to co-purify CB1-interactors involved in these processes, a TAP of synaptosomes that were prepared after acute agonist treatment of mice, or in the presence of agonist in the buffers during the procedure, might be a promising approach. GIRKs, which get activated via CB1 (Kano et al., 2009), have also not been present in the TAP samples, as well as PI3K (Gomez del Pulgar et al., 2000), all of which are downstream effectors of Gβγ instead of Gα subunits, suggesting that interactions mediated by Gβγ may not be stable enough to detect in this TAP approach.

Heterodimerization of GPCRs was shown to be a fundamental property for neural transmission and plasticity (Brugarolas et al., 2014), and for CB1 a number of dimerizing or oligomerizing GPCRs were described (2.3.2). Only two GPCRs were co-purified in the TAPs, which are the neuropeptide Y receptor (NPYR) type 2 (Glu: 0.026, GABA: 0.012) and at very low abundance the μ-OR (Glu: 0.001, GABA: 0.009), of which only the latter was shown to interact with CB1 yet (Ellis et al., 2006; Rios et al., 2006). GPCR heterodimerization is spatially and temporally controlled and all of the CB1-dimerizing GPCRs mentioned in 2.3.2, including μ-OR, are hardly expressed in the hippocampal formation (Lein et al., 2007), therefore the lack of co-purified interacting GPCRs is to be expected. NPYR on the other hand is robustly expressed in the hippocampus and therefore an interesting potential interactor of CB1, since it appears to be specific for glutamatergic neurons, and an interplay of the ECS and neuropeptide Y was shown in the control of energy metabolism in the hypothalamus (Vahatalo et al., 2015).

Taken together, a wide range of already described CB1-interacting proteins could be detected, whereas a few have not been present, possibly due to the reasons mentioned in the particular cases. Nevertheless, this is an important control in order to evaluate the relevance of the dataset of identified proteins. To gain deeper insight into the entirety of the co-purified proteins, and not only single potential interactors, the GO term enrichment and network analyses drew a more comprehensive picture of the functional relevance of all proteins identified in the TAP samples. For reasons of clarity, and because the STRING network analysis does not take into account the abundance of identified proteins, a protein inclusion threshold of a molar ratio of 1% to CB1 was set for these analyses, which should not affect the relevance of single potential interactors of interest with a lower molar ratio, as Crip1a (Glu: 0.009, GABA: 0.008), for instance, a confirmed interactor of CB1, falls just below this threshold. In general, it has to be considered that the

abundance of known interactors of CB1 can help in order to estimate false-positive hits in the MS measurement by setting a known interactor with the lowest abundance as baseline threshold for true positive hits. Nevertheless, it cannot be ruled out that proteins with a lower abundance can still be of significant biological relevance, therefore all proteins detected in the TAP approach have to be considered as potentially interesting CB1-interacting proteins.

The GO analysis of all proteins revealed that the entirety of proteins and their GO annotations reflect known functions of CB1 and actions of this GPCR in different multiprotein signaling subsets (Fig. 4.20). The significant enrichment of membranous and cytoplasmic proteins in the CC ontology reflects the role of CB1 as a membrane protein and associated signaling proteins in or at the membrane as well as in the cytoplasm where they mediate their actions. The BP ontology terms reflect already described functions of CB1 as well, such as nucleotide metabolic processes, which is a fundamental feature of GPCR signaling cascades, or cell communication reflecting the modulation of neurotransmitter release. Other terms, such as behavior or secretion also relate to described functions of CB1, but are rather vague. The MF terms, on the contrary, are specific enough to allow for a comparison with known properties of CB1. $G\alpha_{i/o}$ proteins, which are the major mediators of CB1 signaling, regulate ion channel and transporter activity (Turu and Hunyady, 2010). Protein binding and signal transducer activity are main characteristics of GPCR signaling cascades as well as the catalytic activity of kinases, hydrolases, and lyases. Intriguingly, an enrichment in oxidoreductases was also found, which can be attributed to a number of mitochondrial proteins, indicating further evidence for the existence of mitochondrial fractions of CB1 (Benard et al., 2012; Fisar et al., 2014).

Clustering of the proteins embedded in the network (Fig. 4.19A) led to functional groups with consistent GO annotations (Tab. 4.3). Cluster 1, which contains CB1 itself and its closest predicted interactors based on the calculated confidence values, showed enrichment in ontology terms, which can be directly related to GPCR signaling, such as heterotrimeric G-protein complex, plasma membrane, intracellular signaling cascade, and GTPase activity. The next largest clusters 2 and 3 still show enrichment in nucleotide binding annotations and therefore direct signaling cascade properties regarding the MF ontology, but differ more in regards that proteins are also annotated in glucose metabolism (Lemos et al., 2012) or protein transport. Cluster 4 consists of proteins enriched in mitochondrial functions and mitochondrial cellular compartment. The presence of mitochondria in the TAP input synaptosome preparations was confirmed (Fig. 4.10), and although it has become clear lately that there is a mitochondrial population of CB1 and that it is playing a regulatory role in the respiratory chain, it has been a matter of debate among the scientific community in recent years (Benard et al., 2012; Fisar et al., 2014; Hebert-Chatelain et al., 2014). The

co-purification of mitochondrial proteins involved in these processes using the TAP approach therefore contributes further evidence to the presence of CB1 in mitochondria. The enrichment of proteins annotated to $K^+$ channel activity in Cluster 5 represents a more detailed view of the enrichment of proteins with ion transmembrane transporter activity and channel activity of the GO_Slim annotation of the whole network (Fig. 4.20). It has to be noted that the $K^+$ channels in this cluster are not GIRKs, which are regulated by $G\alpha_{i/o}$ proteins, but voltage-gated $K^+$ channels which are essential for the repolarization of action potentials in neurons. It was shown that the activity of some of these channels is regulated by phosphatidylinositol 4,5-bisphosphate ($PIP_2$) (Kruse et al., 2012). Considering additionally the presence of the $PIP_2$-synthesizing enzyme phosphatidylinositol 5-phosphate 4-kinase (Glu: 0.012, GABA: 0.015), the precursor-synthesizing enzyme phosphatidylinositol 4-kinase (Glu: 0.007, GABA: 0.010), and two $PIP_2$-degrading enzymes type 1 phosphatidylinositol 4,5-bisphosphate 4-phosphatase (Glu: 0.009, GABA: 0.013) and type 2 phosphatidylinositol 4,5-bisphosphate 4-phosphatase (Glu: 0.003, GABA: 0.005), this might hint at a CB1-mediated regulation of not only GIRKs, but voltage-gated $K^+$ channels as well. Intriguingly, a considerable number of proteins in this cluster is specific for GABAergic neurons and also the formerly mentioned enzymes involved in $PIP_2$-synthesis and -degradation show a higher molar ratio to CB1 in the TAP of CB1-SF-C in GABAergic neurons as compared to glutamatergic neurons, suggesting specific CB1-mediated actions via this functional complex predominantly in GABAergic interneurons. Cluster 6 features structural molecule activity and intermediate filament organizational processes in which the corresponding proteins may play a role in integrating the isolated proteins as a part of the protein complexes. The proteins in Cluster 7 generally play roles in transmembrane transporter activity and amino acid transport in neuronal projections or axonal cellular compartment. This fits again as CB1 is dominantly involved in the regulation of neurotransmitter release.

Taken together, the integrative network and GO analyses confirmed that the entirety of purified proteins in the TAPs reflect known functions of CB1 and thereby revealing a high degree of relevance of this dataset. In the context of these findings, all the identified yet unknown potential interactors in the dataset of detected proteins are interesting candidates with a potential functional relevance in CB1 signaling.

A few protein families and groups of functionally related proteins are prominent throughout the dataset of co-purified proteins, and therefore might play important roles in mediating actions of CB1 or in the regulation of CB1. These include a multitude of proteins regulated by $Ca^{2+}$, an important second messenger modulating neuronal activity, a great number of proteins of the Rab family, which are generally involved in budding, transport, docking, and fusion of intracellular

vesicles, and thus, in sorting and trafficking of internalized GPCRs, several 14-3-3 proteins, which exert important scaffolding functions, and a number of RTKs and receptor type tyrosine phsophatases, which were shown to be assembled in multireceptor complexes with GPCRs and mutually modulate downstream signaling pathways (2.2.3).

Cell type-specifically isolated proteins provide a basis for new hypotheses regarding differences in CB1-mediated manifestations of glutamatergic or GABAergic signaling output. Considering the threshold of 1% molar ratio to CB1, out of 571 proteins 33 proteins in the Glu-CB1-SF-C-TAP and 56 proteins in the GABA-CB1-SF-C-TAP were defined as specific for one or the other neuronal subtype (Fig. 4.16; Tab. 4.1). These proteins could play important roles on their own by their functional properties, especially if they have a high abundance and are annotated in clusters with functions directly related to GPCR signaling. Additionally, enrichment of proteins specific for one of the neuronal subtypes in one cluster hints at differences regarding cell type-specific CB1 signaling through the function of this cluster. In the CB1-containing Cluster 1, an even distribution of Glu-CB1-SF-C- and GABA-CB1-SF-C-specific proteins was observed, which have to be considered as candidates to change CB1 signaling in the respective cell type by their own functional properties. Thus, interesting candidates were, for instance, Glu-CB1-SF-C-enriched AC9 (Glu: 0.086, GABA: 0.029), which is a forskolin- and $Ca^{2+}$-insensitive AC isoform or GABA-CB1-SF-C-enriched PKA (Glu: 0.013, GABA: 0.045) (Tab. 4.2). On the other hand, Cluster 5, taken as a whole, clearly shows enrichment of GABA-specific proteins, which might indicate that $K^+$ channel activity in general is more strongly influenced by CB1 in GABAergic interneurons, as discussed above. Another protein to be noted is $G\alpha_z$ (Glu: 0.141, GABA: 0.101), which is member of the $G\alpha_{i/o}$ family of G proteins. The relative abundance to CB1 is in the range of the other co-purified $G\alpha_i$ proteins, which are known to predominantly couple to CB1, and several fold higher than $G\alpha_s$ or $G\alpha_{q/11}$, which have also already been shown to functionally couple to CB1. There is little known about an interaction of CB1 with this G protein subunit, and although per definition it is not specific for one or the other cell type, the difference in abundance between Glu-CB1-SF-C-TAP and GABA-CB1-SF-C-TAP, together with its unconventional signaling properties, might hold the potential to contribute to differential CB1 signaling in glutamatergic neurons and GABAergic interneurons. The role of this protein will be investigated in the next chapter.

Eventually, a few potential points of criticism regarding this study have to be stressed. In neurons, CB1 is considered to be located and to act generally in the presynaptic compartment, thereby decreasing neurotransmitter release after being activated by endocannabinoids produced at the postsynaptic site. It can be argued that the identified interactors cover both presynaptically and postsynaptically located proteins. It was shown that there are compartment-selective actions of

CB1 in polarized cells where the receptor stably accumulates in the axonal plasma membrane after going through cycles of endocytosis and recycling in the somatodendritic compartment, involving specific intracellular pathways, before being delivered to axons (Leterrier et al., 2006). Whereas a CB1-dependent strong decrease of PKA activity can be observed in the nerve terminals, somatodendritic CB1 is constitutively activated by locally produced 2-AG, thereby constitutively inhibiting the cAMP/PKA pathway and ultimately leading to its relocation to the axonal compartment (Ladarre et al., 2014). The identification of interacting proteins that are predominantly located in the postsynapse therefore does not exclude that they are bound in CB1 protein complexes *in vivo*, considering the activity-dependent cycles of endocytosis, recycling, and transport CB1 is undergoing in neurons after its translation.

The conditional Cre-expressing mouse lines drive expression under the NEX promoter in order to target dorsal telencephalic glutamatergic neurons (Goebbels et al., 2006) or the Dlx5/6 promoter in order to target all forebrain GABAergic interneurons (Monory et al., 2006). Expression of the SF-tagged CB1 under control of the NEX promoter spatially resembles endogenous CB1 expression in hippocampal glutamatergic neurons, but only one of the two major populations of perisomatic GABAergic interneurons that are targeted by the Dlx5/6 promoter endogenously express CB1. Cholecystokinin-positive ($CCK^+$) interneurons and parvalbumin (PV)-expressing interneurons constitute these two major populations, and endogenously CB1 is primarily located only on axon terminals of CCK-positive cells (Katona et al., 1999; Marsicano and Lutz, 1999). This might lead to the detection of false positive interactions of CB1 with proteins in PV-expressing interneurons, which do not occur *in vivo* in CCK-expressing interneurons, but is unavoidable due to limitations in the availability of Cre-driving mouse lines. However, it was shown that the majority of GABAergic interneurons in the hippocampus are CCK-positive interneurons in all subregions with the exception of the dorsal subiculum (Whissell et al., 2015), thus expression of the bait CB1-SF-C protein under control of the dlx5/6 promoter can still be considered an appropriate model system in order to address the aims of this study.

On a final note, one technical weakness of the TAP approach in the detection of cell type-specific protein complexes has to be mentioned. The expression of the bait protein was proven to be specific for either neuronal subtype but before the two step purification procedure, synaptosome preparations were lyzed under mild conditions overnight in order to solubilize the membrane proteins. As a consequence thereof, intact cells or cell fractions are disintegrated, and the bait protein might get in contact with other proteins of other cell types, which are theoretically able to bind to the bait protein, but endogenously do not because of the spatial segregation. This might also lead to the detection of false positive protein interactions of Glu-CB1-SF-C with specific

GABAergic proteins or the other way around, or even with glial or astrocytic proteins. In a less severe scenario, it was still possible that the specificity effect calculated by the Glu versus GABA ratio of the ratios of the respective proteins to CB1 (Fig. 4.16) gets diluted by a mixture of specific CB1 protein complexes and free floating proteins of the other cell type, which are still able to bind to the protein complexes during the lysis step. Nevertheless, the dataset of identified proteins does not indicate that there is a significant amount of proteins that do not occur in the respective cell types in which CB1-SF-C was expressed, and specificity for a considerable number of proteins could clearly be determined, which eventually confirms the validity of this approach in its entirety.

Taken together, this study outlines a comprehensive view on a large number of up to now unidentified potentially CB1-interacting proteins and functional groups of proteins. Although the majority of proteins were found in both neuronal subtypes, a number of neuron subtype-specific interactors may pave the way to put forward new hypotheses of how differential CB1 signaling in glutamatergic and GABAergic neurons in the hippocampus may emerge, in particular regarding proteins directly involved in receptor-coupled G protein signaling. Among the cell type-specific proteins in the main clusters of the network analysis (Tab. 4.2), AC9 was identified as a potential CB1 interactor in glutamatergic neurons. Although it was shown to be only marginally inhibited by CB1 in transfected monkey kidney fibroblast-like COS7 cells in early studies (Rhee et al., 1998), it cannot be ruled out that this isoform may play a significant role in transmitting the signaling from $G\alpha_{i/o}$ to downstream effectors in the brain in a cell type-specific manner, since it is not additionally regulated by $Ca^{2+}$ and calmodulin, as is the case with other AC isoforms. Another mechanism may be found in the enrichment of PKA and voltage-gated $K^+$ channels in GABAergic CB1 protein complexes. CB1-mediated activation of $G\alpha_{i/o}$ and subsequent inhibition of AC leads to a decrease in PKA activity. Lower PKA activity leads to a decrease in phosphorylation of voltage-gated $K^+$ channels and thus, a higher activity and potentially increased ability for the neuron to return to the resting state after depolarization. An improved ability of GABAergic interneurons to return to a state of re-excitabilty could counteract the mechanism of CB1-mediated suppression of neurotransmitter release, but is highly speculative. The final outcome would be an overall lower efficiency of CB1 signaling in glutamatergic neurons as compared to GABAergic interneurons, as shown in electrophysiological studies (Azad et al., 2003), but irrespective of the observed several fold stronger direct coupling to G protein signaling in glutamatergic neurons as compared to GABAergic interneurons (Steindel et al., 2013). A potential role of the identified G protein $G\alpha_z$ in cell type-specific CB1 signaling was brought up and will be investigated in more detail in the next section.

# 5 Functional studies on G protein subunit alpha z in CB1-mediated signaling

## 5.1 Introduction

G protein subunit alpha z ($G\alpha_z$) is a member of the $G\alpha_{i/o}$ class of G proteins, although showing a relatively low sequence homology of approximately 60% as compared to $G\alpha_i$. Like other G protein members of this class, it inhibits AC upon activation through a GPCR, but is the only one insensitive to PTX due to a lack of a C-terminal cysteine residue. It is predominantly expressed in neuronal tissues, and was shown to interact with several GPCRs, including adenosine $A_1$ receptor ($A_1$), D2, $\alpha_2$AR, 5-$HT_{1A}$ receptor (5-$HT_{1A}$), muscarinic acetylcholine receptor $M_2$ ($M_2$), and all types of opioid receptors (Ho and Wong, 2001). In addition to its effect on AC, it couples receptors to N-type VGCCs and stimulates GIRKs as shown in sympathetic neurons (Jeong and Ikeda, 1998). Due to a sequence variation in one of the guanine nucleotide-binding regions, $G\alpha_z$ hydrolyzes GTP with much slower kinetics as compared to other Gα subunits, implying that it may be hard to switch off after activation. Another aspect of its unique biochemical characteristics is the possibility of regulating its signaling properties by a large variety of modifications, such as phosphorylation by PKC or p21-activated kinase 1 (PAK1), myristoylation, arachidonoylation, and palmitoylation. Among the family of RGS proteins, at least five members interact with $G\alpha_z$, including RGS10, RGS4, retinal(RET)-RGS1, GAIP, and most specifically RGSZ1, thereby critically controlling the low intrinsic GTP hydrolysis rate of this G protein. Further interactions with other proteins were described, such as G protein-regulated inducer of neurite outgrowth 1 and 2 (GRIN1, GRIN2). Consequently, $G\alpha_z$ should be considered as a functionally unique protein with specialized roles, rather than being a PTX-resistant version of $G\alpha_{i/o}$ proteins (Ho and Wong, 2001) (Fig. 5.1).

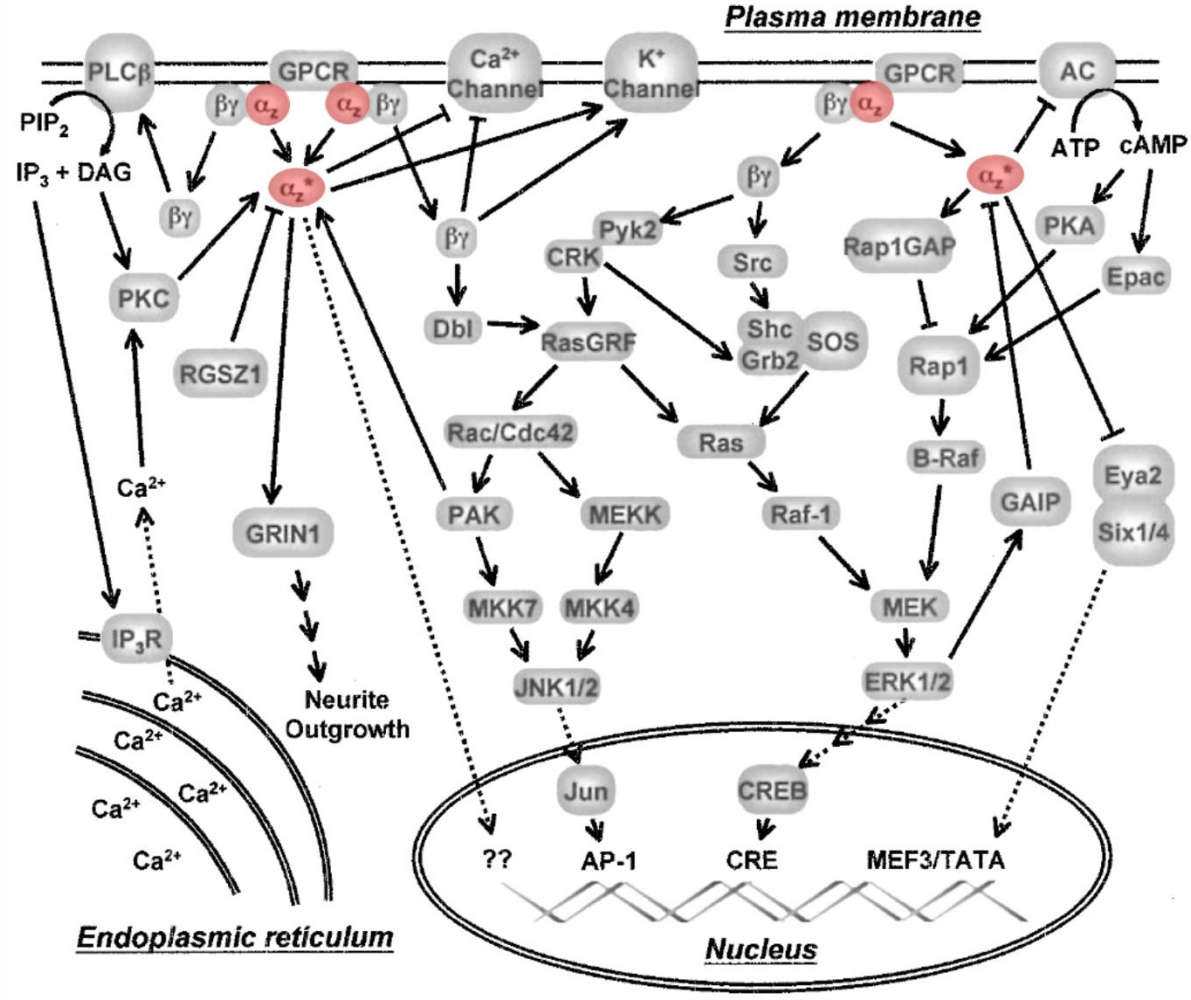


**Fig. 5.1 Signaling pathways involving $G\alpha_z$**

Activation of GPCRs coupled to $G\alpha_z$ (red) leads to the activation and dissociation of $G\alpha_z$ and $G\beta\gamma$ subunits, subsequently inducing a complex network of signaling pathways. Asterisks: activation state. Solid arrows: direct activation. Solid blunted arrows: direct inhibition. Dotted arrows: translocation event. Multiple arrows: activation through a number of steps. AC: adenylyl cyclase. CRE: cAMP-responsive element. CRK: CT10 regulator of kinase. DAG: diacylglycerol. Epac: cAMP-dependent Rap1 guanine nucleotide exchange factor. ERK: extracellular signal-regulated kinase. Eya2: Eyes absent transcription cofactor 2. GAIP: G protein-interacting protein. GPCR: G protein-coupled receptor. Grb2: growth factor receptor-bound protein 2. GRIN1: G protein-regulated inducer of neurite outgrowth 1. $IP_3$: inositol trisphosphate. $IP_3R$: inositol trisphosphate receptor. JNK: Jun N-terminal kinase. MEKK: MEK kinase. MKK4/MKK7: mitogen-activated protein kinase kinases 4 and 7, respectively. PAK: p21-activating kinase. $PIP_2$: phosphatidylinositol 4,5-bisphosphate. PKA: cAMP-activated protein kinase A. PKC: protein kinase C. PLC: phospholipase C. Pyk2: proline-rich tyrosine kinase 2. Rap1GAP: Rap1 GTPase-activating protein. RasGRF: Ras guanine nucleotide-releasing factor. RGSZ1: regulator of G protein signaling Z1. Six1/4: sine oculis homologous transcription factors 1 and 4. SOS: Son of sevenless guanine nucleotide exchange factor (modified from Ho and Wong, 2001).

In growth cones of developing neurons, $G\alpha_z$ was shown to inhibit BDNF-stimulated axonal outgrowth of cortical neurons by acting on downstream effectors of the BDNF signaling pathway without having an inherent effect on growth properties (Hultman et al., 2014).

Behavioral studies have revealed a hypertolerance to morphine in $G\alpha_z$-KO mice, whereas acute morphine treatment-mediated analgesia is only slightly diminished (Hendry et al., 2000; Leck et al., 2004). Strikingly, supraspinal analgesic tolerance produced by cannabinoids and cross-tolerance between CB1 and μ-OR was shown to be mediated by $G\alpha_z$. Stimulation of CB1 with various receptor agonists leads to analgesic tolerance, which is independent from receptor desensitization or loss of G proteins, lasting for more than 14 days, and at the same time reducing morphine analgesia. Morphine administration, on the other hand, produces tolerance for only three days without affecting CB1. These effects are mediated by an interaction of both receptors with the Histidine triad nucleotide-binding protein 1 (HINT1)-RGSZ signaling module, thereby modulating $G\alpha_z$ (Garzon et al., 2009). Other behavioral responses to psychoactive drugs are affected by a loss of $G\alpha_z$ as well. Cocaine caused a more pronounced increase in locomotor activity in $G\alpha_z$-KO mice as compared to wildtype mice, and the antidepressant effects of catecholamine reuptake inhibitors are completely abolished (Yang et al., 2000). $G\alpha_z$-KO mice furthermore show increased levels of anxiety and responses to 5-$HT_{1A}$ stimulation, although these effects are strongly dependent on the genetic background of the mouse strain (van den Buuse et al., 2007).

Among several interesting CB1-interacting proteins, which have the potential to change the signaling output in one neuronal subtype as compared to the other, $G\alpha_z$ was found with a distinct and relatively high abundance to CB1 in glutamatergic neurons (0.141) and GABAergic interneurons (0.101). Although in the analysis of the identified proteins in the TAP samples specificity of a protein for one or the other cell type was defined as a ≥ 2x enrichment in one cell type as compared to the other, $G\alpha_z$ with its unique signaling properties still seems to hold the potential to change the overall signaling output in hippocampal glutamatergic neurons versus GABAergic interneurons. Since the identification of proteins is initially a first step towards understanding signaling, further experiments must be performed in order to investigate if the interaction of CB1 and $G\alpha_z$ is functional.

As a first step, a CoIP of $G\alpha_z$ and CB1 was performed using CB1- and $G\alpha_z$-cotransfected HEK293 cells and hippocampal lysates of AAV-injected mice to confirm the physical interaction obtained in the TAP approach. In order to investigate the coexpression of CB1 and $G\alpha_z$ *in vivo*, we used double fluorescent *in situ* hybridization (dFISH) to determine the spatial expression of the respective mRNAs on brain slices. Finally, using an assay to measure cAMP levels in an *in vitro* system, the functional interaction of CB1 with $G\alpha_z$ was evaluated.

## 5.2 Results

### 5.2.1 Cloning of the $G\alpha_z$ and $G\alpha_o$ CDS into AAV expression plasmids

Two expression vectors based on pAM AAV expression backbones were cloned in order to set the foundation for the development of model systems, which serve for the investigation of a functional interaction of $G\alpha_z$ with CB1. One contains an HA-tagged $G\alpha_z$ CDS, and the other an HA-tagged $G\alpha_o$ CDS, with the latter designed to serve as a control in the following experiments, as this G protein was described as being predominantly activated after CB1 stimulation. In order to obtain the CDS of $G\alpha_z$, RNA from mouse brain was isolated, followed by a reverse transcription of mRNAs to cDNAs using oligo d(T) primers. $G\alpha_z$ cDNA was then amplified in a PCR reaction adding restriction sites at the 5'- and 3'-end of the amplificates to allow the generation of ligation sites at both ends of the CDS using specific restriction enzymes complementary to the linearized plasmid vector backbone. The CDS of $G\alpha_o$ was obtained by a PCR reaction again adding restriction sites at both ends of the CDS and using a $G\alpha_o$ CDS-containing pCIS mammalian expression vector as template (kindly provided by Prof. Dr. Nina Wettschureck, Max-Planck-Institute for Heart and Lung Research, Bad Nauheim, Germany). Both inserts containing the respective G protein CDSs were then, in each case, cloned into a pAM AAV expression backbone containing a CAG promoter, WPRE, AAV2 ITRs, bGHpA, and the CDS for an HA-tag upstream the insertion site for the respective G protein sequence leading to the generation of the plasmids pAM/CAG-HA-G_alpha(z)-WPRE-bGHpA (pAM-HA-$G\alpha_z$) and pAM/CAG-HA-G_alpha(o)-WPRE-bGHpA (pAM-HA-$G\alpha_o$) (Fig. 5.2). Both plasmids were sequenced to exclude mutations and can be used directly for transfections as mammalian expression vectors as well as for the production of AAVs in order to express HA-tagged $G\alpha_z$ (HA-$G\alpha_z$) or HA-tagged $G\alpha_o$ (HA-$G\alpha_o$).

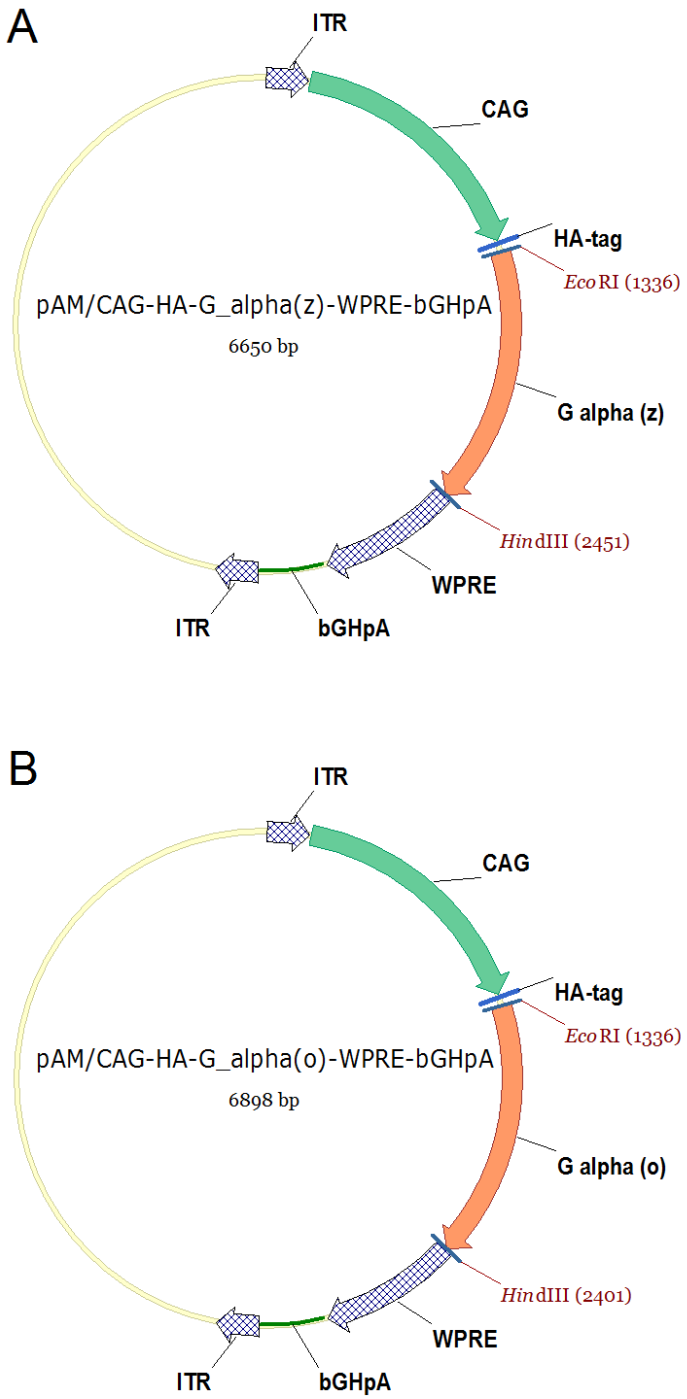


**Fig. 5.2 Plasmid maps of pAM/CAG-HA-G_alpha(z)-WPRE-bGHpA and pAM/CAG-HA-G_alpha(o)-WPRE-bGHpA**

After PCR amplification and addition of restriction sites, the $G\alpha_z$ CDS (**A**) or $G\alpha_o$ CDS (**B**) were cloned into pAM AAV expression vector backbones. Expression is driven under control of a CAG promoter, and an HA-tag CDS upstream the insertion site for the G protein CDS leads to the expression of an HA-tagged $G\alpha_z$ (**A**) or $G\alpha_o$ (**B**), respectively. Both plasmids can be used directly for transfection and subsequent expression of the recombinant proteins *in vitro* or for the production of AAVs. ITR: inverted terminal repeat. CAG: CAG promoter (CMV early enhancer element, promoter, first exon and the first intron of the chicken beta-actin gene and the splice acceptor of the rabbit beta-globin gene). WPRE: woodchuck hepatitis virus posttranscriptional regulatory element. bGHpA: bovine growth hormone polyadenylation signal.

HEK293 cells were transfected with either pAM-HA-Gα$_z$ or pAM-HA-Gα$_o$, and the subsequent expression of HA-Gα$_z$ or HA-Gα$_o$ validated by western blot analysis using a polyclonal antibody directed against an internal epitope of Gα$_z$ or a monoclonal antibody directed against Gα$_o$ (Fig. 5.3).

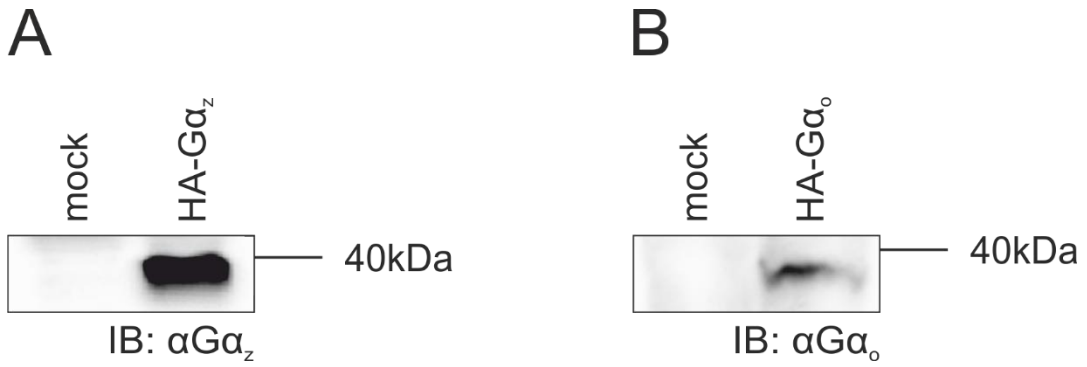


**Fig. 5.3 Western blot analysis of Gα$_z$ or Gα$_o$ overexpression in HEK293 cells**

HEK293 cells were transfected with HA-Gα$_z$ (**A**) or HA-Gα$_o$ (**B**) with mock-transfected cells as negative controls. Protein expression was detected using specific antibodies directed against either Gα$_z$ or Gα$_o$. Specific bands were detectable at around 39kDa according to the molecular weight of both HA-tagged G protein subunits. kDa: kilodalton. IB: immunoblot.

### 5.2.2 Co-immunoprecipitation of CB1 and Gα$_z$

In the TAP approach, Gα$_z$ was co-purified together with CB1. Since the TAP approach can lead to the purification of huge protein complexes, co-purified proteins do not necessarily interact directly with the bait protein. HEK293 cells were co-transfected with HA-Gα$_z$ and CB1-SF-C, which served as source material for subsequent CoIPs in order to validate the interaction of CB1 and Gα$_z$ in another model system and another cellular environment.

Four groups of HEK293 cells were used, transfected with both CB1-SF-C and HA-Gα$_z$, only one of these plasmids, or mock-transfected cells serving as negative controls. According to the TAP protocol, lysis and washing steps were initially performed with 0.3% Brij O10-containing buffer. After performing the CoIP using M2 anti FLAG agarose beads directed against the SF-tag of the CB1 fusion protein (3.8.1), CB1-specific bands were detected in the CB1-SF-C + HA-Gα$_z$ co-transfected and CB1-SF-C-only transfected HEK293 cells, but not in the HA-Gα$_z$ and mock transfected HEK293 cells as shown by western blot using an antibody directed against CB1 (Fig. 5.4A). Using an antibody against Gα$_z$, a specific band at 39kDa in the eluate of CB1-SF-C + HA-Gα$_z$ co-transfected cells indicated a successful co-purification, but was also visible in the HA-Gα$_z$ only transfected cells, which served as a negative control for unspecific binding of HA-Gα$_z$ (Fig. 5.4B). In order to improve the protocol and prevent unspecific binding of HA-Gα$_z$, reaction tubes were changed after each

washing step, the number of washing steps were increased from three up to eight, and various detergents in the washing buffers tested to increase stringency, such as 0.5% Nonidet P-40, 1% Triton X-100, and combinations including 0.1% SDS. No changes were visible in the western blot detection of CB1 and $G\alpha_z$ in the respective samples as compared to the initial approach (Fig. 5.4A, B). The overall band intensities decreased when using SDS in the washing steps, with $G\alpha_z$ hardly detectable in the final eluates but with the same intensity in the co-transfected sample and the $G\alpha_z$ only transfected negative control.

In order to test the CoIP procedure in a less artificial environment with no overexpression of $G\alpha_z$, hippocampal lysates of AAV-Stop-CB1-SF-C-injected NEX-Cre x $CB1^{f/f}$ mice (Glu-CB1-SF-C) and Dlx5/6-Cre x $CB1^{f/f}$ mice (GABA-CB1-SF-C) and non-injected NEX-Cre x $CB1^{f/f}$ mice (Glu-CB1-KO) and Dlx5/6-Cre x $CB1^{f/f}$ mice (GABA-CB1-KO) were taken as source material for another CoIP using a concentration of 1% Brij O10 in the washing buffer. CB1-specific bands were detected in the eluates of Glu-CB1-SF-C mice and GABA-CB1-SF-C mice with a stronger band intensity in the Glu-CB1-SF-C sample as compared to GABA-CB1-SF-C (Fig. 5.4C), in accordance with the expression analysis of CB1-SF-C in this model system (Fig. 4.14). The detection of $G\alpha_z$ again showed signals in each sample running a little lower as compared to the HEK293 cell samples at 38kDa, due to the lack of the HA-tag as only endogenous $G\alpha_z$ is present (Fig. 5.4D). This again indicated a non-specific binding of $G\alpha_z$ in this CoIP approach.

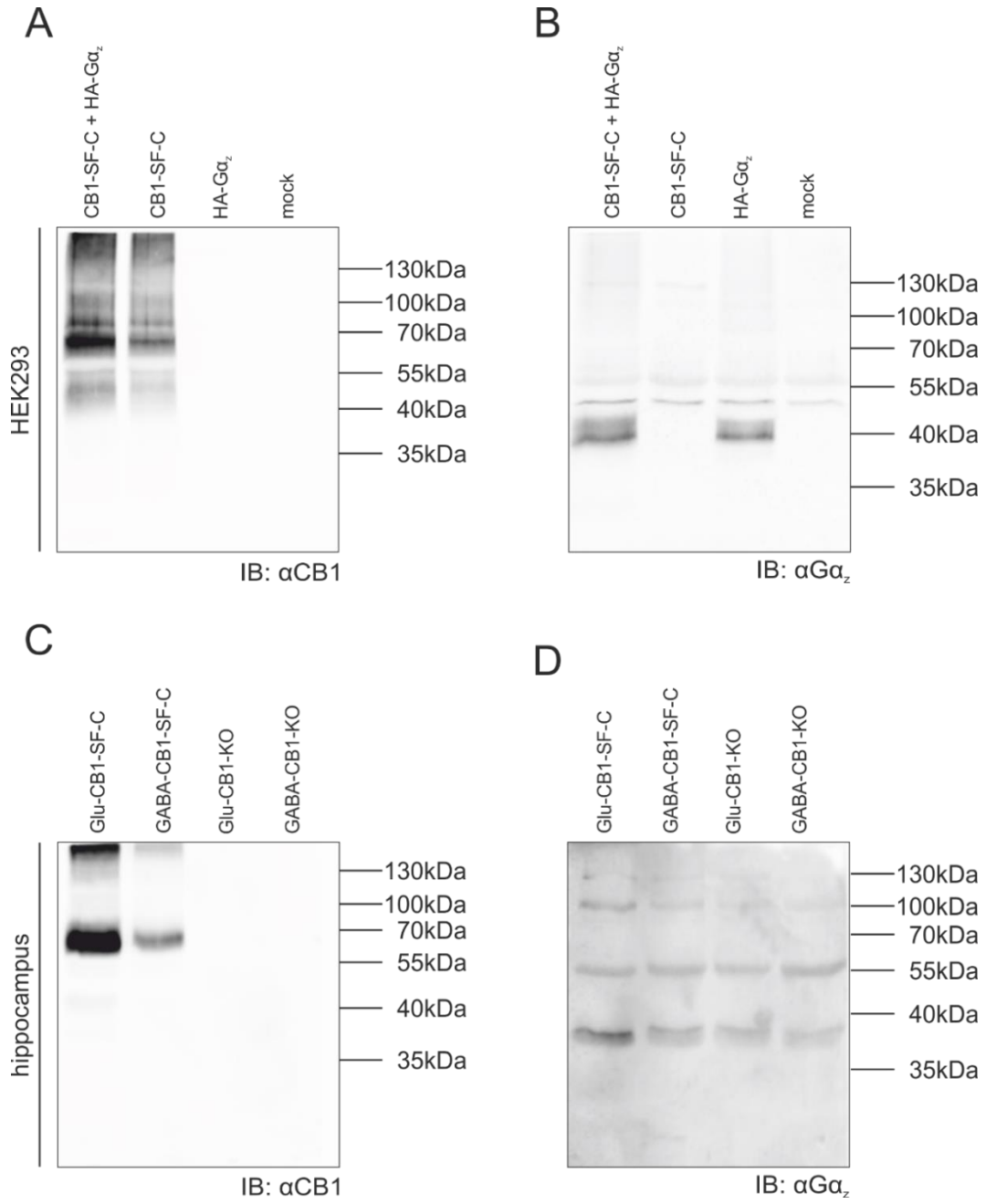


**Fig. 5.4 Co-immunoprecipitation of Gαz with CB1 using transfected HEK293 cells and hippocampal lysates of AAV-injected mice**

Western blot analysis of co-immunoprecipitation experiments using CB1-SF-C and HA-Gαz transfected HEK293 cells (**A**, **B**), and hippocampal lysates of AAV-Stop-CB1-SF-C injected NEX-Cre x CB1$^{f/f}$ mice (Glu-CB1-SF-C) and Dlx5/6-Cre x CB1$^{f/f}$ mice (GABA-CB1-SF-C) and non-injected NEX-Cre x CB1$^{f/f}$ mice (Glu-CB1-KO) and Dlx5/6-Cre x CB1$^{f/f}$ mice (GABA-CB1-KO) as negative controls (**C**, **D**). Experiments were performed using M2 anti FLAG agarose beads directed against the SF-tag of the CB1-SF-C fusion protein. In the HEK293 cell experiments various procedures with different detergents allowed for a successful precipitation of CB1-SF-C (**A**) but with a Gαz-specific signal not only in the co-transfected HEK293 cells, but also in the HA-Gαz only transfected cells serving as a negative control for unspecific binding of HA-Gαz (**B**) (Fig. 5.4A, B representative for all CoIP experiments performed with transfected HEK293 cells with varying procedures as described in the main text). A CoIP of mouse hippocampal lysates after AAV-mediated expression of CB1-SF-C also allowed for the precipitation of CB1-SF-C in the AAV-injected animals (**C**) but again non-specific binding of endogenous Gαz in all samples. kDa: kilodalton. IB: immunoblot.

### 5.2.3 CB1 and $G\alpha_z$ are coexpressed in glutamatergic neurons and GABAergic interneurons in the hippocampus of C57BL/6N mice as evaluated by double fluorescent *in situ* hybridization

In order to investigate the expression of endogenous CB1 and $G\alpha_z$ in the hippocampus, a dFISH assay was performed using labeled riboprobes directed against the respective mRNAs on coronal brain sections (3.1.2). The $G\alpha_z$ CDS obtained for the generation of AAV expression plasmids (5.2.1) was inserted into a pBSIIKS vector backbone and served as template for the T3/T7 RNA polymerase reverse transcription of the $G\alpha_z$ CDS, thereby generating a labeled RNA riboprobe for the detection of $G\alpha_z$ mRNA. For the generation of a riboprobe directed against CB1 mRNA, a CB1 CDS-containing pBSIIKS vector was used, which was generated in our lab. Both riboprobes against CB1 and $G\alpha_z$ were used in a dFISH on coronal brain slices of C57BL/6N mice. CB1 is expressed in glutamatergic neurons and GABAergic interneurons, but the signal intensity between the neuronal subtypes differs to a very high degree, thus confirming the several fold higher expression of CB1 in GABAergic interneurons as compared to glutamatergic neurons (Monory et al., 2006; Steindel et al., 2013). $G\alpha_z$ mRNA shows a similar spatial expression in glutamatergic neurons and in GABAergic interneurons, but with less difference in signal intensity between both types of neurons as compared to CB1 mRNA (Fig. 5.5). Image acquisition set up for saturation of CB1 and $G\alpha_z$ fluorescence signal intensity in glutamatergic neurons leads to a fluorescence signal overexposure in GABAergic interneurons for both mRNAs, which is even more pronounced for CB1 (Fig. 5.5A). The specific signals for the respective mRNAs in glutamatergic neurons are separated when merging the images but visible within the same neurons, thereby validating the coexpression of CB1 and $G\alpha_z$ (Fig. 5.5C). When image acquisition is set up for saturation of both respective riboprobe signals in GABAergic interneurons, the $G\alpha_z$-specific signal is still visible in glutamatergic neurons, albeit weaker, whereas the CB1-specific signal is barely detectable (Fig. 5.5B). All CB1-positive interneurons also show expression of $G\alpha_z$. Due to the high expression of both mRNAs, the signals are hardly separated from each other when merging the images (Fig. 5.5D).

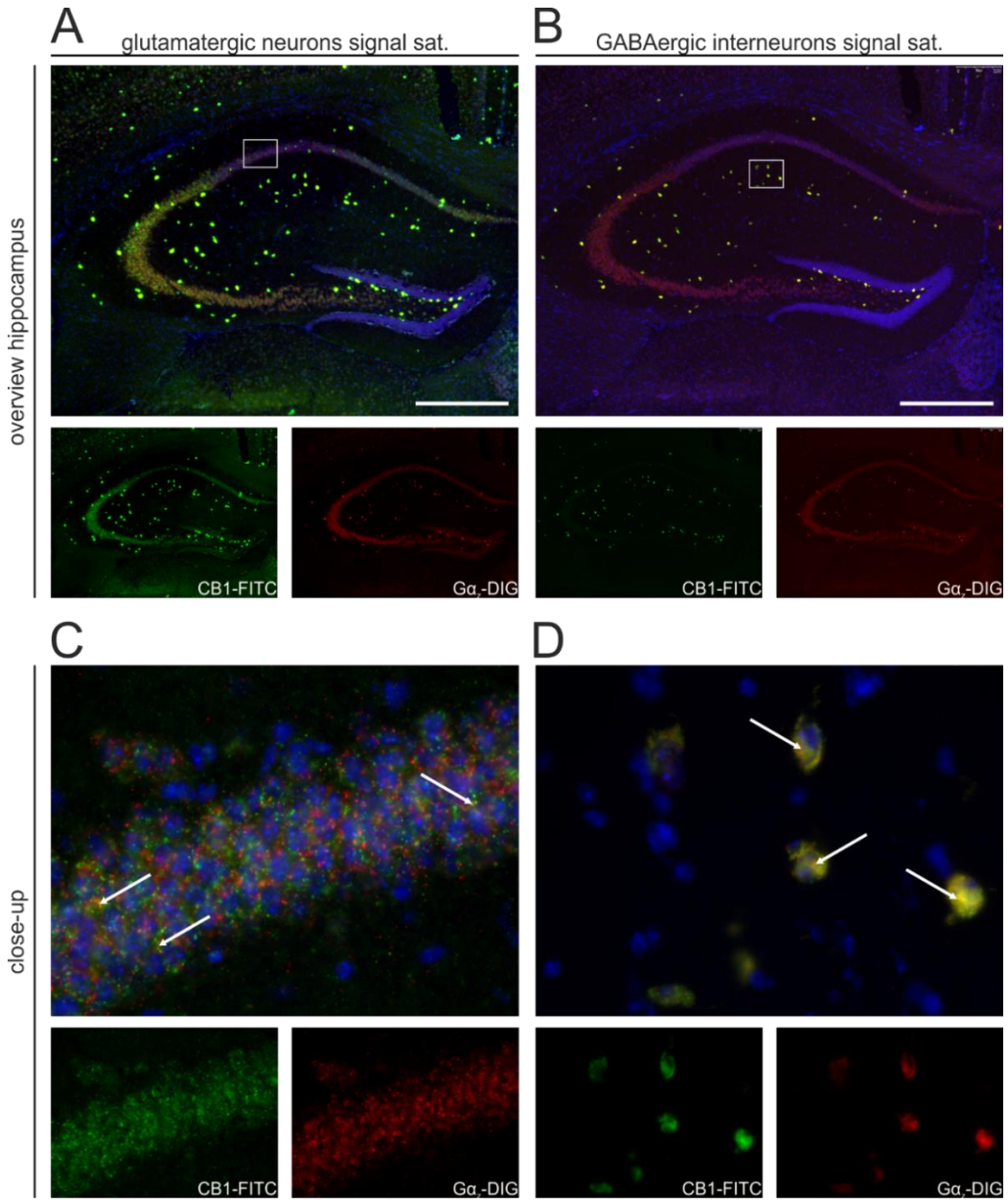


**Fig. 5.5 Coexpression of CB1 and Gα$_z$ in glutamatergic neurons and GABAergic interneurons in mouse hippocampus as evaluated by dFISH**

CB1 and Gα$_z$ are both expressed in glutamatergic neurons and GABAergic interneurons in the hippocampus. Expression of both mRNAs occurs at higher levels in GABAergic interneurons as compared to glutamatergic neurons with a more pronounced difference in CB1 expression between both neuronal subtypes (**A**, **B**). Image acquisition set up for saturation of both riboprobe signals in glutamatergic neurons (left column) leads to an overexposure of both CB1 and Gα$_z$ signals in GABAergic neurons with an even more pronounced difference of CB1 expression between both neuronal subtypes (**A**), and reveals coexpression in the same neurons, as indicated by white arrows, with the single signals clearly distinguishable from each other in the merged image (**C**). Image acquisition set up for saturation of both riboprobe signals in GABAergic interneurons (right column) still allows for a weak detection of Gα$_z$-specific fluorescence signal in glutamatergic neurons, but with a barely detectable CB1 signal in glutamatergic neurons (**B**). CB1 and Gα$_z$ are coexpressed in GABAergic interneurons and show a high expression of both CB1 and Gα$_z$ mRNA with single signals hardly distinguishable from each other as indicated by white arrows (**D**). Green: fluorescein isothiocyanate (FITC)-labeled CB1 mRNA-specific riboprobe (CB1-FITC). Red: digoxigenin (DIG)-labeled Gα$_z$ mRNA-specific riboprobe (Gα$_z$-DIG). Blue: DAPI-stained cell nuclei.

### 5.2.4 $G\alpha_z$ functionally interacts with CB1 after agonist stimulation in an *in vitro* model

CB1 and $G\alpha_z$ are coexpressed in glutamatergic neurons and GABAergic interneurons in the mouse hippocampus, and were co-purified in the TAP approach. However, if there is a functional interaction between these two proteins remained to be clarified. In order to address this issue, an *in vitro* model was established using stably CB1 expressing HEK293 cells (kindly provided by Melanie Wickert from our lab), transiently transfected with either pAM-HA-$G\alpha_z$ (HEK293-CB1 + $G\alpha_z$) pAM-HA-$G\alpha_o$ (HEK293-CB1 + $G\alpha_o$), or mock-transfected without DNA (HEK293-CB1). All cell lines were then in triplicates treated with forskolin in order to induce cAMP production via direct activation of adenylyl cyclase and either the CB1 agonist WIN, vehicle as a control, or WIN with additionally PTX, which inhibits all G proteins of the $G_i$ family, but $G\alpha_z$. At four time points after the treatment (5 min, 10 min, 20 min, and 30 min), the cAMP turnover in the cells was measured using a luciferase-dependent detection system as described in 3.3 (Fig. 5.6). Forskolin with WIN-treated cells were expected to show a lower cAMP production as compared to forskolin with vehicle-treated cells (control) due to the inhibition of adenylyl cyclase via the activation of inhibitory G proteins by CB1. Forskolin with WIN and PTX-treated cells were expected to show a lower cAMP production only in the case of HEK293-CB1 + $G\alpha_z$ if $G\alpha_z$ is activated by CB1 after WIN stimulation because of $G\alpha_z$ being the only PTX-insensitive member of the $G_i$ family.

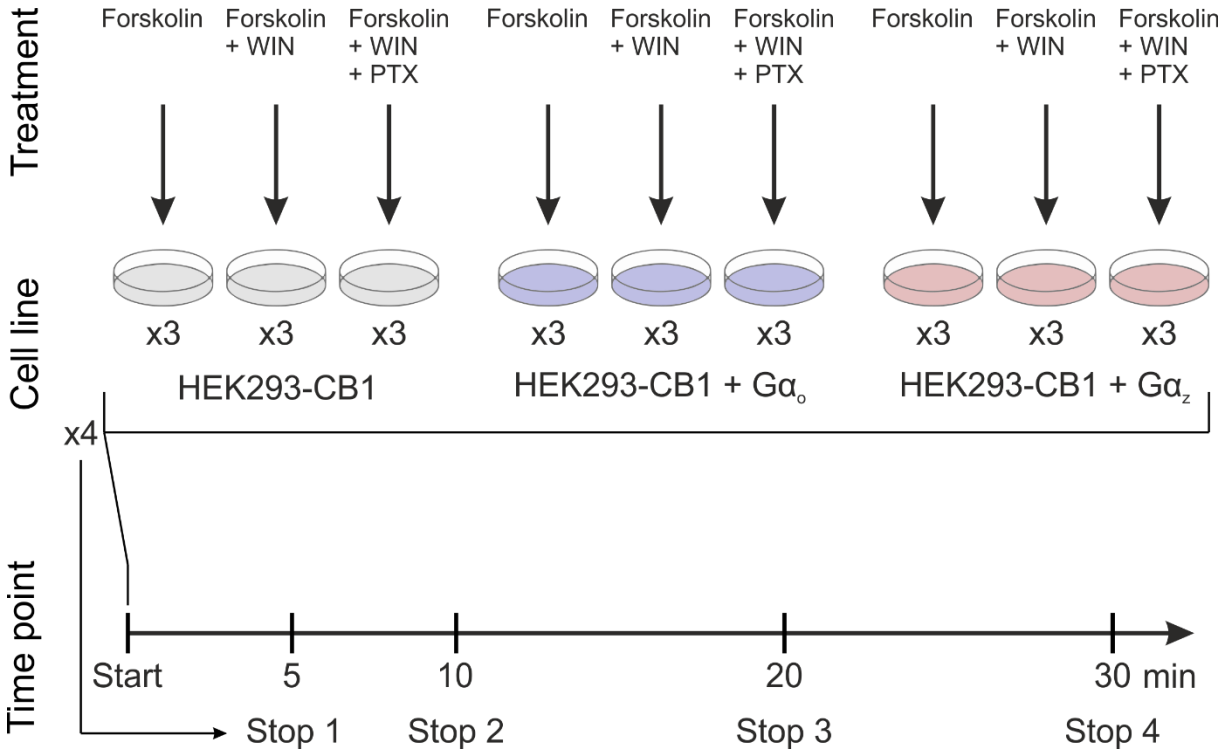


**Fig. 5.6 Schematic diagram of treatment, cells and time points measured in the cAMP assay**

HEK293-CB1, HEK293-CB1 + $G\alpha_o$, and HEK293-CB1 + $G\alpha_z$ cells were treated with either forskolin to measure the baseline cAMP production upon AC activation, forskolin + WIN to measure CB1-mediated inhibition of cAMP production, or forskolin + WIN + PTX to measure CB1-$G\alpha_z$-specific inhibition of cAMP production. The experiment was stopped at four different time points in individual samples and all samples measured in triplicates.

The cAMP turnover 10 min after stimulation showed significant differences in cell line-dependent treatment effects as expected, when the data was analyzed using two-way ANOVA followed by Bonferroni's post-hoc test to evaluate statistical significance. 20 min after stimulation the results showed the same tendencies, although not statistically significant. At both time points, HEK293-CB1 cells showed a lower cAMP production when treated with WIN and WIN + PTX as compared to the vehicle-treated controls. HEK293-CB1 + $G\alpha_o$ cells showed a lower cAMP production after stimulation with WIN and a higher cAMP production after WIN + PTX treatment. In HEK293-CB1 + $G\alpha_z$ cells the effect of PTX inhibiting $G\alpha_{i/o}$ proteins is abolished, indicating a functional interaction of $G\alpha_z$ getting activated by CB1. In contrast, 5 min after treatment, HEK293-CB1 + $G\alpha_z$ cells did not show the expected insensitivity to PTX, instead the cAMP production is increased as compared to the vehicle-treated control similar to HEK293-CB1 + $G\alpha_o$ cells. 30 min after treatment, there is no WIN effect on HEK293-CB1 cells, instead the cAMP production is increased as compared to the vehicle-treated controls (Fig. 5.7).

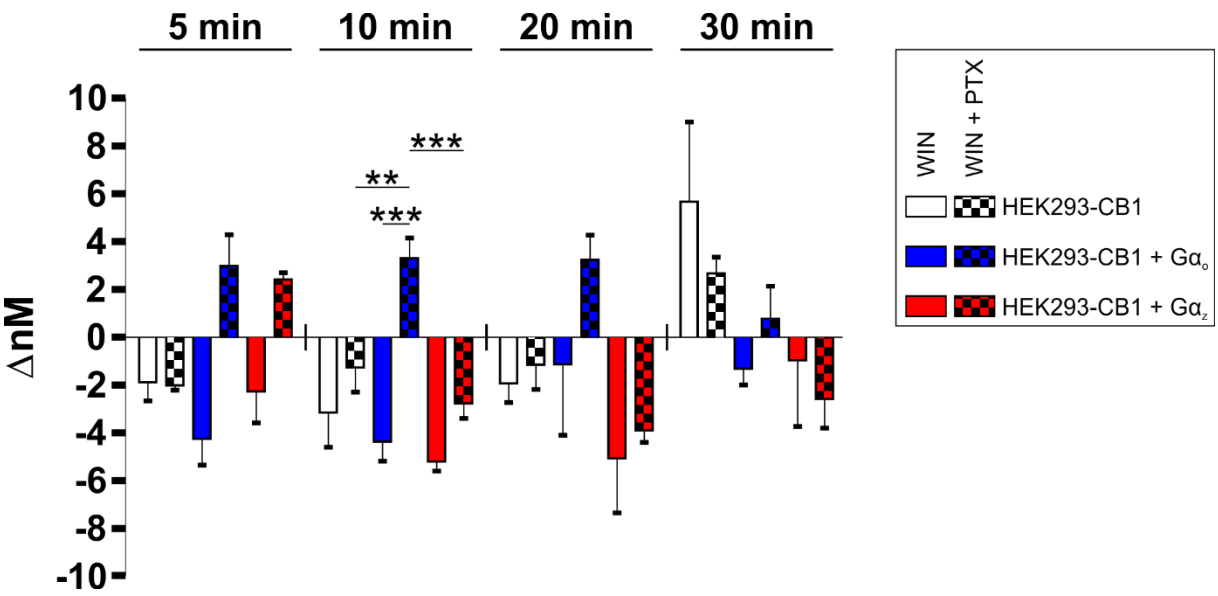


**Fig. 5.7 $G\alpha_z$ functionally interacts with CB1 and inhibits cAMP production after receptor stimulation with WIN in the presence of PTX**

Stably CB1 expressing HEK293 cells (HEK293-CB1), $G\alpha_o$-transfected stably CB1 expressing HEK293 cells (HEK293-CB1 + $G\alpha_o$), and $G\alpha_z$-transfected stably CB1 expressing HEK293 cells (HEK293-CB1 + $G\alpha_z$) cells were treated with forskolin to induce production of cAMP with a concurrent stimulation with the CB1 agonist WIN55,212-2 (WIN) or WIN together with pertussis toxin (WIN + PTX), and compared with forskolin-only-treated controls (n = 3). The difference in cAMP concentration[nM] between WIN- and forskolin-only-treated cells or WIN + PTX- and forskolin-only-treated cells is plotted on the x-axis (in ΔnM) for all cell lines at four different time points (5 min, 10 min, 20 min, 30 min) (independent samples) in order to illustrate stimulation-dependent changes in cAMP production. Statistical significant cell line-dependent treatment effects (two-way ANOVA, followed by Bonferroni's post-hoc test, cell line x treatment effect, $p = 0.006$), could be validated only at 10' after stimulation. WIN + PTX treatment compared to forskolin-only treatment of HEK293-CB1 + $G\alpha_o$ cells led to an increase in cAMP production as compared to a decrease in WIN-treated HEK293-CB1 + $G\alpha_o$ cells, WIN + PTX-treated HEK293-CB1 cells, and WIN + PTX-treated HEK293-CB1 + $G\alpha_z$ cells. All cell lines showed the same tendencies after 20', albeit not statistically significant. 5' after treatment HEK293-CB1 + $G\alpha_z$ cells did not show the expected PTX insensitivity, and a subsequent increase in cAMP after WIN + PTX treatment. 30' after stimulation, the effect of WIN on HEK293-CB1 cells was reversed showing an increase in cAMP production. **: $p < 0.01$. ***: $p < 0.001$.

## 5.3 Discussion

In this part of the thesis, the functional interaction of CB1 with one candidate interactor identified in the TAP approach was evaluated. In a study investigating the analgesic properties of cannabinoids, desensitization and cross-desensitization of supraspinal CB1 and μ-OR was observed, which is mediated by a functional coupling of both receptors to HINT-RGSZ and $G\alpha_z$ in order to produce supraspinal analgesia. In this work, $G\alpha_z$ was successfully co-precipitated with CB1 in periaqueductal gray (PAG) membrane preparations and it could be shown that CB1 promotes a

reversible transfer of this G proteins toward RGSZ2 proteins upon WIN stimulation (Garzon et al., 2009). An interaction with CB1 in other brain areas and its role in a direct transmission of CB1 signaling in the hippocampus, however, was unknown.

First of all, the co-expression of CB1 and its potential interactor $G\alpha_z$ was assessed using dFISH. Visualization of CB1 and $G\alpha_z$ mRNA in the hippocampus of C57BL/6N mice revealed that both mRNAs are coexpressed in glutamatergic principal cells as well as GABAergic interneurons. CB1 is expressed at several fold higher levels in GABAergic interneurons as compared to glutamatergic neurons (Monory et al., 2006; Steindel et al., 2013), which is visible in the dFISH by pronounced differences in fluorescent signal intensities between both cell types. $G\alpha_z$ expression was also higher in GABAergic interneurons but as compared to CB1, the signal intensity difference to glutamatergic neurons was less pronounced (Fig. 5.5). According to the MS quantification of proteins in the TAP samples, $G\alpha_z$ was co-purified with a higher relative abundance to CB1 in glutamatergic neurons. Since the differences in cell type-specific expression of this G protein are lower as compared to CB1, the ratio of $G\alpha_z$ to CB1 appears to be higher in glutamatergic neurons than in GABAergic interneurons, leading potentially to an increase in coupling of CB1 to $G\alpha_z$ in glutamatergic neurons.

In order to substantiate an interaction of CB1 with $G\alpha_z$, various CoIPs were performed using HEK293 cells as a model system to investigate a possible interaction in an alternative cellular environment. Various attempts were made to detect a co-purification of CB1 after pulling down $G\alpha_z$, or alternatively, using several antibodies directed against the respective protein or its tag. Only the use of M2 anti FLAG beads, directed at the CB1-linked SF-tag, led to a successful purification of the target protein. Intriguingly, after pulling down CB1-SF-C using M2 anti FLAG beads, $G\alpha_z$ could be detected in the final eluates, suggesting a successful co-purification and interaction of both proteins. However, in $G\alpha_z$-only-transfected HEK293 cells, which served as a negative control, $G\alpha_z$ has also always been purified in the absence of the SF-tagged CB1 target protein under all conditions tested (Fig. 5.4A, B). Eventually, a successful CoIP could not be performed, but the non-specific binding of $G\alpha_z$ to the M2 anti FLAG beads at least highlighted the usefulness of a two step purification approach in some cases, as $G\alpha_z$ was not present in the TAP NC sample of non-AAV-injected animals, due to the sequential purification using two distinct kinds of beads. This could be further validated by a CoIP (Fig. 5.4C, D) using hippocampal lysates of Glu-CB1-SF-C- and GABA-CB1-SF-C-injected and non-injected control mice expressing only endogenous $G\alpha_z$, which was still co-purified in each case using M2 anti FLAG beads.

In order to evaluate a functional interaction of CB1 with $G\alpha_z$, an *in vitro* model using CB1-stably expressing HEK293 cells was established. A kinetic assay using non-transfected or transiently $G\alpha_z$-

or $G\alpha_o$-transfected HEK293-CB1 cells was successfully performed, measuring the cAMP turnover at four different time points and finally proving a functional PTX-insensitive inhibition of cAMP production upon WIN-stimulation of CB1, mediated by $G\alpha_z$ (Fig. 5.7). These cell line-dependent treatment effects reached significance after 10 min. Interestingly, the non-transfected HEK293-CB1 cells showed an intermediate phenotype between HEK293-CB1 + $G\alpha_o$ and HEK293-CB1 + $G\alpha_z$, which is possibly attributable to the presence of endogenous $G\alpha_z$ in HEK293 cells (Atwood et al., 2011). At 20 min, the same tendencies were observed, albeit not statistically significant. 5 min after treatment, $G\alpha_z$-transfected HEK293-CB1 cells did not show the expected insensitivity to the effect of PTX, which is probably due to the acute treatment of the cells with forskolin, WIN, and PTX at the same time. In other studies using PTX, cells were treated for up to 18 h with PTX in advance (Ahn et al., 2012), in order to preinhibit all PTX-sensitive G proteins of the $G\alpha_{i/o}$ family before the start of the experiment. PTX was shown to be able to rapidly enter the cell and to get activated, although complete ADP-ribosylation of PTX-sensitive $G\alpha_{i/o}$ proteins occurs within 3 h (Kaslow and Burns, 1992). An effect of PTX is thus to be expected within minutes, but 5 min after initiation of the experiment, the reaction of the cell system probably still needs to align to the complex multiple stimulation using three different compounds acting on three different downstream targets. Therefore, no clear response is visible at that time point. 30 min after the treatment, $G\alpha_z$-transfected HEK293-CB1 cells and $G\alpha_o$-transfected HEK293-CB1 cells showed minimal tendencies towards the expected responses, whereas the effect of WIN is completely reversed in non-transfected HEK293-CB1 cells, leading to an even higher activation of AC in addition to the forskolin treatment. This effect needs to be considered an artefact, since there is no explanation of an even higher stimulation of AC as compared to the forskolin-only treated cells. One may speculate that the mixture of compounds and removal of regular growth medium at the start of the experiment leads to stress responses or even cell death or other compensatory mechanisms, which do not allow for an evaluation of the responses after that period of time in this case. As a matter of principle, it could be shown that overexpression of one specific G protein is able to change the preferential coupling of CB1 to the G protein and in consequence leading to altered responses, in addition to the finding that CB1 is able to directly activate $G\alpha_z$. Discovering that the expression ratio of a G protein to a GPCR in a cell is sufficient to change the balance of preferential coupling of the receptor towards a certain G protein further substantiates the hypothesis of $G\alpha_z$ having an impact on differential CB1 signaling in hippocampal glutamatergic neurons and GABAergic interneurons, considering the distinct ratios of expression levels of CB1 to $G\alpha_z$ in both neuronal subtypes as evaluated by the dFISH approach.

Eventually, a functional interaction of CB1 with $G\alpha_z$, a yet unknown candidate interactor identified in the TAP, could be shown. $G\alpha_z$ mediates the inhibition of AC upon stimulation of CB1 with the agonist WIN in HEK293-CB1 cells. The question remains if this interaction occurs *in vivo*, as agonists were characterized as being biased or functionally selective towards certain response pathways by stabilizing different receptor conformations (2.2.1). Therefore, activation of the receptor by endocannabinoids can still lead to the induction of other pathways without any involvement of $G\alpha_z$. The co-purification of $G\alpha_z$ along with the relatively high abundance, on the other hand, is indicative of a role of this G protein in endogenous hippocampal CB1 protein complexes.

If $G\alpha_z$ contributes to differential CB1 signaling in the neuronal subtypes investigated in this study could not be demonstrated. Electrophysiological studies revealed differential cannabinoid-mediated synaptic glutamatergic and GABAergic synaptic transmission in the hippocampus and other brain regions (Kano et al., 2009), and provide the best tool in order to investigate signaling separately on excitatory and inhibitory neurons without the need for expression of recombinant proteins, which might potentially affect intracellular signaling. Assuming that $G\alpha_z$ is more pronouncedly interacting with CB1 in glutamatergic neurons, it seems possible that the observed characteristic of cannabinoid actions on glutamatergic synaptic transmission overriding those on GABAergic synaptic transmission (Azad et al., 2003) is mediated at least partially by the unique signaling properties of this G protein, such as its extraordinarily slow GTP hydrolysis rate. A deletion of $G\alpha_z$ may thus abolish or even reverse the observed decrease in the field potential amplitude despite its effects on both excitatory and inhibitory synaptic transmission, which would be expected to compensate each other. Further investigations of distinct glutamatergic and GABAergic synaptic transmission in the absence of $G\alpha_z$ could then reveal specific changes in one or the other cell type. An attempt to investigate the synaptic transmission upon CB1 stimulation in $G\alpha_z$-KO mice (Hendry et al., 2000) as compared to C57BL/6N mice was made in collaboration with Prof. Dr. Thomas Budde (Institut für Physiologie, Westfälische Wilhelms-Universität, Münster, Germany), but no final conclusions could be made up this time. Therefore, this question still needs to be addressed in the future.

# 6 Conclusion and outlook

The well investigated widespread physiological functions of the ECS, with CB1 playing a pivotal role in mediating these effects, has been strongly contrasting with the knowledge of intracellular CB1 signaling pathways and protein-protein interactions on a molecular level. In the present work, a combination of Cre-expressing mouse lines, AAV vectors, TAP, and deep coverage MS was utilized in order to reveal the composition of CB1 multiprotein complexes in mouse hippocampal glutamatergic neurons and GABAergic interneurons.

Using this approach, a huge dataset of identified co-purified proteins could be generated, depicting the complexity of CB1 signaling and interlinkage with other signaling pathways. Meta-analyses using bioinformatic tools with an integration of database information on protein functions revealed that the entirety of proteins mirrors known physiological properties of CB1 signaling, thereby validating the coherency and high degree of relevance of the obtained dataset. Yet unknown potential interacting proteins and cell type-specifically co-purified proteins were identified. Based on these findings, an extensive basis for the generation of new perspectives for endocannabinoid signaling, which is of steadily growing importance in understanding physiological functions and potential dysregulation in pathophysiology and their clinical implications, has been provided. Further functional studies need to be performed to reveal the functional relevance of interesting target proteins, direct protein interactions, and distinct signaling pathways.

A functional interaction with one co-purified protein, $G\alpha_z$, could be confirmed by exploiting its extraordinary characteristic of being PTX insensitive. However, its role *in vivo*, potentially contributing to differences in glutamatergic and GABAergic CB1 signaling, could not be clarified. Electrophysiological experiments offer the most valuable tool in order to investigate neuronal subtype-specific synaptic transmission. One attempt to measure CB1-mediated effects upon agonist treatment in brain slices and dissecting glutamatergic and GABAergic synaptic transmission in the hippocampus of $G\alpha_z$-KO mice as compared to C57BL/6N mice failed due to technical reasons, but still is the most promising approach to target this question in the future.

A general strategy to target the functionality of further single candidate interactors is a knockout or knockdown of the respective protein using knockout mouse lines or RNA interference (RNAi). Afterwards, known CB1-mediated effects, for instance DSE or DSI, phosphorylation of known

downstream effectors, or axonal guidance and outgrowth can be measured in either brain slices, primary cultures of specific neuronal populations, or other cell lines, and compared to wildtype controls. The output signal after CB1 activation to be measured depends on the interacting protein to be investigated. If a candidate protein has already been described to exert effects that are also known to be mediated by CB1, these effects are to be measured in an appropriate model system. If there is a lack of knowledge about the functional properties of a potential interactor, the best approach in a first step would be the investigation of changes in fundamental effects mediated by CB1, such as electrophysiological measurements of DSE and DSI, or cAMP turnover upon CB1 stimulation and with the concomitant knockout or knockdown of the candidate interactor.

Another method to study direct interactions of two proteins of interest in a high throughput manner was described by combining cell-free protein expression, AlphaScreen technology, and single-molecule fluorescence spectroscopy (Sierecki et al., 2013). This approach allows for a high-throughout investigation of hundreds of pairs of proteins per day and provides information about the state of proteins in monomers, oligomers, or random aggregates, and the stoichiometry of direct protein interactions. Exploiting this technique could provide further information about which of the co-purified proteins in the TAP approach directly interact and thus, give some indication of a hierarchy of binding events, instead of purifying huge multiprotein complexes.

In this work, the combination of AAV-mediated overexpression of the SF-tagged CB1, TAP, and screening for interacting proteins was applied in a spatially well-defined area, in only a subset of neurons in the mouse hippocampus. Now that the purification technique was optimized, this approach can be extended to other brain areas of interest by changing the injection sites of the AAV, and also to other neuronal subtypes, as well as astrocytes, depending on the Cre-driving mouse line. Furthermore, a comparison of the CB1 interactome after agonist or inverse agonist treatment as compared to non-treated animals can be performed, in order to investigate changes in the protein complex composition after stimulation or inhibition of the receptor.

Finally, this study outlines a powerful strategy for an initial screening of region- and cell type-specific CB1 multiprotein complexes and contributes to the general understanding of the complexity of intracellular signaling pathways and protein-protein interactions, in particular regarding the complex biogenesis and trafficking of membrane receptors.

# 7 References


Abramow-Newerly, M., Roy, A.A., Nunn, C., and Chidiac, P. (2006). RGS proteins have a signalling complex: interactions between RGS proteins and GPCRs, effectors, and auxiliary proteins. *Cell Signal 18*, 579-591.

Ahn, K.H., Mahmoud, M.M., and Kendall, D.A. (2012). Allosteric modulator ORG27569 induces CB1 cannabinoid receptor high affinity agonist binding state, receptor internalization, and Gi protein-independent ERK1/2 kinase activation. *J Biol Chem 287*, 12070-12082.

Ahn, K.H., Mahmoud, M.M., Shim, J.Y., and Kendall, D.A. (2013). Distinct roles of beta-arrestin 1 and beta-arrestin 2 in ORG27569-induced biased signaling and internalization of the cannabinoid receptor 1 (CB1). *J Biol Chem 288*, 9790-9800.

Ahrne, E., Molzahn, L., Glatter, T., and Schmidt, A. (2013). Critical assessment of proteome-wide label-free absolute abundance estimation strategies. *Proteomics 13*, 2567-2578.

Alger, B.E., and Kim, J. (2011). Supply and demand for endocannabinoids. *Trends Neurosci 34*, 304-315.

Atwood, B.K., Lopez, J., Wager-Miller, J., Mackie, K., and Straiker, A. (2011). Expression of G protein-coupled receptors and related proteins in HEK293, AtT20, BV2, and N18 cell lines as revealed by microarray analysis. *BMC Genomics 12*, 14.

Azad, S.C., Eder, M., Marsicano, G., Lutz, B., Zieglgansberger, W., and Rammes, G. (2003). Activation of the cannabinoid receptor type 1 decreases glutamatergic and GABAergic synaptic transmission in the lateral amygdala of the mouse. *Learn Mem 10*, 116-128.

Baillie, G.S., Sood, A., McPhee, I., Gall, I., Perry, S.J., Lefkowitz, R.J., and Houslay, M.D. (2003). beta-Arrestin-mediated PDE4 cAMP phosphodiesterase recruitment regulates beta-adrenoceptor switching from Gs to Gi. *Proc Natl Acad Sci U S A 100*, 940-945.

Bellocchio, L., Lafenetre, P., Cannich, A., Cota, D., Puente, N., Grandes, P., Chaouloff, F., Piazza, P.V., and Marsicano, G. (2010). Bimodal control of stimulated food intake by the endocannabinoid system. *Nat Neurosci 13*, 281-283.

Benard, G., Massa, F., Puente, N., Lourenco, J., Bellocchio, L., Soria-Gomez, E., Matias, I., Delamarre, A., Metna-Laurent, M., Cannich, A., et al. (2012). Mitochondrial CB(1) receptors regulate neuronal energy metabolism. *Nat Neurosci 15*, 558-564.

Berghuis, P., Dobszay, M.B., Wang, X., Spano, S., Ledda, F., Sousa, K.M., Schulte, G., Ernfors, P., Mackie, K., Paratcha, G., et al. (2005). Endocannabinoids regulate interneuron migration and morphogenesis by transactivating the TrkB receptor. *Proc Natl Acad Sci U S A 102*, 19115-19120.

Bergmayr, C., Thurner, P., Keuerleber, S., Kudlacek, O., Nanoff, C., Freissmuth, M., and Gruber, C.W. (2013). Recruitment of a cytoplasmic chaperone relay by the A2A adenosine receptor. *J Biol Chem 288*, 28831-28844.

Bisogno, T., Howell, F., Williams, G., Minassi, A., Cascio, M.G., Ligresti, A., Matias, I., Schiano-Moriello, A., Paul, P., Williams, E.J., et al. (2003). Cloning of the first sn1-DAG lipases points to the spatial and temporal regulation of endocannabinoid signaling in the brain. *J Cell Biol 163*, 463-468.

Blankman, J.L., and Cravatt, B.F. (2013). Chemical probes of endocannabinoid metabolism. *Pharmacol Rev 65*, 849-871.

Blankman, J.L., Simon, G.M., and Cravatt, B.F. (2007). A comprehensive profile of brain enzymes that hydrolyze the endocannabinoid 2-arachidonoylglycerol. *Chem Biol 14*, 1347-1356.

Blume, L.C., Eldeeb, K., Bass, C.E., Selley, D.E., and Howlett, A.C. (2015). Cannabinoid receptor interacting protein (CRIP1a) attenuates CB1R signaling in neuronal cells. *Cell Signal 27*, 716-726.

Bosier, B., Hermans, E., and Lambert, D.M. (2009). Concomitant activation of adenylyl cyclase suppresses the opposite influences of CB(1) cannabinoid receptor agonists on tyrosine hydroxylase expression. *Biochem Pharmacol 77*, 216-227.

Bosier, B., Muccioli, G.G., Hermans, E., and Lambert, D.M. (2010). Functionally selective cannabinoid receptor signalling: therapeutic implications and opportunities. *Biochem Pharmacol 80*, 1-12.

Bouaboula, M., Poinot-Chazel, C., Bourrie, B., Canat, X., Calandra, B., Rinaldi-Carmona, M., Le Fur, G., and Casellas, P. (1995). Activation of mitogen-activated protein kinases by stimulation of the central cannabinoid receptor CB1. *Biochem J 312 ( Pt 2)*, 637-641.

Brugarolas, M., Navarro, G., Martinez-Pinilla, E., Angelats, E., Casado, V., Lanciego, J.L., and Franco, R. (2014). G-protein-coupled receptor heteromers as key players in the molecular architecture of the central nervous system. *CNS Neurosci Ther 20*, 703-709.

Cadas, H., Gaillet, S., Beltramo, M., Venance, L., and Piomelli, D. (1996). Biosynthesis of an endogenous cannabinoid precursor in neurons and its control by calcium and cAMP. *J Neurosci 16*, 3934-3942.

Carlin, R.K., Grab, D.J., Cohen, R.S., and Siekevitz, P. (1980). Isolation and characterization of postsynaptic densities from various brain regions: enrichment of different types of postsynaptic densities. *J Cell Biol 86*, 831-845.

Castillo, P.E., Younts, T.J., Chavez, A.E., and Hashimotodani, Y. (2012). Endocannabinoid signaling and synaptic function. *Neuron 76*, 70-81.

Chavez, A.E., Chiu, C.Q., and Castillo, P.E. (2010). TRPV1 activation by endogenous anandamide triggers postsynaptic long-term depression in dentate gyrus. *Nat Neurosci 13*, 1511-1518.

Chen, C., and Okayama, H. (1987). High-efficiency transformation of mammalian cells by plasmid DNA. *Mol Cell Biol 7*, 2745-2752.

Chevaleyre, V., Heifets, B.D., Kaeser, P.S., Sudhof, T.C., and Castillo, P.E. (2007). Endocannabinoid-mediated long-term plasticity requires cAMP/PKA signaling and RIM1alpha. *Neuron 54*, 801-812.

Cline, M.S., Smoot, M., Cerami, E., Kuchinsky, A., Landys, N., Workman, C., Christmas, R., Avila-Campilo, I., Creech, M., Gross, B., et al. (2007). Integration of biological networks and gene expression data using Cytoscape. *Nat Protoc 2*, 2366-2382.

Cravatt, B.F., Giang, D.K., Mayfield, S.P., Boger, D.L., Lerner, R.A., and Gilula, N.B. (1996). Molecular characterization of an enzyme that degrades neuromodulatory fatty-acid amides. *Nature 384*, 83-87.

Daaka, Y., Luttrell, L.M., and Lefkowitz, R.J. (1997). Switching of the coupling of the beta2-adrenergic receptor to different G proteins by protein kinase A. *Nature 390*, 88-91.

Dalton, G.D., and Howlett, A.C. (2012). Cannabinoid CB1 receptors transactivate multiple receptor tyrosine kinases and regulate serine/threonine kinases to activate ERK in neuronal cells. *Br J Pharmacol 165*, 2497-2511.

Daulat, A.M., Maurice, P., Froment, C., Guillaume, J.L., Broussard, C., Monsarrat, B., Delagrange, P., and Jockers, R. (2007). Purification and identification of G protein-coupled receptor protein complexes under native conditions. *Mol Cell Proteomics 6*, 835-844.

Delgado-Peraza, F., Ahn, K., Nogueras-Ortiz, C., Mungrue, I., Mackie, K.P., Kendall, D.A., and Yudowski, G. (2016). Mechanisms of biased beta-arrestin mediated signaling downstream from the cannabinoid 1 receptor. *Mol Pharmacol*.

Derkinderen, P., Valjent, E., Toutant, M., Corvol, J.C., Enslen, H., Ledent, C., Trzaskos, J., Caboche, J., and Girault, J.A. (2003). Regulation of extracellular signal-regulated kinase by cannabinoids in hippocampus. *J Neurosci 23*, 2371-2382.

Devane, W.A., Dysarz, F.A., 3rd, Johnson, M.R., Melvin, L.S., and Howlett, A.C. (1988). Determination and characterization of a cannabinoid receptor in rat brain. *Mol Pharmacol 34*, 605-613.

Devane, W.A., Hanus, L., Breuer, A., Pertwee, R.G., Stevenson, L.A., Griffin, G., Gibson, D., Mandelbaum, A., Etinger, A., and Mechoulam, R. (1992). Isolation and structure of a brain constituent that binds to the cannabinoid receptor. *Science 258*, 1946-1949.

Dewey, W.L. (1986). Cannabinoid pharmacology. *Pharmacol Rev 38*, 151-178.

Di Marzo, V., Fontana, A., Cadas, H., Schinelli, S., Cimino, G., Schwartz, J.C., and Piomelli, D. (1994). Formation and inactivation of endogenous cannabinoid anandamide in central neurons. *Nature 372*, 686-691.

Dinh, T.P., Freund, T.F., and Piomelli, D. (2002). A role for monoglyceride lipase in 2-arachidonoylglycerol inactivation. *Chem Phys Lipids 121*, 149-158.

Distler, U., Kuharev, J., Navarro, P., Levin, Y., Schild, H., and Tenzer, S. (2014). Drift time-specific collision energies enable deep-coverage data-independent acquisition proteomics. *Nat Methods 11*, 167-170.

Distler, U., Schmeisser, M.J., Pelosi, A., Reim, D., Kuharev, J., Weiczner, R., Baumgart, J., Boeckers, T.M., Nitsch, R., Vogt, J., et al. (2014). In-depth protein profiling of the postsynaptic density from mouse hippocampus using data-independent acquisition proteomics. *Proteomics 14*, 2607-2613.

Duc, N.M., Kim, H.R., and Chung, K.Y. (2015). Structural mechanism of G protein activation by G protein-coupled receptor. *Eur J Pharmacol 763*, 214-222.

Dunn, H.A., and Ferguson, S.S. (2015). PDZ Protein Regulation of G Protein-Coupled Receptor Trafficking and Signaling Pathways. *Mol Pharmacol 88*, 624-639.

During, M.J., Young, D., Baer, K., Lawlor, P., and Klugmann, M. (2003). Development and optimization of adeno-associated virus vector transfer into the central nervous system. *Methods Mol Med 76*, 221-236.

Ellis, J., Pediani, J.D., Canals, M., Milasta, S., and Milligan, G. (2006). Orexin-1 receptor-cannabinoid CB1 receptor heterodimerization results in both ligand-dependent and -independent coordinated alterations of receptor localization and function. *J Biol Chem 281*, 38812-38824.

Elphick, M.R., and Egertova, M. (2005). The phylogenetic distribution and evolutionary origins of endocannabinoid signalling. *Handb Exp Pharmacol*, 283-297.

Fabre, B., Lambour, T., Bouyssié, D., Menneteau, T., Monsarrat, B., Burlet-Schiltz, O., and Bousquet-Dubouch, M.-P. (2014). Comparison of label-free quantification methods for the determination of protein complexes subunits stoichiometry. *EuPA Open Proteomics 4*, 82-86.

Fagni, L., Worley, P.F., and Ango, F. (2002). Homer as both a scaffold and transduction molecule. *Sci STKE 2002*, re8.

Falenski, K.W., Carter, D.S., Harrison, A.J., Martin, B.R., Blair, R.E., and DeLorenzo, R.J. (2009). Temporal characterization of changes in hippocampal cannabinoid CB(1) receptor expression following pilocarpine-induced status epilepticus. *Brain Res 1262*, 64-72.

Fisar, Z., Singh, N., and Hroudova, J. (2014). Cannabinoid-induced changes in respiration of brain mitochondria. *Toxicol Lett 231*, 62-71.

Fredriksson, R., Lagerstrom, M.C., Lundin, L.G., and Schioth, H.B. (2003). The G-protein-coupled receptors in the human genome form five main families. Phylogenetic analysis, paralogon groups, and fingerprints. *Mol Pharmacol 63*, 1256-1272.

Gainetdinov, R.R., Premont, R.T., Bohn, L.M., Lefkowitz, R.J., and Caron, M.G. (2004). Desensitization of G protein-coupled receptors and neuronal functions. *Annu Rev Neurosci 27*, 107-144.

Gao, Y., Vasilyev, D.V., Goncalves, M.B., Howell, F.V., Hobbs, C., Reisenberg, M., Shen, R., Zhang, M.Y., Strassle, B.W., Lu, P., et al. (2010). Loss of retrograde endocannabinoid signaling and reduced adult neurogenesis in diacylglycerol lipase knock-out mice. *J Neurosci 30*, 2017-2024.

Gaoni, Y., and Mechoulam, R. (1964). Isolation, Structure, and Partial Synthesis of an Active Constituent of Hashish. *J Am Chem Soc 86*, 1646-+.

Garzon, J., de la Torre-Madrid, E., Rodriguez-Munoz, M., Vicente-Sanchez, A., and Sanchez-Blazquez, P. (2009). Gz mediates the long-lasting desensitization of brain CB1 receptors and is essential for cross-tolerance with morphine. *Mol Pain 5*, 11.

Georgieva, T., Devanathan, S., Stropova, D., Park, C.K., Salamon, Z., Tollin, G., Hruby, V.J., Roeske, W.R., Yamamura, H.I., and Varga, E. (2008). Unique agonist-bound cannabinoid CB1 receptor conformations indicate agonist specificity in signaling. *Eur J Pharmacol 581*, 19-29.

Glass, M., and Felder, C.C. (1997). Concurrent stimulation of cannabinoid CB1 and dopamine D2 receptors augments cAMP accumulation in striatal neurons: evidence for a Gs linkage to the CB1 receptor. *J Neurosci 17*, 5327-5333.

Gloeckner, C.J., Boldt, K., Schumacher, A., Roepman, R., and Ueffing, M. (2007). A novel tandem affinity purification strategy for the efficient isolation and characterisation of native protein complexes. *Proteomics 7*, 4228-4234.

Gloeckner, C.J., Boldt, K., and Ueffing, M. (2009). Strep/FLAG tandem affinity purification (SF-TAP) to study protein interactions. *Curr Protoc Protein Sci Chapter 19*, Unit19 20.

Goebbels, S., Bormuth, I., Bode, U., Hermanson, O., Schwab, M.H., and Nave, K.A. (2006). Genetic targeting of principal neurons in neocortex and hippocampus of NEX-Cre mice. *Genesis 44*, 611-621.

Gomes, I., Ayoub, M.A., Fujita, W., Jaeger, W.C., Pfleger, K.D., and Devi, L.A. (2016). G Protein-Coupled Receptor Heteromers. *Annu Rev Pharmacol Toxicol 56*, 403-425.

Gomez del Pulgar, T., Velasco, G., and Guzman, M. (2000). The CB1 cannabinoid receptor is coupled to the activation of protein kinase B/Akt. *Biochem J 347*, 369-373.

Gonsiorek, W., Lunn, C., Fan, X., Narula, S., Lundell, D., and Hipkin, R.W. (2000). Endocannabinoid 2-arachidonyl glycerol is a full agonist through human type 2 cannabinoid receptor: antagonism by anandamide. *Mol Pharmacol 57*, 1045-1050.

Gonzalez-Maeso, J. (2011). GPCR oligomers in pharmacology and signaling. *Mol Brain 4*, 20.

Gudermann, T., Schoneberg, T., and Schultz, G. (1997). Functional and structural complexity of signal transduction via G-protein-coupled receptors. *Annu Rev Neurosci 20*, 399-427.

Guggenhuber, S., Alpar, A., Chen, R., Schmitz, N., Wickert, M., Mattheus, T., Harasta, A.E., Purrio, M., Kaiser, N., Elphick, M.R., et al. (2016). Cannabinoid receptor-interacting protein Crip1a modulates CB1 receptor signaling in mouse hippocampus. *Brain Struct Funct 221*, 2061-2074.

Guggenhuber, S., Monory, K., Lutz, B., and Klugmann, M. (2010). AAV vector-mediated overexpression of CB1 cannabinoid receptor in pyramidal neurons of the hippocampus protects against seizure-induced excitoxicity. *PLoS One 5*, e15707.

Guggenhuber, S., Romo-Parra, H., Bindila, L., Leschik, J., Lomazzo, E., Remmers, F., Zimmermann, T., Lerner, R., Klugmann, M., Pape, H.C., et al. (2016). Impaired 2-AG Signaling in Hippocampal Glutamatergic Neurons: Aggravation of Anxiety-Like Behavior and Unaltered Seizure Susceptibility. *Int J Neuropsychopharmacol 19*.

Gulyas, A.I., Cravatt, B.F., Bracey, M.H., Dinh, T.P., Piomelli, D., Boscia, F., and Freund, T.F. (2004). Segregation of two endocannabinoid-hydrolyzing enzymes into pre- and postsynaptic compartments in the rat hippocampus, cerebellum and amygdala. *Eur J Neurosci 20*, 441-458.

Guo, J., and Ikeda, S.R. (2004). Endocannabinoids modulate N-type calcium channels and G-protein-coupled inwardly rectifying potassium channels via CB1 cannabinoid receptors heterologously expressed in mammalian neurons. *Mol Pharmacol 65*, 665-674.

Hamm, H.E., and Gilchrist, A. (1996). Heterotrimeric G proteins. *Curr Opin Cell Biol 8*, 189-196.

Hauck, B., Chen, L., and Xiao, W. (2003). Generation and characterization of chimeric recombinant AAV vectors. *Mol Ther 7*, 419-425.

Hay, D.L., and Pioszak, A.A. (2016). Receptor Activity-Modifying Proteins (RAMPs): New Insights and Roles. *Annu Rev Pharmacol Toxicol 56*, 469-487.

Hayashi, M.K., Ames, H.M., and Hayashi, Y. (2006). Tetrameric hub structure of postsynaptic scaffolding protein homer. *J Neurosci 26*, 8492-8501.

Hebert-Chatelain, E., Reguero, L., Puente, N., Lutz, B., Chaouloff, F., Rossignol, R., Piazza, P.V., Benard, G., Grandes, P., and Marsicano, G. (2014). Cannabinoid control of brain bioenergetics: Exploring the subcellular localization of the CB1 receptor. *Mol Metab 3*, 495-504.

Helenius, A., and Simons, K. (1975). Solubilization of membranes by detergents. *Biochim Biophys Acta 415*, 29-79.

Hendry, I.A., Kelleher, K.L., Bartlett, S.E., Leck, K.J., Reynolds, A.J., Heydon, K., Mellick, A., Megirian, D., and Matthaei, K.I. (2000). Hypertolerance to morphine in G(z alpha)-deficient mice. *Brain Res 870*, 10-19.

Henry, D.J., and Chavkin, C. (1995). Activation of inwardly rectifying potassium channels (GIRK1) by co-expressed rat brain cannabinoid receptors in Xenopus oocytes. *Neurosci Lett 186*, 91-94.

Herkenham, M., Lynn, A.B., Little, M.D., Johnson, M.R., Melvin, L.S., de Costa, B.R., and Rice, K.C. (1990). Cannabinoid receptor localization in brain. *Proc Natl Acad Sci U S A 87*, 1932-1936.

Hermanson, D.J., Hartley, N.D., Gamble-George, J., Brown, N., Shonesy, B.C., Kingsley, P.J., Colbran, R.J., Reese, J., Marnett, L.J., and Patel, S. (2013). Substrate-selective COX-2 inhibition decreases anxiety via endocannabinoid activation. *Nat Neurosci 16*, 1291-1298.

Ho, M.K., and Wong, Y.H. (2001). G(z) signaling: emerging divergence from G(i) signaling. *Oncogene 20*, 1615-1625.

Howlett, A.C., Qualy, J.M., and Khachatrian, L.L. (1986). Involvement of Gi in the inhibition of adenylate cyclase by cannabimimetic drugs. *Mol Pharmacol 29*, 307-313.

Huang da, W., Sherman, B.T., and Lempicki, R.A. (2009). Systematic and integrative analysis of large gene lists using DAVID bioinformatics resources. *Nat Protoc 4*, 44-57.

Hudson, B.D., Hebert, T.E., and Kelly, M.E. (2010). Physical and functional interaction between CB1 cannabinoid receptors and beta2-adrenoceptors. *Br J Pharmacol 160*, 627-642.

Hultman, R., Kumari, U., Michel, N., and Casey, P.J. (2014). Galphaz regulates BDNF-induction of axon growth in cortical neurons. *Mol Cell Neurosci 58*, 53-61.

Jensen, L.J., Kuhn, M., Stark, M., Chaffron, S., Creevey, C., Muller, J., Doerks, T., Julien, P., Roth, A., Simonovic, M., et al. (2009). STRING 8--a global view on proteins and their functional interactions in 630 organisms. *Nucleic Acids Res 37*, D412-416.

Jeong, S.W., and Ikeda, S.R. (1998). G protein alpha subunit G alpha z couples neurotransmitter receptors to ion channels in sympathetic neurons. *Neuron 21*, 1201-1212.

Jin, W., Brown, S., Roche, J.P., Hsieh, C., Celver, J.P., Kovoor, A., Chavkin, C., and Mackie, K. (1999). Distinct domains of the CB1 cannabinoid receptor mediate desensitization and internalization. *J Neurosci 19*, 3773-3780.

Joost, P., and Methner, A. (2002). Phylogenetic analysis of 277 human G-protein-coupled receptors as a tool for the prediction of orphan receptor ligands. *Genome Biol 3*, RESEARCH0063.

Jung, H.W., Park, I., and Ghil, S. (2014). Cannabinoid receptor activation inhibits cell cycle progression by modulating 14-3-3beta. *Cell Mol Biol Lett 19*, 347-360.

Kano, M., Ohno-Shosaku, T., Hashimotodani, Y., Uchigashima, M., and Watanabe, M. (2009). Endocannabinoid-mediated control of synaptic transmission. *Physiol Rev 89*, 309-380.

Kaslow, H.R., and Burns, D.L. (1992). Pertussis toxin and target eukaryotic cells: binding, entry, and activation. *FASEB J 6*, 2684-2690.

Katona, I., and Freund, T.F. (2012). Multiple functions of endocannabinoid signaling in the brain. *Annu Rev Neurosci 35*, 529-558.

Katona, I., Sperlagh, B., Sik, A., Kafalvi, A., Vizi, E.S., Mackie, K., and Freund, T.F. (1999). Presynaptically located CB1 cannabinoid receptors regulate GABA release from axon terminals of specific hippocampal interneurons. *J Neurosci 19*, 4544-4558.

Kearn, C.S., Blake-Palmer, K., Daniel, E., Mackie, K., and Glass, M. (2005). Concurrent stimulation of cannabinoid CB1 and dopamine D2 receptors enhances heterodimer formation: a mechanism for receptor cross-talk? *Mol Pharmacol 67*, 1697-1704.

Kenakin, T. (2011). Functional selectivity and biased receptor signaling. *J Pharmacol Exp Ther 336*, 296-302.

Klausberger, T., Marton, L.F., O'Neill, J., Huck, J.H., Dalezios, Y., Fuentealba, P., Suen, W.Y., Papp, E., Kaneko, T., Watanabe, M., et al. (2005). Complementary roles of cholecystokinin- and parvalbumin-expressing GABAergic neurons in hippocampal network oscillations. *J Neurosci 25*, 9782-9793.

Klugmann, M., Symes, C.W., Leichtlein, C.B., Klaussner, B.K., Dunning, J., Fong, D., Young, D., and During, M.J. (2005). AAV-mediated hippocampal expression of short and long Homer 1 proteins differentially affect cognition and seizure activity in adult rats. *Mol Cell Neurosci 28*, 347-360.

Korzeniewski, B. (2001). Cybernetic Formulation of the Definition of Life. *Journal of Theoretical Biology 209*, 275-286.

Koshland, D.E., Jr. (2002). Special essay. The seven pillars of life. *Science 295*, 2215-2216.

Kouznetsova, M., Kelley, B., Shen, M., and Thayer, S.A. (2002). Desensitization of cannabinoid-mediated presynaptic inhibition of neurotransmission between rat hippocampal neurons in culture. *Mol Pharmacol 61*, 477-485.

Kozak, K.R., Rowlinson, S.W., and Marnett, L.J. (2000). Oxygenation of the endocannabinoid, 2-arachidonylglycerol, to glyceryl prostaglandins by cyclooxygenase-2. *J Biol Chem 275*, 33744-33749.

Kreitzer, A.C., and Regehr, W.G. (2001). Retrograde inhibition of presynaptic calcium influx by endogenous cannabinoids at excitatory synapses onto Purkinje cells. *Neuron 29*, 717-727.

Kruse, M., Hammond, G.R., and Hille, B. (2012). Regulation of voltage-gated potassium channels by PI(4,5)P2. *J Gen Physiol 140*, 189-205.

Kurose, H. (2003). Gα12 and Gα13 as key regulatory mediator in signal transduction. *Life Sciences 74*, 155-161.

Ladarre, D., Roland, A.B., Biedzinski, S., Ricobaraza, A., and Lenkei, Z. (2014). Polarized cellular patterns of endocannabinoid production and detection shape cannabinoid signaling in neurons. *Front Cell Neurosci 8*, 426.

Lauckner, J.E., Hille, B., and Mackie, K. (2005). The cannabinoid agonist WIN55,212-2 increases intracellular calcium via CB1 receptor coupling to Gq/11 G proteins. *Proc Natl Acad Sci U S A 102*, 19144-19149.

Leck, K.J., Bartlett, S.E., Smith, M.T., Megirian, D., Holgate, J., Powell, K.L., Matthaei, K.I., and Hendry, I.A. (2004). Deletion of guanine nucleotide binding protein alpha z subunit in mice induces a gene dose dependent tolerance to morphine. *Neuropharmacology 46*, 836-846.

Lein, E.S., Hawrylycz, M.J., Ao, N., Ayres, M., Bensinger, A., Bernard, A., Boe, A.F., Boguski, M.S., Brockway, K.S., Byrnes, E.J., et al. (2007). Genome-wide atlas of gene expression in the adult mouse brain. *Nature 445*, 168-176.

Lemos, C., Valerio-Fernandes, A., Ghisleni, G.C., Ferreira, S.G., Ledent, C., de Ceballos, M.L., and Kofalvi, A. (2012). Impaired hippocampal glucoregulation in the cannabinoid CB1 receptor knockout mice as revealed by an optimized in vitro experimental approach. *J Neurosci Methods 204*, 366-373.

Leterrier, C., Laine, J., Darmon, M., Boudin, H., Rossier, J., and Lenkei, Z. (2006). Constitutive activation drives compartment-selective endocytosis and axonal targeting of type 1 cannabinoid receptors. *J Neurosci 26*, 3141-3153.

Lin, F.T., Chen, W., Shenoy, S., Cong, M., Exum, S.T., and Lefkowitz, R.J. (2002). Phosphorylation of beta-arrestin2 regulates its function in internalization of beta(2)-adrenergic receptors. *Biochemistry 41*, 10692-10699.

Losonczy, A., Biro, A.A., and Nusser, Z. (2004). Persistently active cannabinoid receptors mute a subpopulation of hippocampal interneurons. *Proc Natl Acad Sci U S A 101*, 1362-1367.

Low, M.J. (2011). Agnostic about in vivo inverse agonism of agouti-related peptide. *Endocrinology 152*, 1731-1733.

Luttrell, L.M. (2014). Minireview: More than just a hammer: ligand "bias" and pharmaceutical discovery. *Mol Endocrinol 28*, 281-294.

Luttrell, L.M. (2008). Reviews in molecular biology and biotechnology: transmembrane signaling by G protein-coupled receptors. *Mol Biotechnol 39*, 239-264.

Luttrell, L.M., Ferguson, S.S., Daaka, Y., Miller, W.E., Maudsley, S., Della Rocca, G.J., Lin, F., Kawakatsu, H., Owada, K., Luttrell, D.K., et al. (1999). Beta-arrestin-dependent formation of beta2 adrenergic receptor-Src protein kinase complexes. *Science 283*, 655-661.

Luttrell, L.M., Hawes, B.E., van Biesen, T., Luttrell, D.K., Lansing, T.J., and Lefkowitz, R.J. (1996). Role of c-Src tyrosine kinase in G protein-coupled receptor- and Gbetagamma subunit-mediated activation of mitogen-activated protein kinases. *J Biol Chem 271*, 19443-19450.

Luttrell, L.M., and Lefkowitz, R.J. (2002). The role of beta-arrestins in the termination and transduction of G-protein-coupled receptor signals. *J Cell Sci 115*, 455-465.

Lutz, B., Marsicano, G., Maldonado, R., and Hillard, C.J. (2015). The endocannabinoid system in guarding against fear, anxiety and stress. *Nat Rev Neurosci 16*, 705-718.

Maccarrone, M., Guzman, M., Mackie, K., Doherty, P., and Harkany, T. (2014). Programming of neural cells by (endo)cannabinoids: from physiological rules to emerging therapies. *Nat Rev Neurosci 15*, 786-801.

Mackie, K., and Hille, B. (1992). Cannabinoids inhibit N-type calcium channels in neuroblastoma-glioma cells. *Proc Natl Acad Sci U S A 89*, 3825-3829.

Maejima, T., Hashimoto, K., Yoshida, T., Aiba, A., and Kano, M. (2001). Presynaptic inhibition caused by retrograde signal from metabotropic glutamate to cannabinoid receptors. *Neuron 31*, 463-475.

Maere, S., Heymans, K., and Kuiper, M. (2005). BiNGO: a Cytoscape plugin to assess overrepresentation of gene ontology categories in biological networks. *Bioinformatics 21*, 3448-3449.

Magalhaes, A.C., Dunn, H., and Ferguson, S.S. (2012). Regulation of GPCR activity, trafficking and localization by GPCR-interacting proteins. *Br J Pharmacol 165*, 1717-1736.

Maroso, M., Szabo, G.G., Kim, H.K., Alexander, A., Bui, A.D., Lee, S.H., Lutz, B., and Soltesz, I. (2016). Cannabinoid Control of Learning and Memory through HCN Channels. *Neuron 89*, 1059-1073.

Marsicano, G., Goodenough, S., Monory, K., Hermann, H., Eder, M., Cannich, A., Azad, S.C., Cascio, M.G., Gutierrez, S.O., van der Stelt, M., et al. (2003). CB1 cannabinoid receptors and on-demand defense against excitotoxicity. *Science 302*, 84-88.

Marsicano, G., and Kuner, R. (2008). Anatomical distribution of receptor, ligands and enzymes in the brain and in the spinal cord: circuitries and neurochemistry. In Cannabinoids and the brain, A. Köfalvi, ed. (New York: Springer), pp. 161-201.

Marsicano, G., and Lutz, B. (1999). Expression of the cannabinoid receptor CB1 in distinct neuronal subpopulations in the adult mouse forebrain. *Eur J Neurosci 11*, 4213-4225.

Marsicano, G., Wotjak, C.T., Azad, S.C., Bisogno, T., Rammes, G., Cascio, M.G., Hermann, H., Tang, J., Hofmann, C., Zieglgansberger, W., et al. (2002). The endogenous cannabinoid system controls extinction of aversive memories. *Nature 418*, 530-534.

Martini, L., Waldhoer, M., Pusch, M., Kharazia, V., Fong, J., Lee, J.H., Freissmuth, C., and Whistler, J.L. (2007). Ligand-induced down-regulation of the cannabinoid 1 receptor is mediated by the G-protein-coupled receptor-associated sorting protein GASP1. *FASEB J 21*, 802-811.

Mato, S., Lafourcade, M., Robbe, D., Bakiri, Y., and Manzoni, O.J. (2008). Role of the cyclic-AMP/PKA cascade and of P/Q-type Ca++ channels in endocannabinoid-mediated long-term depression in the nucleus accumbens. *Neuropharmacology 54*, 87-94.

Matsuda, L.A., Lolait, S.J., Brownstein, M.J., Young, A.C., and Bonner, T.I. (1990). Structure of a cannabinoid receptor and functional expression of the cloned cDNA. *Nature 346*, 561-564.

Maudsley, S., Pierce, K.L., Zamah, A.M., Miller, W.E., Ahn, S., Daaka, Y., Lefkowitz, R.J., and Luttrell, L.M. (2000). The beta(2)-adrenergic receptor mediates extracellular signal-regulated kinase activation via assembly of a multi-receptor complex with the epidermal growth factor receptor. *J Biol Chem 275*, 9572-9580.

McPartland, J.M., Matias, I., Di Marzo, V., and Glass, M. (2006). Evolutionary origins of the endocannabinoid system. *Gene 370*, 64-74.

Mechoulam, R., Ben-Shabat, S., Hanus, L., Ligumsky, M., Kaminski, N.E., Schatz, A.R., Gopher, A., Almog, S., Martin, B.R., Compton, D.R., et al. (1995). Identification of an endogenous 2-monoglyceride, present in canine gut, that binds to cannabinoid receptors. *Biochem Pharmacol 50*, 83-90.

Mechoulam, R., Hanus, L.O., Pertwee, R., and Howlett, A.C. (2014). Early phytocannabinoid chemistry to endocannabinoids and beyond. *Nat Rev Neurosci 15*, 757-764.

Mechoulam, R., and Parker, L.A. (2013). The endocannabinoid system and the brain. *Annu Rev Psychol 64*, 21-47.

Monory, K., Massa, F., Egertova, M., Eder, M., Blaudzun, H., Westenbroek, R., Kelsch, W., Jacob, W., Marsch, R., Ekker, M., et al. (2006). The endocannabinoid system controls key epileptogenic circuits in the hippocampus. *Neuron 51*, 455-466.

Morris, J.H., Apeltsin, L., Newman, A.M., Baumbach, J., Wittkop, T., Su, G., Bader, G.D., and Ferrin, T.E. (2011). clusterMaker: a multi-algorithm clustering plugin for Cytoscape. *BMC Bioinformatics 12*, 436.

Muller, H.J. (1955). Life. *Science 121*, 1-9.

Munro, S., Thomas, K.L., and Abu-Shaar, M. (1993). Molecular characterization of a peripheral receptor for cannabinoids. *Nature 365*, 61-65.

Navarrete, M., and Araque, A. (2008). Endocannabinoids mediate neuron-astrocyte communication. *Neuron 57*, 883-893.

Navarrete, M., and Araque, A. (2010). Endocannabinoids potentiate synaptic transmission through stimulation of astrocytes. *Neuron 68*, 113-126.

Navarro, G., Carriba, P., Gandia, J., Ciruela, F., Casado, V., Cortes, A., Mallol, J., Canela, E.I., Lluis, C., and Franco, R. (2008). Detection of heteromers formed by cannabinoid CB1, dopamine D2, and adenosine A2A G-protein-coupled receptors by combining bimolecular fluorescence complementation and bioluminescence energy transfer. *ScientificWorldJournal 8*, 1088-1097.

Niehaus, J.L., Liu, Y., Wallis, K.T., Egertova, M., Bhartur, S.G., Mukhopadhyay, S., Shi, S., He, H., Selley, D.E., Howlett, A.C., et al. (2007). CB1 cannabinoid receptor activity is modulated by the cannabinoid receptor interacting protein CRIP 1a. *Mol Pharmacol 72*, 1557-1566.

Njoo, C., Agarwal, N., Lutz, B., and Kuner, R. (2015). The Cannabinoid Receptor CB1 Interacts with the WAVE1 Complex and Plays a Role in Actin Dynamics and Structural Plasticity in Neurons. *PLoS Biol 13*, e1002286.

Ogura, Y., Parsons, W.H., Kamat, S.S., and Cravatt, B.F. (2016). A calcium-dependent acyltransferase that produces N-acyl phosphatidylethanolamines. *Nat Chem Biol*.

Ohno-Shosaku, T., and Kano, M. (2014). Endocannabinoid-mediated retrograde modulation of synaptic transmission. *Curr Opin Neurobiol 29*, 1-8.

Ohno-Shosaku, T., Maejima, T., and Kano, M. (2001). Endogenous cannabinoids mediate retrograde signals from depolarized postsynaptic neurons to presynaptic terminals. *Neuron 29*, 729-738.

Ohno-Shosaku, T., Tsubokawa, H., Mizushima, I., Yoneda, N., Zimmer, A., and Kano, M. (2002). Presynaptic cannabinoid sensitivity is a major determinant of depolarization-induced retrograde suppression at hippocampal synapses. *J Neurosci 22*, 3864-3872.

Ozaita, A., Puighermanal, E., and Maldonado, R. (2007). Regulation of PI3K/Akt/GSK-3 pathway by cannabinoids in the brain. *J Neurochem 102*, 1105-1114.

Pankow, S., Bamberger, C., Calzolari, D., Martinez-Bartolome, S., Lavallee-Adam, M., Balch, W.E., and Yates, J.R., 3rd. (2015). F508 CFTR interactome remodelling promotes rescue of cystic fibrosis. *Nature 528*, 510-516.

Parsons, L.H., and Hurd, Y.L. (2015). Endocannabinoid signalling in reward and addiction. *Nat Rev Neurosci 16*, 579-594.

Perry, S.J., Baillie, G.S., Kohout, T.A., McPhee, I., Magiera, M.M., Ang, K.L., Miller, W.E., McLean, A.J., Conti, M., Houslay, M.D., et al. (2002). Targeting of cyclic AMP degradation to beta 2-adrenergic receptors by beta-arrestins. *Science 298*, 834-836.

Pertwee, R.G. (1972). The ring test: a quantitative method for assessing the 'cataleptic' effect of cannabis in mice. *Br J Pharmacol 46*, 753-763.

Piomelli, D. (2003). The molecular logic of endocannabinoid signalling. *Nat Rev Neurosci 4*, 873-884.

Prenderville, J.A., Kelly, A.M., and Downer, E.J. (2015). The role of cannabinoids in adult neurogenesis. *Br J Pharmacol 172*, 3950-3963.

Prenzel, N., Zwick, E., Daub, H., Leserer, M., Abraham, R., Wallasch, C., and Ullrich, A. (1999). EGF receptor transactivation by G-protein-coupled receptors requires metalloproteinase cleavage of proHB-EGF. *Nature 402*, 884-888.

Prigogine, I. (1980). From being to becoming : time and complexity in the physical sciences (San Francisco: W. H. Freeman).

Puighermanal, E., Marsicano, G., Busquets-Garcia, A., Lutz, B., Maldonado, R., and Ozaita, A. (2009). Cannabinoid modulation of hippocampal long-term memory is mediated by mTOR signaling. *Nat Neurosci 12*, 1152-1158.

Rankovic, Z., Brust, T.F., and Bohn, L.M. (2016). Biased agonism: An emerging paradigm in GPCR drug discovery. *Bioorg Med Chem Lett 26*, 241-250.

Rasmussen, S.G., DeVree, B.T., Zou, Y., Kruse, A.C., Chung, K.Y., Kobilka, T.S., Thian, F.S., Chae, P.S., Pardon, E., Calinski, D., et al. (2011). Crystal structure of the beta2 adrenergic receptor-Gs protein complex. *Nature 477*, 549-555.

Regehr, W.G., Carey, M.R., and Best, A.R. (2009). Activity-dependent regulation of synapses by retrograde messengers. *Neuron 63*, 154-170.

Rehm, H., and Rehm, H. (2006). Protein biochemistry and proteomics (Amsterdam ; Boston: Elsevier, Academic Press).

Reiter, E., Ahn, S., Shukla, A.K., and Lefkowitz, R.J. (2012). Molecular mechanism of beta-arrestin-biased agonism at seven-transmembrane receptors. *Annu Rev Pharmacol Toxicol 52*, 179-197.

Rey, A.A., Purrio, M., Viveros, M.P., and Lutz, B. (2012). Biphasic effects of cannabinoids in anxiety responses: CB1 and GABA(B) receptors in the balance of GABAergic and glutamatergic neurotransmission. *Neuropsychopharmacology 37*, 2624-2634.

Rhee, M.H., Bayewitch, M., Avidor-Reiss, T., Levy, R., and Vogel, Z. (1998). Cannabinoid receptor activation differentially regulates the various adenylyl cyclase isozymes. *J Neurochem 71*, 1525-1534.

Richichi, C., Lin, E.J., Stefanin, D., Colella, D., Ravizza, T., Grignaschi, G., Veglianese, P., Sperk, G., During, M.J., and Vezzani, A. (2004). Anticonvulsant and antiepileptogenic effects mediated by adeno-associated virus vector neuropeptide Y expression in the rat hippocampus. *J Neurosci 24*, 3051-3059.

Rigaut, G., Shevchenko, A., Rutz, B., Wilm, M., Mann, M., and Seraphin, B. (1999). A generic protein purification method for protein complex characterization and proteome exploration. *Nat Biotechnol 17*, 1030-1032.

Rios, C., Gomes, I., and Devi, L.A. (2006). mu opioid and CB1 cannabinoid receptor interactions: reciprocal inhibition of receptor signaling and neuritogenesis. *Br J Pharmacol 148*, 387-395.

Roberto, M., Cruz, M., Bajo, M., Siggins, G.R., Parsons, L.H., and Schweitzer, P. (2010). The endocannabinoid system tonically regulates inhibitory transmission and depresses the effect of ethanol in central amygdala. *Neuropsychopharmacology 35*, 1962-1972.

Roche, J.P., Bounds, S., Brown, S., and Mackie, K. (1999). A mutation in the second transmembrane region of the CB1 receptor selectively disrupts G protein signaling and prevents receptor internalization. *Mol Pharmacol 56*, 611-618.

Roland, A.B., Ricobaraza, A., Carrel, D., Jordan, B.M., Rico, F., Simon, A., Humbert-Claude, M., Ferrier, J., McFadden, M.H., Scheuring, S., et al. (2014). Cannabinoid-induced actomyosin contractility shapes neuronal morphology and growth. *Elife 3*, e03159.

Ross, E.M., and Wilkie, T.M. (2000). GTPase-activating proteins for heterotrimeric G proteins: regulators of G protein signaling (RGS) and RGS-like proteins. *Annu Rev Biochem 69*, 795-827.

Rozenfeld, R., Bushlin, I., Gomes, I., Tzavaras, N., Gupta, A., Neves, S., Battini, L., Gusella, G.L., Lachmann, A., Ma'ayan, A., et al. (2012). Receptor heteromerization expands the repertoire of cannabinoid signaling in rodent neurons. *PLoS One 7*, e29239.

Russo, E.B., Jiang, H.E., Li, X., Sutton, A., Carboni, A., del Bianco, F., Mandolino, G., Potter, D.J., Zhao, Y.X., Bera, S., et al. (2008). Phytochemical and genetic analyses of ancient cannabis from Central Asia. *J Exp Bot 59*, 4171-4182.

Schmidt, P.M., Sparrow, L.G., Attwood, R.M., Xiao, X., Adams, T.E., and McKimm-Breschkin, J.L. (2012). Taking down the FLAG! How insect cell expression challenges an established tag-system. *PLoS One 7*, e37779.

Schrödinger, E. (1945). What is life? The physical aspect of the living cell (Cambridge Eng. New York: The University press; The Macmillan company).

Scripture, E.W. (1893). Consciousness under the Influence of Cannabis Indica. *Science 22*, 233-234.

Seachrist, J.L., and Ferguson, S.S. (2003). Regulation of G protein-coupled receptor endocytosis and trafficking by Rab GTPases. *Life Sci 74*, 225-235.

Seifert, R., and Wenzel-Seifert, K. (2002). Constitutive activity of G-protein-coupled receptors: cause of disease and common property of wild-type receptors. *Naunyn Schmiedebergs Arch Pharmacol 366*, 381-416.

Shenoy, S.K., McDonald, P.H., Kohout, T.A., and Lefkowitz, R.J. (2001). Regulation of receptor fate by ubiquitination of activated beta 2-adrenergic receptor and beta-arrestin. *Science 294*, 1307-1313.

Sierecki, E., Giles, N., Polinkovsky, M., Moustaqil, M., Alexandrov, K., and Gambin, Y. (2013). A cell-free approach to accelerate the study of protein-protein interactions in vitro. *Interface Focus 3*, 20130018.

Slanina, K.A., and Schweitzer, P. (2005). Inhibition of cyclooxygenase-2 elicits a CB1-mediated decrease of excitatory transmission in rat CA1 hippocampus. *Neuropharmacology 49*, 653-659.

Smith, T.H., Blume, L.C., Straiker, A., Cox, J.O., David, B.G., McVoy, J.R., Sayers, K.W., Poklis, J.L., Abdullah, R.A., Egertova, M., et al. (2015). Cannabinoid receptor-interacting protein 1a modulates CB1 receptor signaling and regulation. *Mol Pharmacol 87*, 747-765.

Soltesz, I., Alger, B.E., Kano, M., Lee, S.H., Lovinger, D.M., Ohno-Shosaku, T., and Watanabe, M. (2015). Weeding out bad waves: towards selective cannabinoid circuit control in epilepsy. *Nat Rev Neurosci 16*, 264-277.

Steindel, F., Lerner, R., Haring, M., Ruehle, S., Marsicano, G., Lutz, B., and Monory, K. (2013). Neuron-type specific cannabinoid-mediated G protein signalling in mouse hippocampus. *J Neurochem 124*, 795-807.

Sudhof, T.C., and Malenka, R.C. (2008). Understanding synapses: past, present, and future. *Neuron 60*, 469-476.

Tanimura, A., Yamazaki, M., Hashimotodani, Y., Uchigashima, M., Kawata, S., Abe, M., Kita, Y., Hashimoto, K., Shimizu, T., Watanabe, M., et al. (2010). The endocannabinoid 2-arachidonoylglycerol produced by diacylglycerol lipase alpha mediates retrograde suppression of synaptic transmission. *Neuron 65*, 320-327.

Tebano, M.T., Martire, A., and Popoli, P. (2012). Adenosine A(2A)-cannabinoid CB(1) receptor interaction: an integrative mechanism in striatal glutamatergic neurotransmission. *Brain Res 1476*, 108-118.

Tsetsenis, T., Younts, T.J., Chiu, C.Q., Kaeser, P.S., Castillo, P.E., and Sudhof, T.C. (2011). Rab3B protein is required for long-term depression of hippocampal inhibitory synapses and for normal reversal learning. *Proc Natl Acad Sci U S A 108*, 14300-14305.

Tsokolov, S.A. (2009). Why is the definition of life so elusive? Epistemological considerations. *Astrobiology 9*, 401-412.

Turu, G., and Hunyady, L. (2010). Signal transduction of the CB1 cannabinoid receptor. *J Mol Endocrinol 44*, 75-85.

Vahatalo, L.H., Ruohonen, S.T., Makela, S., Ailanen, L., Penttinen, A.M., Stormi, T., Kauko, T., Piscitelli, F., Silvestri, C., Savontaus, E., et al. (2015). Role of the endocannabinoid system in obesity induced by neuropeptide Y overexpression in noradrenergic neurons. *Nutr Diabetes 5*, e151.

van Biesen, T., Hawes, B.E., Luttrell, D.K., Krueger, K.M., Touhara, K., Porfiri, E., Sakaue, M., Luttrell, L.M., and Lefkowitz, R.J. (1995). Receptor-tyrosine-kinase- and G beta gamma-mediated MAP kinase activation by a common signalling pathway. *Nature 376*, 781-784.

van den Buuse, M., Martin, S., Holgate, J., Matthaei, K., and Hendry, I. (2007). Mice deficient in the alpha subunit of G(z) show changes in pre-pulse inhibition, anxiety and responses to 5-HT(1A) receptor stimulation, which are strongly dependent on the genetic background. *Psychopharmacology (Berl) 195*, 273-283.

Venkatakrishnan, A.J., Deupi, X., Lebon, G., Tate, C.G., Schertler, G.F., and Babu, M.M. (2013). Molecular signatures of G-protein-coupled receptors. *Nature 494*, 185-194.

Vinals, X., Moreno, E., Lanfumey, L., Cordomi, A., Pastor, A., de La Torre, R., Gasperini, P., Navarro, G., Howell, L.A., Pardo, L., et al. (2015). Cognitive Impairment Induced by Delta9-tetrahydrocannabinol Occurs through Heteromers between Cannabinoid CB1 and Serotonin 5-HT2A Receptors. *PLoS Biol 13*, e1002194.

Whissell, P.D., Cajanding, J.D., Fogel, N., and Kim, J.C. (2015). Comparative density of CCK- and PV-GABA cells within the cortex and hippocampus. *Frontiers in Neuroanatomy 9*.

Whistler, J.L., Enquist, J., Marley, A., Fong, J., Gladher, F., Tsuruda, P., Murray, S.R., and Von Zastrow, M. (2002). Modulation of postendocytic sorting of G protein-coupled receptors. *Science 297*, 615-620.

Wickman, K.D., and Clapham, D.E. (1995). G-protein regulation of ion channels. *Curr Opin Neurobiol 5*, 278-285.

Wiener, N. (1948). Cybernetics. *Sci Am 179*, 14-18.

Wilson, R.I., and Nicoll, R.A. (2001). Endogenous cannabinoids mediate retrograde signalling at hippocampal synapses. *Nature 410*, 588-592.

Yang, J., Wu, J., Kowalska, M.A., Dalvi, A., Prevost, N., O'Brien, P.J., Manning, D., Poncz, M., Lucki, I., Blendy, J.A., et al. (2000). Loss of signaling through the G protein, Gz, results in abnormal platelet activation and altered responses to psychoactive drugs. *Proc Natl Acad Sci U S A 97*, 9984-9989.

Zogopoulos, P., Vasileiou, I., Patsouris, E., and Theocharis, S. (2013). The neuroprotective role of endocannabinoids against chemical-induced injury and other adverse effects. *J Appl Toxicol 33*, 246-264.

# 8 Appendix

## 8.1 Proteins identified in TAP samples

### Tab. 8.1 Proteins identified in the TAP samples of N-SF-CB1- and CB1-SF-C-transfected HEK293 cells

All proteins identified in the TAP samples of N-SF-CB1- and CB1-SF-C-transfected HEK293 cells and non-transfected negative controls (NC). Two individual samples were measured, respectively, in four technical replicates and mean values for all proteins calculated for each sample (mean NC (n=4); mean N-SF-CB1 1 (n=4); mean N-SF-CB1 (n=4); mean CB1-SF-C 1 (n=4); mean CB1-SF-C 2 (n=4)). description: detailed description of the identified protein including official gene symbol. accession: UniProtKB accession number of the protein. log2 ratio N-SF-CB1 vs NC: ratio of mean protein abundance in N-SF-CB1 samples relative to NC on a logarithmic scale. log2 ratio CB1-SF-C vs NC: ratio of mean protein abundance in CB1-SF-C samples relative to NC on a logarithmic scale.

| description | accession | mean NC (n=4) | mean N-SF-CB1 1 (n=4) | mean N-SF-CB1 2 (n=4) | mean CB1-SF-C 1 (n=4) | mean CB1-SF-C 2 (n=4) | log2 ratio N-SF-CB1 vs NC | log2 ratio CB1-SF-C vs NC |
|---|---|---|---|---|---|---|---|---|
| Cannabinoid receptor 1 OS=Homo sapiens GN=CNR1 PE=1 SV=1 | P21554 | 0 | 5879 | 4276 | 29443 | 42770 | 9,9893 | 12,8182 |
| Calnexin OS=Homo sapiens GN=CANX PE=1 SV=2 | P27824 | 0 | 0 | 0 | 10923 | 18930 | | 11,5441 |
| Tubulin alpha-1B chain OS=Homo sapiens GN=TUBA1B PE=1 SV=1 | P68363 | 0 | 1202 | 1212 | 4130 | 6808 | 7,9213 | 10,0964 |
| Ubiquitin-60S ribosomal protein L40 OS=Homo sapiens GN=UBA52 PE=1 SV=2 | P62987 | 0 | 0 | 0 | 2463 | 5853 | | 9,7015 |
| Cornifin-A OS=Homo sapiens GN=SPRR1A PE=1 SV=2 | P35321 | 0 | 0 | 0 | 0 | 3000 | | 8,2337 |
| Tubulin beta chain OS=Homo sapiens GN=TUBB PE=1 SV=2 | P07437 | 0 | 0 | 0 | 2127 | 2579 | | 8,8816 |
| Leucine-rich repeat-containing protein 59 OS=Homo sapiens GN=LRRC59 PE=1 SV=1 | Q96AG4 | 0 | 0 | 0 | 1302 | 1963 | | 8,3551 |
| Transmembrane protein 33 OS=Homo sapiens GN=TMEM33 PE=1 SV=2 | P57088 | 0 | 0 | 0 | 0 | 1858 | | 7,5454 |
| Glyceraldehyde-3-phosphate dehydrogenase OS=Homo sapiens GN=GAPDH PE=1 SV=3 | P04406 | 0 | 0 | 0 | 0 | 1748 | | 7,4581 |
| Catechol O-methyltransferase OS=Homo sapiens GN=COMT PE=1 SV=2 | P21964 | 0 | 0 | 0 | 0 | 1681 | | 7,4017 |
| Heat shock protein HSP 90-beta OS=Homo sapiens GN=HSP90AB1 PE=1 SV=4 | P08238 | 0 | 0 | 0 | 1298 | 1654 | | 8,2104 |
| Calmodulin-like protein 5 OS=Homo sapiens GN=CALML5 PE=1 SV=2 | Q9NZT1 | 0 | 0 | 0 | 1102 | 1502 | | 8,0301 |
| ATP synthase subunit alpha, mitochondrial OS=Homo sapiens GN=ATP5A1 PE=1 SV=1 | P25705 | 0 | 0 | 0 | 0 | 1434 | | 7,1739 |
| 60S ribosomal protein L27a OS=Homo sapiens GN=RPL27A PE=1 SV=2 | P46776 | 0 | 0 | 0 | 1085 | 1379 | | 7,9507 |
| Desmoglein-1 OS=Homo sapiens GN=DSG1 PE=1 SV=2 | Q02413 | 0 | 0 | 0 | 0 | 1362 | | 7,1001 |
| Sodium/potassium-transporting ATPase subunit alpha-1 OS=Homo sapiens GN=ATP1A1 PE=1 SV=1 | P05023 | 0 | 0 | 0 | 0 | 1328 | | 7,0639 |
| Fatty acid-binding protein, epidermal OS=Homo sapiens GN=FABP5 PE=1 SV=3 | Q01469 | 0 | 0 | 0 | 0 | 1245 | | 6,9710 |
| Actin, cytoplasmic 1 OS=Homo sapiens GN=ACTB PE=1 SV=1 | P60709 | 0 | 0 | 0 | 0 | 1243 | | 6,9698 |
| Tubulin beta-4B chain OS=Homo sapiens GN=TUBB4B PE=1 SV=1 | P68371 | 0 | 0 | 0 | 1042 | 1202 | | 7,8167 |
| Annexin A2 OS=Homo sapiens GN=ANXA2 PE=1 SV=2 | P07355 | 0 | 0 | 0 | 0 | 1114 | | 6,8125 |
| Propionyl-CoA carboxylase beta chain, mitochondrial OS=Homo sapiens GN=PCCB PE=1 SV=3 | P05166 | 0 | 1863 | 1319 | 2904 | 1036 | 8,3182 | 8,6257 |
| Pyruvate carboxylase, mitochondrial OS=Homo sapiens GN=PC PE=1 SV=2 | P11498 | 0 | 1440 | 1172 | 2293 | 1005 | 8,0347 | 8,3698 |

## Tab. 8.2 Proteins identified in the samples of Glu-CB1-SF-C-TAP and GABA-CB1-SF-C-TAP

All proteins identified in the Glu-CB1-SF-C-TAP and GABA-CB1-SF-C-TAP. Specificity was defined as a ≥ 2x enrichment of the abundance of a protein in one cell type compared to the other and highlighted with green (Glu-CB1-SF-C-TAP) or red (GABA-CB1-SF-C-TAP) background. description: detailed description of the identified protein including official gene symbol. accession: UniProtKB accession number of the protein. molar ratio vs CB1 GABA: molar ratio of the identified protein in the GABA-CB1-SF-C-TAP sample relative to CB1 in the GABA-CB1-SF-C-TAP sample. molar ratio vs CB1 Glu: molar ratio of the identified protein in the Glu-CB1-SF-C-TAP sample relative to CB1 in the Glu-CB1-SF-C-TAP sample. average molar ratio vs CB1: average of molar ratio of the identified protein relative to CB1 in the Glu-CB1-SF-C-TAP and GABA-CB1-SF-C-TAP samples. log2 ratio GABA vs Glu: ratio of abundance relative to CB1 of identified protein in GABA-CB1-SF-C-TAP vs Glu-CB1-SF-C-TAP sample on a logarithmic scale. Specificity of a protein for a cell type is defined as the log2 value exceeds or equals the absolute value of 1.

| Description | accession | molar ratio vs CB1 GABA | molar ratio vs CB1 Glu | average molar ratio vs CB1 | log2 ratio GABA vs Glu |
|---|---|---|---|---|---|
| Cannabinoid receptor 1 OS=Mus musculus GN=Cnr1 PE=2 SV=1 | P47746 | 1,0000 | 1,0000 | 1,0000 | -0,07 |
| Guanine nucleotide-binding protein G(o) subunit alpha OS=Mus musculus GN=Gnao1 PE=1 SV=3 | P18872 | 0,4280 | 0,4736 | 0,4513 | -0,21 |
| Sodium/potassium-transporting ATPase subunit alpha-3 OS=Mus musculus GN=Atp1a3 PE=1 SV=1 | Q6PIC6 | 0,4593 | 0,4044 | 0,4312 | 0,12 |
| Tubulin alpha-4A chain OS=Mus musculus GN=Tuba4a PE=1 SV=1 | P68368 | 0,3458 | 0,3158 | 0,3305 | 0,06 |
| Glyceraldehyde-3-phosphate dehydrogenase OS=Mus musculus GN=Gapdh PE=1 SV=2 | P16858 | 0,3158 | 0,3012 | 0,3083 | 0,00 |
| Tubulin alpha-8 chain OS=Mus musculus GN=Tuba8 PE=1 SV=1 | Q9JJZ2 | 0,3089 | 0,2950 | 0,3018 | 0,00 |
| ATP synthase subunit alpha, mitochondrial OS=Mus musculus GN=Atp5a1 PE=1 SV=1 | Q03265 | 0,2834 | 0,2811 | 0,2822 | -0,06 |
| Sodium/potassium-transporting ATPase subunit beta-1 OS=Mus musculus GN=Atp1b1 PE=1 SV=1 | P14094 | 0,3108 | 0,2546 | 0,2820 | 0,22 |
| Alpha-enolase OS=Mus musculus GN=Eno1 PE=1 SV=3 | P17182 | 0,2885 | 0,2199 | 0,2534 | 0,32 |
| Guanine nucleotide-binding protein G(I)/G(S)/G(T) subunit beta-1 OS=Mus musculus GN=Gnb1 PE=1 SV=3 | P62874 | 0,2189 | 0,2717 | 0,2459 | -0,38 |
| Sodium/potassium-transporting ATPase subunit alpha-1 OS=Mus musculus GN=Atp1a1 PE=1 SV=1 | Q8VDN2 | 0,2577 | 0,2275 | 0,2423 | 0,11 |
| Keratin, type II cytoskeletal 1 OS=Mus musculus GN=Krt1 PE=1 SV=4 | P04104 | 0,2340 | 0,2445 | 0,2394 | -0,13 |
| Actin, cytoplasmic 1 OS=Mus musculus GN=Actb PE=1 SV=1 | P60710 | 0,2508 | 0,2246 | 0,2374 | 0,09 |
| Syntaxin-1B OS=Mus musculus GN=Stx1b PE=1 SV=1 | P61264 | 0,2537 | 0,2094 | 0,2311 | 0,21 |
| Synaptic vesicle glycoprotein 2A OS=Mus musculus GN=Sv2a PE=1 SV=1 | Q9JIS5 | 0,2531 | 0,2016 | 0,2268 | 0,26 |
| Ig gamma-1 chain C region, membrane-bound form OS=Mus musculus GN=Ighg1 PE=1 SV=2 | P01869 | 0,2609 | 0,1798 | 0,2194 | 0,47 |
| Visinin-like protein 1 OS=Mus musculus GN=Vsnl1 PE=1 SV=2 | P62761 | 0,2457 | 0,1904 | 0,2174 | 0,30 |
| Calcium-dependent secretion activator 1 OS=Mus musculus GN=Cadps PE=1 SV=3 | Q80TJ1 | 0,2349 | 0,1956 | 0,2148 | 0,20 |
| Excitatory amino acid transporter 1 OS=Mus musculus GN=Slc1a3 PE=1 SV=2 | P56564 | 0,2157 | 0,1867 | 0,2009 | 0,14 |
| Guanine nucleotide-binding protein G(i) subunit alpha-1 OS=Mus musculus GN=Gnai1 PE=2 SV=1 | B2RSH2 | 0,1739 | 0,2159 | 0,1954 | -0,38 |
| Synaptotagmin-1 OS=Mus musculus GN=Syt1 PE=1 SV=1 | P46096 | 0,1943 | 0,1951 | 0,1947 | -0,07 |
| Synaptophysin OS=Mus musculus GN=Syp PE=1 SV=2 | Q62277 | 0,2039 | 0,1810 | 0,1922 | 0,11 |
| Keratin, type II cytoskeletal 79 OS=Mus musculus GN=Krt79 PE=2 SV=2 | Q8VED5 | 0,1613 | 0,2128 | 0,1877 | -0,47 |
| Serine/threonine-protein phosphatase 2B catalytic subunit alpha isoform OS=Mus musculus GN=Ppp3ca PE=1 SV=1 | P63328 | 0,1849 | 0,1800 | 0,1824 | -0,03 |
| Sodium/potassium-transporting ATPase subunit alpha-2 OS=Mus musculus GN=Atp1a2 PE=1 SV=1 | Q6PIE5 | 0,1915 | 0,1593 | 0,1750 | 0,20 |
| Vesicle-associated membrane protein 2 OS=Mus musculus GN=Vamp2 PE=1 SV=2 | P63044 | 0,1767 | 0,1489 | 0,1625 | 0,18 |
| Ras-related C3 botulinum toxin substrate 1 OS=Mus musculus GN=Rac1 PE=1 SV=1 | P63001 | 0,1365 | 0,1576 | 0,1473 | -0,27 |
| Excitatory amino acid transporter 2 OS=Mus musculus GN=Slc1a2 PE=1 SV=1 | P43006 | 0,1318 | 0,1584 | 0,1454 | -0,33 |
| ATP synthase subunit beta, mitochondrial OS=Mus musculus GN=Atp5b PE=1 SV=2 | P56480 | 0,1364 | 0,1510 | 0,1438 | -0,21 |
| Synaptic vesicle glycoprotein 2B OS=Mus musculus GN=Sv2b PE=1 SV=1 | Q8BG39 | 0,1293 | 0,1550 | 0,1424 | -0,33 |
| Mitochondrial glutamate carrier 1 OS=Mus musculus GN=Slc25a22 PE=1 SV=1 | Q9D6M3 | 0,1496 | 0,1339 | 0,1416 | 0,09 |
| Neuronal membrane glycoprotein M6-b OS=Mus musculus GN=Gpm6b PE=1 SV=2 | P35803 | 0,1257 | 0,1478 | 0,1371 | -0,30 |
| Ras-related protein Rab-30 OS=Mus musculus GN=Rab30 PE=2 SV=1 | Q923S9 | 0,1347 | 0,1364 | 0,1356 | -0,08 |
| Synaptogyrin-3 OS=Mus musculus GN=Syngr3 PE=1 SV=1 | Q8R191 | 0,1393 | 0,1292 | 0,1341 | 0,04 |
| Plasma membrane calcium-transporting ATPase 2 OS=Mus musculus GN=Atp2b2 PE=1 SV=2 | Q9R0K7 | 0,1610 | 0,1079 | 0,1338 | 0,51 |
| Myelin proteolipid protein OS=Mus musculus GN=Plp1 PE=1 SV=2 | P60202 | 0,1364 | 0,1308 | 0,1335 | -0,01 |
| Sarcoplasmic/endoplasmic reticulum calcium ATPase 2 OS=Mus musculus GN=Atp2a2 PE=1 SV=2 | O55143 | 0,1400 | 0,1255 | 0,1326 | 0,09 |
| Pyruvate kinase PKM OS=Mus musculus GN=Pkm PE=1 SV=4 | P52480 | 0,1497 | 0,1110 | 0,1299 | 0,37 |
| Guanine nucleotide-binding protein G(i) subunit alpha-2 OS=Mus musculus GN=Gnai2 PE=1 SV=5 | P08752 | 0,1243 | 0,1271 | 0,1257 | -0,10 |
| Calnexin OS=Mus musculus GN=Canx PE=1 SV=1 | P35564 | 0,1432 | 0,1030 | 0,1226 | 0,41 |
| Dipeptidyl aminopeptidase-like protein 6 OS=Mus musculus GN=Dpp6 PE=1 SV=1 | Q9Z218 | 0,1364 | 0,1083 | 0,1220 | 0,27 |
| Guanine nucleotide-binding protein G(z) subunit alpha OS=Mus musculus GN=Gnaz PE=2 SV=4 | O70443 | 0,1015 | 0,1409 | 0,1216 | -0,54 |
| 40S ribosomal protein S25 OS=Mus musculus GN=Rps25 PE=2 SV=1 | P62852 | 0,1463 | 0,0968 | 0,1210 | 0,53 |
| DnaJ homolog subfamily C member 5 OS=Mus musculus GN=Dnajc5 PE=1 SV=1 | P60904 | 0,1360 | 0,1038 | 0,1195 | 0,32 |
| Tubulin beta-4A chain OS=Mus musculus GN=Tubb4a PE=1 SV=3 | Q9D6F9 | 0,1152 | 0,1162 | 0,1157 | -0,08 |
| Vesicular glutamate transporter 1 OS=Mus musculus GN=Slc17a7 PE=2 SV=2 | Q3TXX4 | 0,0811 | 0,1482 | 0,1154 | -0,94 |
| Guanine nucleotide-binding protein G(I)/G(S)/G(T) subunit beta-2 OS=Mus musculus GN=Gnb2 PE=1 SV=3 | P62880 | 0,0948 | 0,1347 | 0,1152 | -0,57 |
| 4F2 cell-surface antigen heavy chain OS=Mus musculus GN=Slc3a2 PE=1 SV=1 | P10852 | 0,1233 | 0,1068 | 0,1149 | 0,14 |

| | | | | | |
|---|---|---|---|---|---|
| NADH dehydrogenase [ubiquinone] 1 alpha subcomplex subunit 4 OS=Mus musculus GN=Ndufa4 PE=1 SV=2 | Q62425 | 0,1161 | 0,1132 | 0,1146 | -0,03 |
| ADP/ATP translocase 1 OS=Mus musculus GN=Slc25a4 PE=1 SV=4 | P48962 | 0,1139 | 0,1142 | 0,1141 | -0,07 |
| Synaptotagmin-3 OS=Mus musculus GN=Syt3 PE=1 SV=2 | O35681 | 0,1000 | 0,1266 | 0,1136 | -0,41 |
| Endoplasmin OS=Mus musculus GN=Hsp90b1 PE=1 SV=2 | P08113 | 0,1083 | 0,1183 | 0,1134 | -0,19 |
| Sodium channel subunit beta-2 OS=Mus musculus GN=Scn2b PE=1 SV=1 | Q56A07 | 0,1173 | 0,1086 | 0,1129 | 0,04 |
| ATP synthase subunit gamma, mitochondrial OS=Mus musculus GN=Atp5c1 PE=1 SV=1 | Q91VR2 | 0,1093 | 0,1152 | 0,1123 | -0,14 |
| D-beta-hydroxybutyrate dehydrogenase, mitochondrial OS=Mus musculus GN=Bdh1 PE=1 SV=2 | Q80XN0 | 0,1141 | 0,1094 | 0,1117 | -0,01 |
| Proline-rich transmembrane protein 2 OS=Mus musculus GN=Prrt2 PE=1 SV=1 | E9PUL5 | 0,0813 | 0,1392 | 0,1109 | -0,84 |
| Tubulin beta-3 chain OS=Mus musculus GN=Tubb3 PE=1 SV=1 | Q9ERD7 | 0,0990 | 0,1200 | 0,1097 | -0,35 |
| Hippocalcin-like protein 4 OS=Mus musculus GN=Hpcal4 PE=2 SV=3 | Q8BGZ1 | 0,0797 | 0,1369 | 0,1090 | -0,85 |
| Ras-related protein Rab-14 OS=Mus musculus GN=Rab14 PE=1 SV=3 | Q91V41 | 0,1125 | 0,1044 | 0,1084 | 0,04 |
| Secretory carrier-associated membrane protein 5 OS=Mus musculus GN=Scamp5 PE=2 SV=1 | Q9JKD3 | 0,1099 | 0,1068 | 0,1083 | -0,03 |
| Keratin, type II cuticular Hb3 OS=Mus musculus GN=Krt83 PE=2 SV=2 | Q6IMF0 | 0,0905 | 0,1249 | 0,1081 | -0,53 |
| Ras-related protein Rab-1B OS=Mus musculus GN=Rab1b PE=1 SV=1 | Q9D1G1 | 0,1001 | 0,1136 | 0,1070 | -0,25 |
| Calcium/calmodulin-dependent protein kinase type II subunit alpha OS=Mus musculus GN=Camk2a PE=1 SV=2 | P11798 | 0,0936 | 0,1155 | 0,1048 | -0,37 |
| Vesicle-fusing ATPase OS=Mus musculus GN=Nsf PE=1 SV=2 | P46460 | 0,1049 | 0,1040 | 0,1044 | -0,05 |
| Tubulin beta-2A chain OS=Mus musculus GN=Tubb2a PE=1 SV=1 | Q7TMM9 | 0,1087 | 0,0979 | 0,1032 | 0,08 |
| Receptor-type tyrosine-protein phosphatase S OS=Mus musculus GN=Ptprs PE=1 SV=1 | B0V2N1 | 0,0788 | 0,1220 | 0,1009 | -0,70 |
| 2',3'-cyclic-nucleotide 3'-phosphodiesterase OS=Mus musculus GN=Cnp PE=1 SV=3 | P16330 | 0,0995 | 0,1002 | 0,0998 | -0,08 |
| Cell division control protein 42 homolog OS=Mus musculus GN=Cdc42 PE=1 SV=2 | P60766 | 0,0997 | 0,0966 | 0,0982 | -0,02 |
| Synaptogyrin-1 OS=Mus musculus GN=Syngr1 PE=1 SV=2 | O55100 | 0,1005 | 0,0932 | 0,0968 | 0,04 |
| Neuronal membrane glycoprotein M6-a OS=Mus musculus GN=Gpm6a PE=1 SV=1 | P35802 | 0,0856 | 0,1058 | 0,0959 | -0,37 |
| 14-3-3 protein zeta/delta OS=Mus musculus GN=Ywhaz PE=1 SV=1 | P63101 | 0,0935 | 0,0921 | 0,0928 | -0,05 |
| Syntaxin-1A OS=Mus musculus GN=Stx1a PE=1 SV=3 | O35526 | 0,0873 | 0,0952 | 0,0913 | -0,19 |
| Keratin, type II cytoskeletal 75 OS=Mus musculus GN=Krt75 PE=1 SV=1 | Q8BGZ7 | 0,0957 | 0,0860 | 0,0907 | 0,09 |
| Tubulin beta-4B chain OS=Mus musculus GN=Tubb4b PE=1 SV=1 | P68372 | 0,0895 | 0,0871 | 0,0883 | -0,03 |
| Ras-related protein Rab-3A OS=Mus musculus GN=Rab3a PE=1 SV=1 | P63011 | 0,0817 | 0,0890 | 0,0854 | -0,19 |
| Ras-related protein Rab-3C OS=Mus musculus GN=Rab3c PE=1 SV=1 | P62823 | 0,0846 | 0,0855 | 0,0850 | -0,08 |
| NADH dehydrogenase [ubiquinone] 1 alpha subcomplex subunit 10, mitochondrial OS=Mus musculus GN=Ndufa10 PE=1 SV=1 | Q99LC3 | 0,0772 | 0,0916 | 0,0845 | -0,31 |
| Heat shock cognate 71 kDa protein OS=Mus musculus GN=Hspa8 PE=1 SV=1 | P63017 | 0,1006 | 0,0680 | 0,0839 | 0,50 |
| 14-3-3 protein theta OS=Mus musculus GN=Ywhaq PE=1 SV=1 | P68254 | 0,0877 | 0,0788 | 0,0831 | 0,09 |
| Protein RUFY3 OS=Mus musculus GN=Rufy3 PE=1 SV=1 | Q9D394 | 0,0686 | 0,0946 | 0,0819 | -0,53 |
| Neuroplastin OS=Mus musculus GN=Nptn PE=1 SV=3 | P97300 | 0,0836 | 0,0802 | 0,0819 | -0,01 |
| Contactin-associated protein 1 OS=Mus musculus GN=Cntnap1 PE=2 SV=2 | O54991 | 0,0915 | 0,0695 | 0,0802 | 0,33 |
| Synaptosomal-associated protein 25 OS=Mus musculus GN=Snap25 PE=1 SV=1 | P60879 | 0,0890 | 0,0699 | 0,0792 | 0,28 |
| Ketimine reductase mu-crystallin OS=Mus musculus GN=Crym PE=1 SV=1 | O54983 | 0,0647 | 0,0915 | 0,0784 | -0,57 |
| Sodium/potassium-transporting ATPase subunit beta-2 OS=Mus musculus GN=Atp1b2 PE=1 SV=2 | P14231 | 0,0933 | 0,0620 | 0,0773 | 0,52 |
| Keratin, type II cytoskeletal 6A OS=Mus musculus GN=Krt6a PE=2 SV=3 | P50446 | 0,0967 | 0,0579 | 0,0769 | 0,67 |
| Ras-related protein Rab-3B OS=Mus musculus GN=Rab3b PE=1 SV=1 | Q9CZT8 | 0,0796 | 0,0723 | 0,0759 | 0,07 |
| Ras-related protein Rab-10 OS=Mus musculus GN=Rab10 PE=1 SV=1 | P61027 | 0,0721 | 0,0776 | 0,0749 | -0,17 |
| Very-long-chain (3R)-3-hydroxyacyl-[acyl-carrier protein] dehydratase 3 OS=Mus musculus GN=ptplad1 PE=1 SV=2 | Q8K2C9 | 0,0807 | 0,0694 | 0,0749 | 0,15 |
| ADP-ribosylation factor 5 OS=Mus musculus GN=Arf5 PE=1 SV=2 | P84084 | 0,0716 | 0,0780 | 0,0749 | -0,19 |
| Tubulin beta-5 chain OS=Mus musculus GN=Tubb5 PE=1 SV=1 | P99024 | 0,0813 | 0,0684 | 0,0747 | 0,18 |
| ADP/ATP translocase 2 OS=Mus musculus GN=Slc25a5 PE=1 SV=3 | P51881 | 0,0799 | 0,0688 | 0,0742 | 0,15 |
| Voltage-dependent calcium channel gamma-8 subunit OS=Mus musculus GN=Cacng8 PE=1 SV=1 | Q8VHW2 | 0,0621 | 0,0852 | 0,0739 | -0,52 |
| Sodium/calcium exchanger 1 OS=Mus musculus GN=Slc8a1 PE=1 SV=1 | P70414 | 0,0535 | 0,0921 | 0,0733 | -0,85 |
| Keratin, type I cytoskeletal 42 OS=Mus musculus GN=Krt42 PE=1 SV=1 | Q6IFX2 | 0,0789 | 0,0665 | 0,0725 | 0,18 |
| 78 kDa glucose-regulated protein OS=Mus musculus GN=Hspa5 PE=1 SV=3 | P20029 | 0,1034 | 0,0398 | 0,0709 | 1,31 |
| Ras-related protein Rab-18 OS=Mus musculus GN=Rab18 PE=2 SV=2 | P35293 | 0,0728 | 0,0673 | 0,0700 | 0,05 |
| Glycogen phosphorylase, brain form OS=Mus musculus GN=Pygb PE=1 SV=3 | Q8CI94 | 0,0611 | 0,0782 | 0,0698 | -0,42 |
| CaM kinase-like vesicle-associated protein OS=Mus musculus GN=Camkv PE=1 SV=2 | Q3UHL1 | 0,0587 | 0,0804 | 0,0698 | -0,52 |
| Ephrin type-A receptor 4 OS=Mus musculus GN=Epha4 PE=1 SV=2 | Q03137 | 0,0355 | 0,1024 | 0,0697 | -1,60 |
| Centrosomal protein of 152 kDa OS=Mus musculus GN=Cep152 PE=1 SV=1 | A2AUM9 | 0,0704 | 0,0652 | 0,0677 | 0,05 |
| Immunoglobulin superfamily member 8 OS=Mus musculus GN=Igsf8 PE=1 SV=2 | Q8R366 | 0,0589 | 0,0761 | 0,0677 | -0,44 |
| LanC-like protein 2 OS=Mus musculus GN=Lancl2 PE=1 SV=1 | Q9JJK2 | 0,0659 | 0,0665 | 0,0662 | -0,08 |
| Phosphatidate cytidylyltransferase 2 OS=Mus musculus GN=Cds2 PE=1 SV=1 | Q99L43 | 0,0600 | 0,0696 | 0,0649 | -0,28 |
| Ras-related protein Rap-1A OS=Mus musculus GN=Rap1a PE=2 SV=1 | P62835 | 0,0639 | 0,0654 | 0,0647 | -0,10 |
| Phosphate carrier protein, mitochondrial OS=Mus musculus GN=Slc25a3 PE=1 SV=1 | Q8VEM8 | 0,0637 | 0,0645 | 0,0641 | -0,08 |
| Potassium voltage-gated channel subfamily A member 2 OS=Mus musculus GN=Kcna2 PE=1 SV=1 | P63141 | 0,0663 | 0,0611 | 0,0636 | 0,05 |
| Dephospho-CoA kinase domain-containing protein OS=Mus musculus GN=Dcakd PE=2 SV=1 | Q8BHC4 | 0,0659 | 0,0613 | 0,0636 | 0,04 |
| Pyruvate carboxylase, mitochondrial OS=Mus musculus GN=Pc PE=1 SV=1 | Q05920 | 0,0732 | 0,0528 | 0,0627 | 0,41 |
| Plexin-A4 OS=Mus musculus GN=Plxna4 PE=1 SV=3 | Q80UG2 | 0,0577 | 0,0641 | 0,0610 | -0,22 |
| Protein kinase C gamma type OS=Mus musculus GN=Prkcg PE=1 SV=1 | P63318 | 0,0345 | 0,0846 | 0,0601 | -1,36 |
| Keratin, type II cytoskeletal 6B OS=Mus musculus GN=Krt6b PE=2 SV=3 | Q9Z331 | 0,0545 | 0,0653 | 0,0600 | -0,33 |
| Solute carrier family 2, facilitated glucose transporter member 3 OS=Mus musculus GN=Slc2a3 PE=1 SV=1 | P32037 | 0,0599 | 0,0593 | 0,0596 | -0,05 |
| Adenylate cyclase type 9 OS=Mus musculus GN=Adcy9 PE=1 SV=1 | P51830 | 0,0291 | 0,0861 | 0,0583 | -1,63 |
| Disintegrin and metalloproteinase domain-containing protein 22 OS=Mus musculus GN=Adam22 PE=1 SV=2 | Q9R1V6 | 0,0545 | 0,0612 | 0,0579 | -0,23 |
| Neuron-specific calcium-binding protein hippocalcin OS=Mus musculus GN=Hpca PE=1 SV=2 | P84075 | 0,0393 | 0,0755 | 0,0579 | -1,01 |
| Ras-related protein Rab-39B OS=Mus musculus GN=Rab39b PE=2 SV=1 | Q8BHC1 | 0,0525 | 0,0623 | 0,0575 | -0,31 |
| Isocitrate dehydrogenase [NAD] subunit alpha, mitochondrial OS=Mus musculus GN=Idh3a PE=1 SV=1 | Q9D6R2 | 0,0577 | 0,0570 | 0,0573 | -0,05 |
| Serine/threonine-protein phosphatase 2B catalytic subunit beta isoform OS=Mus musculus GN=Ppp3cb PE=1 SV=2 | P48453 | 0,0604 | 0,0544 | 0,0573 | 0,09 |
| FXYD domain-containing ion transport regulator 7 OS=Mus musculus GN=Fxyd7 PE=2 SV=1 | P59648 | 0,0300 | 0,0833 | 0,0573 | -1,54 |
| Ig kappa chain C region OS=Mus musculus PE=1 SV=1 | P01837 | 0,0604 | 0,0541 | 0,0572 | 0,09 |
| Electron transfer flavoprotein subunit alpha, mitochondrial OS=Mus musculus GN=Etfa PE=1 SV=2 | Q99LC5 | 0,0551 | 0,0557 | 0,0554 | -0,08 |
| ADP-ribosylation factor 2 OS=Mus musculus GN=Arf2 PE=1 SV=2 | Q8BSL7 | 0,0574 | 0,0533 | 0,0553 | 0,04 |
| Vesicular inhibitory amino acid transporter OS=Mus musculus GN=Slc32a1 PE=1 SV=3 | O35633 | 0,1074 | 0,0047 | 0,0549 | 4,45 |

| | | | | | |
|---|---|---|---|---|---|
| Keratin, type I cytoskeletal 14 OS=Mus musculus GN=Krt14 PE=1 SV=2 | Q61781 | 0,0520 | 0,0562 | 0,0542 | -0,18 |
| Keratin, type II cuticular Hb2 OS=Mus musculus GN=Krt82 PE=2 SV=2 | Q99M74 | 0,0440 | 0,0638 | 0,0541 | -0,60 |
| Ras-related protein Rab-5A OS=Mus musculus GN=Rab5a PE=1 SV=1 | Q9CQD1 | 0,0548 | 0,0516 | 0,0531 | 0,02 |
| Rabphilin-3A OS=Mus musculus GN=Rph3a PE=1 SV=2 | P47708 | 0,0549 | 0,0509 | 0,0528 | 0,04 |
| Mast/stem cell growth factor receptor Kit OS=Mus musculus GN=Kit PE=1 SV=3 | P05532 | 0,0397 | 0,0653 | 0,0528 | -0,79 |
| Neurofilament heavy polypeptide OS=Mus musculus GN=Nefh PE=1 SV=3 | P19246 | 0,0449 | 0,0590 | 0,0521 | -0,46 |
| Clathrin coat assembly protein AP180 OS=Mus musculus GN=Snap91 PE=1 SV=1 | Q61548 | 0,0499 | 0,0519 | 0,0509 | -0,12 |
| Synaptotagmin-7 OS=Mus musculus GN=Syt7 PE=1 SV=1 | Q9R0N7 | 0,0363 | 0,0631 | 0,0500 | -0,87 |
| Acetyl-CoA acetyltransferase, mitochondrial OS=Mus musculus GN=Acat1 PE=1 SV=1 | Q8QZT1 | 0,0402 | 0,0576 | 0,0491 | -0,59 |
| Gamma-glutamyltransferase 7 OS=Mus musculus GN=Ggt7 PE=2 SV=2 | Q99JP7 | 0,0457 | 0,0517 | 0,0488 | -0,25 |
| Alpha-1,3/1,6-mannosyltransferase ALG2 OS=Mus musculus GN=Alg2 PE=2 SV=2 | Q9DBE8 | 0,0464 | 0,0509 | 0,0487 | -0,20 |
| Ras-related protein Rab-5C OS=Mus musculus GN=Rab5c PE=1 SV=2 | P35278 | 0,0553 | 0,0419 | 0,0485 | 0,33 |
| Succinyl-CoA ligase [ADP-forming] subunit beta, mitochondrial OS=Mus musculus GN=Sucla2 PE=1 SV=2 | Q9Z2I9 | 0,0480 | 0,0483 | 0,0481 | -0,07 |
| Cytochrome b-c1 complex subunit 2, mitochondrial OS=Mus musculus GN=Uqcrc2 PE=1 SV=1 | Q9DB77 | 0,0370 | 0,0577 | 0,0476 | -0,71 |
| Ig kappa chain V-II region 26-10 OS=Mus musculus PE=1 SV=1 | P01631 | 0,0563 | 0,0393 | 0,0476 | 0,45 |
| Sodium-dependent neutral amino acid transporter SLC6A17 OS=Mus musculus GN=Slc6a17 PE=1 SV=1 | Q8BJI1 | 0,0551 | 0,0388 | 0,0468 | 0,44 |
| Estradiol 17-beta-dehydrogenase 12 OS=Mus musculus GN=Hsd17b12 PE=2 SV=1 | O70503 | 0,0521 | 0,0416 | 0,0468 | 0,26 |
| Synapsin-2 OS=Mus musculus GN=Syn2 PE=1 SV=2 | Q64332 | 0,0422 | 0,0510 | 0,0467 | -0,34 |
| Elongation factor Tu, mitochondrial OS=Mus musculus GN=Tufm PE=1 SV=1 | Q8BFR5 | 0,0503 | 0,0433 | 0,0467 | 0,15 |
| 6-phosphofructokinase, muscle type OS=Mus musculus GN=Pfkm PE=1 SV=3 | P47857 | 0,0456 | 0,0472 | 0,0464 | -0,12 |
| Protein lunapark OS=Mus musculus GN=Lnp PE=1 SV=1 | Q7TQ95 | 0,0509 | 0,0411 | 0,0459 | 0,24 |
| Guanine nucleotide-binding protein G(q) subunit alpha OS=Mus musculus GN=Gnaq PE=1 SV=4 | P21279 | 0,0368 | 0,0545 | 0,0458 | -0,63 |
| Heat shock 70 kDa protein 12A OS=Mus musculus GN=Hspa12a PE=1 SV=1 | Q8K0U4 | 0,0410 | 0,0504 | 0,0458 | -0,36 |
| Dihydropyrimidinase-related protein 2 OS=Mus musculus GN=Dpysl2 PE=1 SV=2 | O08553 | 0,0481 | 0,0429 | 0,0455 | 0,10 |
| Myelin-oligodendrocyte glycoprotein OS=Mus musculus GN=Mog PE=1 SV=1 | Q61885 | 0,0489 | 0,0419 | 0,0453 | 0,16 |
| Inactive dipeptidyl peptidase 10 OS=Mus musculus GN=Dpp10 PE=2 SV=1 | Q6NXK7 | 0,0599 | 0,0310 | 0,0451 | 0,88 |
| Keratin, type II cuticular Hb1 OS=Mus musculus GN=Krt81 PE=2 SV=2 | Q9ERE2 | 0,0180 | 0,0707 | 0,0450 | -2,04 |
| Drebrin OS=Mus musculus GN=Dbn1 PE=1 SV=4 | Q9QXS6 | 0,0378 | 0,0518 | 0,0450 | -0,52 |
| Ectonucleoside triphosphate diphosphohydrolase 2 OS=Mus musculus GN=Entpd2 PE=1 SV=2 | O55026 | 0,0517 | 0,0384 | 0,0449 | 0,36 |
| Monoglyceride lipase OS=Mus musculus GN=Mgll PE=1 SV=1 | O35678 | 0,0643 | 0,0262 | 0,0448 | 1,23 |
| Intercellular adhesion molecule 5 OS=Mus musculus GN=Icam5 PE=1 SV=2 | Q60625 | 0,0342 | 0,0548 | 0,0447 | -0,75 |
| Protein tweety homolog 1 OS=Mus musculus GN=Ttyh1 PE=1 SV=1 | Q9D3A9 | 0,0484 | 0,0402 | 0,0442 | 0,20 |
| Secretory carrier-associated membrane protein 3 OS=Mus musculus GN=Scamp3 PE=1 SV=3 | O35609 | 0,0410 | 0,0461 | 0,0436 | -0,24 |
| Ganglioside-induced differentiation-associated protein 1 OS=Mus musculus GN=Gdap1 PE=1 SV=1 | O88741 | 0,0429 | 0,0439 | 0,0434 | -0,10 |
| Neutral amino acid transporter A OS=Mus musculus GN=Slc1a4 PE=1 SV=1 | O35874 | 0,0530 | 0,0342 | 0,0433 | 0,57 |
| 60 kDa heat shock protein, mitochondrial OS=Mus musculus GN=Hspd1 PE=1 SV=1 | P63038 | 0,0449 | 0,0413 | 0,0431 | 0,05 |
| Elongation factor 1-alpha 1 OS=Mus musculus GN=Eef1a1 PE=1 SV=3 | P10126 | 0,0479 | 0,0379 | 0,0428 | 0,27 |
| Heat shock 70 kDa protein 1-like OS=Mus musculus GN=Hspa1l PE=2 SV=4 | P16627 | 0,0369 | 0,0484 | 0,0428 | -0,46 |
| Glutamate decarboxylase 1 OS=Mus musculus GN=Gad1 PE=2 SV=2 | P48318 | 0,0755 | 0,0113 | 0,0427 | 2,67 |
| Guanine nucleotide-binding protein G(k) subunit alpha OS=Mus musculus GN=Gnai3 PE=1 SV=3 | Q9DC51 | 0,0351 | 0,0495 | 0,0425 | -0,56 |
| Membrane-associated progesterone receptor component 1 OS=Mus musculus GN=Pgrmc1 PE=1 SV=4 | O55022 | 0,0410 | 0,0430 | 0,0420 | -0,14 |
| Septin-7 OS=Mus musculus GN=Sept7 PE=1 SV=1 | O55131 | 0,0266 | 0,0564 | 0,0418 | -1,15 |
| Triosephosphate isomerase OS=Mus musculus GN=Tpi1 PE=1 SV=4 | P17751 | 0,0505 | 0,0333 | 0,0417 | 0,53 |
| 14-3-3 protein beta/alpha OS=Mus musculus GN=Ywhab PE=1 SV=3 | Q9CQV8 | 0,0367 | 0,0461 | 0,0415 | -0,40 |
| Astrotactin-1 OS=Mus musculus GN=Astn1 PE=2 SV=4 | Q61137 | 0,0376 | 0,0446 | 0,0412 | -0,31 |
| Actin, aortic smooth muscle OS=Mus musculus GN=Acta2 PE=1 SV=1 | P62737 | 0,0441 | 0,0379 | 0,0409 | 0,15 |
| Ras-related protein Rab-2B OS=Mus musculus GN=Rab2b PE=2 SV=1 | P59279 | 0,0445 | 0,0374 | 0,0408 | 0,18 |
| Potassium voltage-gated channel subfamily A member 1 OS=Mus musculus GN=Kcna1 PE=1 SV=1 | P16388 | 0,0313 | 0,0494 | 0,0406 | -0,72 |
| Protein FAM49A OS=Mus musculus GN=Fam49a PE=2 SV=1 | Q8BHZ0 | 0,0418 | 0,0392 | 0,0405 | 0,02 |
| Mitochondrial import inner membrane translocase subunit TIM50 OS=Mus musculus GN=Timm50 PE=1 SV=1 | Q9D880 | 0,0385 | 0,0423 | 0,0405 | -0,20 |
| Semaphorin-4B OS=Mus musculus GN=Sema4b PE=1 SV=2 | Q62179 | 0,0256 | 0,0542 | 0,0402 | -1,15 |
| Basigin OS=Mus musculus GN=Bsg PE=1 SV=2 | P18572 | 0,0423 | 0,0379 | 0,0400 | 0,09 |
| Proline-rich transmembrane protein 3 OS=Mus musculus GN=Prrt3 PE=1 SV=1 | Q6PE13 | 0,0325 | 0,0464 | 0,0396 | -0,58 |
| Transmembrane protein 132A OS=Mus musculus GN=Tmem132a PE=2 SV=2 | Q922P8 | 0,0316 | 0,0464 | 0,0391 | -0,62 |
| GTP-binding protein Di-Ras2 OS=Mus musculus GN=Diras2 PE=2 SV=1 | Q5PR73 | 0,0378 | 0,0396 | 0,0387 | -0,13 |
| Calcium/calmodulin-dependent protein kinase type II subunit beta OS=Mus musculus GN=Camk2b PE=1 SV=2 | P28652 | 0,0378 | 0,0389 | 0,0384 | -0,11 |
| Beta-soluble NSF attachment protein OS=Mus musculus GN=Napb PE=1 SV=2 | P28663 | 0,0383 | 0,0380 | 0,0381 | -0,06 |
| Junction plakoglobin OS=Mus musculus GN=Jup PE=1 SV=3 | Q02257 | 0,0404 | 0,0358 | 0,0380 | 0,11 |
| Myelin basic protein OS=Mus musculus GN=Mbp PE=1 SV=2 | P04370 | 0,0340 | 0,0417 | 0,0380 | -0,36 |
| ADP-ribosylation factor 1 OS=Mus musculus GN=Arf1 PE=1 SV=2 | P84078 | 0,0321 | 0,0434 | 0,0379 | -0,50 |
| Glutamine synthetase OS=Mus musculus GN=Glul PE=1 SV=6 | P15105 | 0,0402 | 0,0356 | 0,0379 | 0,11 |
| Trifunctional enzyme subunit alpha, mitochondrial OS=Mus musculus GN=Hadha PE=1 SV=1 | Q8BMS1 | 0,0388 | 0,0362 | 0,0375 | 0,03 |
| Long-chain-fatty-acid--CoA ligase ACSBG1 OS=Mus musculus GN=Acsbg1 PE=1 SV=1 | Q99PU5 | 0,0440 | 0,0312 | 0,0374 | 0,43 |
| E3 ubiquitin-protein ligase UBR2 OS=Mus musculus GN=Ubr2 PE=1 SV=2 | Q6WKZ8 | 0,0408 | 0,0339 | 0,0373 | 0,20 |
| 14-3-3 protein gamma OS=Mus musculus GN=Ywhag PE=1 SV=2 | P61982 | 0,0420 | 0,0328 | 0,0373 | 0,29 |
| OX-2 membrane glycoprotein OS=Mus musculus GN=Cd200 PE=1 SV=1 | O54901 | 0,0404 | 0,0342 | 0,0372 | 0,17 |
| Rho-related GTP-binding protein RhoB OS=Mus musculus GN=Rhob PE=1 SV=1 | P62746 | 0,0337 | 0,0404 | 0,0371 | -0,33 |
| NADH dehydrogenase [ubiquinone] iron-sulfur protein 7, mitochondrial OS=Mus musculus GN=Ndufs7 PE=1 SV=1 | Q9DC70 | 0,0298 | 0,0438 | 0,0369 | -0,62 |
| Integral membrane protein 2B OS=Mus musculus GN=Itm2b PE=2 SV=1 | O89051 | 0,0370 | 0,0367 | 0,0369 | -0,05 |
| Activin receptor type-1 OS=Mus musculus GN=Acvr1 PE=2 SV=2 | P37172 | 0,0412 | 0,0322 | 0,0366 | 0,29 |
| Leucine-zipper-like transcriptional regulator 1 OS=Mus musculus GN=Lztr1 PE=2 SV=2 | Q9CQ33 | 0,0222 | 0,0502 | 0,0366 | -1,24 |
| ADP-ribosylation factor-like protein 8B OS=Mus musculus GN=Arl8b PE=2 SV=1 | Q9CQW2 | 0,0354 | 0,0376 | 0,0365 | -0,16 |
| Latrophilin-1 OS=Mus musculus GN=Lphn1 PE=1 SV=2 | Q80TR1 | 0,0380 | 0,0345 | 0,0362 | 0,07 |
| Heat shock protein HSP 90-beta OS=Mus musculus GN=Hsp90ab1 PE=1 SV=3 | P11499 | 0,0332 | 0,0388 | 0,0361 | -0,29 |
| Sodium- and chloride-dependent GABA transporter 3 OS=Mus musculus GN=Slc6a11 PE=1 SV=2 | P31650 | 0,0382 | 0,0339 | 0,0360 | 0,10 |
| Sideroflexin-5 OS=Mus musculus GN=Sfxn5 PE=1 SV=2 | Q925N0 | 0,0382 | 0,0334 | 0,0358 | 0,13 |

| | | | | | |
|---|---|---|---|---|---|
| 14-3-3 protein epsilon OS=Mus musculus GN=Ywhae PE=1 SV=1 | P62259 | 0,0375 | 0,0328 | 0,0351 | 0,13 |
| Keratin, type I cuticular Ha4 OS=Mus musculus GN=Krt34 PE=2 SV=1 | Q9D646 | 0,0174 | 0,0518 | 0,0350 | -1,65 |
| Protein NipSnap homolog 1 OS=Mus musculus GN=Nipsnap1 PE=1 SV=1 | O55125 | 0,0343 | 0,0353 | 0,0348 | -0,11 |
| Prohibitin OS=Mus musculus GN=Phb PE=1 SV=1 | P67778 | 0,0461 | 0,0239 | 0,0347 | 0,88 |
| Protein FAM49B OS=Mus musculus GN=Fam49b PE=2 SV=1 | Q921M7 | 0,0335 | 0,0356 | 0,0346 | -0,16 |
| Glutamate decarboxylase 2 OS=Mus musculus GN=Gad2 PE=2 SV=1 | P48320 | 0,0570 | 0,0119 | 0,0339 | 2,20 |
| Sodium- and chloride-dependent GABA transporter 1 OS=Mus musculus GN=Slc6a1 PE=1 SV=2 | P31648 | 0,0599 | 0,0089 | 0,0338 | 2,68 |
| Rho-related GTP-binding protein RhoG OS=Mus musculus GN=Rhog PE=2 SV=1 | P84096 | 0,0362 | 0,0314 | 0,0338 | 0,14 |
| Vesicle-associated membrane protein 1 OS=Mus musculus GN=Vamp1 PE=1 SV=1 | Q62442 | 0,0442 | 0,0237 | 0,0337 | 0,83 |
| V-type proton ATPase subunit H OS=Mus musculus GN=Atp6v1h PE=1 SV=1 | Q8BVE3 | 0,0306 | 0,0365 | 0,0336 | -0,32 |
| Amine oxidase [flavin-containing] B OS=Mus musculus GN=Maob PE=1 SV=4 | Q8BW75 | 0,0372 | 0,0300 | 0,0335 | 0,24 |
| Potassium voltage-gated channel subfamily C member 2 OS=Mus musculus GN=Kcnc2 PE=1 SV=1 | Q14B80 | 0,0626 | 0,0053 | 0,0333 | 3,49 |
| ATP synthase subunit O, mitochondrial OS=Mus musculus GN=Atp5o PE=1 SV=1 | Q9DB20 | 0,0297 | 0,0363 | 0,0331 | -0,36 |
| Keratin, type I cytoskeletal 15 OS=Mus musculus GN=Krt15 PE=1 SV=2 | Q61414 | 0,0236 | 0,0421 | 0,0331 | -0,90 |
| 6-phosphofructokinase type C OS=Mus musculus GN=Pfkp PE=1 SV=1 | Q9WUA3 | 0,0327 | 0,0326 | 0,0327 | -0,06 |
| Potassium/sodium hyperpolarization-activated cyclic nucleotide-gated channel 1 OS=Mus musculus GN=Hcn1 PE=1 SV=1 | O88704 | 0,0469 | 0,0185 | 0,0324 | 1,28 |
| Peroxiredoxin-2 OS=Mus musculus GN=Prdx2 PE=1 SV=3 | Q61171 | 0,0422 | 0,0224 | 0,0321 | 0,84 |
| V-type proton ATPase catalytic subunit A OS=Mus musculus GN=Atp6v1a PE=1 SV=2 | P50516 | 0,0271 | 0,0365 | 0,0319 | -0,49 |
| Protein kinase C beta type OS=Mus musculus GN=Prkcb PE=1 SV=4 | P68404 | 0,0292 | 0,0340 | 0,0316 | -0,28 |
| Neurocalcin-delta OS=Mus musculus GN=Ncald PE=1 SV=4 | Q91X97 | 0,0368 | 0,0266 | 0,0316 | 0,40 |
| Neurochondrin OS=Mus musculus GN=Ncdn PE=1 SV=1 | Q9Z0E0 | 0,0295 | 0,0327 | 0,0311 | -0,21 |
| Neuroligin-3 OS=Mus musculus GN=Nlgn3 PE=1 SV=2 | Q8BYM5 | 0,0340 | 0,0282 | 0,0310 | 0,20 |
| Solute carrier family 12 member 5 OS=Mus musculus GN=Slc12a5 PE=1 SV=2 | Q91V14 | 0,0272 | 0,0346 | 0,0310 | -0,41 |
| Voltage-gated potassium channel subunit beta-2 OS=Mus musculus GN=Kcnab2 PE=2 SV=1 | P62482 | 0,0322 | 0,0292 | 0,0307 | 0,07 |
| RELT-like protein 2 OS=Mus musculus GN=Rell2 PE=2 SV=1 | Q8BRJ3 | 0,0351 | 0,0262 | 0,0305 | 0,36 |
| Synaptoporin OS=Mus musculus GN=Synpr PE=1 SV=1 | Q8BGN8 | 0,0345 | 0,0266 | 0,0305 | 0,31 |
| Thyrotropin-releasing hormone-degrading ectoenzyme OS=Mus musculus GN=Trhde PE=2 SV=1 | Q8K093 | 0,0299 | 0,0308 | 0,0303 | -0,11 |
| Serine/threonine-protein phosphatase 2A 65 kDa regulatory subunit A beta isoform OS=Mus musculus GN=Ppp2r1b PE=1 SV=2 | Q7TNP2 | 0,0338 | 0,0270 | 0,0303 | 0,26 |
| Band 4.1-like protein 1 OS=Mus musculus GN=Epb41l1 PE=1 SV=2 | Q9Z2H5 | 0,0414 | 0,0196 | 0,0303 | 1,01 |
| Receptor-type tyrosine-protein phosphatase delta OS=Mus musculus GN=Ptprd PE=1 SV=3 | Q64487 | 0,0352 | 0,0254 | 0,0302 | 0,41 |
| Catechol O-methyltransferase OS=Mus musculus GN=Comt PE=1 SV=2 | O88587 | 0,0341 | 0,0264 | 0,0302 | 0,31 |
| Cell cycle exit and neuronal differentiation protein 1 OS=Mus musculus GN=Cend1 PE=1 SV=1 | Q9JKC6 | 0,0342 | 0,0262 | 0,0301 | 0,32 |
| Tubulin beta-2B chain OS=Mus musculus GN=Tubb2b PE=1 SV=1 | Q9CWF2 | 0,0278 | 0,0322 | 0,0300 | -0,28 |
| Ras-related protein Rab-15 OS=Mus musculus GN=Rab15 PE=1 SV=1 | Q8K386 | 0,0264 | 0,0335 | 0,0300 | -0,41 |
| Calcineurin subunit B type 1 OS=Mus musculus GN=Ppp3r1 PE=1 SV=3 | Q63810 | 0,0286 | 0,0309 | 0,0298 | -0,18 |
| Elongation factor 2 OS=Mus musculus GN=Eef2 PE=1 SV=2 | P58252 | 0,0432 | 0,0166 | 0,0296 | 1,31 |
| Keratin, type II cytoskeletal 4 OS=Mus musculus GN=Krt4 PE=1 SV=2 | P07744 | 0,0173 | 0,0411 | 0,0295 | -1,31 |
| Ras-related protein Rap-2b OS=Mus musculus GN=Rap2b PE=1 SV=1 | P61226 | 0,0237 | 0,0347 | 0,0293 | -0,61 |
| Prosaposin receptor GPR37L1 OS=Mus musculus GN=Gpr37l1 PE=2 SV=2 | Q99JG2 | 0,0317 | 0,0268 | 0,0292 | 0,17 |
| WASH complex subunit 7 OS=Mus musculus GN=Kiaa1033 PE=2 SV=2 | Q3UMB9 | 0,0393 | 0,0186 | 0,0287 | 1,01 |
| Synaptosomal-associated protein 47 OS=Mus musculus GN=Snap47 PE=1 SV=1 | Q8R570 | 0,0333 | 0,0244 | 0,0287 | 0,38 |
| Keratin, type II cuticular Hb5 OS=Mus musculus GN=Krt85 PE=2 SV=2 | Q9Z2T6 | 0,0090 | 0,0475 | 0,0287 | -2,47 |
| Probable phospholipid-transporting ATPase IIA OS=Mus musculus GN=Atp9a PE=2 SV=3 | O70228 | 0,0290 | 0,0279 | 0,0285 | -0,01 |
| cAMP-dependent protein kinase type II-alpha regulatory subunit OS=Mus musculus GN=Prkar2a PE=1 SV=2 | P12367 | 0,0446 | 0,0131 | 0,0285 | 1,70 |
| Complement component 1 Q subcomponent-binding protein, mitochondrial OS=Mus musculus GN=C1qbp PE=1 SV=1 | O35658 | 0,0408 | 0,0161 | 0,0282 | 1,27 |
| Probable cationic amino acid transporter OS=Mus musculus GN=Slc7a14 PE=2 SV=1 | Q8BXR1 | 0,0293 | 0,0268 | 0,0280 | 0,06 |
| Regulator of G-protein signaling 7-binding protein OS=Mus musculus GN=Rgs7bp PE=1 SV=1 | Q8BQP9 | 0,0286 | 0,0273 | 0,0280 | 0,00 |
| 6-phosphofructokinase, liver type OS=Mus musculus GN=Pfkl PE=1 SV=4 | P12382 | 0,0271 | 0,0286 | 0,0279 | -0,14 |
| Contactin-1 OS=Mus musculus GN=Cntn1 PE=1 SV=1 | P12960 | 0,0317 | 0,0241 | 0,0278 | 0,32 |
| Ras-related protein Rab-21 OS=Mus musculus GN=Rab21 PE=1 SV=4 | P35282 | 0,0297 | 0,0259 | 0,0278 | 0,13 |
| Keratin, type I cuticular Ha5 OS=Mus musculus GN=Krt35 PE=2 SV=1 | Q497I4 | 0,0100 | 0,0445 | 0,0276 | -2,22 |
| Guanine nucleotide-binding protein G(I)/G(S)/G(O) subunit gamma-3 OS=Mus musculus GN=Gng3 PE=1 SV=1 | P63216 | 0,0215 | 0,0333 | 0,0275 | -0,70 |
| Alpha-soluble NSF attachment protein OS=Mus musculus GN=Napa PE=1 SV=1 | Q9DB05 | 0,0108 | 0,0430 | 0,0273 | -2,07 |
| Catenin beta-1 OS=Mus musculus GN=Ctnnb1 PE=1 SV=1 | Q02248 | 0,0319 | 0,0223 | 0,0270 | 0,45 |
| cAMP-dependent protein kinase type II-beta regulatory subunit OS=Mus musculus GN=Prkar2b PE=1 SV=3 | P31324 | 0,0436 | 0,0111 | 0,0270 | 1,91 |
| Zinc transporter ZIP12 OS=Mus musculus GN=Slc39a12 PE=2 SV=1 | Q5FWH7 | 0,0291 | 0,0246 | 0,0268 | 0,17 |
| Sideroflexin-3 OS=Mus musculus GN=Sfxn3 PE=1 SV=1 | Q91V61 | 0,0296 | 0,0239 | 0,0267 | 0,24 |
| C-terminal-binding protein 1 OS=Mus musculus GN=Ctbp1 PE=1 SV=2 | O88712 | 0,0234 | 0,0297 | 0,0266 | -0,41 |
| Peroxiredoxin-5, mitochondrial OS=Mus musculus GN=Prdx5 PE=1 SV=2 | P99029 | 0,0299 | 0,0233 | 0,0265 | 0,29 |
| Dihydropyrimidinase-related protein 1 OS=Mus musculus GN=Crmp1 PE=1 SV=1 | P97427 | 0,0196 | 0,0328 | 0,0263 | -0,81 |
| ADP-ribosylation factor 4 OS=Mus musculus GN=Arf4 PE=1 SV=2 | P61750 | 0,0264 | 0,0256 | 0,0260 | -0,03 |
| Lysosome-associated membrane glycoprotein 5 OS=Mus musculus GN=Lamp5 PE=1 SV=2 | Q9D387 | 0,0444 | 0,0082 | 0,0259 | 2,36 |
| Redox-regulatory protein FAM213A OS=Mus musculus GN=Fam213a PE=1 SV=2 | Q9CYH2 | 0,0262 | 0,0253 | 0,0257 | -0,02 |
| Receptor-type tyrosine-protein phosphatase-like N OS=Mus musculus GN=Ptprn PE=1 SV=2 | Q60673 | 0,0372 | 0,0146 | 0,0256 | 1,29 |
| Neural cell adhesion molecule 2 OS=Mus musculus GN=Ncam2 PE=2 SV=1 | O35136 | 0,0361 | 0,0156 | 0,0256 | 1,14 |
| Mitochondrial import receptor subunit TOM22 homolog OS=Mus musculus GN=Tomm22 PE=2 SV=3 | Q9CPQ3 | 0,0271 | 0,0241 | 0,0256 | 0,10 |
| Glutamate receptor 2 OS=Mus musculus GN=Gria2 PE=1 SV=3 | P23819 | 0,0189 | 0,0314 | 0,0253 | -0,80 |
| 14-3-3 protein eta OS=Mus musculus GN=Ywhah PE=1 SV=2 | P68510 | 0,0244 | 0,0251 | 0,0248 | -0,10 |
| Probable phospholipid-transporting ATPase IA OS=Mus musculus GN=Atp8a1 PE=1 SV=1 | P70704 | 0,0232 | 0,0261 | 0,0247 | -0,23 |
| Cell adhesion molecule 2 OS=Mus musculus GN=Cadm2 PE=1 SV=2 | Q8BLQ9 | 0,0271 | 0,0222 | 0,0246 | 0,22 |
| Protein NDRG4 OS=Mus musculus GN=Ndrg4 PE=1 SV=1 | Q8BTG7 | 0,0374 | 0,0120 | 0,0244 | 1,58 |
| Hepatocyte cell adhesion molecule OS=Mus musculus GN=Hepacam PE=1 SV=2 | Q640R3 | 0,0288 | 0,0202 | 0,0244 | 0,45 |
| Catenin alpha-1 OS=Mus musculus GN=Ctnna1 PE=1 SV=1 | P26231 | 0,0198 | 0,0287 | 0,0244 | -0,60 |
| Mesoderm-specific transcript protein OS=Mus musculus GN=Mest PE=2 SV=1 | Q07646 | 0,0304 | 0,0186 | 0,0243 | 0,64 |
| Monocarboxylate transporter 1 OS=Mus musculus GN=Slc16a1 PE=1 SV=1 | P53986 | 0,0297 | 0,0192 | 0,0243 | 0,57 |
| Protocadherin-19 OS=Mus musculus GN=Pcdh19 PE=2 SV=3 | Q80TF3 | 0,0270 | 0,0217 | 0,0243 | 0,24 |

| | | | | | |
|---|---|---|---|---|---|
| Syntaxin-binding protein 5-like OS=Mus musculus GN=Stxbp5l PE=2 SV=1 | Q5DQR4 | 0,0222 | 0,0262 | 0,0242 | -0,31 |
| Ras-related protein Rab-5B OS=Mus musculus GN=Rab5b PE=1 SV=1 | P61021 | 0,0264 | 0,0220 | 0,0242 | 0,19 |
| Integral membrane protein 2C OS=Mus musculus GN=Itm2c PE=2 SV=2 | Q91VK4 | 0,0182 | 0,0298 | 0,0241 | -0,78 |
| Serine/threonine-protein phosphatase 2A 65 kDa regulatory subunit A alpha isoform OS=Mus musculus GN=Ppp2r1a PE=1 SV=3 | Q76MZ3 | 0,0252 | 0,0228 | 0,0240 | 0,08 |
| Protein NDRG2 OS=Mus musculus GN=Ndrg2 PE=1 SV=1 | Q9QYG0 | 0,0239 | 0,0240 | 0,0239 | -0,07 |
| Protein QIL1 OS=Mus musculus GN=Qil1 PE=2 SV=1 | Q8R404 | 0,0224 | 0,0253 | 0,0239 | -0,24 |
| Ankyrin repeat and sterile alpha motif domain-containing protein 1B OS=Mus musculus GN=Anks1b PE=1 SV=3 | Q8BIZ1 | 0,0269 | 0,0209 | 0,0239 | 0,30 |
| Cofilin-1 OS=Mus musculus GN=Cfl1 PE=1 SV=3 | P18760 | 0,0261 | 0,0216 | 0,0238 | 0,21 |
| Potassium voltage-gated channel subfamily A member 4 OS=Mus musculus GN=Kcna4 PE=1 SV=2 | Q61423 | 0,0170 | 0,0302 | 0,0237 | -0,90 |
| CD99 antigen-like protein 2 OS=Mus musculus GN=Cd99l2 PE=1 SV=1 | Q8BIF0 | 0,0328 | 0,0148 | 0,0236 | 1,08 |
| GTP-binding nuclear protein Ran OS=Mus musculus GN=Ran PE=1 SV=3 | P62827 | 0,0197 | 0,0272 | 0,0235 | -0,53 |
| Potassium voltage-gated channel subfamily C member 1 OS=Mus musculus GN=Kcnc1 PE=2 SV=1 | P15388 | 0,0407 | 0,0065 | 0,0232 | 2,58 |
| Syntaxin-binding protein 1 OS=Mus musculus GN=Stxbp1 PE=1 SV=2 | O08599 | 0,0289 | 0,0176 | 0,0231 | 0,65 |
| Tyrosine-protein kinase Fyn OS=Mus musculus GN=Fyn PE=1 SV=4 | P39688 | 0,0217 | 0,0240 | 0,0229 | -0,21 |
| Protein NDRG3 OS=Mus musculus GN=Ndrg3 PE=1 SV=1 | Q9QYF9 | 0,0238 | 0,0215 | 0,0226 | 0,08 |
| Calpain-5 OS=Mus musculus GN=Capn5 PE=2 SV=1 | O08688 | 0,0170 | 0,0279 | 0,0225 | -0,78 |
| Ras-related protein Rab-1A OS=Mus musculus GN=Rab1A PE=1 SV=3 | P62821 | 0,0235 | 0,0215 | 0,0225 | 0,06 |
| Ras-related C3 botulinum toxin substrate 3 OS=Mus musculus GN=Rac3 PE=1 SV=1 | P60764 | 0,0225 | 0,0219 | 0,0222 | -0,02 |
| Protein THEM6 OS=Mus musculus GN=Them6 PE=2 SV=1 | Q80ZW2 | 0,0221 | 0,0221 | 0,0221 | -0,07 |
| Receptor-type tyrosine-protein phosphatase N2 OS=Mus musculus GN=Ptprn2 PE=1 SV=2 | P80560 | 0,0286 | 0,0159 | 0,0221 | 0,78 |
| L-lactate dehydrogenase B chain OS=Mus musculus GN=Ldhb PE=1 SV=2 | P16125 | 0,0329 | 0,0113 | 0,0218 | 1,47 |
| F-actin-capping protein subunit alpha-2 OS=Mus musculus GN=Capza2 PE=1 SV=3 | P47754 | 0,0196 | 0,0239 | 0,0218 | -0,36 |
| cGMP-dependent 3',5'-cyclic phosphodiesterase OS=Mus musculus GN=Pde2a PE=1 SV=3 | Q922S4 | 0,0145 | 0,0287 | 0,0218 | -1,05 |
| Serine/threonine-protein phosphatase 2A catalytic subunit alpha isoform OS=Mus musculus GN=Ppp2ca PE=1 SV=1 | P63330 | 0,0267 | 0,0171 | 0,0218 | 0,58 |
| Thioredoxin-related transmembrane protein 2 OS=Mus musculus GN=Tmx2 PE=2 SV=1 | Q9D710 | 0,0227 | 0,0208 | 0,0217 | 0,06 |
| Elongation factor 1-gamma OS=Mus musculus GN=Eef1g PE=1 SV=3 | Q9D8N0 | 0,0256 | 0,0179 | 0,0217 | 0,45 |
| Catenin alpha-2 OS=Mus musculus GN=Ctnna2 PE=1 SV=3 | Q61301 | 0,0239 | 0,0195 | 0,0216 | 0,22 |
| Alpha/beta hydrolase domain-containing protein 17B OS=Mus musculus GN=Abhd17b PE=2 SV=1 | Q7M759 | 0,0243 | 0,0189 | 0,0215 | 0,29 |
| Succinate dehydrogenase [ubiquinone] flavoprotein subunit, mitochondrial OS=Mus musculus GN=Sdha PE=1 SV=1 | Q8K2B3 | 0,0226 | 0,0204 | 0,0215 | 0,09 |
| Keratin, type I cuticular Ha1 OS=Mus musculus GN=Krt31 PE=2 SV=2 | Q61765 | 0,0120 | 0,0305 | 0,0214 | -1,42 |
| Neural cell adhesion molecule 1 OS=Mus musculus GN=Ncam1 PE=1 SV=3 | P13595 | 0,0263 | 0,0167 | 0,0214 | 0,59 |
| Septin-5 OS=Mus musculus GN=Sept5 PE=1 SV=2 | Q9Z2Q6 | 0,0162 | 0,0264 | 0,0214 | -0,77 |
| Metabotropic glutamate receptor 2 OS=Mus musculus GN=Grm2 PE=1 SV=2 | Q14BI2 | 0,0087 | 0,0334 | 0,0213 | -2,01 |
| Tubulin polymerization-promoting protein OS=Mus musculus GN=Tppp PE=1 SV=1 | Q7TQD2 | 0,0222 | 0,0205 | 0,0213 | 0,05 |
| NADH dehydrogenase [ubiquinone] 1 alpha subcomplex subunit 9, mitochondrial OS=Mus musculus GN=Ndufa9 PE=1 SV=2 | Q9DC69 | 0,0204 | 0,0221 | 0,0213 | -0,18 |
| Tyrosine-protein phosphatase non-receptor type substrate 1 OS=Mus musculus GN=Sirpa PE=1 SV=1 | P97797 | 0,0227 | 0,0197 | 0,0212 | 0,14 |
| Dynein light chain 1, cytoplasmic OS=Mus musculus GN=Dynll1 PE=1 SV=1 | P63168 | 0,0220 | 0,0201 | 0,0211 | 0,07 |
| T-cell immunomodulatory protein OS=Mus musculus GN=Itfg1 PE=2 SV=2 | Q99KW9 | 0,0222 | 0,0198 | 0,0209 | 0,10 |
| Neuroligin-2 OS=Mus musculus GN=Nlgn2 PE=1 SV=2 | Q69ZK9 | 0,0243 | 0,0177 | 0,0209 | 0,38 |
| Kinesin-like protein KIF3B OS=Mus musculus GN=Kif3b PE=1 SV=1 | Q61771 | 0,0234 | 0,0184 | 0,0209 | 0,28 |
| Pyruvate dehydrogenase E1 component subunit beta, mitochondrial OS=Mus musculus GN=Pdhb PE=1 SV=1 | Q9D051 | 0,0187 | 0,0228 | 0,0208 | -0,35 |
| Proline-rich transmembrane protein 1 OS=Mus musculus GN=Prrt1 PE=1 SV=1 | O35449 | 0,0179 | 0,0232 | 0,0206 | -0,44 |
| Protein KIAA1045 OS=Mus musculus GN=Kiaa1045 PE=2 SV=2 | Q80TL4 | 0,0192 | 0,0220 | 0,0206 | -0,26 |
| Guanine nucleotide-binding protein G(olf) subunit alpha OS=Mus musculus GN=Gnal PE=1 SV=1 | Q8CGK7 | 0,0321 | 0,0095 | 0,0205 | 1,68 |
| Cell death-inducing p53-target protein 1 OS=Mus musculus GN=Cdip1 PE=2 SV=1 | Q9DB75 | 0,0210 | 0,0200 | 0,0205 | 0,00 |
| Serine/threonine-protein phosphatase 2B catalytic subunit gamma isoform OS=Mus musculus GN=Ppp3cc PE=2 SV=1 | P48455 | 0,0177 | 0,0229 | 0,0204 | -0,44 |
| Keratin, type II cytoskeletal 72 OS=Mus musculus GN=Krt72 PE=3 SV=1 | Q6IME9 | 0,0180 | 0,0226 | 0,0204 | -0,39 |
| Keratin, type I cuticular Ha3-I OS=Mus musculus GN=Krt33a PE=2 SV=1 | Q8K0Y2 | 0,0086 | 0,0315 | 0,0203 | -1,94 |
| Disks large homolog 4 OS=Mus musculus GN=Dlg4 PE=1 SV=1 | Q62108 | 0,0207 | 0,0197 | 0,0202 | 0,01 |
| T-complex protein 1 subunit eta OS=Mus musculus GN=Cct7 PE=1 SV=1 | P80313 | 0,0210 | 0,0194 | 0,0201 | 0,05 |
| L-lactate dehydrogenase A chain OS=Mus musculus GN=Ldha PE=1 SV=3 | P06151 | 0,0261 | 0,0143 | 0,0200 | 0,80 |
| Gamma-soluble NSF attachment protein OS=Mus musculus GN=Napg PE=1 SV=1 | Q9CWZ7 | 0,0209 | 0,0186 | 0,0197 | 0,10 |
| Uncharacterized protein C2orf47 homolog, mitochondrial OS=Mus musculus PE=2 SV=1 | Q8BHE8 | 0,0144 | 0,0247 | 0,0197 | -0,84 |
| CD81 antigen OS=Mus musculus GN=Cd81 PE=1 SV=2 | P35762 | 0,0273 | 0,0120 | 0,0195 | 1,12 |
| Long-chain fatty acid transport protein 4 OS=Mus musculus GN=Slc27a4 PE=1 SV=1 | Q91VE0 | 0,0138 | 0,0249 | 0,0195 | -0,92 |
| Syntaxin-16 OS=Mus musculus GN=Stx16 PE=1 SV=3 | Q8BVI5 | 0,0209 | 0,0179 | 0,0194 | 0,16 |
| Uncharacterized membrane protein C1orf95 homolog OS=Mus musculus PE=2 SV=1 | Q0VBF8 | 0,0105 | 0,0278 | 0,0193 | -1,48 |
| Neuropeptide Y receptor type 2 OS=Mus musculus GN=Npy2r PE=2 SV=2 | P97295 | 0,0122 | 0,0259 | 0,0192 | -1,15 |
| PEX5-related protein OS=Mus musculus GN=Pex5l PE=1 SV=2 | Q8C437 | 0,0247 | 0,0139 | 0,0192 | 0,76 |
| Calcium-binding mitochondrial carrier protein SCaMC-3 OS=Mus musculus GN=Slc25a23 PE=2 SV=1 | Q6GQS1 | 0,0135 | 0,0241 | 0,0190 | -0,90 |
| Potassium channel subfamily K member 1 OS=Mus musculus GN=Kcnk1 PE=2 SV=2 | O08581 | 0,0266 | 0,0116 | 0,0189 | 1,14 |
| Guanine nucleotide-binding protein subunit alpha-11 OS=Mus musculus GN=Gna11 PE=1 SV=1 | P21278 | 0,0173 | 0,0204 | 0,0189 | -0,30 |
| Histone H3.2 OS=Mus musculus GN=Hist1h3b PE=1 SV=2 | P84228 | 0,0264 | 0,0116 | 0,0188 | 1,12 |
| Dehydrogenase/reductase SDR family member 1 OS=Mus musculus GN=Dhrs1 PE=2 SV=1 | Q99L04 | 0,0287 | 0,0092 | 0,0188 | 1,57 |
| Guanine nucleotide-binding protein G(s) subunit alpha isoforms XLas OS=Mus musculus GN=Gnas PE=2 SV=1 | Q6R0H7 | 0,0185 | 0,0189 | 0,0187 | -0,10 |
| Ras-related protein Rab-33A OS=Mus musculus GN=Rab33a PE=2 SV=1 | P97950 | 0,0168 | 0,0204 | 0,0186 | -0,34 |
| XK-related protein 4 OS=Mus musculus GN=Xkr4 PE=1 SV=1 | Q5GH67 | 0,0204 | 0,0169 | 0,0186 | 0,21 |
| Calcium-activated potassium channel subunit alpha-1 OS=Mus musculus GN=Kcnma1 PE=1 SV=2 | Q08460 | 0,0118 | 0,0248 | 0,0185 | -1,13 |
| Protein kinase C epsilon type OS=Mus musculus GN=Prkce PE=1 SV=1 | P16054 | 0,0151 | 0,0216 | 0,0184 | -0,59 |
| Alpha/beta hydrolase domain-containing protein 17A OS=Mus musculus GN=Abhd17a PE=2 SV=1 | Q99JW1 | 0,0164 | 0,0202 | 0,0184 | -0,37 |
| Synaptotagmin-2 OS=Mus musculus GN=Syt2 PE=1 SV=1 | P46097 | 0,0316 | 0,0054 | 0,0182 | 2,47 |
| Fatty aldehyde dehydrogenase OS=Mus musculus GN=Aldh3a2 PE=2 SV=2 | P47740 | 0,0206 | 0,0159 | 0,0182 | 0,31 |
| Glycerol-3-phosphate dehydrogenase, mitochondrial OS=Mus musculus GN=Gpd2 PE=1 SV=2 | Q64521 | 0,0201 | 0,0163 | 0,0182 | 0,23 |
| Ras-related protein Rab-35 OS=Mus musculus GN=Rab35 PE=1 SV=1 | Q6PHN9 | 0,0176 | 0,0186 | 0,0181 | -0,15 |
| Endoplasmic reticulum resident protein 44 OS=Mus musculus GN=Erp44 PE=1 SV=1 | Q9D1Q6 | 0,0315 | 0,0053 | 0,0181 | 2,50 |
| Protein kinase C alpha type OS=Mus musculus GN=Prkca PE=1 SV=3 | P20444 | 0,0179 | 0,0183 | 0,0181 | -0,09 |

| | | | | | |
|---|---|---|---|---|---|
| Retinol dehydrogenase 14 OS=Mus musculus GN=Rdh14 PE=2 SV=1 | Q9ERI6 | 0,0174 | 0,0188 | 0,0181 | -0,18 |
| Guanine nucleotide-binding protein G(I)/G(S)/G(O) subunit gamma-2 OS=Mus musculus GN=Gng2 PE=2 SV=2 | P63213 | 0,0192 | 0,0170 | 0,0181 | 0,11 |
| Glutamate receptor 1 OS=Mus musculus GN=Gria1 PE=1 SV=1 | P23818 | 0,0130 | 0,0226 | 0,0179 | -0,87 |
| Copine-6 OS=Mus musculus GN=Cpne6 PE=2 SV=1 | Q9Z140 | 0,0170 | 0,0186 | 0,0179 | -0,20 |
| Ras-related protein Rab-9B OS=Mus musculus GN=Rab9b PE=2 SV=1 | Q8BHH2 | 0,0163 | 0,0193 | 0,0178 | -0,30 |
| 40S ribosomal protein S2 OS=Mus musculus GN=Rps2 PE=2 SV=3 | P25444 | 0,0228 | 0,0130 | 0,0178 | 0,74 |
| Potassium voltage-gated channel subfamily C member 3 OS=Mus musculus GN=Kcnc3 PE=1 SV=2 | Q63959 | 0,0243 | 0,0114 | 0,0177 | 1,03 |
| Receptor-type tyrosine-protein phosphatase alpha OS=Mus musculus GN=Ptpra PE=1 SV=3 | P18052 | 0,0187 | 0,0167 | 0,0177 | 0,10 |
| Syntaxin-12 OS=Mus musculus GN=Stx12 PE=1 SV=1 | Q9ER00 | 0,0218 | 0,0137 | 0,0177 | 0,60 |
| Secretory carrier-associated membrane protein 1 OS=Mus musculus GN=Scamp1 PE=1 SV=1 | Q8K021 | 0,0181 | 0,0171 | 0,0176 | 0,02 |
| Phosphatidylinositide phosphatase SAC1 OS=Mus musculus GN=Sacm1l PE=2 SV=1 | Q9EP69 | 0,0195 | 0,0157 | 0,0176 | 0,24 |
| NACHT and WD repeat domain-containing protein 1 OS=Mus musculus GN=Nwd1 PE=2 SV=2 | A6H603 | 0,0165 | 0,0186 | 0,0176 | -0,24 |
| Ubiquitin thioesterase OTUB1 OS=Mus musculus GN=Otub1 PE=1 SV=2 | Q7TQI3 | 0,0182 | 0,0170 | 0,0176 | 0,04 |
| NT-3 growth factor receptor OS=Mus musculus GN=Ntrk3 PE=1 SV=1 | Q6VNS1 | 0,0166 | 0,0185 | 0,0176 | -0,23 |
| Ras-related protein Rab-2A OS=Mus musculus GN=Rab2a PE=1 SV=1 | P53994 | 0,0185 | 0,0165 | 0,0175 | 0,10 |
| Hexokinase-1 OS=Mus musculus GN=Hk1 PE=1 SV=3 | P17710 | 0,0159 | 0,0189 | 0,0175 | -0,31 |
| Guanine nucleotide-binding protein subunit alpha-13 OS=Mus musculus GN=Gna13 PE=1 SV=1 | P27601 | 0,0201 | 0,0149 | 0,0175 | 0,37 |
| Ras-related protein Rab-31 OS=Mus musculus GN=Rab31 PE=1 SV=1 | Q921E2 | 0,0224 | 0,0126 | 0,0174 | 0,76 |
| Probable G-protein coupled receptor 158 OS=Mus musculus GN=Gpr158 PE=1 SV=2 | Q8C419 | 0,0166 | 0,0182 | 0,0174 | -0,20 |
| YjeF N-terminal domain-containing protein 3 OS=Mus musculus GN=Yjefn3 PE=2 SV=2 | F6W8I0 | 0,0181 | 0,0165 | 0,0172 | 0,07 |
| Probable phospholipid-transporting ATPase VA OS=Mus musculus GN=Atp10a PE=2 SV=4 | O54827 | 0,0155 | 0,0189 | 0,0172 | -0,36 |
| GTPase NRas OS=Mus musculus GN=Nras PE=2 SV=1 | P08556 | 0,0152 | 0,0191 | 0,0172 | -0,39 |
| Plexin-A1 OS=Mus musculus GN=Plxna1 PE=1 SV=1 | P70206 | 0,0117 | 0,0224 | 0,0172 | -1,00 |
| Ephrin type-B receptor 2 OS=Mus musculus GN=Ephb2 PE=1 SV=2 | P54763 | 0,0175 | 0,0167 | 0,0171 | -0,01 |
| Transforming protein RhoA OS=Mus musculus GN=Rhoa PE=1 SV=1 | Q9QUI0 | 0,0140 | 0,0199 | 0,0170 | -0,57 |
| Receptor-type tyrosine-protein phosphatase epsilon OS=Mus musculus GN=Ptpre PE=1 SV=3 | P49446 | 0,0229 | 0,0111 | 0,0168 | 0,98 |
| ADP-ribosylation factor 6 OS=Mus musculus GN=Arf6 PE=1 SV=2 | P62331 | 0,0217 | 0,0120 | 0,0168 | 0,79 |
| Cholesterol 24-hydroxylase OS=Mus musculus GN=Cyp46a1 PE=2 SV=1 | Q9WVK8 | 0,0173 | 0,0162 | 0,0167 | 0,03 |
| Fatty-acid amide hydrolase 1 OS=Mus musculus GN=Faah PE=2 SV=1 | O08914 | 0,0156 | 0,0178 | 0,0167 | -0,26 |
| Serine racemase OS=Mus musculus GN=Srr PE=1 SV=1 | Q9QZX7 | 0,0147 | 0,0186 | 0,0167 | -0,41 |
| Protein phosphatase 1H OS=Mus musculus GN=Ppm1h PE=1 SV=1 | Q3UYC0 | 0,0179 | 0,0154 | 0,0166 | 0,15 |
| Gamma-aminobutyric acid type B receptor subunit 1 OS=Mus musculus GN=Gabbr1 PE=1 SV=1 | Q9WV18 | 0,0199 | 0,0134 | 0,0165 | 0,50 |
| Isobutyryl-CoA dehydrogenase, mitochondrial OS=Mus musculus GN=Acad8 PE=1 SV=2 | Q9D7B6 | 0,0161 | 0,0168 | 0,0165 | -0,13 |
| Sodium channel subunit beta-1 OS=Mus musculus GN=Scn1b PE=2 SV=1 | P97952 | 0,0186 | 0,0144 | 0,0165 | 0,30 |
| Keratin, type I cuticular Ha6 OS=Mus musculus GN=Krt36 PE=1 SV=1 | B1AQ75 | 0,0174 | 0,0154 | 0,0164 | 0,11 |
| BMP/retinoic acid-inducible neural-specific protein 1 OS=Mus musculus GN=Brinp1 PE=2 SV=1 | Q920P3 | 0,0131 | 0,0195 | 0,0164 | -0,63 |
| Histone H3.1 OS=Mus musculus GN=Hist1h3a PE=1 SV=2 | P68433 | 0,0224 | 0,0106 | 0,0163 | 1,01 |
| Ras-related protein Rap-2a OS=Mus musculus GN=Rap2a PE=1 SV=2 | Q80ZJ1 | 0,0154 | 0,0172 | 0,0163 | -0,23 |
| Keratin, type II cytoskeletal 1b OS=Mus musculus GN=Krt77 PE=1 SV=1 | Q6IFZ6 | 0,0175 | 0,0151 | 0,0163 | 0,15 |
| Protein shisa-6 homolog OS=Mus musculus GN=Shisa6 PE=1 SV=1 | Q3UH99 | 0,0156 | 0,0169 | 0,0163 | -0,18 |
| Cytochrome b-c1 complex subunit Rieske, mitochondrial OS=Mus musculus GN=Uqcrfs1 PE=1 SV=1 | Q9CR68 | 0,0164 | 0,0161 | 0,0163 | -0,03 |
| GTP-binding protein Di-Ras1 OS=Mus musculus GN=Diras1 PE=2 SV=1 | Q91Z61 | 0,0187 | 0,0136 | 0,0161 | 0,39 |
| Succinate dehydrogenase [ubiquinone] iron-sulfur subunit, mitochondrial OS=Mus musculus GN=Sdhb PE=1 SV=1 | Q9CQA3 | 0,0171 | 0,0150 | 0,0160 | 0,13 |
| Netrin receptor UNC5C OS=Mus musculus GN=Unc5c PE=1 SV=1 | O08747 | 0,0162 | 0,0155 | 0,0159 | -0,01 |
| Membrane protein MLC1 OS=Mus musculus GN=Mlc1 PE=2 SV=1 | Q8VHK5 | 0,0186 | 0,0132 | 0,0158 | 0,42 |
| Clusterin OS=Mus musculus GN=Clu PE=1 SV=1 | Q06890 | 0,0219 | 0,0100 | 0,0158 | 1,06 |
| Serine/threonine-protein kinase DCLK2 OS=Mus musculus GN=Dclk2 PE=1 SV=1 | Q6PGN3 | 0,0166 | 0,0150 | 0,0158 | 0,09 |
| 40S ribosomal protein S14 OS=Mus musculus GN=Rps14 PE=2 SV=3 | P62264 | 0,0175 | 0,0141 | 0,0158 | 0,24 |
| Leucine-rich repeat and immunoglobulin-like domain-containing nogo receptor-interacting protein 1 OS=Mus musculus GN=Lingo1 PE=1 SV=1 | Q9D1T0 | 0,0113 | 0,0200 | 0,0158 | -0,89 |
| Gamma-aminobutyric acid receptor subunit beta-3 OS=Mus musculus GN=Gabrb3 PE=2 SV=1 | P63080 | 0,0134 | 0,0180 | 0,0157 | -0,49 |
| Mitochondrial 2-oxoglutarate/malate carrier protein OS=Mus musculus GN=Slc25a11 PE=1 SV=3 | Q9CR62 | 0,0157 | 0,0157 | 0,0157 | -0,07 |
| Isocitrate dehydrogenase [NAD] subunit gamma 1, mitochondrial OS=Mus musculus GN=Idh3g PE=1 SV=1 | P70404 | 0,0149 | 0,0164 | 0,0157 | -0,20 |
| Sarcoplasmic/endoplasmic reticulum calcium ATPase 1 OS=Mus musculus GN=Atp2a1 PE=2 SV=1 | Q8R429 | 0,0185 | 0,0129 | 0,0156 | 0,45 |
| 3-ketoacyl-CoA thiolase, mitochondrial OS=Mus musculus GN=Acaa2 PE=1 SV=3 | Q8BWT1 | 0,0157 | 0,0156 | 0,0156 | -0,05 |
| cAMP-dependent protein kinase catalytic subunit beta OS=Mus musculus GN=Prkacb PE=1 SV=2 | P68181 | 0,0163 | 0,0150 | 0,0156 | 0,06 |
| NADH-ubiquinone oxidoreductase 75 kDa subunit, mitochondrial OS=Mus musculus GN=Ndufs1 PE=1 SV=2 | Q91VD9 | 0,0208 | 0,0105 | 0,0156 | 0,91 |
| Aconitate hydratase, mitochondrial OS=Mus musculus GN=Aco2 PE=1 SV=1 | Q99KI0 | 0,0166 | 0,0144 | 0,0155 | 0,14 |
| Very-long-chain enoyl-CoA reductase OS=Mus musculus GN=Tecr PE=2 SV=1 | Q9CY27 | 0,0158 | 0,0151 | 0,0154 | 0,00 |
| Serine/threonine-protein phosphatase PP1-beta catalytic subunit OS=Mus musculus GN=Ppp1cb PE=1 SV=3 | P62141 | 0,0174 | 0,0136 | 0,0154 | 0,29 |
| GTP-binding protein Rheb OS=Mus musculus GN=Rheb PE=1 SV=1 | Q921J2 | 0,0181 | 0,0128 | 0,0154 | 0,44 |
| ADP-ribosylation factor-like protein 8A OS=Mus musculus GN=Arl8a PE=2 SV=1 | Q8VEH3 | 0,0172 | 0,0135 | 0,0153 | 0,29 |
| Protocadherin-8 OS=Mus musculus GN=Pcdh8 PE=2 SV=1 | Q7TSK3 | 0,0205 | 0,0102 | 0,0152 | 0,95 |
| Cell adhesion molecule 1 OS=Mus musculus GN=Cadm1 PE=1 SV=2 | Q8R5M8 | 0,0199 | 0,0108 | 0,0152 | 0,82 |
| ATP-binding cassette sub-family A member 7 OS=Mus musculus GN=Abca7 PE=1 SV=1 | Q91V24 | 0,0088 | 0,0211 | 0,0151 | -1,33 |
| IQ motif and SEC7 domain-containing protein 1 OS=Mus musculus GN=Iqsec1 PE=1 SV=2 | Q8R0S2 | 0,0176 | 0,0127 | 0,0151 | 0,40 |
| Protein FAM171A2 OS=Mus musculus GN=Fam171a2 PE=1 SV=1 | A2A699 | 0,0179 | 0,0121 | 0,0149 | 0,50 |
| Serine/threonine-protein kinase DCLK1 OS=Mus musculus GN=Dclk1 PE=1 SV=1 | Q9JLM8 | 0,0155 | 0,0141 | 0,0148 | 0,07 |
| Epimerase family protein SDR39U1 OS=Mus musculus GN=Sdr39u1 PE=2 SV=1 | Q5M8N4 | 0,0116 | 0,0178 | 0,0148 | -0,69 |
| E3 ubiquitin-protein ligase MGRN1 OS=Mus musculus GN=Mgrn1 PE=1 SV=2 | Q9D074 | 0,0188 | 0,0109 | 0,0148 | 0,72 |
| Tumor protein p63-regulated gene 1-like protein OS=Mus musculus GN=Tprg1l PE=1 SV=1 | Q9DBS2 | 0,0150 | 0,0144 | 0,0147 | -0,01 |
| Saccharopine dehydrogenase-like oxidoreductase OS=Mus musculus GN=Sccpdh PE=2 SV=1 | Q8R127 | 0,0170 | 0,0123 | 0,0146 | 0,40 |
| Attractin OS=Mus musculus GN=Atrn PE=2 SV=3 | Q9WU60 | 0,0169 | 0,0122 | 0,0145 | 0,41 |
| Carnitine O-palmitoyltransferase 1, liver isoform OS=Mus musculus GN=Cpt1a PE=1 SV=4 | P97742 | 0,0174 | 0,0117 | 0,0145 | 0,51 |
| Ras-related protein Rab-24 OS=Mus musculus GN=Rab24 PE=1 SV=2 | P35290 | 0,0105 | 0,0181 | 0,0144 | -0,86 |
| Protein phosphatase 1E OS=Mus musculus GN=Ppm1e PE=1 SV=2 | Q80TL0 | 0,0170 | 0,0119 | 0,0144 | 0,44 |

| | | | | | |
|---|---|---|---|---|---|
| Potassium voltage-gated channel subfamily A member 3 OS=Mus musculus GN=Kcna3 PE=2 SV=3 | P16390 | 0,0269 | 0,0024 | 0,0144 | 3,41 |
| Heat shock protein 105 kDa OS=Mus musculus GN=Hsph1 PE=1 SV=2 | Q61699 | 0,0156 | 0,0131 | 0,0143 | 0,18 |
| GTPase HRas OS=Mus musculus GN=Hras1 PE=1 SV=2 | Q61411 | 0,0140 | 0,0145 | 0,0143 | -0,12 |
| Ras-related protein Rap-1b OS=Mus musculus GN=Rap1b PE=2 SV=2 | Q99JI6 | 0,0168 | 0,0119 | 0,0143 | 0,44 |
| V-type proton ATPase subunit B, brain isoform OS=Mus musculus GN=Atp6v1b2 PE=1 SV=1 | P62814 | 0,0155 | 0,0131 | 0,0143 | 0,18 |
| Gamma-aminobutyric acid receptor subunit beta-1 OS=Mus musculus GN=Gabrb1 PE=1 SV=1 | P50571 | 0,0135 | 0,0149 | 0,0142 | -0,21 |
| Complexin-2 OS=Mus musculus GN=Cplx2 PE=1 SV=1 | P84086 | 0,0146 | 0,0137 | 0,0142 | 0,03 |
| Ganglioside-induced differentiation-associated protein 1-like 1 OS=Mus musculus GN=Gdap1l1 PE=2 SV=1 | Q8VE33 | 0,0143 | 0,0139 | 0,0141 | -0,02 |
| Armadillo repeat-containing protein 10 OS=Mus musculus GN=Armc10 PE=1 SV=1 | Q9D0L7 | 0,0144 | 0,0138 | 0,0141 | -0,01 |
| Gamma-aminobutyric acid receptor subunit gamma-2 OS=Mus musculus GN=Gabrg2 PE=1 SV=3 | P22723 | 0,0143 | 0,0138 | 0,0141 | -0,02 |
| Mitochondrial Rho GTPase 1 OS=Mus musculus GN=Rhot1 PE=2 SV=1 | Q8BG51 | 0,0147 | 0,0134 | 0,0140 | 0,07 |
| 40S ribosomal protein S3 OS=Mus musculus GN=Rps3 PE=1 SV=1 | P62908 | 0,0162 | 0,0117 | 0,0139 | 0,40 |
| Inactive hydroxysteroid dehydrogenase-like protein 1 OS=Mus musculus GN=Hsdl1 PE=2 SV=1 | Q8BTX9 | 0,0144 | 0,0134 | 0,0139 | 0,03 |
| ATP-binding cassette sub-family B member 7, mitochondrial OS=Mus musculus GN=Abcb7 PE=1 SV=3 | Q61102 | 0,0137 | 0,0140 | 0,0138 | -0,09 |
| BRI3-binding protein OS=Mus musculus GN=Bri3bp PE=2 SV=1 | Q8BXV2 | 0,0159 | 0,0117 | 0,0138 | 0,38 |
| 1-acyl-sn-glycerol-3-phosphate acyltransferase alpha OS=Mus musculus GN=Agpat1 PE=2 SV=1 | O35083 | 0,0135 | 0,0139 | 0,0137 | -0,12 |
| Leucine-rich repeat and fibronectin type III domain-containing protein 1 OS=Mus musculus GN=Lrfn1 PE=1 SV=1 | Q2WF71 | 0,0153 | 0,0120 | 0,0136 | 0,28 |
| Stress-70 protein, mitochondrial OS=Mus musculus GN=Hspa9 PE=1 SV=3 | P38647 | 0,0160 | 0,0112 | 0,0136 | 0,45 |
| Ephrin type-B receptor 1 OS=Mus musculus GN=Ephb1 PE=1 SV=1 | Q8CBF3 | 0,0127 | 0,0144 | 0,0136 | -0,24 |
| Phospholipase D3 OS=Mus musculus GN=Pld3 PE=2 SV=1 | O35405 | 0,0159 | 0,0113 | 0,0136 | 0,43 |
| Hippocalcin-like protein 1 OS=Mus musculus GN=Hpcal1 PE=2 SV=2 | P62748 | 0,0101 | 0,0167 | 0,0135 | -0,80 |
| Plexin-C1 OS=Mus musculus GN=Plxnc1 PE=1 SV=1 | Q9QZC2 | 0,0144 | 0,0125 | 0,0134 | 0,15 |
| Complement C1q-like protein 3 OS=Mus musculus GN=C1ql3 PE=1 SV=1 | Q9ESN4 | 0,0088 | 0,0178 | 0,0134 | -1,09 |
| Cytochrome c oxidase subunit 4 isoform 1, mitochondrial OS=Mus musculus GN=Cox4i1 PE=1 SV=2 | P19783 | 0,0136 | 0,0130 | 0,0133 | -0,01 |
| ADP-ribosylation factor-like protein 1 OS=Mus musculus GN=Arl1 PE=2 SV=1 | P61211 | 0,0177 | 0,0091 | 0,0133 | 0,90 |
| Mitochondrial pyruvate carrier 2 OS=Mus musculus GN=Mpc2 PE=1 SV=1 | Q9D023 | 0,0128 | 0,0138 | 0,0133 | -0,17 |
| Trimeric intracellular cation channel type A OS=Mus musculus GN=Tmem38a PE=1 SV=2 | Q3TMP8 | 0,0138 | 0,0128 | 0,0133 | 0,04 |
| Synaptojanin-1 OS=Mus musculus GN=Synj1 PE=1 SV=3 | Q8CHC4 | 0,0145 | 0,0120 | 0,0132 | 0,21 |
| Active breakpoint cluster region-related protein OS=Mus musculus GN=Abr PE=1 SV=1 | Q5SSL4 | 0,0135 | 0,0129 | 0,0132 | -0,01 |
| Phosphatidylinositol 5-phosphate 4-kinase type-2 beta OS=Mus musculus GN=Pip4k2b PE=1 SV=1 | Q80XI4 | 0,0149 | 0,0115 | 0,0132 | 0,30 |
| Neurofascin OS=Mus musculus GN=Nfasc PE=1 SV=1 | Q810U3 | 0,0149 | 0,0115 | 0,0132 | 0,31 |
| MAGUK p55 subfamily member 2 OS=Mus musculus GN=Mpp2 PE=1 SV=1 | Q9WV34 | 0,0132 | 0,0131 | 0,0132 | -0,06 |
| Peroxiredoxin-1 OS=Mus musculus GN=Prdx1 PE=1 SV=1 | P35700 | 0,0165 | 0,0096 | 0,0130 | 0,72 |
| Tetraspanin-7 OS=Mus musculus GN=Tspan7 PE=2 SV=2 | Q62283 | 0,0144 | 0,0115 | 0,0130 | 0,26 |
| ATP-sensitive inward rectifier potassium channel 10 OS=Mus musculus GN=Kcnj10 PE=1 SV=1 | Q9JM63 | 0,0169 | 0,0090 | 0,0129 | 0,84 |
| Immunity-related GTPase family M protein 1 OS=Mus musculus GN=Irgm1 PE=1 SV=1 | Q60766 | 0,0219 | 0,0042 | 0,0129 | 2,31 |
| Cell adhesion molecule 3 OS=Mus musculus GN=Cadm3 PE=1 SV=1 | Q99N28 | 0,0163 | 0,0095 | 0,0128 | 0,72 |
| Destrin OS=Mus musculus GN=Dstn PE=1 SV=3 | Q9R0P5 | 0,0134 | 0,0122 | 0,0128 | 0,07 |
| Mitochondrial glutamate carrier 2 OS=Mus musculus GN=Slc25a18 PE=2 SV=4 | Q9DB41 | 0,0129 | 0,0125 | 0,0127 | -0,02 |
| C2 domain-containing protein 2-like OS=Mus musculus GN=C2cd2l PE=1 SV=3 | Q80X80 | 0,0117 | 0,0134 | 0,0126 | -0,27 |
| Zinc transporter 1 OS=Mus musculus GN=Slc30a1 PE=1 SV=1 | Q60738 | 0,0107 | 0,0144 | 0,0126 | -0,50 |
| Mitochondrial coenzyme A transporter SLC25A42 OS=Mus musculus GN=Slc25a42 PE=2 SV=1 | Q8R0Y8 | 0,0123 | 0,0128 | 0,0126 | -0,13 |
| Cytoplasmic FMR1-interacting protein 2 OS=Mus musculus GN=Cyfip2 PE=1 SV=2 | Q5SQX6 | 0,0115 | 0,0136 | 0,0126 | -0,31 |
| Guanine nucleotide-binding protein G(I)/G(S)/G(T) subunit beta-3 OS=Mus musculus GN=Gnb3 PE=1 SV=2 | Q61011 | 0,0104 | 0,0145 | 0,0125 | -0,54 |
| Leukocyte surface antigen CD47 OS=Mus musculus GN=Cd47 PE=1 SV=2 | Q61735 | 0,0161 | 0,0090 | 0,0125 | 0,77 |
| BMP/retinoic acid-inducible neural-specific protein 2 OS=Mus musculus GN=Brinp2 PE=2 SV=1 | Q6DFY8 | 0,0127 | 0,0120 | 0,0124 | 0,01 |
| Beta-centractin OS=Mus musculus GN=Actr1b PE=1 SV=1 | Q8R5C5 | 0,0110 | 0,0137 | 0,0124 | -0,39 |
| Neuromodulin OS=Mus musculus GN=Gap43 PE=1 SV=1 | P06837 | 0,0125 | 0,0122 | 0,0123 | -0,04 |
| Ephrin type-A receptor 6 OS=Mus musculus GN=Epha6 PE=2 SV=2 | Q62413 | 0,0131 | 0,0115 | 0,0123 | 0,11 |
| Regulator of G-protein signaling 7 OS=Mus musculus GN=Rgs7 PE=1 SV=2 | O54829 | 0,0109 | 0,0136 | 0,0123 | -0,39 |
| Contactin-associated protein-like 2 OS=Mus musculus GN=Cntnap2 PE=1 SV=2 | Q9CPW0 | 0,0155 | 0,0091 | 0,0122 | 0,70 |
| PRA1 family protein 2 OS=Mus musculus GN=Praf2 PE=2 SV=1 | Q9JIG8 | 0,0144 | 0,0101 | 0,0122 | 0,44 |
| Myosin-14 OS=Mus musculus GN=Myh14 PE=1 SV=1 | Q6URW6 | 0,0173 | 0,0072 | 0,0122 | 1,19 |
| Microtubule-associated protein tau OS=Mus musculus GN=Mapt PE=1 SV=3 | P10637 | 0,0083 | 0,0158 | 0,0121 | -1,00 |
| Ephrin-B2 OS=Mus musculus GN=Efnb2 PE=1 SV=1 | P52800 | 0,0145 | 0,0097 | 0,0121 | 0,51 |
| AP-2 complex subunit beta OS=Mus musculus GN=Ap2b1 PE=1 SV=1 | Q9DBG3 | 0,0122 | 0,0119 | 0,0120 | -0,03 |
| Ras-related protein Rab-8A OS=Mus musculus GN=Rab8a PE=1 SV=2 | P55258 | 0,0132 | 0,0109 | 0,0120 | 0,21 |
| Methylcrotonoyl-CoA carboxylase subunit alpha, mitochondrial OS=Mus musculus GN=Mccc1 PE=1 SV=2 | Q99MR8 | 0,0151 | 0,0090 | 0,0120 | 0,67 |
| WD repeat-containing protein 7 OS=Mus musculus GN=Wdr7 PE=1 SV=3 | Q920I9 | 0,0110 | 0,0129 | 0,0120 | -0,29 |
| AP-2 complex subunit mu OS=Mus musculus GN=Ap2m1 PE=1 SV=1 | P84091 | 0,0111 | 0,0125 | 0,0119 | -0,24 |
| Dehydrogenase/reductase SDR family member 7 OS=Mus musculus GN=Dhrs7 PE=2 SV=2 | Q9CXR1 | 0,0116 | 0,0120 | 0,0118 | -0,11 |
| Uncharacterized aarF domain-containing protein kinase 1 OS=Mus musculus GN=Adck1 PE=2 SV=1 | Q9D0L4 | 0,0130 | 0,0105 | 0,0117 | 0,24 |
| Gamma-aminobutyric acid receptor subunit beta-2 OS=Mus musculus GN=Gabrb2 PE=1 SV=2 | P63137 | 0,0110 | 0,0124 | 0,0117 | -0,24 |
| Transmembrane protein 106B OS=Mus musculus GN=Tmem106b PE=1 SV=1 | Q80X71 | 0,0141 | 0,0093 | 0,0117 | 0,53 |
| Vesicle-associated membrane protein-associated protein B OS=Mus musculus GN=Vapb PE=2 SV=3 | Q9QY76 | 0,0128 | 0,0106 | 0,0116 | 0,20 |
| Gamma-aminobutyric acid receptor subunit alpha-2 OS=Mus musculus GN=Gabra2 PE=1 SV=1 | P26048 | 0,0113 | 0,0119 | 0,0116 | -0,14 |
| Propionyl-CoA carboxylase alpha chain, mitochondrial OS=Mus musculus GN=Pcca PE=1 SV=2 | Q91ZA3 | 0,0150 | 0,0083 | 0,0116 | 0,79 |
| Ephrin type-A receptor 5 OS=Mus musculus GN=Epha5 PE=1 SV=2 | Q60629 | 0,0089 | 0,0141 | 0,0116 | -0,73 |
| Syntaxin-binding protein 5 OS=Mus musculus GN=Stxbp5 PE=1 SV=3 | Q8K400 | 0,0106 | 0,0125 | 0,0115 | -0,31 |
| NAD-dependent protein deacetylase sirtuin-2 OS=Mus musculus GN=Sirt2 PE=1 SV=2 | Q8VDQ8 | 0,0133 | 0,0099 | 0,0115 | 0,36 |
| Aspartyl/asparaginyl beta-hydroxylase OS=Mus musculus GN=Asph PE=2 SV=1 | Q8BSY0 | 0,0170 | 0,0063 | 0,0115 | 1,36 |
| Vesicle-associated membrane protein-associated protein A OS=Mus musculus GN=Vapa PE=1 SV=2 | Q9WV55 | 0,0115 | 0,0114 | 0,0114 | -0,06 |
| Guanine nucleotide-binding protein G(I)/G(S)/G(O) subunit gamma-4 OS=Mus musculus GN=Gng4 PE=2 SV=1 | P50153 | 0,0113 | 0,0115 | 0,0114 | -0,10 |
| Netrin receptor UNC5A OS=Mus musculus GN=Unc5a PE=2 SV=1 | Q8K1S4 | 0,0074 | 0,0151 | 0,0113 | -1,10 |
| Apoptosis-inducing factor 1, mitochondrial OS=Mus musculus GN=Aifm1 PE=1 SV=1 | Q9Z0X1 | 0,0118 | 0,0109 | 0,0113 | 0,05 |
| Sphingomyelin phosphodiesterase 3 OS=Mus musculus GN=Smpd3 PE=1 SV=1 | Q9JJY3 | 0,0090 | 0,0135 | 0,0113 | -0,65 |

| | | | | | |
|---|---|---|---|---|---|
| AP-2 complex subunit alpha-1 OS=Mus musculus GN=Ap2a1 PE=1 SV=1 | P17426 | 0,0117 | 0,0109 | 0,0113 | 0,04 |
| Mitochondrial translocator assembly and maintenance protein 41 homolog OS=Mus musculus GN=Tamm41 PE=2 SV=2 | Q3TUH1 | 0,0112 | 0,0113 | 0,0112 | -0,08 |
| Protein arginine N-methyltransferase 8 OS=Mus musculus GN=Prmt8 PE=2 SV=2 | Q6PAK3 | 0,0109 | 0,0115 | 0,0112 | -0,14 |
| Type 1 phosphatidylinositol 4,5-bisphosphate 4-phosphatase OS=Mus musculus GN=Tmem55b PE=1 SV=1 | Q3TWL2 | 0,0134 | 0,0091 | 0,0112 | 0,49 |
| Plexin-A2 OS=Mus musculus GN=Plxna2 PE=1 SV=2 | P70207 | 0,0085 | 0,0137 | 0,0111 | -0,76 |
| Protein disulfide-isomerase TMX3 OS=Mus musculus GN=Tmx3 PE=1 SV=2 | Q8BXZ1 | 0,0121 | 0,0102 | 0,0111 | 0,18 |
| Vesicular glutamate transporter 3 OS=Mus musculus GN=Slc17a8 PE=2 SV=1 | Q8BFU8 | 0,0119 | 0,0103 | 0,0111 | 0,14 |
| 60S ribosomal protein L27a OS=Mus musculus GN=Rpl27a PE=2 SV=5 | P14115 | 0,0102 | 0,0118 | 0,0110 | -0,27 |
| Activin receptor type-1B OS=Mus musculus GN=Acvr1b PE=1 SV=1 | Q61271 | 0,0068 | 0,0151 | 0,0110 | -1,21 |
| Protein FAM210A OS=Mus musculus GN=Fam210a PE=2 SV=1 | Q8BGY7 | 0,0104 | 0,0116 | 0,0110 | -0,23 |
| Potassium voltage-gated channel subfamily KQT member 2 OS=Mus musculus GN=Kcnq2 PE=1 SV=1 | Q9Z351 | 0,0108 | 0,0112 | 0,0110 | -0,13 |
| Protocadherin gamma-A4 OS=Mus musculus GN=Pcdhga4 PE=2 SV=1 | Q91XY4 | 0,0113 | 0,0107 | 0,0110 | 0,02 |
| Thioredoxin-related transmembrane protein 4 OS=Mus musculus GN=Tmx4 PE=2 SV=2 | Q8C0L0 | 0,0122 | 0,0098 | 0,0109 | 0,25 |
| DnaJ homolog subfamily A member 1 OS=Mus musculus GN=Dnaja1 PE=1 SV=1 | P63037 | 0,0114 | 0,0104 | 0,0109 | 0,07 |
| cAMP-dependent protein kinase catalytic subunit alpha OS=Mus musculus GN=Prkaca PE=1 SV=3 | P05132 | 0,0161 | 0,0060 | 0,0109 | 1,36 |
| Elongation factor 1-alpha 2 OS=Mus musculus GN=Eef1a2 PE=1 SV=1 | P62631 | 0,0109 | 0,0108 | 0,0108 | -0,04 |
| 60S ribosomal protein L9 OS=Mus musculus GN=Rpl9 PE=2 SV=2 | P51410 | 0,0116 | 0,0100 | 0,0108 | 0,16 |
| Creatine kinase U-type, mitochondrial OS=Mus musculus GN=Ckmt1 PE=1 SV=1 | P30275 | 0,0137 | 0,0079 | 0,0107 | 0,72 |
| Neurexin-1 OS=Mus musculus GN=Nrxn1 PE=1 SV=3 | Q9CS84 | 0,0112 | 0,0102 | 0,0107 | 0,07 |
| Zinc transporter ZIP10 OS=Mus musculus GN=Slc39a10 PE=1 SV=1 | Q6P5F6 | 0,0099 | 0,0114 | 0,0107 | -0,27 |
| BDNF/NT-3 growth factors receptor OS=Mus musculus GN=Ntrk2 PE=1 SV=1 | P15209 | 0,0126 | 0,0088 | 0,0107 | 0,45 |
| Vesicle-trafficking protein SEC22b OS=Mus musculus GN=Sec22b PE=1 SV=3 | O08547 | 0,0121 | 0,0093 | 0,0107 | 0,31 |
| TOM1-like protein 2 OS=Mus musculus GN=Tom1l2 PE=2 SV=1 | Q5SRX1 | 0,0110 | 0,0103 | 0,0106 | 0,03 |
| Dynein light chain 2, cytoplasmic OS=Mus musculus GN=Dynll2 PE=1 SV=1 | Q9D0M5 | 0,0126 | 0,0087 | 0,0106 | 0,47 |
| Cadherin-2 OS=Mus musculus GN=Cdh2 PE=1 SV=2 | P15116 | 0,0128 | 0,0084 | 0,0105 | 0,54 |
| Ras-related C3 botulinum toxin substrate 2 OS=Mus musculus GN=Rac2 PE=2 SV=1 | Q05144 | 0,0143 | 0,0069 | 0,0105 | 0,98 |
| S-phase kinase-associated protein 1 OS=Mus musculus GN=Skp1 PE=1 SV=3 | Q9WTX5 | 0,0129 | 0,0082 | 0,0105 | 0,58 |
| Glycogen synthase kinase-3 beta OS=Mus musculus GN=Gsk3b PE=1 SV=2 | Q9WV60 | 0,0115 | 0,0095 | 0,0105 | 0,21 |
| Dual specificity mitogen-activated protein kinase kinase 1 OS=Mus musculus GN=Map2k1 PE=1 SV=2 | P31938 | 0,0100 | 0,0108 | 0,0104 | -0,19 |
| Puromycin-sensitive aminopeptidase OS=Mus musculus GN=Npepps PE=1 SV=2 | Q11011 | 0,0135 | 0,0074 | 0,0104 | 0,80 |
| Septin-2 OS=Mus musculus GN=Sept2 PE=1 SV=2 | P42208 | 0,0116 | 0,0093 | 0,0104 | 0,25 |
| Neuronal pentraxin receptor OS=Mus musculus GN=Nptxr PE=1 SV=1 | Q99J85 | 0,0097 | 0,0110 | 0,0104 | -0,24 |
| Ubiquitin carboxyl-terminal hydrolase 5 OS=Mus musculus GN=Usp5 PE=1 SV=1 | P56399 | 0,0108 | 0,0100 | 0,0104 | 0,04 |
| Ras-related protein Rab-27B OS=Mus musculus GN=Rab27b PE=1 SV=3 | Q99P58 | 0,0140 | 0,0069 | 0,0104 | 0,96 |
| Protein tweety homolog 3 OS=Mus musculus GN=Ttyh3 PE=1 SV=1 | Q6P5F7 | 0,0121 | 0,0087 | 0,0103 | 0,40 |
| Copine-4 OS=Mus musculus GN=Cpne4 PE=1 SV=1 | Q8BLR2 | 0,0076 | 0,0127 | 0,0102 | -0,81 |
| Ras-related protein Rab-33B OS=Mus musculus GN=Rab33b PE=1 SV=1 | O35963 | 0,0102 | 0,0102 | 0,0102 | -0,07 |
| ATPase family AAA domain-containing protein 3 OS=Mus musculus GN=Atad3 PE=1 SV=1 | Q925I1 | 0,0107 | 0,0096 | 0,0101 | 0,08 |
| Keratin, type I cytoskeletal 18 OS=Mus musculus GN=Krt18 PE=1 SV=5 | P05784 | 0,0151 | 0,0054 | 0,0101 | 1,43 |
| Disintegrin and metalloproteinase domain-containing protein 11 OS=Mus musculus GN=Adam11 PE=1 SV=2 | Q9R1V4 | 0,0101 | 0,0101 | 0,0101 | -0,07 |
| Mitofusin-2 OS=Mus musculus GN=Mfn2 PE=1 SV=3 | Q80U63 | 0,0094 | 0,0107 | 0,0100 | -0,26 |
| Proton myo-inositol cotransporter OS=Mus musculus GN=Slc2a13 PE=2 SV=2 | Q3UHK1 | 0,0124 | 0,0078 | 0,0100 | 0,60 |
| Importin subunit beta-1 OS=Mus musculus GN=Kpnb1 PE=1 SV=2 | P70168 | 0,0096 | 0,0104 | 0,0100 | -0,18 |
| Cell cycle control protein 50A OS=Mus musculus GN=Tmem30a PE=1 SV=1 | Q8VEK0 | 0,0107 | 0,0093 | 0,0100 | 0,13 |
| Diacylglycerol kinase epsilon OS=Mus musculus GN=Dgke PE=2 SV=1 | Q9R1C6 | 0,0094 | 0,0105 | 0,0100 | -0,23 |
| ADP-ribosylation factor-like protein 10 OS=Mus musculus GN=Arl10 PE=2 SV=2 | Q9QXJ4 | 0,0098 | 0,0101 | 0,0100 | -0,11 |
| Myristoylated alanine-rich C-kinase substrate OS=Mus musculus GN=Marcks PE=1 SV=2 | P26645 | 0,0116 | 0,0085 | 0,0100 | 0,38 |
| Palmitoyl-protein thioesterase 1 OS=Mus musculus GN=Ppt1 PE=2 SV=2 | O88531 | 0,0117 | 0,0083 | 0,0100 | 0,43 |
| Adenylate cyclase type 1 OS=Mus musculus GN=Adcy1 PE=2 SV=2 | O88444 | 0,0114 | 0,0084 | 0,0099 | 0,36 |
| Immunoglobulin superfamily containing leucine-rich repeat protein 2 OS=Mus musculus GN=Islr2 PE=1 SV=1 | Q5RKR3 | 0,0031 | 0,0163 | 0,0099 | -2,47 |
| Thioredoxin-dependent peroxide reductase, mitochondrial OS=Mus musculus GN=Prdx3 PE=1 SV=1 | P20108 | 0,0111 | 0,0085 | 0,0098 | 0,32 |
| Peroxiredoxin-4 OS=Mus musculus GN=Prdx4 PE=1 SV=1 | O08807 | 0,0118 | 0,0079 | 0,0098 | 0,51 |
| Catenin delta-2 OS=Mus musculus GN=Ctnnd2 PE=1 SV=1 | O35927 | 0,0112 | 0,0084 | 0,0098 | 0,34 |
| Emerin OS=Mus musculus GN=Emd PE=1 SV=1 | O08579 | 0,0102 | 0,0093 | 0,0098 | 0,07 |
| Glutamate dehydrogenase 1, mitochondrial OS=Mus musculus GN=Glud1 PE=1 SV=1 | P26443 | 0,0108 | 0,0088 | 0,0098 | 0,23 |
| 14-3-3 protein sigma OS=Mus musculus GN=Sfn PE=1 SV=2 | O70456 | 0,0152 | 0,0045 | 0,0098 | 1,69 |
| Protein Dos OS=Mus musculus GN=Dos PE=1 SV=3 | Q66L44 | 0,0097 | 0,0098 | 0,0097 | -0,09 |
| Interleukin-1 receptor accessory protein OS=Mus musculus GN=Il1rap PE=1 SV=1 | Q61730 | 0,0096 | 0,0098 | 0,0097 | -0,09 |
| Keratin, type II cytoskeletal 2 oral OS=Mus musculus GN=Krt76 PE=2 SV=1 | Q3UV17 | 0,0103 | 0,0092 | 0,0097 | 0,10 |
| LanC-like protein 1 OS=Mus musculus GN=Lancl1 PE=1 SV=1 | O89112 | 0,0093 | 0,0100 | 0,0097 | -0,16 |
| Profilin-2 OS=Mus musculus GN=Pfn2 PE=1 SV=3 | Q9JJV2 | 0,0105 | 0,0089 | 0,0096 | 0,18 |
| CDP-diacylglycerol--glycerol-3-phosphate 3-phosphatidyltransferase, mitochondrial OS=Mus musculus GN=Pgs1 PE=2 SV=1 | Q8BHF7 | 0,0106 | 0,0087 | 0,0096 | 0,23 |
| DnaJ homolog subfamily A member 2 OS=Mus musculus GN=Dnaja2 PE=1 SV=1 | Q9QYJ0 | 0,0096 | 0,0096 | 0,0096 | -0,07 |
| F-actin-capping protein subunit beta OS=Mus musculus GN=Capzb PE=1 SV=3 | P47757 | 0,0096 | 0,0097 | 0,0096 | -0,08 |
| Microtubule-associated protein 6 OS=Mus musculus GN=Map6 PE=1 SV=2 | Q7TSJ2 | 0,0102 | 0,0089 | 0,0095 | 0,14 |
| HCLS1-associated protein X-1 OS=Mus musculus GN=Hax1 PE=1 SV=1 | O35387 | 0,0075 | 0,0115 | 0,0095 | -0,69 |
| Metallo-beta-lactamase domain-containing protein 2 OS=Mus musculus GN=Mblac2 PE=2 SV=2 | Q8BL86 | 0,0112 | 0,0079 | 0,0095 | 0,43 |
| Serine incorporator 1 OS=Mus musculus GN=Serinc1 PE=1 SV=1 | Q9QZI8 | 0,0102 | 0,0088 | 0,0095 | 0,15 |
| Serine/threonine-protein phosphatase PP1-alpha catalytic subunit OS=Mus musculus GN=Ppp1ca PE=1 SV=1 | P62137 | 0,0097 | 0,0093 | 0,0095 | 0,00 |
| Vesicular glutamate transporter 2 OS=Mus musculus GN=Slc17a6 PE=1 SV=1 | Q8BLE7 | 0,0073 | 0,0116 | 0,0095 | -0,73 |
| Dynamin-like 120 kDa protein, mitochondrial OS=Mus musculus GN=Opa1 PE=1 SV=1 | P58281 | 0,0104 | 0,0086 | 0,0095 | 0,20 |
| Fumarylacetoacetate hydrolase domain-containing protein 2A OS=Mus musculus GN=Fahd2 PE=1 SV=1 | Q3TC72 | 0,0085 | 0,0103 | 0,0094 | -0,35 |
| Alpha/beta hydrolase domain-containing protein 17C OS=Mus musculus GN=Abhd17c PE=2 SV=2 | Q8VCV1 | 0,0089 | 0,0098 | 0,0094 | -0,21 |
| Gamma-aminobutyric acid receptor subunit alpha-1 OS=Mus musculus GN=Gabra1 PE=1 SV=1 | P62812 | 0,0100 | 0,0088 | 0,0094 | 0,12 |
| 3-mercaptopyruvate sulfurtransferase OS=Mus musculus GN=Mpst PE=1 SV=3 | Q99J99 | 0,0081 | 0,0106 | 0,0094 | -0,47 |
| Ras-related protein R-Ras2 OS=Mus musculus GN=Rras2 PE=1 SV=1 | P62071 | 0,0092 | 0,0093 | 0,0093 | -0,08 |

| | | | | | |
|---|---|---|---|---|---|
| Opalin OS=Mus musculus GN=Opalin PE=1 SV=1 | Q7M750 | 0,0100 | 0,0085 | 0,0093 | 0,16 |
| MAGUK p55 subfamily member 6 OS=Mus musculus GN=Mpp6 PE=1 SV=1 | Q9JLB0 | 0,0107 | 0,0079 | 0,0093 | 0,36 |
| Neuronal-specific septin-3 OS=Mus musculus GN=Sept3 PE=1 SV=2 | Q9Z1S5 | 0,0048 | 0,0134 | 0,0092 | -1,55 |
| 60S ribosomal protein L14 OS=Mus musculus GN=Rpl14 PE=2 SV=3 | Q9CR57 | 0,0078 | 0,0106 | 0,0092 | -0,50 |
| Argininosuccinate synthase OS=Mus musculus GN=Ass1 PE=1 SV=1 | P16460 | 0,0082 | 0,0102 | 0,0092 | -0,37 |
| Actin-related protein 3 OS=Mus musculus GN=Actr3 PE=1 SV=3 | Q99JY9 | 0,0116 | 0,0070 | 0,0092 | 0,67 |
| Guanine deaminase OS=Mus musculus GN=Gda PE=1 SV=1 | Q9R111 | 0,0089 | 0,0095 | 0,0092 | -0,17 |
| Ras-related protein Rab-6A OS=Mus musculus GN=Rab6a PE=1 SV=4 | P35279 | 0,0101 | 0,0083 | 0,0092 | 0,21 |
| Endophilin-B2 OS=Mus musculus GN=Sh3glb2 PE=2 SV=2 | Q8R3V5 | 0,0094 | 0,0089 | 0,0092 | 0,01 |
| Isocitrate dehydrogenase [NADP], mitochondrial OS=Mus musculus GN=Idh2 PE=1 SV=3 | P54071 | 0,0091 | 0,0092 | 0,0091 | -0,08 |
| H-2 class I histocompatibility antigen, D-B alpha chain OS=Mus musculus GN=H2-D1 PE=1 SV=2 | P01899 | 0,0157 | 0,0028 | 0,0091 | 2,41 |
| Semaphorin-4A OS=Mus musculus GN=Sema4a PE=1 SV=2 | Q62178 | 0,0098 | 0,0084 | 0,0091 | 0,16 |
| Metal transporter CNNM1 OS=Mus musculus GN=Cnnm1 PE=1 SV=5 | Q0GA42 | 0,0133 | 0,0051 | 0,0091 | 1,33 |
| Ras-related protein Rab-12 OS=Mus musculus GN=Rab12 PE=1 SV=3 | P35283 | 0,0090 | 0,0091 | 0,0091 | -0,08 |
| Solute carrier family 2, facilitated glucose transporter member 1 OS=Mus musculus GN=Slc2a1 PE=1 SV=4 | P17809 | 0,0083 | 0,0097 | 0,0090 | -0,29 |
| Bardet-Biedl syndrome 7 protein homolog OS=Mus musculus GN=Bbs7 PE=1 SV=1 | Q8K2G4 | 0,0056 | 0,0123 | 0,0090 | -1,20 |
| V-type proton ATPase 116 kDa subunit a isoform 1 OS=Mus musculus GN=Atp6v0a1 PE=1 SV=3 | Q9Z1G4 | 0,0120 | 0,0062 | 0,0090 | 0,89 |
| Putative tyrosine-protein phosphatase auxilin OS=Mus musculus GN=Dnajc6 PE=2 SV=2 | Q80TZ3 | 0,0090 | 0,0090 | 0,0090 | -0,07 |
| Tripeptidyl-peptidase 1 OS=Mus musculus GN=Tpp1 PE=1 SV=2 | O89023 | 0,0084 | 0,0094 | 0,0089 | -0,23 |
| Gamma-enolase OS=Mus musculus GN=Eno2 PE=1 SV=2 | P17183 | 0,0112 | 0,0068 | 0,0089 | 0,66 |
| Phenylalanine--tRNA ligase alpha subunit OS=Mus musculus GN=Farsa PE=2 SV=1 | Q8C0C7 | 0,0074 | 0,0102 | 0,0088 | -0,52 |
| Aldehyde dehydrogenase, mitochondrial OS=Mus musculus GN=Aldh2 PE=1 SV=1 | P47738 | 0,0087 | 0,0089 | 0,0088 | -0,10 |
| Atlastin-1 OS=Mus musculus GN=Atl1 PE=1 SV=1 | Q8BH66 | 0,0085 | 0,0091 | 0,0088 | -0,15 |
| Neuropilin and tolloid-like protein 1 OS=Mus musculus GN=Neto1 PE=1 SV=2 | Q8R4I7 | 0,0134 | 0,0044 | 0,0088 | 1,55 |
| Long-chain-fatty-acid--CoA ligase 4 OS=Mus musculus GN=Acsl4 PE=2 SV=2 | Q9QUJ7 | 0,0104 | 0,0072 | 0,0088 | 0,48 |
| Mitochondrial import receptor subunit TOM20 homolog OS=Mus musculus GN=Tomm20 PE=1 SV=1 | Q9DCC8 | 0,0088 | 0,0087 | 0,0088 | -0,05 |
| Transmembrane 9 superfamily member 2 OS=Mus musculus GN=Tm9sf2 PE=2 SV=1 | P58021 | 0,0094 | 0,0081 | 0,0087 | 0,15 |
| NADH dehydrogenase [ubiquinone] iron-sulfur protein 2, mitochondrial OS=Mus musculus GN=Ndufs2 PE=1 SV=1 | Q91WD5 | 0,0090 | 0,0083 | 0,0087 | 0,05 |
| NADH dehydrogenase [ubiquinone] iron-sulfur protein 3, mitochondrial OS=Mus musculus GN=Ndufs3 PE=1 SV=2 | Q9DCT2 | 0,0099 | 0,0075 | 0,0087 | 0,32 |
| Quinone oxidoreductase-like protein 2 OS=Mus musculus PE=1 SV=1 | Q3UNZ8 | 0,0102 | 0,0072 | 0,0087 | 0,44 |
| Cadherin-11 OS=Mus musculus GN=Cdh11 PE=1 SV=1 | P55288 | 0,0096 | 0,0078 | 0,0087 | 0,23 |
| Prostaglandin E synthase 2 OS=Mus musculus GN=Ptges2 PE=1 SV=3 | Q8BWM0 | 0,0091 | 0,0082 | 0,0087 | 0,09 |
| T-complex protein 1 subunit delta OS=Mus musculus GN=Cct4 PE=1 SV=3 | P80315 | 0,0080 | 0,0092 | 0,0086 | -0,27 |
| Roundabout homolog 1 OS=Mus musculus GN=Robo1 PE=1 SV=1 | O89026 | 0,0074 | 0,0097 | 0,0086 | -0,45 |
| Protein FAM189A1 OS=Mus musculus GN=Fam189a1 PE=2 SV=3 | Q6A044 | 0,0041 | 0,0129 | 0,0086 | -1,72 |
| F-box/LRR-repeat protein 16 OS=Mus musculus GN=Fbxl16 PE=2 SV=1 | A2RT62 | 0,0075 | 0,0095 | 0,0086 | -0,41 |
| Cyclin-dependent kinase 5 OS=Mus musculus GN=Cdk5 PE=1 SV=1 | P49615 | 0,0083 | 0,0087 | 0,0085 | -0,13 |
| Heterogeneous nuclear ribonucleoprotein K OS=Mus musculus GN=Hnrnpk PE=1 SV=1 | P61979 | 0,0138 | 0,0034 | 0,0085 | 1,95 |
| Cytochrome b-c1 complex subunit 8 OS=Mus musculus GN=Uqcrq PE=1 SV=3 | Q9CQ69 | 0,0068 | 0,0101 | 0,0085 | -0,64 |
| Contactin-associated protein like 5-1 OS=Mus musculus GN=Cntnap5a PE=2 SV=1 | Q0V8T9 | 0,0134 | 0,0037 | 0,0084 | 1,80 |
| CB1 cannabinoid receptor-interacting protein 1 OS=Mus musculus GN=Cnrip1 PE=1 SV=1 | Q5M8N0 | 0,0079 | 0,0089 | 0,0084 | -0,24 |
| Serine/threonine-protein phosphatase 2A 55 kDa regulatory subunit B delta isoform OS=Mus musculus GN=Ppp2r2d PE=2 SV=1 | Q925E7 | 0,0075 | 0,0093 | 0,0084 | -0,39 |
| Protein disulfide-isomerase A3 OS=Mus musculus GN=Pdia3 PE=1 SV=2 | P27773 | 0,0142 | 0,0028 | 0,0084 | 2,25 |
| Beta-actin-like protein 2 OS=Mus musculus GN=Actbl2 PE=1 SV=1 | Q8BFZ3 | 0,0068 | 0,0099 | 0,0084 | -0,61 |
| V-type proton ATPase subunit d 1 OS=Mus musculus GN=Atp6v0d1 PE=1 SV=2 | P51863 | 0,0114 | 0,0055 | 0,0083 | 0,99 |
| Prolactin regulatory element-binding protein OS=Mus musculus GN=Preb PE=1 SV=1 | Q9WUQ2 | 0,0089 | 0,0078 | 0,0083 | 0,12 |
| Calsyntenin-3 OS=Mus musculus GN=Clstn3 PE=1 SV=1 | Q99JH7 | 0,0116 | 0,0052 | 0,0083 | 1,10 |
| Tumor necrosis factor receptor superfamily member 21 OS=Mus musculus GN=Tnfrsf21 PE=1 SV=2 | Q9EPU5 | 0,0083 | 0,0083 | 0,0083 | -0,08 |
| Peptidyl-prolyl cis-trans isomerase FKBP8 OS=Mus musculus GN=Fkbp8 PE=1 SV=2 | O35465 | 0,0089 | 0,0077 | 0,0083 | 0,14 |
| Gamma-aminobutyric acid type B receptor subunit 2 OS=Mus musculus GN=Gabbr2 PE=1 SV=2 | Q80T41 | 0,0102 | 0,0063 | 0,0082 | 0,62 |
| Cadherin-9 OS=Mus musculus GN=Cdh9 PE=2 SV=2 | P70407 | 0,0099 | 0,0066 | 0,0082 | 0,51 |
| Sodium-coupled neutral amino acid transporter 1 OS=Mus musculus GN=Slc38a1 PE=1 SV=1 | Q8K2P7 | 0,0115 | 0,0050 | 0,0082 | 1,13 |
| Phosphatidylinositol 4-kinase type 2-alpha OS=Mus musculus GN=Pi4k2a PE=1 SV=1 | Q2TBE6 | 0,0098 | 0,0067 | 0,0082 | 0,49 |
| Diacylglycerol kinase beta OS=Mus musculus GN=Dgkb PE=2 SV=2 | Q6NS52 | 0,0066 | 0,0096 | 0,0082 | -0,60 |
| Rootletin OS=Mus musculus GN=Crocc PE=1 SV=2 | Q8CJ40 | 0,0091 | 0,0072 | 0,0081 | 0,28 |
| Catechol O-methyltransferase domain-containing protein 1 OS=Mus musculus GN=Comtd1 PE=2 SV=1 | Q8BIG7 | 0,0075 | 0,0087 | 0,0081 | -0,29 |
| Uncharacterized protein KIAA0513 OS=Mus musculus GN=Kiaa0513 PE=2 SV=1 | Q8R0A7 | 0,0114 | 0,0049 | 0,0081 | 1,14 |
| Sulfide:quinone oxidoreductase, mitochondrial OS=Mus musculus GN=Sqrdl PE=1 SV=3 | Q9R112 | 0,0088 | 0,0074 | 0,0081 | 0,19 |
| Reticulon-4 OS=Mus musculus GN=Rtn4 PE=1 SV=2 | Q99P72 | 0,0107 | 0,0055 | 0,0081 | 0,89 |
| Electron transfer flavoprotein subunit beta OS=Mus musculus GN=Etfb PE=1 SV=3 | Q9DCW4 | 0,0083 | 0,0077 | 0,0080 | 0,04 |
| ADP/ATP translocase 4 OS=Mus musculus GN=Slc25a31 PE=2 SV=1 | Q3V132 | 0,0081 | 0,0078 | 0,0080 | -0,01 |
| Succinyl-CoA ligase [GDP-forming] subunit beta, mitochondrial OS=Mus musculus GN=Suclg2 PE=1 SV=3 | Q9Z2I8 | 0,0099 | 0,0061 | 0,0080 | 0,63 |
| Myelin-associated glycoprotein OS=Mus musculus GN=Mag PE=1 SV=2 | P20917 | 0,0088 | 0,0072 | 0,0080 | 0,23 |
| Tissue factor OS=Mus musculus GN=F3 PE=1 SV=2 | P20352 | 0,0090 | 0,0068 | 0,0079 | 0,34 |
| Calcium/calmodulin-dependent protein kinase type II subunit gamma OS=Mus musculus GN=Camk2g PE=1 SV=1 | Q923T9 | 0,0092 | 0,0066 | 0,0079 | 0,42 |
| T-complex protein 1 subunit alpha OS=Mus musculus GN=Tcp1 PE=1 SV=3 | P11983 | 0,0083 | 0,0074 | 0,0078 | 0,11 |
| Large neutral amino acids transporter small subunit 1 OS=Mus musculus GN=Slc7a5 PE=1 SV=2 | Q9Z127 | 0,0089 | 0,0068 | 0,0078 | 0,33 |
| Amyloid beta A4 protein OS=Mus musculus GN=App PE=1 SV=3 | P12023 | 0,0087 | 0,0071 | 0,0078 | 0,23 |
| Monoacylglycerol lipase ABHD12 OS=Mus musculus GN=Abhd12 PE=1 SV=2 | Q99LR1 | 0,0077 | 0,0079 | 0,0078 | -0,11 |
| AFG3-like protein 2 OS=Mus musculus GN=Afg3l2 PE=1 SV=1 | Q8JZQ2 | 0,0079 | 0,0077 | 0,0078 | -0,04 |
| Cytosolic acyl coenzyme A thioester hydrolase OS=Mus musculus GN=Acot7 PE=1 SV=2 | Q91V12 | 0,0082 | 0,0074 | 0,0078 | 0,08 |
| Sodium/hydrogen exchanger 1 OS=Mus musculus GN=Slc9a1 PE=1 SV=1 | Q61165 | 0,0066 | 0,0090 | 0,0078 | -0,52 |
| Calcium/calmodulin-dependent protein kinase type II subunit delta OS=Mus musculus GN=Camk2d PE=1 SV=1 | Q6PHZ2 | 0,0094 | 0,0062 | 0,0078 | 0,54 |
| Syntaxin-7 OS=Mus musculus GN=Stx7 PE=1 SV=3 | O70439 | 0,0096 | 0,0060 | 0,0078 | 0,60 |
| Vascular endothelial growth factor receptor 2 OS=Mus musculus GN=Kdr PE=1 SV=1 | P35918 | 0,0033 | 0,0120 | 0,0077 | -1,93 |
| Receptor-type tyrosine-protein phosphatase R OS=Mus musculus GN=Ptprr PE=1 SV=1 | Q62132 | 0,0085 | 0,0070 | 0,0077 | 0,23 |

| | | | | | |
|---|---|---|---|---|---|
| Sarcoplasmic/endoplasmic reticulum calcium ATPase 3 OS=Mus musculus GN=Atp2a3 PE=2 SV=3 | Q64518 | 0,0086 | 0,0069 | 0,0077 | 0,26 |
| Probable G-protein coupled receptor 162 OS=Mus musculus GN=Gpr162 PE=2 SV=2 | Q3UN16 | 0,0076 | 0,0078 | 0,0077 | -0,12 |
| Activator of 90 kDa heat shock protein ATPase homolog 1 OS=Mus musculus GN=Ahsa1 PE=2 SV=2 | Q8BK64 | 0,0076 | 0,0079 | 0,0077 | -0,12 |
| BTB/POZ domain-containing protein KCTD12 OS=Mus musculus GN=Kctd12 PE=1 SV=1 | Q6WVG3 | 0,0096 | 0,0059 | 0,0077 | 0,63 |
| Thioredoxin-related transmembrane protein 1 OS=Mus musculus GN=Tmx1 PE=1 SV=1 | Q8VBT0 | 0,0078 | 0,0076 | 0,0077 | -0,03 |
| Protocadherin alpha-4 OS=Mus musculus GN=Pcdha4 PE=1 SV=1 | O88689 | 0,0085 | 0,0069 | 0,0077 | 0,22 |
| Annexin A1 OS=Mus musculus GN=Anxa1 PE=1 SV=2 | P10107 | 0,0123 | 0,0033 | 0,0077 | 1,81 |
| Calcium/calmodulin-dependent protein kinase type 1D OS=Mus musculus GN=Camk1d PE=1 SV=2 | Q8BW96 | 0,0061 | 0,0090 | 0,0076 | -0,63 |
| Glycogen phosphorylase, muscle form OS=Mus musculus GN=Pygm PE=1 SV=3 | Q9WUB3 | 0,0066 | 0,0084 | 0,0075 | -0,42 |
| Heat shock 70 kDa protein 4L OS=Mus musculus GN=Hspa4l PE=1 SV=2 | P48722 | 0,0073 | 0,0077 | 0,0075 | -0,15 |
| Vacuolar protein sorting-associated protein 35 OS=Mus musculus GN=Vps35 PE=1 SV=1 | Q9EQH3 | 0,0079 | 0,0071 | 0,0075 | 0,08 |
| Receptor-type tyrosine-protein phosphatase T OS=Mus musculus GN=Ptprt PE=2 SV=2 | Q99M80 | 0,0138 | 0,0015 | 0,0075 | 3,18 |
| Retinol dehydrogenase 11 OS=Mus musculus GN=Rdh11 PE=2 SV=2 | Q9QYF1 | 0,0090 | 0,0060 | 0,0075 | 0,51 |
| NADH dehydrogenase [ubiquinone] flavoprotein 1, mitochondrial OS=Mus musculus GN=Ndufv1 PE=1 SV=1 | Q91YT0 | 0,0068 | 0,0081 | 0,0075 | -0,32 |
| AP-2 complex subunit alpha-2 OS=Mus musculus GN=Ap2a2 PE=1 SV=2 | P17427 | 0,0076 | 0,0073 | 0,0074 | -0,01 |
| Neuronal calcium sensor 1 OS=Mus musculus GN=Ncs1 PE=2 SV=3 | Q8BNY6 | 0,0096 | 0,0054 | 0,0074 | 0,76 |
| FERM, RhoGEF and pleckstrin domain-containing protein 1 OS=Mus musculus GN=Farp1 PE=1 SV=1 | F8VPU2 | 0,0081 | 0,0067 | 0,0074 | 0,20 |
| Hypoxanthine-guanine phosphoribosyltransferase OS=Mus musculus GN=Hprt1 PE=1 SV=3 | P00493 | 0,0105 | 0,0043 | 0,0074 | 1,23 |
| Reticulon-1 OS=Mus musculus GN=Rtn1 PE=1 SV=1 | Q8K0T0 | 0,0078 | 0,0069 | 0,0073 | 0,13 |
| Isocitrate dehydrogenase [NADP] cytoplasmic OS=Mus musculus GN=Idh1 PE=1 SV=2 | O88844 | 0,0065 | 0,0081 | 0,0073 | -0,38 |
| Long-chain fatty acid transport protein 1 OS=Mus musculus GN=Slc27a1 PE=1 SV=1 | Q60714 | 0,0070 | 0,0075 | 0,0073 | -0,16 |
| Actin-related protein 2 OS=Mus musculus GN=Actr2 PE=1 SV=1 | P61161 | 0,0086 | 0,0059 | 0,0072 | 0,48 |
| Leucine-rich repeat-containing protein 57 OS=Mus musculus GN=Lrrc57 PE=2 SV=1 | Q9D1G5 | 0,0067 | 0,0077 | 0,0072 | -0,26 |
| ATP-binding cassette sub-family B member 9 OS=Mus musculus GN=Abcb9 PE=2 SV=1 | Q9JJ59 | 0,0091 | 0,0054 | 0,0072 | 0,70 |
| Propionyl-CoA carboxylase beta chain, mitochondrial OS=Mus musculus GN=Pccb PE=1 SV=2 | Q99MN9 | 0,0103 | 0,0043 | 0,0072 | 1,21 |
| AP-3 complex subunit mu-2 OS=Mus musculus GN=Ap3m2 PE=2 SV=1 | Q8R2R9 | 0,0054 | 0,0089 | 0,0072 | -0,80 |
| Phytanoyl-CoA hydroxylase-interacting protein OS=Mus musculus GN=Phyhip PE=1 SV=1 | Q8K0S0 | 0,0065 | 0,0078 | 0,0072 | -0,34 |
| Ankyrin repeat domain-containing protein 46 OS=Mus musculus GN=Ankrd46 PE=2 SV=1 | Q8BTZ5 | 0,0091 | 0,0054 | 0,0072 | 0,68 |
| Bcl-2-like protein 13 OS=Mus musculus GN=Bcl2l13 PE=1 SV=2 | P59017 | 0,0079 | 0,0065 | 0,0072 | 0,22 |
| Potassium-transporting ATPase alpha chain 2 OS=Mus musculus GN=Atp12a PE=1 SV=3 | Q9Z1W8 | 0,0071 | 0,0072 | 0,0072 | -0,08 |
| Lysosomal alpha-glucosidase OS=Mus musculus GN=Gaa PE=1 SV=2 | P70699 | 0,0074 | 0,0070 | 0,0072 | 0,02 |
| Trifunctional enzyme subunit beta, mitochondrial OS=Mus musculus GN=Hadhb PE=1 SV=1 | Q99JY0 | 0,0086 | 0,0058 | 0,0072 | 0,52 |
| Serine/threonine-protein phosphatase PP1-gamma catalytic subunit OS=Mus musculus GN=Ppp1cc PE=1 SV=1 | P63087 | 0,0083 | 0,0061 | 0,0072 | 0,38 |
| Mitochondrial import inner membrane translocase subunit Tim23 OS=Mus musculus GN=Timm23 PE=2 SV=1 | Q9WTQ8 | 0,0076 | 0,0067 | 0,0072 | 0,11 |
| Sodium/potassium-transporting ATPase subunit beta-3 OS=Mus musculus GN=Atp1b3 PE=1 SV=1 | P97370 | 0,0089 | 0,0055 | 0,0072 | 0,62 |
| Neogenin OS=Mus musculus GN=Neo1 PE=1 SV=1 | P97798 | 0,0059 | 0,0083 | 0,0071 | -0,56 |
| Muscarinic acetylcholine receptor M1 OS=Mus musculus GN=Chrm1 PE=2 SV=2 | P12657 | 0,0064 | 0,0079 | 0,0071 | -0,38 |
| 60S acidic ribosomal protein P0 OS=Mus musculus GN=Rplp0 PE=1 SV=3 | P14869 | 0,0071 | 0,0071 | 0,0071 | -0,07 |
| 3-ketodihydrosphingosine reductase OS=Mus musculus GN=Kdsr PE=2 SV=1 | Q6GV12 | 0,0082 | 0,0060 | 0,0071 | 0,39 |
| 40S ribosomal protein S13 OS=Mus musculus GN=Rps13 PE=2 SV=2 | P62301 | 0,0112 | 0,0032 | 0,0071 | 1,75 |
| Cysteine and glycine-rich protein 1 OS=Mus musculus GN=Csrp1 PE=1 SV=3 | P97315 | 0,0102 | 0,0041 | 0,0071 | 1,25 |
| ADP-ribosyl cyclase 1 OS=Mus musculus GN=Cd38 PE=1 SV=2 | P56528 | 0,0086 | 0,0056 | 0,0070 | 0,56 |
| Tetraspanin-18 OS=Mus musculus GN=Tspan18 PE=2 SV=1 | Q80WR1 | 0,0027 | 0,0111 | 0,0070 | -2,10 |
| 40S ribosomal protein S18 OS=Mus musculus GN=Rps18 PE=1 SV=3 | P62270 | 0,0071 | 0,0069 | 0,0070 | -0,03 |
| Copine-7 OS=Mus musculus GN=Cpne7 PE=2 SV=1 | Q0VE82 | 0,0062 | 0,0077 | 0,0070 | -0,39 |
| Ras-related protein Rab-22A OS=Mus musculus GN=Rab22a PE=1 SV=2 | P35285 | 0,0066 | 0,0074 | 0,0070 | -0,24 |
| Leucine-rich repeat and fibronectin type-III domain-containing protein 5 OS=Mus musculus GN=Lrfn5 PE=1 SV=1 | Q8BXA0 | 0,0087 | 0,0053 | 0,0070 | 0,63 |
| Chondroitin sulfate proteoglycan 5 OS=Mus musculus GN=Cspg5 PE=1 SV=2 | Q71M36 | 0,0098 | 0,0042 | 0,0070 | 1,15 |
| C-type lectin domain family 2 member L OS=Mus musculus GN=Clec2l PE=4 SV=1 | P0C7M9 | 0,0088 | 0,0052 | 0,0069 | 0,71 |
| Acyl-CoA synthetase family member 2, mitochondrial OS=Mus musculus GN=Acsf2 PE=1 SV=1 | Q8VCW8 | 0,0079 | 0,0060 | 0,0069 | 0,31 |
| Amyloid beta A4 precursor protein-binding family B member 1 OS=Mus musculus GN=Apbb1 PE=1 SV=3 | Q9QXJ1 | 0,0071 | 0,0068 | 0,0069 | 0,01 |
| Heat shock-related 70 kDa protein 2 OS=Mus musculus GN=Hspa2 PE=1 SV=2 | P17156 | 0,0073 | 0,0065 | 0,0069 | 0,10 |
| NMDA receptor synaptonuclear signaling and neuronal migration factor OS=Mus musculus GN=Nsmf PE=1 SV=1 | Q99NF2 | 0,0060 | 0,0078 | 0,0069 | -0,45 |
| ATP synthase F(0) complex subunit B1, mitochondrial OS=Mus musculus GN=Atp5f1 PE=1 SV=1 | Q9CQQ7 | 0,0073 | 0,0065 | 0,0069 | 0,10 |
| Cysteine-rich protein 2 OS=Mus musculus GN=Crip2 PE=1 SV=1 | Q9DCT8 | 0,0104 | 0,0036 | 0,0069 | 1,48 |
| Plexin-D1 OS=Mus musculus GN=Plxnd1 PE=1 SV=1 | Q3UH93 | 0,0034 | 0,0102 | 0,0069 | -1,66 |
| Glutamate receptor 3 OS=Mus musculus GN=Gria3 PE=1 SV=2 | Q9Z2W9 | 0,0063 | 0,0073 | 0,0068 | -0,27 |
| Leucine-rich repeat and fibronectin type-III domain-containing protein 4 OS=Mus musculus GN=Lrfn4 PE=1 SV=1 | Q80XU8 | 0,0079 | 0,0057 | 0,0068 | 0,40 |
| Abhydrolase domain-containing protein 16A OS=Mus musculus GN=Abhd16a PE=1 SV=3 | Q9Z1Q2 | 0,0070 | 0,0066 | 0,0068 | 0,02 |
| ADP-ribosylation factor-like protein 15 OS=Mus musculus GN=Arl15 PE=2 SV=1 | Q8BGR6 | 0,0048 | 0,0086 | 0,0067 | -0,90 |
| Hexaprenyldihydroxybenzoate methyltransferase, mitochondrial OS=Mus musculus GN=Coq3 PE=1 SV=1 | Q8BMS4 | 0,0067 | 0,0068 | 0,0067 | -0,09 |
| Semaphorin-4D OS=Mus musculus GN=Sema4d PE=1 SV=2 | O09126 | 0,0073 | 0,0061 | 0,0067 | 0,21 |
| Protein lifeguard 2 OS=Mus musculus GN=Faim2 PE=2 SV=1 | Q8K097 | 0,0068 | 0,0065 | 0,0066 | -0,01 |
| 40S ribosomal protein S8 OS=Mus musculus GN=Rps8 PE=2 SV=2 | P62242 | 0,0066 | 0,0067 | 0,0066 | -0,09 |
| Syntaxin-17 OS=Mus musculus GN=Stx17 PE=1 SV=1 | Q9D0I4 | 0,0054 | 0,0078 | 0,0066 | -0,60 |
| Surfeit locus protein 4 OS=Mus musculus GN=Surf4 PE=2 SV=1 | Q64310 | 0,0069 | 0,0063 | 0,0066 | 0,08 |
| Calcineurin B homologous protein 1 OS=Mus musculus GN=Chp1 PE=1 SV=2 | P61022 | 0,0078 | 0,0054 | 0,0066 | 0,45 |
| Phosphoglycerate kinase 1 OS=Mus musculus GN=Pgk1 PE=1 SV=4 | P09411 | 0,0097 | 0,0036 | 0,0066 | 1,37 |
| Cathepsin B OS=Mus musculus GN=Ctsb PE=1 SV=2 | P10605 | 0,0077 | 0,0054 | 0,0066 | 0,45 |
| 2-methoxy-6-polyprenyl-1,4-benzoquinol methylase, mitochondrial OS=Mus musculus GN=Coq5 PE=2 SV=2 | Q9CXI0 | 0,0064 | 0,0067 | 0,0065 | -0,14 |
| Ubiquitin carboxyl-terminal hydrolase 46 OS=Mus musculus GN=Usp46 PE=1 SV=1 | P62069 | 0,0059 | 0,0071 | 0,0065 | -0,32 |
| Cystine/glutamate transporter OS=Mus musculus GN=Slc7a11 PE=1 SV=1 | Q9WTR6 | 0,0065 | 0,0065 | 0,0065 | -0,06 |
| 2'-5'-oligoadenylate synthase 1A OS=Mus musculus GN=Oas1a PE=2 SV=2 | P11928 | 0,0111 | 0,0022 | 0,0065 | 2,28 |
| PH and SEC7 domain-containing protein 3 OS=Mus musculus GN=Psd3 PE=1 SV=2 | Q2PFD7 | 0,0050 | 0,0079 | 0,0065 | -0,73 |
| Ras-related protein Rab-6B OS=Mus musculus GN=Rab6b PE=1 SV=1 | P61294 | 0,0077 | 0,0053 | 0,0065 | 0,47 |
| Contactin-associated protein like 5-3 OS=Mus musculus GN=Cntnap5c PE=2 SV=1 | Q0V8T7 | 0,0086 | 0,0044 | 0,0065 | 0,89 |

| | | | | | |
|---|---|---|---|---|---|
| Tetraspanin-2 OS=Mus musculus GN=Tspan2 PE=1 SV=1 | Q922J6 | 0,0068 | 0,0061 | 0,0065 | 0,11 |
| Protein NDRG1 OS=Mus musculus GN=Ndrg1 PE=1 SV=1 | Q62433 | 0,0066 | 0,0063 | 0,0064 | -0,01 |
| Leucine-rich repeat and fibronectin type-III domain-containing protein 3 OS=Mus musculus GN=Lrfn3 PE=1 SV=1 | Q8BLY3 | 0,0072 | 0,0056 | 0,0064 | 0,29 |
| Guanine nucleotide-binding protein subunit beta-5 OS=Mus musculus GN=Gnb5 PE=1 SV=1 | P62881 | 0,0059 | 0,0069 | 0,0064 | -0,28 |
| Phosphoglycerate mutase 1 OS=Mus musculus GN=Pgam1 PE=1 SV=3 | Q9DBJ1 | 0,0090 | 0,0038 | 0,0064 | 1,16 |
| Synaptotagmin-12 OS=Mus musculus GN=Syt12 PE=2 SV=1 | Q920N7 | 0,0067 | 0,0060 | 0,0063 | 0,10 |
| Sphingomyelin phosphodiesterase 2 OS=Mus musculus GN=Smpd2 PE=1 SV=1 | O70572 | 0,0067 | 0,0060 | 0,0063 | 0,09 |
| Ribonuclease inhibitor OS=Mus musculus GN=Rnh1 PE=1 SV=1 | Q91VI7 | 0,0079 | 0,0048 | 0,0063 | 0,64 |
| Cell adhesion molecule 4 OS=Mus musculus GN=Cadm4 PE=1 SV=1 | Q8R464 | 0,0080 | 0,0047 | 0,0063 | 0,70 |
| Cyclin-Y OS=Mus musculus GN=Ccny PE=1 SV=1 | Q8BGU5 | 0,0058 | 0,0068 | 0,0063 | -0,29 |
| Serine/threonine-protein phosphatase 5 OS=Mus musculus GN=Ppp5c PE=1 SV=3 | Q60676 | 0,0068 | 0,0058 | 0,0063 | 0,16 |
| Protein transport protein Sec61 subunit alpha isoform 1 OS=Mus musculus GN=Sec61a1 PE=2 SV=2 | P61620 | 0,0074 | 0,0051 | 0,0062 | 0,46 |
| Transmembrane protein 132E OS=Mus musculus GN=Tmem132e PE=2 SV=1 | Q6IEE6 | 0,0099 | 0,0027 | 0,0062 | 1,78 |
| Vacuolar protein sorting-associated protein 45 OS=Mus musculus GN=Vps45 PE=1 SV=1 | P97390 | 0,0065 | 0,0059 | 0,0062 | 0,07 |
| Mitogen-activated protein kinase 1 OS=Mus musculus GN=Mapk1 PE=1 SV=3 | P63085 | 0,0057 | 0,0067 | 0,0062 | -0,31 |
| 60S ribosomal protein L7 OS=Mus musculus GN=Rpl7 PE=2 SV=2 | P14148 | 0,0062 | 0,0062 | 0,0062 | -0,06 |
| 40S ribosomal protein S15 OS=Mus musculus GN=Rps15 PE=2 SV=2 | P62843 | 0,0091 | 0,0034 | 0,0062 | 1,36 |
| 4-aminobutyrate aminotransferase, mitochondrial OS=Mus musculus GN=Abat PE=1 SV=1 | P61922 | 0,0056 | 0,0066 | 0,0061 | -0,29 |
| Diacylglycerol kinase gamma OS=Mus musculus GN=Dgkg PE=2 SV=1 | Q91WG7 | 0,0062 | 0,0060 | 0,0061 | -0,01 |
| RING finger protein 157 OS=Mus musculus GN=Rnf157 PE=2 SV=2 | Q3TEL6 | 0,0066 | 0,0056 | 0,0061 | 0,16 |
| TBC1 domain family member 24 OS=Mus musculus GN=Tbc1d24 PE=2 SV=2 | Q3UUG6 | 0,0072 | 0,0051 | 0,0061 | 0,44 |
| Transmembrane protein 151A OS=Mus musculus GN=Tmem151a PE=1 SV=1 | Q6GQT5 | 0,0057 | 0,0064 | 0,0061 | -0,22 |
| Disks large homolog 1 OS=Mus musculus GN=Dlg1 PE=1 SV=1 | Q811D0 | 0,0058 | 0,0063 | 0,0061 | -0,20 |
| Prostamide/prostaglandin F synthase OS=Mus musculus GN=Fam213b PE=1 SV=1 | Q9DB60 | 0,0065 | 0,0057 | 0,0061 | 0,12 |
| Phytanoyl-CoA hydroxylase-interacting protein-like OS=Mus musculus GN=Phyhipl PE=2 SV=1 | Q8BGT8 | 0,0098 | 0,0024 | 0,0060 | 1,96 |
| Leucine-rich glioma-inactivated protein 1 OS=Mus musculus GN=Lgi1 PE=1 SV=1 | Q9JIA1 | 0,0047 | 0,0073 | 0,0060 | -0,70 |
| 40S ribosomal protein S16 OS=Mus musculus GN=Rps16 PE=2 SV=4 | P14131 | 0,0058 | 0,0062 | 0,0060 | -0,16 |
| Lysocardiolipin acyltransferase 1 OS=Mus musculus GN=Lclat1 PE=2 SV=2 | Q3UN02 | 0,0064 | 0,0056 | 0,0060 | 0,11 |
| Ras-related protein Rap-2c OS=Mus musculus GN=Rap2c PE=1 SV=1 | Q8BU31 | 0,0062 | 0,0058 | 0,0060 | 0,03 |
| WD repeat domain phosphoinositide-interacting protein 2 OS=Mus musculus GN=Wipi2 PE=1 SV=1 | Q80W47 | 0,0060 | 0,0060 | 0,0060 | -0,08 |
| Protein disulfide-isomerase OS=Mus musculus GN=P4hb PE=1 SV=2 | P09103 | 0,0103 | 0,0018 | 0,0060 | 2,45 |
| AP-3 complex subunit beta-2 OS=Mus musculus GN=Ap3b2 PE=1 SV=2 | Q9JME5 | 0,0063 | 0,0056 | 0,0059 | 0,12 |
| Ephrin type-A receptor 7 OS=Mus musculus GN=Epha7 PE=1 SV=2 | Q61772 | 0,0060 | 0,0058 | 0,0059 | -0,02 |
| ES1 protein homolog, mitochondrial OS=Mus musculus GN=D10Jhu81e PE=1 SV=1 | Q9D172 | 0,0055 | 0,0062 | 0,0059 | -0,23 |
| Solute carrier family 25 member 51 OS=Mus musculus GN=Slc25a51 PE=2 SV=1 | Q5HZI9 | 0,0056 | 0,0061 | 0,0059 | -0,18 |
| Guanine nucleotide-binding protein subunit beta-4 OS=Mus musculus GN=Gnb4 PE=2 SV=4 | P29387 | 0,0068 | 0,0050 | 0,0059 | 0,36 |
| Pyridoxal kinase OS=Mus musculus GN=Pdxk PE=1 SV=1 | Q8K183 | 0,0082 | 0,0036 | 0,0058 | 1,10 |
| Histidine triad nucleotide-binding protein 3 OS=Mus musculus GN=Hint3 PE=2 SV=1 | Q9CPS6 | 0,0056 | 0,0061 | 0,0058 | -0,20 |
| Dolichol-phosphate mannosyltransferase OS=Mus musculus GN=Dpm1 PE=2 SV=1 | O70152 | 0,0064 | 0,0053 | 0,0058 | 0,22 |
| Protein phosphatase 1A OS=Mus musculus GN=Ppm1a PE=1 SV=1 | P49443 | 0,0066 | 0,0051 | 0,0058 | 0,31 |
| Kinesin-like protein KIF17 OS=Mus musculus GN=Kif17 PE=1 SV=1 | Q99PW8 | 0,0073 | 0,0044 | 0,0058 | 0,67 |
| Creatine kinase B-type OS=Mus musculus GN=Ckb PE=1 SV=1 | Q04447 | 0,0085 | 0,0032 | 0,0058 | 1,34 |
| [Pyruvate dehydrogenase (acetyl-transferring)] kinase isozyme 2, mitochondrial OS=Mus musculus GN=Pdk2 PE=1 SV=2 | Q9JK42 | 0,0058 | 0,0057 | 0,0058 | -0,06 |
| Neuroligin 4-like OS=Mus musculus GN=Nlgn4l PE=1 SV=1 | B0F2B4 | 0,0071 | 0,0045 | 0,0058 | 0,60 |
| Endoplasmic reticulum-Golgi intermediate compartment protein 1 OS=Mus musculus GN=Ergic1 PE=1 SV=1 | Q9DC16 | 0,0065 | 0,0050 | 0,0058 | 0,31 |
| Long-chain-fatty-acid--CoA ligase 1 OS=Mus musculus GN=Acsl1 PE=1 SV=2 | P41216 | 0,0058 | 0,0057 | 0,0057 | -0,06 |
| Aldehyde dehydrogenase X, mitochondrial OS=Mus musculus GN=Aldh1b1 PE=1 SV=1 | Q9CZS1 | 0,0047 | 0,0067 | 0,0057 | -0,58 |
| Alpha-adducin OS=Mus musculus GN=Add1 PE=1 SV=2 | Q9QYC0 | 0,0065 | 0,0050 | 0,0057 | 0,30 |
| Alpha-centractin OS=Mus musculus GN=Actr1a PE=2 SV=1 | P61164 | 0,0052 | 0,0062 | 0,0057 | -0,31 |
| Bone morphogenetic protein receptor type-1A OS=Mus musculus GN=Bmpr1a PE=2 SV=1 | P36895 | 0,0060 | 0,0054 | 0,0057 | 0,06 |
| 60S ribosomal protein L11 OS=Mus musculus GN=Rpl11 PE=1 SV=4 | Q9CXW4 | 0,0070 | 0,0044 | 0,0057 | 0,58 |
| Myosin-9 OS=Mus musculus GN=Myh9 PE=1 SV=4 | Q8VDD5 | 0,0082 | 0,0033 | 0,0057 | 1,25 |
| Voltage-gated potassium channel subunit beta-1 OS=Mus musculus GN=Kcnab1 PE=2 SV=2 | P63143 | 0,0074 | 0,0039 | 0,0057 | 0,85 |
| Thioredoxin OS=Mus musculus GN=Txn PE=1 SV=3 | P10639 | 0,0074 | 0,0040 | 0,0057 | 0,80 |
| Neuroligin-1 OS=Mus musculus GN=Nlgn1 PE=1 SV=2 | Q99K10 | 0,0053 | 0,0059 | 0,0056 | -0,24 |
| Enoyl-CoA delta isomerase 1, mitochondrial OS=Mus musculus GN=Eci1 PE=1 SV=2 | P42125 | 0,0056 | 0,0056 | 0,0056 | -0,07 |
| Brain acid soluble protein 1 OS=Mus musculus GN=Basp1 PE=1 SV=3 | Q91XV3 | 0,0065 | 0,0047 | 0,0056 | 0,41 |
| V-type proton ATPase subunit C 1 OS=Mus musculus GN=Atp6v1c1 PE=1 SV=4 | Q9Z1G3 | 0,0053 | 0,0058 | 0,0056 | -0,18 |
| Transmembrane protein 114 OS=Mus musculus GN=Tmem114 PE=1 SV=1 | Q9D563 | 0,0020 | 0,0089 | 0,0056 | -2,19 |
| Poly(rC)-binding protein 1 OS=Mus musculus GN=Pcbp1 PE=1 SV=1 | P60335 | 0,0064 | 0,0048 | 0,0056 | 0,35 |
| Pyruvate dehydrogenase E1 component subunit alpha, somatic form, mitochondrial OS=Mus musculus GN=Pdha1 PE=1 SV=1 | P35486 | 0,0054 | 0,0057 | 0,0055 | -0,13 |
| 60S ribosomal protein L22 OS=Mus musculus GN=Rpl22 PE=2 SV=2 | P67984 | 0,0070 | 0,0041 | 0,0055 | 0,71 |
| Monoacylglycerol lipase ABHD6 OS=Mus musculus GN=Abhd6 PE=2 SV=1 | Q8R2Y0 | 0,0058 | 0,0052 | 0,0055 | 0,10 |
| Dual specificity mitogen-activated protein kinase kinase 4 OS=Mus musculus GN=Map2k4 PE=1 SV=2 | P47809 | 0,0053 | 0,0057 | 0,0055 | -0,17 |
| Latrophilin-3 OS=Mus musculus GN=Lphn3 PE=2 SV=3 | Q80TS3 | 0,0058 | 0,0052 | 0,0055 | 0,10 |
| Glycerol-3-phosphate dehydrogenase 1-like protein OS=Mus musculus GN=Gpd1l PE=1 SV=2 | Q3ULJ0 | 0,0050 | 0,0059 | 0,0055 | -0,29 |
| Ras-related protein Rab-26 OS=Mus musculus GN=Rab26 PE=1 SV=1 | Q504M8 | 0,0037 | 0,0071 | 0,0054 | -1,02 |
| P2Y purinoceptor 12 OS=Mus musculus GN=P2ry12 PE=2 SV=1 | Q9CPV9 | 0,0060 | 0,0049 | 0,0054 | 0,21 |
| ATP synthase subunit s, mitochondrial OS=Mus musculus GN=Atp5s PE=2 SV=1 | Q9CRA7 | 0,0052 | 0,0056 | 0,0054 | -0,17 |
| Amine oxidase [flavin-containing] A OS=Mus musculus GN=Maoa PE=1 SV=3 | Q64133 | 0,0048 | 0,0060 | 0,0054 | -0,40 |
| Syntaxin-6 OS=Mus musculus GN=Stx6 PE=1 SV=1 | Q9JKK1 | 0,0049 | 0,0058 | 0,0054 | -0,31 |
| Fructose-bisphosphate aldolase A OS=Mus musculus GN=Aldoa PE=1 SV=2 | P05064 | 0,0074 | 0,0035 | 0,0054 | 1,03 |
| Carbonyl reductase [NADPH] 1 OS=Mus musculus GN=Cbr1 PE=1 SV=3 | P48758 | 0,0050 | 0,0056 | 0,0054 | -0,23 |
| LETM1 and EF-hand domain-containing protein 1, mitochondrial OS=Mus musculus GN=Letm1 PE=2 SV=1 | Q9Z2I0 | 0,0059 | 0,0048 | 0,0054 | 0,23 |
| ADP-ribosylation factor-like protein 5A OS=Mus musculus GN=Arl5a PE=2 SV=1 | Q80ZU0 | 0,0057 | 0,0048 | 0,0053 | 0,18 |
| Carnitine O-palmitoyltransferase 1, brain isoform OS=Mus musculus GN=Cpt1c PE=1 SV=1 | Q8BGD5 | 0,0054 | 0,0051 | 0,0053 | 0,00 |

| | | | | | |
|---|---|---|---|---|---|
| 60S ribosomal protein L38 OS=Mus musculus GN=Rpl38 PE=2 SV=3 | Q9JJI8 | 0,0060 | 0,0045 | 0,0053 | 0,35 |
| Dihydrolipoyl dehydrogenase, mitochondrial OS=Mus musculus GN=Dld PE=1 SV=2 | O08749 | 0,0055 | 0,0050 | 0,0053 | 0,06 |
| Ras-related protein Rab-8B OS=Mus musculus GN=Rab8b PE=1 SV=1 | P61028 | 0,0046 | 0,0059 | 0,0052 | -0,44 |
| Ubiquitin carboxyl-terminal hydrolase isozyme L1 OS=Mus musculus GN=Uchl1 PE=1 SV=1 | Q9R0P9 | 0,0061 | 0,0044 | 0,0052 | 0,41 |
| Glucose 1,6-bisphosphate synthase OS=Mus musculus GN=Pgm2l1 PE=1 SV=1 | Q8CAA7 | 0,0052 | 0,0052 | 0,0052 | -0,05 |
| Neuropilin-1 OS=Mus musculus GN=Nrp1 PE=1 SV=2 | P97333 | 0,0039 | 0,0065 | 0,0052 | -0,82 |
| Acylglycerol kinase, mitochondrial OS=Mus musculus GN=Agk PE=1 SV=1 | Q9ESW4 | 0,0050 | 0,0054 | 0,0052 | -0,18 |
| Acyl-CoA:lysophosphatidylglycerol acyltransferase 1 OS=Mus musculus GN=Lpgat1 PE=2 SV=1 | Q91YX5 | 0,0058 | 0,0045 | 0,0052 | 0,30 |
| Dynamin-1-like protein OS=Mus musculus GN=Dnm1l PE=1 SV=2 | Q8K1M6 | 0,0060 | 0,0044 | 0,0052 | 0,39 |
| Neuronal proto-oncogene tyrosine-protein kinase Src OS=Mus musculus GN=Src PE=1 SV=4 | P05480 | 0,0047 | 0,0055 | 0,0051 | -0,29 |
| H(+)/Cl(-) exchange transporter 3 OS=Mus musculus GN=Clcn3 PE=1 SV=2 | P51791 | 0,0058 | 0,0045 | 0,0051 | 0,29 |
| Vascular endothelial growth factor receptor 1 OS=Mus musculus GN=Flt1 PE=1 SV=1 | P35969 | 0,0039 | 0,0063 | 0,0051 | -0,77 |
| 40S ribosomal protein S9 OS=Mus musculus GN=Rps9 PE=2 SV=3 | Q6ZWN5 | 0,0055 | 0,0048 | 0,0051 | 0,13 |
| Ras-related protein Rab-7a OS=Mus musculus GN=Rab7a PE=1 SV=2 | P51150 | 0,0064 | 0,0039 | 0,0051 | 0,63 |
| Guanylate cyclase soluble subunit beta-1 OS=Mus musculus GN=Gucy1b3 PE=2 SV=1 | O54865 | 0,0058 | 0,0045 | 0,0051 | 0,30 |
| Sprouty-related, EVH1 domain-containing protein 1 OS=Mus musculus GN=Spred1 PE=1 SV=1 | Q924S8 | 0,0066 | 0,0036 | 0,0051 | 0,81 |
| Cytochrome c1, heme protein, mitochondrial OS=Mus musculus GN=Cyc1 PE=1 SV=1 | Q9D0M3 | 0,0047 | 0,0053 | 0,0050 | -0,25 |
| Alpha-actinin-1 OS=Mus musculus GN=Actn1 PE=1 SV=1 | Q7TPR4 | 0,0061 | 0,0040 | 0,0050 | 0,54 |
| Casein kinase I isoform gamma-1 OS=Mus musculus GN=Csnk1g1 PE=1 SV=2 | Q8BTH8 | 0,0037 | 0,0063 | 0,0050 | -0,85 |
| Synaptojanin-2-binding protein OS=Mus musculus GN=Synj2bp PE=1 SV=1 | Q9D6K5 | 0,0053 | 0,0046 | 0,0050 | 0,14 |
| NADH dehydrogenase [ubiquinone] iron-sulfur protein 8, mitochondrial OS=Mus musculus GN=Ndufs8 PE=1 SV=1 | Q8K3J1 | 0,0050 | 0,0050 | 0,0050 | -0,05 |
| Voltage-dependent L-type calcium channel subunit beta-4 OS=Mus musculus GN=Cacnb4 PE=1 SV=2 | Q8R0S4 | 0,0057 | 0,0042 | 0,0050 | 0,37 |
| Transmembrane protein 33 OS=Mus musculus GN=Tmem33 PE=2 SV=1 | Q9CR67 | 0,0057 | 0,0042 | 0,0049 | 0,36 |
| Lipid phosphate phosphatase-related protein type 4 OS=Mus musculus GN=Lppr4 PE=2 SV=2 | Q7TME0 | 0,0049 | 0,0049 | 0,0049 | -0,08 |
| Mu-type opioid receptor OS=Mus musculus GN=Oprm1 PE=1 SV=1 | P42866 | 0,0088 | 0,0012 | 0,0049 | 2,81 |
| L-2-hydroxyglutarate dehydrogenase, mitochondrial OS=Mus musculus GN=L2hgdh PE=1 SV=1 | Q91YP0 | 0,0044 | 0,0053 | 0,0049 | -0,31 |
| 1-acyl-sn-glycerol-3-phosphate acyltransferase gamma OS=Mus musculus GN=Agpat3 PE=1 SV=2 | Q9D517 | 0,0048 | 0,0049 | 0,0049 | -0,08 |
| Pyrroline-5-carboxylate reductase 2 OS=Mus musculus GN=Pycr2 PE=2 SV=1 | Q922Q4 | 0,0049 | 0,0048 | 0,0048 | -0,03 |
| Guanine nucleotide-binding protein subunit alpha-12 OS=Mus musculus GN=Gna12 PE=1 SV=3 | P27600 | 0,0060 | 0,0036 | 0,0048 | 0,65 |
| [Pyruvate dehydrogenase (acetyl-transferring)] kinase isozyme 1, mitochondrial OS=Mus musculus GN=Pdk1 PE=2 SV=2 | Q8BFP9 | 0,0044 | 0,0051 | 0,0048 | -0,28 |
| Calcium/calmodulin-dependent 3',5'-cyclic nucleotide phosphodiesterase 1A OS=Mus musculus GN=Pde1a PE=2 SV=2 | Q61481 | 0,0046 | 0,0049 | 0,0048 | -0,15 |
| Ras-related protein Rab-27A OS=Mus musculus GN=Rab27a PE=1 SV=1 | Q9ERI2 | 0,0047 | 0,0048 | 0,0047 | -0,10 |
| Protein transport protein Sec61 subunit alpha isoform 2 OS=Mus musculus GN=Sec61a2 PE=2 SV=3 | Q9JLR1 | 0,0052 | 0,0043 | 0,0047 | 0,22 |
| WD repeat-containing protein 37 OS=Mus musculus GN=Wdr37 PE=2 SV=1 | Q8CBE3 | 0,0051 | 0,0043 | 0,0047 | 0,18 |
| Protein spinster homolog 1 OS=Mus musculus GN=Spns1 PE=2 SV=1 | Q8R0G7 | 0,0059 | 0,0036 | 0,0047 | 0,64 |
| Eukaryotic initiation factor 4A-I OS=Mus musculus GN=Eif4a1 PE=1 SV=1 | P60843 | 0,0064 | 0,0031 | 0,0047 | 0,98 |
| Membrane-associated progesterone receptor component 2 OS=Mus musculus GN=Pgrmc2 PE=1 SV=2 | Q80UU9 | 0,0049 | 0,0045 | 0,0047 | 0,05 |
| Heat shock 70 kDa protein 12B OS=Mus musculus GN=Hspa12b PE=1 SV=1 | Q9CZJ2 | 0,0036 | 0,0056 | 0,0047 | -0,69 |
| Neural proliferation differentiation and control protein 1 OS=Mus musculus GN=Npdc1 PE=2 SV=2 | Q64322 | 0,0046 | 0,0047 | 0,0047 | -0,11 |
| Plastin-3 OS=Mus musculus GN=Pls3 PE=1 SV=3 | Q99K51 | 0,0066 | 0,0027 | 0,0046 | 1,22 |
| 60S ribosomal protein L17 OS=Mus musculus GN=Rpl17 PE=2 SV=3 | Q9CPR4 | 0,0045 | 0,0048 | 0,0046 | -0,16 |
| Interferon-inducible GTPase 1 OS=Mus musculus GN=Iigp1 PE=1 SV=2 | Q9QZ85 | 0,0073 | 0,0020 | 0,0046 | 1,83 |
| 60S ribosomal protein L19 OS=Mus musculus GN=Rpl19 PE=1 SV=1 | P84099 | 0,0043 | 0,0048 | 0,0046 | -0,24 |
| Sodium-dependent phosphate transport protein 1 OS=Mus musculus GN=Slc17a1 PE=1 SV=2 | Q61983 | 0,0049 | 0,0043 | 0,0046 | 0,11 |
| Golgi phosphoprotein 3 OS=Mus musculus GN=Golph3 PE=1 SV=1 | Q9CRA5 | 0,0060 | 0,0032 | 0,0046 | 0,82 |
| Serine/threonine-protein phosphatase 2A catalytic subunit beta isoform OS=Mus musculus GN=Ppp2cb PE=1 SV=1 | P62715 | 0,0038 | 0,0053 | 0,0046 | -0,56 |
| Electroneutral sodium bicarbonate exchanger 1 OS=Mus musculus GN=Slc4a8 PE=2 SV=1 | Q8JZR6 | 0,0071 | 0,0021 | 0,0045 | 1,69 |
| Rho-related GTP-binding protein RhoF OS=Mus musculus GN=Rhof PE=2 SV=1 | Q8BYP3 | 0,0044 | 0,0045 | 0,0045 | -0,09 |
| AP-1 complex subunit beta-1 OS=Mus musculus GN=Ap1b1 PE=1 SV=2 | O35643 | 0,0049 | 0,0041 | 0,0045 | 0,18 |
| Ras-related protein Rab-3D OS=Mus musculus GN=Rab3d PE=1 SV=1 | P35276 | 0,0044 | 0,0045 | 0,0045 | -0,13 |
| 40S ribosomal protein S15a OS=Mus musculus GN=Rps15a PE=2 SV=2 | P62245 | 0,0048 | 0,0041 | 0,0044 | 0,15 |
| Aspartate aminotransferase, mitochondrial OS=Mus musculus GN=Got2 PE=1 SV=1 | P05202 | 0,0057 | 0,0032 | 0,0044 | 0,76 |
| Apolipoprotein O OS=Mus musculus GN=Apoo PE=2 SV=1 | Q9DCZ4 | 0,0046 | 0,0042 | 0,0044 | 0,07 |
| Myosin-8 OS=Mus musculus GN=Myh8 PE=2 SV=2 | P13542 | 0,0041 | 0,0047 | 0,0044 | -0,26 |
| Glial fibrillary acidic protein OS=Mus musculus GN=Gfap PE=1 SV=4 | P03995 | 0,0064 | 0,0024 | 0,0044 | 1,38 |
| Cytosolic non-specific dipeptidase OS=Mus musculus GN=Cndp2 PE=1 SV=1 | Q9D1A2 | 0,0057 | 0,0031 | 0,0044 | 0,79 |
| Regulator of G-protein signaling 14 OS=Mus musculus GN=Rgs14 PE=1 SV=2 | P97492 | 0,0023 | 0,0063 | 0,0043 | -1,50 |
| D-3-phosphoglycerate dehydrogenase OS=Mus musculus GN=Phgdh PE=1 SV=3 | Q61753 | 0,0038 | 0,0049 | 0,0043 | -0,43 |
| Probable arginine--tRNA ligase, mitochondrial OS=Mus musculus GN=Rars2 PE=1 SV=1 | Q3U186 | 0,0040 | 0,0046 | 0,0043 | -0,29 |
| Potassium-transporting ATPase alpha chain 1 OS=Mus musculus GN=Atp4a PE=1 SV=3 | Q64436 | 0,0031 | 0,0055 | 0,0043 | -0,89 |
| Ninein OS=Mus musculus GN=Nin PE=2 SV=3 | Q61043 | 0,0057 | 0,0029 | 0,0043 | 0,91 |
| DnaJ homolog subfamily A member 3, mitochondrial OS=Mus musculus GN=Dnaja3 PE=1 SV=1 | Q99M87 | 0,0042 | 0,0043 | 0,0043 | -0,12 |
| Chromodomain-helicase-DNA-binding protein 4 OS=Mus musculus GN=Chd4 PE=1 SV=1 | Q6PDQ2 | 0,0042 | 0,0043 | 0,0042 | -0,10 |
| Medium-chain specific acyl-CoA dehydrogenase, mitochondrial OS=Mus musculus GN=Acadm PE=1 SV=1 | P45952 | 0,0041 | 0,0043 | 0,0042 | -0,14 |
| Plexin-B2 OS=Mus musculus GN=Plxnb2 PE=1 SV=1 | B2RXS4 | 0,0049 | 0,0036 | 0,0042 | 0,38 |
| [Pyruvate dehydrogenase (acetyl-transferring)] kinase isozyme 3, mitochondrial OS=Mus musculus GN=Pdk3 PE=2 SV=1 | Q922H2 | 0,0036 | 0,0048 | 0,0042 | -0,49 |
| Ras-related protein Ral-A OS=Mus musculus GN=Rala PE=1 SV=1 | P63321 | 0,0046 | 0,0038 | 0,0042 | 0,20 |
| Vesicular integral-membrane protein VIP36 OS=Mus musculus GN=Lman2 PE=2 SV=2 | Q9DBH5 | 0,0050 | 0,0033 | 0,0041 | 0,54 |
| Peroxisome biogenesis factor 1 OS=Mus musculus GN=Pex1 PE=1 SV=2 | Q5BL07 | 0,0049 | 0,0033 | 0,0041 | 0,52 |
| 40S ribosomal protein S17 OS=Mus musculus GN=Rps17 PE=1 SV=2 | P63276 | 0,0034 | 0,0047 | 0,0041 | -0,53 |
| Succinyl-CoA:3-ketoacid coenzyme A transferase 1, mitochondrial OS=Mus musculus GN=Oxct1 PE=1 SV=1 | Q9D0K2 | 0,0048 | 0,0033 | 0,0040 | 0,47 |
| Type 2 phosphatidylinositol 4,5-bisphosphate 4-phosphatase OS=Mus musculus GN=Tmem55a PE=1 SV=1 | Q9CZX7 | 0,0048 | 0,0033 | 0,0040 | 0,48 |
| Ras-related protein Rab-9A OS=Mus musculus GN=Rab9a PE=1 SV=1 | Q9R0M6 | 0,0037 | 0,0043 | 0,0040 | -0,27 |
| Gamma-aminobutyric acid receptor subunit alpha-5 OS=Mus musculus GN=Gabra5 PE=1 SV=1 | Q8BHJ7 | 0,0031 | 0,0048 | 0,0040 | -0,69 |
| Guanine nucleotide-binding protein G(I)/G(S)/G(O) subunit gamma-10 OS=Mus musculus GN=Gng10 PE=3 SV=1 | Q9CXP8 | 0,0037 | 0,0043 | 0,0040 | -0,28 |
| Actin-related protein 3B OS=Mus musculus GN=Actr3b PE=2 SV=1 | Q641P0 | 0,0047 | 0,0033 | 0,0040 | 0,44 |

| | | | | | |
|---|---|---|---|---|---|
| Calcium-binding mitochondrial carrier protein SCaMC-2 OS=Mus musculus GN=Slc25a25 PE=2 SV=1 | A2ASZ8 | 0,0040 | 0,0039 | 0,0039 | -0,06 |
| Sodium channel subunit beta-4 OS=Mus musculus GN=Scn4b PE=2 SV=1 | Q7M729 | 0,0037 | 0,0041 | 0,0039 | -0,23 |
| Poly(rC)-binding protein 2 OS=Mus musculus GN=Pcbp2 PE=1 SV=1 | Q61990 | 0,0051 | 0,0026 | 0,0038 | 0,87 |
| Leucyl-cystinyl aminopeptidase OS=Mus musculus GN=Lnpep PE=1 SV=1 | Q8C129 | 0,0044 | 0,0031 | 0,0037 | 0,45 |
| StAR-related lipid transfer protein 3 OS=Mus musculus GN=Stard3 PE=2 SV=1 | Q61542 | 0,0039 | 0,0035 | 0,0037 | 0,11 |
| Syntaxin-binding protein 6 OS=Mus musculus GN=Stxbp6 PE=2 SV=1 | Q8R3T5 | 0,0042 | 0,0033 | 0,0037 | 0,29 |
| Protein-tyrosine kinase 2-beta OS=Mus musculus GN=Ptk2b PE=1 SV=2 | Q9QVP9 | 0,0027 | 0,0046 | 0,0037 | -0,83 |
| Protein rogdi homolog OS=Mus musculus GN=Rogdi PE=2 SV=2 | Q3TDK6 | 0,0041 | 0,0033 | 0,0037 | 0,26 |
| Peroxisomal biogenesis factor 19 OS=Mus musculus GN=Pex19 PE=1 SV=1 | Q8VCI5 | 0,0049 | 0,0026 | 0,0037 | 0,86 |
| Four and a half LIM domains protein 1 OS=Mus musculus GN=Fhl1 PE=1 SV=3 | P97447 | 0,0047 | 0,0027 | 0,0037 | 0,76 |
| Casein kinase I isoform gamma-3 OS=Mus musculus GN=Csnk1g3 PE=1 SV=2 | Q8C4X2 | 0,0038 | 0,0035 | 0,0036 | 0,07 |
| Inositol monophosphatase 1 OS=Mus musculus GN=Impa1 PE=1 SV=1 | O55023 | 0,0043 | 0,0029 | 0,0036 | 0,49 |
| Cysteine desulfurase, mitochondrial OS=Mus musculus GN=Nfs1 PE=2 SV=3 | Q9Z1J3 | 0,0034 | 0,0038 | 0,0036 | -0,23 |
| Transmembrane emp24 domain-containing protein 10 OS=Mus musculus GN=Tmed10 PE=2 SV=1 | Q9D1D4 | 0,0046 | 0,0026 | 0,0036 | 0,77 |
| Protein phosphatase PTC7 homolog OS=Mus musculus GN=Pptc7 PE=2 SV=1 | Q6NVE9 | 0,0035 | 0,0036 | 0,0036 | -0,10 |
| E3 ubiquitin-protein ligase TRIM32 OS=Mus musculus GN=Trim32 PE=1 SV=2 | Q8CH72 | 0,0034 | 0,0036 | 0,0035 | -0,17 |
| RasGAP-activating-like protein 1 OS=Mus musculus GN=Rasal1 PE=2 SV=2 | Q9Z268 | 0,0023 | 0,0046 | 0,0035 | -1,07 |
| Keratin, type I cuticular Ha2 OS=Mus musculus GN=Krt32 PE=2 SV=2 | Q62168 | 0,0015 | 0,0054 | 0,0035 | -1,95 |
| 60S ribosomal protein L23 OS=Mus musculus GN=Rpl23 PE=1 SV=1 | P62830 | 0,0024 | 0,0044 | 0,0034 | -0,94 |
| Beta-enolase OS=Mus musculus GN=Eno3 PE=1 SV=3 | P21550 | 0,0045 | 0,0023 | 0,0034 | 0,87 |
| Peptidyl-tRNA hydrolase 2, mitochondrial OS=Mus musculus GN=Ptrh2 PE=2 SV=1 | Q8R2Y8 | 0,0037 | 0,0031 | 0,0034 | 0,22 |
| Rho-related GTP-binding protein RhoQ OS=Mus musculus GN=Rhoq PE=1 SV=2 | Q8R527 | 0,0049 | 0,0019 | 0,0034 | 1,28 |
| Mitochondrial Rho GTPase 2 OS=Mus musculus GN=Rhot2 PE=2 SV=1 | Q8JZN7 | 0,0037 | 0,0028 | 0,0032 | 0,33 |
| Rho-related GTP-binding protein RhoC OS=Mus musculus GN=Rhoc PE=1 SV=2 | Q62159 | 0,0035 | 0,0030 | 0,0032 | 0,16 |
| Dihydropyrimidinase-related protein 3 OS=Mus musculus GN=Dpysl3 PE=1 SV=1 | Q62188 | 0,0028 | 0,0035 | 0,0032 | -0,39 |
| Raftlin-2 OS=Mus musculus GN=Rftn2 PE=2 SV=3 | Q8CHX7 | 0,0032 | 0,0031 | 0,0032 | -0,02 |
| F-actin-capping protein subunit alpha-1 OS=Mus musculus GN=Capza1 PE=1 SV=4 | P47753 | 0,0043 | 0,0021 | 0,0032 | 0,96 |
| Neurensin-1 OS=Mus musculus GN=Nrsn1 PE=2 SV=1 | P97799 | 0,0040 | 0,0023 | 0,0031 | 0,74 |
| Keratin, type I cytoskeletal 25 OS=Mus musculus GN=Krt25 PE=1 SV=1 | Q8VCW2 | 0,0024 | 0,0037 | 0,0030 | -0,68 |
| Mitogen-activated protein kinase 3 OS=Mus musculus GN=Mapk3 PE=1 SV=5 | Q63844 | 0,0028 | 0,0033 | 0,0030 | -0,29 |
| Tubulin gamma-1 chain OS=Mus musculus GN=Tubg1 PE=1 SV=1 | P83887 | 0,0031 | 0,0030 | 0,0030 | 0,00 |
| Actin-related protein 2/3 complex subunit 4 OS=Mus musculus GN=Arpc4 PE=1 SV=3 | P59999 | 0,0037 | 0,0024 | 0,0030 | 0,57 |
| 26S proteasome non-ATPase regulatory subunit 5 OS=Mus musculus GN=Psmd5 PE=1 SV=4 | Q8BJY1 | 0,0027 | 0,0032 | 0,0030 | -0,31 |
| MAP6 domain-containing protein 1 OS=Mus musculus GN=Map6d1 PE=1 SV=1 | Q14BB9 | 0,0037 | 0,0022 | 0,0030 | 0,70 |
| Activin receptor type-1C OS=Mus musculus GN=Acvr1c PE=2 SV=3 | Q8K348 | 0,0026 | 0,0032 | 0,0029 | -0,37 |
| Alpha-actinin-4 OS=Mus musculus GN=Actn4 PE=1 SV=1 | P57780 | 0,0059 | 0,0000 | 0,0029 | 5,00 |
| Sodium channel subunit beta-3 OS=Mus musculus GN=Scn3b PE=2 SV=1 | Q8BHK2 | 0,0024 | 0,0030 | 0,0027 | -0,42 |
| Platelet-derived growth factor receptor beta OS=Mus musculus GN=Pdgfrb PE=1 SV=1 | P05622 | 0,0053 | 0,0000 | 0,0026 | 5,00 |
| Sprouty-related, EVH1 domain-containing protein 2 OS=Mus musculus GN=Spred2 PE=1 SV=1 | Q924S7 | 0,0036 | 0,0016 | 0,0026 | 1,08 |
| Glutathione S-transferase Mu 2 OS=Mus musculus GN=Gstm2 PE=1 SV=2 | P15626 | 0,0024 | 0,0027 | 0,0026 | -0,27 |
| Potassium voltage-gated channel subfamily C member 4 OS=Mus musculus GN=Kcnc4 PE=2 SV=1 | Q8R1C0 | 0,0037 | 0,0013 | 0,0025 | 1,43 |
| H-2 class I histocompatibility antigen, D-K alpha chain OS=Mus musculus GN=H2-D1 PE=1 SV=1 | P14426 | 0,0034 | 0,0016 | 0,0025 | 1,03 |
| NADH dehydrogenase (ubiquinone) complex I, assembly factor 6 OS=Mus musculus GN=Ndufaf6 PE=1 SV=1 | A2AIL4 | 0,0022 | 0,0026 | 0,0024 | -0,30 |
| Apoptotic protease-activating factor 1 OS=Mus musculus GN=Apaf1 PE=1 SV=3 | O88879 | 0,0024 | 0,0023 | 0,0024 | -0,02 |
| Glutamate receptor 4 OS=Mus musculus GN=Gria4 PE=1 SV=2 | Q9Z2W8 | 0,0031 | 0,0017 | 0,0024 | 0,78 |
| Contactin-associated protein like 5-2 OS=Mus musculus GN=Cntnap5b PE=2 SV=1 | Q0V8T8 | 0,0029 | 0,0017 | 0,0023 | 0,68 |
| Receptor-type tyrosine-protein kinase FLT3 OS=Mus musculus GN=Flt3 PE=1 SV=1 | Q00342 | 0,0035 | 0,0010 | 0,0022 | 1,81 |
| Dihydropyrimidinase-related protein 4 OS=Mus musculus GN=Dpysl4 PE=1 SV=1 | O35098 | 0,0021 | 0,0022 | 0,0022 | -0,18 |
| Potassium voltage-gated channel subfamily A member 5 OS=Mus musculus GN=Kcna5 PE=2 SV=2 | Q61762 | 0,0022 | 0,0020 | 0,0021 | 0,02 |
| Keratin, type II cuticular Hb4 OS=Mus musculus GN=Krt84 PE=2 SV=2 | Q99M73 | 0,0018 | 0,0023 | 0,0020 | -0,41 |
| Leucine-rich repeat and immunoglobulin-like domain-containing nogo receptor-interacting protein 2 OS=Mus musculus GN=Lingo2 PE=2 SV=1 | Q3URE9 | 0,0023 | 0,0018 | 0,0020 | 0,28 |
| Golgi-associated plant pathogenesis-related protein 1 OS=Mus musculus GN=Glipr2 PE=2 SV=3 | Q9CYL5 | 0,0038 | 0,0000 | 0,0019 | 5,00 |
| Glycogen phosphorylase, liver form OS=Mus musculus GN=Pygl PE=1 SV=4 | Q9ET01 | 0,0021 | 0,0016 | 0,0019 | 0,37 |
| Probable phospholipid-transporting ATPase IC OS=Mus musculus GN=Atp8b1 PE=1 SV=2 | Q148W0 | 0,0000 | 0,0035 | 0,0018 | -5,00 |
| Glutathione S-transferase Mu 1 OS=Mus musculus GN=Gstm1 PE=1 SV=2 | P10649 | 0,0018 | 0,0017 | 0,0018 | -0,02 |
| E3 ubiquitin-protein ligase MARCH1 OS=Mus musculus GN=March1 PE=1 SV=2 | Q6NZQ8 | 0,0000 | 0,0034 | 0,0017 | -5,00 |
| Macrophage colony-stimulating factor 1 receptor OS=Mus musculus GN=Csf1r PE=1 SV=3 | P09581 | 0,0012 | 0,0020 | 0,0016 | -0,85 |
| Alsin OS=Mus musculus GN=Als2 PE=1 SV=3 | Q920R0 | 0,0000 | 0,0031 | 0,0016 | -5,00 |
| Ras-related protein Rab-39A OS=Mus musculus GN=Rab39a PE=2 SV=1 | Q8BHD0 | 0,0015 | 0,0012 | 0,0013 | 0,23 |
| Anion exchange protein 3 OS=Mus musculus GN=Slc4a3 PE=1 SV=2 | P16283 | 0,0014 | 0,0012 | 0,0013 | 0,22 |
| Synaptotagmin-9 OS=Mus musculus GN=Syt9 PE=1 SV=2 | Q9R0N9 | 0,0015 | 0,0008 | 0,0012 | 0,79 |
| Ras-related protein Rab-13 OS=Mus musculus GN=Rab13 PE=1 SV=1 | Q9DD03 | 0,0009 | 0,0012 | 0,0011 | -0,48 |
| Ephrin type-A receptor 2 OS=Mus musculus GN=Epha2 PE=1 SV=3 | Q03145 | 0,0007 | 0,0013 | 0,0010 | -0,90 |
| Tubulin beta-1 chain OS=Mus musculus GN=Tubb1 PE=1 SV=1 | A2AQ07 | 0,0014 | 0,0006 | 0,0010 | 1,06 |
| GTP-binding nuclear protein Ran, testis-specific isoform OS=Mus musculus GN=Rasl2-9 PE=2 SV=1 | Q61820 | 0,0019 | 0,0000 | 0,0009 | 5,00 |
| Keratin, type II cytoskeletal 7 OS=Mus musculus GN=Krt7 PE=1 SV=1 | Q9DCV7 | 0,0009 | 0,0003 | 0,0006 | 1,39 |
| Keratin, type II cytoskeletal 8 OS=Mus musculus GN=Krt8 PE=1 SV=4 | P11679 | 0,0005 | 0,0006 | 0,0005 | -0,35 |
| Tyrosine-protein kinase Lyn OS=Mus musculus GN=Lyn PE=1 SV=4 | P25911 | 0,0008 | 0,0000 | 0,0004 | 5,00 |

## 8.2 Plasmid sequences

### pAM/CAG-N-SF-CB1-WPRE-bGHpA (pAM-N-SF-CB1)

tagctgcgcgctcgctcgctcactgaggccgcccgggcaaagcccgggcgtcgggcgacctttggtcgcccggcctcagtgagcga
gcgagcgcgcagagagggagtggccaactccatcactaggggttccttgtagttaatgattaacccgccatgctacttatctacgtagc
catgctctaggtaccattgacgtcaataatgacgtatgttcccatagtaacgccaatagggactttccattgacgtcaatgggtggactatt
tacggtaaactgcccacttggcagtacatcaagtgtatcatatgccaagtacgccccctattgacgtcaatgacggtaaatggcccgcct
ggcattatgcccagtacatgaccttatgggactttcctacttggcagtacatctacgtattagtcatcgctattaccatggtcgaggtgagc
cccacgttctgcttcactctccccatctcccccccctccccacccccaattttgtatttatttatttttttaattattttgtgcagcgatgggggcg
gggggggggggggggcgcgcgccaggcggggcggggcggggcgaggggcggggcggggcgaggcggagaggtgcggc
ggcagccaatcagagcggcgcgctccgaaagtttccttttatggcgaggcggcggcggcggccctataaaaagcgaagcgcgc
ggcgggcgggagtcgctgcgacgctgccttcgccccgtgccccgctccgccgccgcctcgcgccgcccgccccggctctgactgacc
gcgttactcccacaggtgagcgggcgggacggcccttctcctccgggctgtaattagcgcttggtttaatgacggcttgtttcttttctgt
ggctgcgtgaaagccttgaggggctccgggagggcccttttgtgcgggggggagcggctcggggctgtccgcgggggggacggctgc
cttcgggggggacggggcagggcggggttcggcttctggcgtgtgaccggcggctctagagcctctgctaaccatgttcatgccttct
tctttttcctacagctcctgggcaacgtgctggttattgtgctgtctcatcattttggcaaagaattggatccatgtacccgtacgacgtccc
ggactacgcgaagtcgatcctagatggccttgcagacaccaccttccgtaccatcaccacagacctcctctacgtgggctcgaatgacat
tcagtatgaagatatcaaaggagacatggcatccaaattaggatacttcccacagaaattccctctaacttccttcaggggtagtcccttcc
aagaaaagatgaccgcaggagacaacggaggaaccggtgattacaaggacgatgacgacaaaggcagcgcttctgcctggagcca
ccctcaattcgaaaagggtggaggcagtggaggagggtcaggtggaggctcctggtcccatccccagtttgagaaaggggcaaccg
gtggaggctccccgttggtcccagcaggagacacaacaaacattacagagttctataacaagtctctctcgtcgttcaaggagaatgag
gagaacatccagtgtggggagaactttatggacatggagtgctttatgattctgaatcccagccagcagctggccatcgctgtactgtcc
ctcacactgggcaccttcacggttctggagaacctactggtgctgtgtgtcatcctgcactcccgcagtctccgatgcaggccttcctacc
acttcatcggcagcctggcagtggccgacctcctgggaagtgtcatttttgtgtacagctttgttgacttccatgtattccaccgtaaagac
agccccaatgtgtttctgttcaaactgggtggggttacagcctccttcacagcttctgtgggcagcctgttcctcacagccatcgacaggt
acatatccattcacaggcctctggcctataagaggatcgtcaccaggcccaaggccgttgtggccttttgcctgatgtggactatcgcaat
agtaatcgctgtgttgcctctcctgggctggaactgcaagaagctgcaatctgtttgctcggacattttcccactcattgacgagacctacc
tgatgttctggattggggtgaccagtgtgctgctgttcattgtgtacgcgtacatgtacattctctggaaggctcacagccacgcggt
ccgcatgattcagcgtgggacccagaagagcatcatcatccacacgtcagaagacggcaaggtgcaggtgacccggcctgaccaag
cccgcatggacattaggctggccaaaaccctggttctgatcctggtggtgttgatcatctgctggggccctctgcttgcgatcatggtgta
tgacgtcttcgggaagatgaacaagcttatcaagacggtgtttgccttctgcagtatgctctgcctgctgaactccaccgtgaaccccatc
atctatgctctgaggagcaaggacctgagacatgctttccgaagcatgttcccttcgtgcgaaggcaccgcacagcctctagacaacag
catgggggactcagactgcctgcacaagcacgccaacaacacagccagcatgcacagggccgcggagagctgcatcaagagcacc
gttaagatcgcgaaggtgaccatgtctgtgtccacagacacgtccgccgaggctctgtgagctgctgcttttgtgaattcgatatcaagc
ttatcgataatcaacctctggattacaaaatttgtgaaagattgactggtattcttaactatgttgctccttttacgctatgtggatacgctgct
ttaatgcctttgtatcatgctattgcttcccgtatggctttcattttctcctccttgtataaatcctggttgctgtctctttatgaggagttgtggc
ccgttgtcaggcaacgtggcgtggtgtgcactgtgtttgctgacgcaacccccactggttggggcattgccaccacctgtcagctccttt
ccgggactttcgctttccccctccctattgccacggcggaactcatcgccgcctgccttgcccgctgctggacaggggctcggctgttgg
gcactgacaattccgtggtgttgtcggggaaatcatcgtcctttccttggctgctcgcctgtgttgccacctggattctgcgcgggacgtc
cttctgctacgtcccttcggccctcaatccagcggaccttccttcccgcggcctgctgccggctctgcggcctcttccgcgtcttcgccttc
gccctcagacgagtcggatctccctttgggccgcctccccgcatcgataccgtcgactcgctgatcagcctcgactgtgccttctagttgc
cagccatctgttgtttgcccctcccccgtgccttccttgaccctggaaggtgccactcccactgtccttttcctaataaaatgaggaaattgca
tcgcattgtctgagtaggtgtcattctattctgggggggtggggtggggcaggacagcaagggggaggattgggaagacaatagcag
gcatgctggggatgcggtgggctctatggcttctgaggcggaaagaaccagctggggctcgactagagcatggctacgtagataagt
agcatggcgggttaatcattaactacaaggaacccctagtgatggagttggccactccctctctgcgcgctcgctcgctcactgaggcc
gggcgaccaaaggtcgcccgacgcccgggctttgcccgggcggcctcagtgagcgagcgagcgcgcagagcttttgcaaaagcct

aggcctccaaaaaagcctcctcactacttctggaatagctcagaggccgaggcggcctcggcctctgcataaataaaaaaaattagtca
gccatggggcggagaatgggcggaactgggcggagttaggggcgggatgggcggagttaggggcgggactatggttgctgact
aattgagatgcatgctttgcatacttctgcctgctggggagcctggggactttccacacctggttgctgactaattgagatgcatgctttgc
atacttctgcctgctggggagcctggggactttccacaccctaactgacacacattccacagctgcattaatgaatcggccaacgcgcgg
ggagaggcggtttgcgtattgggcgctcttccgcttcctcgctcactgactcgctgcgctcggtcgttcggctgcggcgagcggtatca
gctcactcaaaggcggtaatacggttatccacagaatcaggggataacgcaggaaagaacatgtgagcaaaaggccagcaaaaggc
caggaaccgtaaaaaggccgcgttgctggcgtttttccataggctccgccccccctgacgagcatcacaaaaatcgacgctcaagtcaga
ggtggcgaaacccgacaggactataaagataccaggcgtttcccccctggaagctccctcgtgcgctctcctgttccgaccctgccgctta
ccggatacctgtccgcctttctcccttcgggaagcgtggcgctttctcatagctcacgctgtaggtatctcagttcggtgtaggtcgttcgc
tccaagctgggctgtgtgcacgaacccccccgttcagcccgaccgctgcgccttatccggtaactatcgtcttgagtccaacccggtaaga
cacgacttatcgccactggcagcagccactggtaacaggattagcagagcgaggtatgtaggcggtgctacagagttcttgaagtggt
ggcctaactacggctacactagaagaacagtatttggtatctgcgctctgctgaagccagttaccttcggaaaaagagttggtagctctt
gatccggcaaacaaaccaccgctggtagcggtggttttttttgtttgcaagcagcagattacgcgcagaaaaaaaggatctcaagaagat
cctttgatcttttctacggggtctgacgctcagtggaacgaaaactcacgttaagggattttggtcatgagattatcaaaaaggatcttcac
ctagatccttttaaattaaaaatgaagttttaaatcaatctaaagtatatatgagtaaacttggtctgacagttaccaatgcttaatcagtgag
gcacctatctcagcgatctgtctatttcgttcatccatagttgcctgactccccgtcgtgtagataactacgatacgggagggcttaccatct
ggccccagtgctgcaatgataccgcgagacccacgctcaccggctccagatttatcagcaataaaccagccagccggaagggccgag
cgcagaagtggtcctgcaactttatccgcctccatccagtctattaattgttgccgggaagctagagtaagtagttcgccagttaatagttt
gcgcaacgttgttgccattgctacaggcatcgtggtgtcacgctcgtcgtttggtatggcttcattcagctccggttcccaacgatcaagg
cgagttacatgatcccccatgttgtgcaaaaaagcggttagctccttcggtcctccgatcgttgtcagaagtaagttggccgcagtgttat
cactcatggttatggcagcactgcataattctcttactgtcatgccatccgtaagatgcttttctgtgactggtgagtactcaaccaagtcatt
ctgagaatagtgtatgcggcgaccgagttgctcttgcccggcgtcaatacgggataataccgcgccacatagcagaactttaaaagtgc
tcatcattggaaaacgttcttcggggcgaaaactctcaaggatcttaccgctgttgagatccagttcgatgtaacccactcgtgcacccaa
ctgatcttcagcatcttttactttcaccagcgtttctgggtgagcaaaaacaggaaggcaaaatgccgcaaaaaagggaataagggcga
cacggaaatgttgaatactcatactcttccttttcaatattattgaagcatttatcagggttattgtctcatgagcggatacatatttgaatgt
atttagaaaaataaacaaataggggttccgcgcacatttccccgaaaagtgccacctgacgtctaagaaaccattattatcatgacattaa
cctataaaaataggcgtatcacgaggccctttcgtctcgcgcgtttcggtgatgacggtgaaaacctctgacacatgcagctcccggag
acggtcacagcttgtctgtaagcggatgccgggagcagacaagcccgtcagggcgcgtcagcgggtgttggcgggtgtcggggct
ggcttaactatgcggcatcagagcagattgtactgagagtgcaccattcgacgctctcccttatgcgactcctgcattaggaagcagccc
agtagtaggttgaggccgttgagcaccgccgccgcaaggaatggtgcatgcaaggagatggcgcccaacagtcccccggccacgg
ggcctgccaccatacccacgccgaaacaagcgctcatgagcccgaagtggcgagcccgatcttccccatcggtgatgtcggcgatata
ggcgccagcaaccgcacctgtggcgccggtgatgccggccacgatgcgtccggcgtagaggatctggctagcgatgaccctgctga
ttggttcgctgaccatttccgggtgcgggacggcgttaccagaaactcagaaggttcgtccaaccaaaccgactctgacggcagtttac
gagagagatgatagggtctgcttcagtaagccagatgctacacaattaggcttgtacatattgtcgttagaacgcggctacaattaatac
ataaccttatgtatcatacacatacgatttaggtgacactatagaatacacggaattaattc

**pAM/CAG-CB1-SF-C-WPRE-bGHpA (pAM-CB1-SF-C)**

tagctgcgcgctcgctcgctcactgaggccgcccgggcaaagcccgggcgtcgggcgacctttggtcgcccggcctcagtgagcga
gcgagcgcgcagagagggagtggccaactccatcactaggggttccttgtagttaatgattaacccgccatgctacttatctacgtagc
catgctctaggtaccattgacgtcaataatgacgtatgttcccatagtaacgccaatagggactttccattgacgtcaatgggtggactatt
tacggtaaactgcccacttggcagtacatcaagtgtatcatatgccaagtacgccccctattgacgtcaatgacggtaaatggcccgcct
ggcattatgcccagtacatgaccttatgggactttcctacttggcagtacatctacgtattagtcatcgctattaccatggtcgaggtgagc
cccacgttctgcttcactctccccatctccccccccctccccacccccaattttgtatttatttatttttttaattattttgtgcagcgatgggggcg
gggggggggggggggcgcgcgccaggcggggcggggcggggcgaggggcggggcggggcgaggcggagaggtgcggc
ggcagccaatcagagcggcgcgctccgaaagtttccttttatggcgaggcggcggcggcggccctataaaaagcgaagcgcgc
ggcgggcgggagtcgctgcgacgctgccttcgccccgtgccccgctccgccgccgcctcgcgccgcccgccccggctctgactgacc
gcgttactcccacaggtgagcgggcgggacggcccttctcctccgggctgtaattagcgcttggtttaatgacggcttgtttcttttctgt

ggctgcgtgaaagccttgaggggctccgggagggccctttgtgcgggggagcggctcggggctgtccgcgggggacggctgc
cttcgggggggacggggcagggcggggttcggcttctggcgtgtgaccggcggctctagagcctctgctaaccatgttcatgccttct
tctttttcctacagctcctgggcaacgtgctggttattgtgctgtctcatcattttggcaaagaattggatccactcgagtggagctcggatc
ctcagtcacgttgagcctggcctaatcaaagactgaggttatgaagtcgatcttagacggccttgcagataccaccttccgtaccatcacc
acagacctcctctacgtgggctcaaatgacattcagtacgaagatatcaaaggagacatggcatccaaattaggatacttcccacagaaa
ttccctctaacttccttcaggggtagtcccttccaagaaaagatgacggcaggagacaactccccgttggttccagcaggagacacaac
caacattacagagttctataacaagtctctctcatcgttcaaggagaacgaggacaacatccagtgtggggagaattttatggacatgga
gtgcttcatgattctgaatcccagccagcagctggccatcgctgtcctgtccctcaccctgggcaccttcacggttctggagaacctgctg
gtgctatgtgtcatccttcactcccgcagtctccgatgcaggccttcctaccacttcattggcagcctggcggtggccgatctcctgggaa
gtgtcatctttgtctacagctttgttgacttccacgtgttccaccgcaaagatagtcccaatgtgtttctgttcaaactgggtggggttaccg
cctccttcacagcatctgtgggcagcctgttcctcacggccatcgacaggtacatatccattcacaggcctctggcctataagaggatcgt
caccaggcccaaggccgtagtggccttttgcttgatgtggactattgcaatagtaattgctgtgttgcctctcctgggctggaactgcaag
aagctgcaatctgtttgctcagacatcttcccactcattgatgaaacctacctgatgttctggatcggagtcaccagtgtgctgttgctgttc
attgtgtatgcatacatgtacattctctggaaggctcacagccacgcagttcgcatgatccagcgtggaacccagaaaagcatcatcattc
acacctcagaagatggcaaggtgcaggtgacacggcctgaccaagcccgcatggacattaggctggccaaaaccctggttctgatcct
ggtggtgttgatcatctgctggggccctctgcttgcgatcatggtgtatgatgtctttgggaagatgaacaagcttatcaagacggtgttt
gccttctgtagtatgctctgcctgctgaactccaccgtgaaccccatcatctatgctctgaggagcaaggacctgagacatgctttccgca
gcatgttcccttcatgtgaaggcactgcgcagcctctagataacagcatgggggactcagactgcctgcacaagcacgccaataacaca
gccagcatgcacagggccgcggaaagctgcatcaagagcactgttaagatcgccaaggtgaccatgtctgtgtccacagacacgtctg
ccgaggctctgggcggcggcacggtaccgcgggcccgggatccaccggtctccgcttggagccaccctcagtttgagaaaggcggt
gggtcaggaggaggctctggaggtgggagctggtcccatccccaattcgagaaaggcgccagtggggaagactacaaggatgacg
acgataagtgagcggccgctcgagcatgcatctagagggccctattctatagtgtcacctaaatgctagagctcgcgactagtcgattc
gaattcgatatcaagcttatcgataatcaacctctggattacaaaatttgtgaaagattgactggtattcttaactatgttgctccttttacgct
atgtggatacgctgctttaatgcctttgtatcatgctattgcttcccgtatggctttcattttctcctccttgtataaatcctggttgctgtctctttt
atgaggagttgtggcccgttgtcaggcaacgtggcgtggtgtgcactgtgtttgctgacgcaacccccactggttggggcattgccacc
acctgtcagctcctttccgggactttcgctttcccccctccctattgccacggcggaactcatcgccgcctgccttgcccgctgctggacagg
ggctcggctgttgggcactgacaattccgtggtgttgtcggggaaatcatcgtcctttccttggctgctcgcctgtgttgccacctggatt
ctgcgcgggacgtccttctgctacgtcccttcggccctcaatccagcggaccttccttcccgcggcctgctgccggctctgcggcctcttc
cgcgtcttcgccttcgccctcagacgagtcggatctccctttgggccgcctccccgcatcgataccgtcgactcgctgatcagcctcgact
gtgccttctagttgccagccatctgttgtttgcccctcccccgtgccttccttgaccctggaaggtgccactcccactgtcctttcctaataaa
atgaggaaattgcatcgcattgtctgagtaggtgtcattctattctgggggggtggggtggggcaggacagcaagggggaggattgg
gaagacaatagcaggcatgctggggatgcggtgggctctatggcttctgaggcggaaagaaccagctggggctcgactagagcatg
gctacgtagataagtagcatggcgggttaatcattaactacaaggaacccctagtgatggagttggccactccctctctgcgcgctcgct
cgctcactgaggccgggcgaccaaaggtcgcccgacgcccgggctttgcccgggcggcctcagtgagcgagcgagcgcgcagag
ctttttgcaaaagcctaggcctccaaaaaagcctcctcactacttctggaatagctcagaggccgaggcggcctcggcctctgcataaat
aaaaaaaattagtcagccatggggcggagaatgggcggaactgggcggagttaggggcgggatgggcggagttaggggcggga
ctatggttgctgactaattgagatgcatgctttgcatacttctgcctgctggggagcctggggactttccacacctggttgctgactaattg
agatgcatgctttgcatacttctgcctgctggggagcctggggactttccacaccctaactgacacacattccacagctgcattaatgaat
cggccaacgcgcggggagaggcggtttgcgtattgggcgctcttccgcttcctcgctcactgactcgctgcgctcggtcgttcggctgc
ggcgagcggtatcagctcactcaaaggcggtaatacggttatccacagaatcaggggataacgcaggaaagaacatgtgagcaaaa
ggccagcaaaaggccaggaaccgtaaaaaggccgcgttgctggcgtttttccataggctccgccccccctgacgagcatcacaaaaatc
gacgctcaagtcagaggtggcgaaacccgacaggactataaagataccaggcgtttcccccctggaagctccctcgtgcgctctcctgtt
ccgaccctgccgcttaccggatacctgtccgcctttctcccttcgggaagcgtggcgctttctatagctcacgctgtaggtatctcagttc
ggtgtaggtcgttcgctccaagctgggctgtgtgcacgaacccccccgttcagcccgaccgctgcgccttatccggtaactatcgtcttga
gtccaacccggtaagacacgacttatcgccactggcagcagccactggtaacaggattagcagagcgaggtatgtaggcggtgctac
agagttcttgaagtggtggcctaactacggctacactagaagaacagtatttggtatctgcgctctgctgaagccagttaccttcggaaa
aagagttggtagctcttgatccggcaaacaaaccaccgctggtagcggtggttttttgtttgcaagcagcagattacgcgcagaaaaa
aaggatctcaagaagatcctttgatcttttctacggggtctgacgctcagtggaacgaaaactcacgttaagggattttggtcatgagatt
atcaaaaaggatcttcacctagatccttttaaattaaaaatgaagttttaaatcaatctaaagtatatatgagtaaacttggtctgacagttac
caatgcttaatcagtgaggcacctatctcagcgatctgtctatttcgttcatccatagttgcctgactccccgtcgtgtagataactacgata
cgggagggcttaccatctggccccagtgctgcaatgataccgcgagacccacgctcaccggctccagatttatcagcaataaaccagcc
agccggaagggccgagcgcagaagtggtcctgcaactttatccgcctccatccagtctattaattgttgccgggaagctagagtaagta

gttcgccagttaatagtttgcgcaacgttgttgccattgctacaggcatcgtggtgtcacgctcgtcgtttggtatggcttcattcagctcc
ggttcccaacgatcaaggcgagttacatgatcccccatgttgtgcaaaaaagcggttagctccttcggtcctccgatcgttgtcagaagt
aagttggccgcagtgttatcactcatggttatggcagcactgcataattctcttactgtcatgccatccgtaagatgcttttctgtgactggt
gagtactcaaccaagtcattctgagaatagtgtatgcggcgaccgagttgctcttgcccggcgtcaatacgggataataccgcgccaca
tagcagaactttaaaagtgctcatcattggaaaacgttcttcggggcgaaaactctcaaggatcttaccgctgttgagatccagttcgatg
taacccactcgtgcacccaactgatcttcagcatcttttactttcaccagcgtttctgggtgagcaaaaacaggaaggcaaaatgccgcaa
aaaagggaataagggcgacacggaaatgttgaatactcatactcttccttttcaatattattgaagcatttatcagggttattgtctcatga
gcggatacatatttgaatgtatttagaaaaataaacaaatagggttccgcgcacatttccccgaaaagtgccacctgacgtctaagaaa
ccattattatcatgacattaacctataaaaataggcgtatcacgaggccctttcgtctcgcgcgtttcggtgatgacggtgaaaacctctga
cacatgcagctcccggagacggtcacagcttgtctgtaagcggatgccgggagcagacaagcccgtcagggcgcgtcagcgggtgt
tggcgggtgtcggggctggcttaactatgcggcatcagagcagattgtactgagagtgcaccattcgacgctctcccttatgcgactcct
gcattaggaagcagcccagtagtaggttgaggccgttgagcaccgccgccgcaaggaatggtgcatgcaaggagatggcgcccaac
agtcccccggccacggggcctgccaccatacccacgccgaaacaagcgctcatgagcccgaagtggcgagcccgatcttccccatcg
gtgatgtcggcgatataggcgccagcaaccgcacctgtggcgccggtgatgccggccacgatgcgtccggcgtagaggatctggct
agcgatgaccctgctgattggttcgctgaccatttccgggtgcgggacggcgttaccagaaactcagaaggttcgtccaaccaaaccg
actctgacggcagtttacgagagagatgatagggtctgcttcagtaagccagatgctacacaattaggcttgtacatattgtcgttagaa
cgcggctacaattaatacataaccttatgtatcatacacatacgatttaggtgacactatagaatacacggaattaattc

**pAM/CAG-Stop-N-SF-CB1-WPRE-bGHpA (pAM-Stop-N-SF-CB1)**

tagctgcgcgctcgctcgctcactgaggccgcccgggcaaagcccgggcgtcgggcgacctttggtcgcccggcctcagtgagcga
gcgagcgcgcagagagggagtggccaactccatcactaggggttccttgtagttaatgattaacccgccatgctacttatctacgtagc
catgctctaggtacctaatatcacaaactggaaatgtctatcaatatatagttgctctagttattaatagtaatcaattacggggtcattagtt
catagcccatatatggagttccgcgttacataacttacggtaaatggcccgcctggctgaccgcccaacgacccccgcccattgacgtca
ataatgacgtatgttcccatagtaacgccaatagggactttccattgacgtcaatgggtggactatttacggtaaactgcccacttggcag
tacatcaagtgtatcatatgccaagtacgccccctattgacgtcaatgacggtaaatggcccgcctggcattatgcccagtacatgacctt
atgggactttcctacttggcagtacatctacgtattagtcatcgctattaccatggtcgaggtgagccccacgttctgcttcactctccccat
ctccccccccctccccacccccaattttgtatttatttatttttttaattattttgtgcagcgatgggggcgggggggggggggggcgcgcg
ccaggcggggcggggcggggcgaggggcggggcggggcgaggcggagaggtgcggcggcagccaatcagagcggcgcgct
ccgaaagtttccttttatggcgaggcggcggcggcggccctataaaaagcgaagcgcgcggcgggcgggagtcgctgcgacg
ctgccttcgccccgtgccccgctccgccgccgcctcgcgccgcccgccccggctctgactgaccgcgttactcccacaggtgagcggg
cgggacggcccttctcctccgggctgtaattagcgcttggtttaatgacggcttgtttcttttctgtggctgcgtgaaagccttgaggggc
tccgggagggcccttttgtgcgggggggagcggctcggggctgtccgcgggggggacggctgccttcgggggggacggggcagggc
ggggttcggcttctggcgtgtgaccggcggctctagagcctctgctaaccatgttcatgccttcttctttttcctacagctcctgggcaacg
tgctggttattgtgctgtctcatcattttggcaaagaaatcataacttcgtatagcatacattatacgaagttatgcaataaaaagacagaat
aaaacgcacggtgttgggtcgtttgttcataaacgcggggttcggtcccaggaataaaatatctttatttttcattacatctgtgtgttggttt
tttgtgtgaatcgatagtactaacatacgctctccatcaaaacaaaacgaaacaaaacaaactagcaaaataggctgtccccagtgcaag
tgcaggtgccagaacatttctctataacttcgtatagcatacattatacgaagttatttaattaaatggacagcaaaggttcgtcgcagaaa
gggtcccgcctgctcctgctgctggtggtgtcaaatctactcttgtgccagggtgtggtctccggtaccgagctcggatccatgtacccg
tacgacgtcccggactacgcgaagtcgatcctagatggccttgcagacaccaccttccgtaccatcaccacagacctcctctacgtgggc
tcgaatgacattcagtatgaagatatcaaaggagacatggcatccaaattaggatacttcccacagaaattccctctaacttccttcaggg
gtagtcccttccaagaaaagatgaccgcaggagacaacggaggaaccggtgattacaaggacgatgacgacaaaggcagcgcttct
gcctggagccaccctcaattcgaaaagggtggaggcagtggaggagggtcaggtggaggctcctggtcccatccccagtttgagaa
aggggcaaccggtggaggctccccgttggtcccagcaggagacacaacaaacattacagagttctataacaagtctctctcgtcgttca
aggagaatgaggagaacatccagtgtggggagaactttatggacatggagtgctttatgattctgaatcccagccagcagctggccat
cgctgtactgtccctcacactgggcaccttcacggttctggagaacctactggtgctgtgtgtcatcctgcactcccgcagtctccgatgc
aggccttcctaccacttcatcggcagcctggcagtggccgacctcctgggaagtgtcatttttgtgtacagctttgttgacttccatgtattc
caccgtaaagacagccccaatgtgtttctgttcaaactgggtggggttacagcctccttcacagcttctgtgggcagcctgttcctcacag
ccatcgacaggtacatatccattcacaggcctctggcctataagaggatcgtcaccaggcccaaggccgttgtggccttttgcctgatgt
ggactatcgcaatagtaatcgctgtgttgcctctcctgggctggaactgcaagaagctgcaatctgtttgctcggacattttcccactcatt
gacgagacctacctgatgttctggattggggtgaccagtgtgctgctgctgttcattgtgtacgcgtacatgtacattctctggaaggctc

acagccacgcggtccgcatgattcagcgtgggacccagaagagcatcatcatccacacgtcagaagacggcaaggtgcaggtgacc
cggcctgaccaagcccgcatggacattaggctggccaaaaccctggttctgatcctggtggtgttgatcatctgctggggccctctgctt
gcgatcatggtgtatgacgtcttcgggaagatgaacaagcttatcaagacggtgtttgccttctgcagtatgctctgcctgctgaactcca
ccgtgaaccccatcatctatgctctgaggagcaaggacctgagacatgctttccgaagcatgttcccttcgtgcgaaggcaccgcacag
cctctagacaacagcatgggggactcagactgcctgcacaagcacgccaacaacacagccagcatgcacagggccgcggagagctg
catcaagagcaccgttaagatcgcgaaggtgaccatgtctgtgtccacagacacgtccgccgaggctctgtgagctgctgcttttgtga
attcgatatcaagcttatcgataatcaacctctggattacaaaatttgtgaaagattgactggtattcttaactatgttgctccttttacgctat
gtggatacgctgctttaatgcctttgtatcatgctattgcttcccgtatggctttcattttctcctccttgtataaatcctggttgctgtctctttat
gaggagttgtggcccgttgtcaggcaacgtggcgtggtgtgcactgtgtttgctgacgcaacccccactggttggggcattgccacca
cctgtcagctcctttccgggactttcgctttcccctccctattgccacggcggaactcatcgccgcctgccttgcccgctgctggacagg
ggctcggctgttgggcactgacaattccgtggtgttgtcggggaaatcatcgtcctttccttggctgctcgcctgtgttgccacctggatt
ctgcgcgggacgtccttctgctacgtcccttcggccctcaatccagcggaccttccttcccgcggcctgctgccggctctgcggcctcttc
cgcgtcttcgccttcgccctcagacgagtcggatctccctttgggccgcctccccgcatcgataccgtcgactcgctgatcagcctcgact
gtgccttctagttgccagccatctgttgtttgcccctcccccgtgccttccttgaccctggaaggtgccactcccactgtcctttcctaataaa
atgaggaaattgcatcgcattgtctgagtaggtgtcattctattctgggggggtggggtggggcaggacagcaagggggaggattgg
gaagacaatagcaggcatgctggggatgcggtgggctctatggcttctgaggcggaaagaaccagctggggctcgactagagcatg
gctacgtagataagtagcatggcgggttaatcattaactacaaggaacccctagtgatggagttggccactccctctctgcgcgctcgct
cgctcactgaggccgggcgaccaaaggtcgcccgacgcccgggctttgcccgggcggcctcagtgagcgagcgagcgcgcagag
ctttttgcaaaagcctaggcctccaaaaaagcctcctcactacttctggaatagctcagaggccgaggcggcctcggcctctgcataaat
aaaaaaaattagtcagccatggggcggagaatgggcggaactgggcggagttaggggcgggatgggcggagttaggggcgggga
ctatggttgctgactaattgagatgcatgctttgcatacttctgcctgctggggagcctggggactttccacacctggttgctgactaattg
agatgcatgctttgcatacttctgcctgctggggagcctggggactttccacaccctaactgacacacattccacagctgcattaatgaat
cggccaacgcgcggggagaggcggtttgcgtattgggcgctcttccgcttcctcgctcactgactcgctgcgctcggtcgttcggctgc
ggcgagcggtatcagctcactcaaaggcggtaatacggttatccacagaatcaggggataacgcaggaaagaacatgtgagcaaaa
ggccagcaaaaggccaggaaccgtaaaaaggccgcgttgctggcgtttttccataggctccgccccccctgacgagcatcacaaaaatc
gacgctcaagtcagaggtggcgaaacccgacaggactataaagataccaggcgtttcccccctggaagctccctcgtgcgctctcctgtt
ccgaccctgccgcttaccggatacctgtccgcctttctcccttcgggaagcgtggcgctttctatagctcacgctgtaggtatctcagttc
ggtgtaggtcgttcgctccaagctgggctgtgtgcacgaacccccgttcagcccgaccgctgcgccttatccggtaactatcgtcttga
gtccaacccggtaagacacgacttatcgccactggcagcagccactggtaacaggattagcagagcgaggtatgtaggcggtgctac
agagttcttgaagtggtggcctaactacggctacactagaagaacagtatttggtatctgcgctctgctgaagccagttaccttcggaaa
aagagttggtagctcttgatccggcaaacaaaccaccgctggtagcggtggttttttgtttgcaagcagcagattacgcgcagaaaaa
aaggatctcaagaagatcctttgatcttttctacggggtctgacgctcagtggaacgaaaactcacgttaagggattttggtcatgagatt
atcaaaaaggatcttcacctagatccttttaaattaaaaatgaagttttaaatcaatctaaagtatatatgagtaaacttggtctgacagttac
caatgcttaatcagtgaggcacctatctcagcgatctgtctatttcgttcatccatagttgcctgactccccgtcgtgtagataactacgata
cgggagggcttaccatctggccccagtgctgcaatgataccgcgagacccacgctcaccggctccagatttatcagcaataaaccagcc
agccggaagggccgagcgcagaagtggtcctgcaactttatccgcctccatccagtctattaattgttgccgggaagctagagtaagta
gttcgccagttaatagtttgcgcaacgttgttgccattgctacaggcatcgtggtgtcacgctcgtcgtttggtatggcttcattcagctcc
ggttcccaacgatcaaggcgagttacatgatcccccatgttgtgcaaaaaagcggttagctccttcggtcctccgatcgttgtcagaagt
aagttggccgcagtgttatcactcatggttatggcagcactgcataattctcttactgtcatgccatccgtaagatgcttttctgtgactggt
gagtactcaaccaagtcattctgagaatagtgtatgcggcgaccgagttgctcttgcccggcgtcaatacgggataataccgcgccaca
tagcagaactttaaaagtgctcatcattggaaaacgttcttcggggcgaaaactctcaaggatcttaccgctgttgagatccagttcgatg
taacccactcgtgcacccaactgatcttcagcatcttttactttcaccagcgtttctgggtgagcaaaaacaggaaggcaaaatgccgcaa
aaaagggaataagggcgacacggaaatgttgaatactcatactcttccttttttcaatattattgaagcatttatcagggttattgtctcatga
gcggatacatatttgaatgtatttagaaaaataaacaaatagggggttccgcgcacatttccccgaaaagtgccacctgacgtctaagaaa
ccattattatcatgacattaacctataaaaataggcgtatcacgaggccctttcgtctcgcgcgtttcggtgatgacggtgaaaacctctga
cacatgcagctcccggagacggtcacagcttgtctgtaagcggatgccgggagcagacaagcccgtcagggcgcgtcagcgggtgt
tggcgggtgtcggggctggcttaactatgcggcatcagagcagattgtactgagagtgcaccattcgacgctctcccttatgcgactcct
gcattaggaagcagcccagtagtaggttgaggccgttgagcaccgccgccgcaaggaatggtgcatgcaaggagatggcgcccaac
agtcccccggccacggggcctgccaccatacccacgccgaaacaagcgctcatgagcccgaagtggcgagcccgatcttccccatcg
gtgatgtcggcgatataggcgccagcaaccgcacctgtggcgccggtgatgccggccacgatgcgtccggcgtagaggatctggct
agcgatgaccctgctgattggttcgctgaccatttccgggtgcgggacggcgttaccagaaactcagaaggttcgtccaaccaaaccg

actctgacggcagtttacgagagagatgatagggtctgcttcagtaagccagatgctacacaattaggcttgtacatattgtcgttagaa
cgcggctacaattaatacataaccttatgtatcatacacatacgatttaggtgacactatagaatacacggaattaattc

### pAM/CAG-Stop-CB1-SF-C-WPRE-bGHpA (pAM-Stop-CB1-SF-C)

tagctgcgcgctcgctcgctcactgaggccgcccgggcaaagcccgggcgtcgggcgacctttggtcgcccggcctcagtgagcga
gcgagcgcgcagagagggagtggccaactccatcactaggggttccttgtagttaatgattaacccgccatgctacttatctacgtagc
catgctctaggtacctaatatcacaaactggaaatgtctatcaatatatagttgctctagttattaatagtaatcaattacggggtcattagtt
catagcccatatatggagttccgcgttacataacttacggtaaatggcccgcctggctgaccgcccaacgacccccgcccattgacgtca
ataatgacgtatgttcccatagtaacgccaatagggactttccattgacgtcaatgggtggactatttacggtaaactgcccacttggcag
tacatcaagtgtatcatatgccaagtacgcccccctattgacgtcaatgacggtaaatggcccgcctggcattatgcccagtacatgacctt
atgggactttcctacttggcagtacatctacgtattagtcatcgctattaccatggtcgaggtgagccccacgttctgcttcactctccccat
ctccccccccctccccacccccaattttgtatttatttatttttttaattattttgtgcagcgatgggggcgggggggggggggggcgcgcg
ccaggcggggcggggcggggcgaggggcggggcggggcgaggcggagaggtgcggcggcagccaatcagagcggcgcgct
ccgaaagtttccttttatggcgaggcggcggcggcggccctataaaaagcgaagcgcgcggcgggcgggagtcgctgcgacg
ctgccttcgccccgtgccccgctccgccgccgcctcgcgccgcccgccccggctctgactgaccgcgttactcccacaggtgagcggg
cgggacggcccttctcctccgggctgtaattagcgcttggtttaatgacggcttgtttcttttctgtggctgcgtgaaagccttgaggggc
tccgggagggcccttttgtgcgggggggagcggctcggggctgtccgcgggggggacggctgccttcgggggggacggggcagggc
ggggttcggcttctggcgtgtgaccggcggctctagagcctctgctaaccatgttcatgccttcttctttttcctacagctcctgggcaacg
tgctggttattgtgctgtctcatcattttggcaaagaaatcataacttcgtatagcatacattatacgaagttatgcaataaaaagacagaat
aaaacgcacggtgttgggtcgtttgttcataaacgcggggttcggtcccaggaataaaatatctttattttcattacatctgtgtgttggttt
tttgtgtgaatcgatagtactaacatacgctctccatcaaaacaaaacgaaacaaaacaaactagcaaaataggctgtccccagtgcaag
tgcaggtgccagaacatttctctataacttcgtatagcatacattatacgaagttatttaattaaatgaagtcgatcttagacggccttgcag
ataccaccttccgtaccatcaccacagacctcctctacgtgggctcaaatgacattcagtacgaagatatcaaaggagacatggcatcca
aattaggatacttcccacagaaattccctctaacttccttcaggggtagtcccttccaagaaaagatgacggcaggagacaactccccgtt
ggttccagcaggagacacaaccaacattacagagttctataacaagtctctctcatcgttcaaggagaacgaggacaacatccagtgtg
gggagaattttatggacatggagtgcttcatgattctgaatcccagccagcagctggccatcgctgtcctgtccctcaccctgggcacctt
cacggttctggagaacctgctggtgctatgtgtcatccttcactcccgcagtctccgatgcaggccttcctaccacttcattggcagcctgg
cggtggccgatctcctgggaagtgtcatctttgtctacagctttgttgacttccacgtgttccaccgcaaagatagtcccaatgtgtttctgt
tcaaactgggtggggttaccgcctccttcacagcatctgtgggcagcctgttcctcacggccatcgacaggtacatatccattcacaggc
ctctggcctataagaggatcgtcaccaggcccaaggccgtagtggccttttgcttgatgtggactattgcaatagtaattgctgtgttgcc
tctcctgggctggaactgcaagaagctgcaatctgtttgctcagacatcttcccactcattgatgaaacctacctgatgttctggatcggag
tcaccagtgtgctgttgctgttcattgtgtatgcatacatgtacattctctggaaggctcacagccacgcagttcgcatgatccagcgtgg
aacccagaaaagcatcatcattcacacctcagaagatggcaaggtgcaggtgacacggcctgaccaagcccgcatggacattaggct
ggccaaaaccctggttctgatcctggtggtgttgatcatctgctggggccctctgcttgcgatcatggtgtatgatgtctttgggaagatg
aacaagcttatcaagacggtgtttgccttctgtagtatgctctgcctgctgaactccaccgtgaaccccatcatctatgctctgaggagcaa
ggacctgagacatgctttccgcagcatgttcccttcatgtgaaggcactgcgcagcctctagataacagcatgggggactcagactgcc
tgcacaagcacgccaataacacagccagcatgcacagggccgcggaaagctgcatcaagagcactgttaagatcgccaaggtgacc
atgtctgtgtccacagacacgtctgccgaggctctgggcggcggcacggtaccgcgggcccgggatccaccggtctccgcttggagc
caccctcagtttgagaaaggcggtgggtcaggaggaggctctggaggtgggagctggtcccatccccaattcgagaaaggcgccag
tggggaagactacaaggatgacgacgataagtgagcggccgctcgagcatgcatctagagggccctattctatagtgtcacctaaatg
ctagagctcgcgactagtcgattcgaattcgatatcaagcttatcgataatcaacctctggattacaaaatttgtgaaagattgactggtat
tcttaactatgttgctccttttacgctatgtggatacgctgctttaatgcctttgtatcatgctattgcttcccgtatggctttcattttctcctcctt
gtataaatcctggttgctgtctctttatgaggagttgtggcccgttgtcaggcaacgtggcgtggtgtgcactgtgtttgctgacgcaacc
cccactggttggggcattgccaccacctgtcagctcctttccgggactttcgctttcccccctccctattgccacggcggaactcatcgccgc
ctgccttgcccgctgctggacaggggctcggctgttgggcactgacaattccgtggtgttgtcggggaaatcatcgtcctttccttggct
gctcgcctgtgttgccacctggattctgcgcgggacgtccttctgctacgtcccttcggccctcaatccagcggaccttccttcccgcggc
ctgctgccggctctgcggcctcttccgcgtcttcgccttcgccctcagacgagtcggatctccctttgggccgcctccccgcatcgataccc
gtcgactcgctgatcagcctcgactgtgccttctagttgccagccatctgttgtttgcccctcccccgtgccttccttgaccctggaaggtg
ccactcccactgtcctttcctaataaaatgaggaaattgcatcgcattgtctgagtaggtgtcattctattctgggggggtggggtggggca
ggacagcaagggggaggattgggaagacaatagcaggcatgctggggatgcggtgggctctatggcttctgaggcggaaagaac

cagctggggctcgactagagcatggctacgtagataagtagcatggcgggttaatcattaactacaaggaacccctagtgatggagtt
ggccactccctctctgcgcgctcgctcgctcactgaggccgggcgaccaaaggtcgcccgacgcccgggctttgcccgggcggcctc
agtgagcgagcgagcgcgcagagcttttgcaaaagcctaggcctccaaaaaagcctcctcactacttctggaatagctcagaggccg
aggcggcctcggcctctgcataaataaaaaaaattagtcagccatggggcggagaatgggcggaactgggcggagttaggggcgg
gatgggcggagttaggggcgggactatggttgctgactaattgagatgcatgctttgcatacttctgcctgctggggagcctggggac
tttccacacctggttgctgactaattgagatgcatgctttgcatacttctgcctgctggggagcctggggactttccacaccctaactgaca
cacattccacagctgcattaatgaatcggccaacgcgcggggagaggcggtttgcgtattgggcgctcttccgcttcctcgctcactgac
tcgctgcgctcggtcgttcggctgcggcgagcggtatcagctcactcaaaggcggtaatacggttatccacagaatcaggggataacg
caggaaagaacatgtgagcaaaaggccagcaaaaggccaggaaccgtaaaaaggccgcgttgctggcgtttttccataggctccgcc
cccctgacgagcatcacaaaaatcgacgctcaagtcagaggtggcgaaacccgacaggactataaagataccaggcgtttcccccctgg
aagctccctcgtgcgctctcctgttccgaccctgccgcttaccggatacctgtccgcctttctcccttcgggaagcgtggcgctttctcata
gctcacgctgtaggtatctcagttcggtgtaggtcgttcgctccaagctgggctgtgtgcacgaacccccccgttcagcccgaccgctgc
gccttatccggtaactatcgtcttgagtccaacccggtaagacacgacttatcgccactggcagcagccactggtaacaggattagcag
agcgaggtatgtaggcggtgctacagagttcttgaagtggtggcctaactacggctacactagaagaacagtatttggtatctgcgctc
tgctgaagccagttaccttcggaaaaagagttggtagctcttgatccggcaaacaaaccaccgctggtagcggtggtttttttgtttgcaa
gcagcagattacgcgcagaaaaaaaggatctcaagaagatcctttgatcttttctacggggtctgacgctcagtggaacgaaaactcac
gttaagggattttggtcatgagattatcaaaaaggatcttcacctagatccttttaaattaaaaatgaagttttaaatcaatctaaagtatata
tgagtaaacttggtctgacagttaccaatgcttaatcagtgaggcacctatctcagcgatctgtctatttcgttcatccatagttgcctgactc
cccgtcgtgtagataactacgatacgggagggcttaccatctggccccagtgctgcaatgataccgcgagacccacgctcaccggctcc
agatttatcagcaataaaccagccagccggaagggccgagcgcagaagtggtcctgcaactttatccgcctccatccagtctattaattg
ttgccgggaagctagagtaagtagttcgccagttaatagtttgcgcaacgttgttgccattgctacaggcatcgtggtgtcacgctcgtc
gtttggtatggcttcattcagctccggttcccaacgatcaaggcgagttacatgatcccccatgttgtgcaaaaaagcggttagctccttc
ggtcctccgatcgttgtcagaagtaagttggccgcagtgttatcactcatggttatggcagcactgcataattctcttactgtcatgccatc
cgtaagatgcttttctgtgactggtgagtactcaaccaagtcattctgagaatagtgtatgcggcgaccgagttgctcttgcccggcgtca
atacgggataataccgcgccacatagcagaactttaaaagtgctcatcattggaaaacgttcttcggggcgaaaactctcaaggatctta
ccgctgttgagatccagttcgatgtaacccactcgtgcacccaactgatcttcagcatcttttactttcaccagcgtttctgggtgagcaaaa
acaggaaggcaaaatgccgcaaaaaagggaataagggcgacacggaaatgttgaatactcatactcttcctttttcaatattattgaagc
atttatcagggttattgtctcatgagcggatacatatttgaatgtatttagaaaaataaacaaatagggttccgcgcacatttccccgaaa
agtgccacctgacgtctaagaaaccattattatcatgacattaacctataaaaataggcgtatcacgaggccctttcgtctcgcgcgtttcg
gtgatgacggtgaaaacctctgacacatgcagctcccggagacggtcacagcttgtctgtaagcggatgccgggagcagacaagccc
gtcagggcgcgtcagcgggtgttggcgggtgtcggggctggcttaactatgcggcatcagagcagattgtactgagagtgcaccatt
cgacgctctcccttatgcgactcctgcattaggaagcagcccagtagtaggttgaggccgttgagcaccgccgccgcaaggaatggtg
catgcaaggagatggcgcccaacagtcccccggccacggggcctgccaccatacccacgccgaaacaagcgctcatgagcccgaag
tggcgagcccgatcttccccatcggtgatgtcggcgatataggcgccagcaaccgcacctgtggcgccggtgatgccggccacgatg
cgtccggcgtagaggatctggctagcgatgaccctgctgattggttcgctgaccatttccgggtgcgggacggcgttaccagaaactc
agaaggttcgtccaaccaaaccgactctgacggcagtttacgagagagatgatagggtctgcttcagtaagccagatgctacacaatta
ggcttgtacatattgtcgttagaacgcggctacaattaatacataaccttatgtatcatacacatacgatttaggtgacactatagaatacac
ggaattaattc

**pAM/CAG-HA-G_alpha(z)-WPRE-bGHpA (pAM-HA-G$\alpha_z$)**

tagctgcgcgctcgctcgctcactgaggccgcccgggcaaagcccgggcgtcgggcgacctttggtcgcccggcctcagtgagcga
gcgagcgcgcagagagggagtggccaactccatcactaggggttccttgtagttaatgattaacccgccatgctacttatctacgtagc
catgctctaggtacctaatatcacaaactggaaatgtctatcaatatatagttgctctagttattaatagtaatcaattacggggtcattagtt
catagcccatatatggagttccgcgttacataacttacggtaaatggcccgcctggctgaccgcccaacgacccccgcccattgacgtca
ataatgacgtatgttcccatagtaacgccaatagggactttccattgacgtcaatgggtggactatttacggtaaactgcccacttggcag
tacatcaagtgtatcatatgccaagtacgccccctattgacgtcaatgacggtaaatggcccgcctggcattatgcccagtacatgacctt
atgggactttcctacttggcagtacatctacgtattagtcatcgctattaccatggtcgaggtgagccccacgttctgcttcactctccccat
ctccccccccctccccacccccaattttgtatttatttatttttttaattattttgtgcagcgatgggggcgggggggggggggggcgcgcg
ccaggcggggcggggcggggcgaggggcggggcggggcgaggcggagaggtgcggcggcagccaatcagagcggcgcgct
ccgaaagtttccttttatggcgaggcggcggcggcggccctataaaaagcgaagcgcgcggcgggcgggagtcgctgcgacg

ctgccttcgccccgtgccccgctccgccgccgcctcgcgccgcccgccccggctctgactgaccgcgttactcccacaggtgagcggg
cgggacggcccttctcctccgggctgtaattagcgcttggtttaatgacggcttgtttcttttctgtggctgcgtgaaagccttgaggggc
tccgggagggcccttttgtgcgggggggagcggctcggggctgtccgcgggggggacggctgccttcgggggggacggggcagggc
ggggttcggcttctggcgtgtgaccggcggctctagagcctctgctaaccatgttcatgccttcttcttttttcctacagctcctgggcaacg
tgctggttattgtgctgtctcatcattttggcaaagaattggatctcgagatccatgtatccgtatgatgttcctgattatgctagcctcgaat
tcatgggatgtcggcaaagctcagaggaaaaagaggcagcgaggcggtcccggagaattgaccgccacctgcgctccgaaagcca
gcggcagcgccgtgaaatcaaacttctcctgctgggcaccagcaactcgggcaagagcaccatcgtcaagcagatgaagatcatccac
agcgggggcttcaacctggacgcctgcaaggagtacaagcccctcatcatctacaacgccatcgactcgctgacccggatcatccggg
ccctggctgccctcaagatcgatttccacaaccctgaccgtgcctacgacgctgtgcagctctttgctctgactggcccagcagagagca
agggtgagattacacctgagctgctgggtgtcatgcgacggctctgggctgacccaggggcccaggcctgctttggccgctctagcg
agtaccacctggaggacaatgcagcctactacctgaacgacctggagcgcatcgcagcgcccgactacatccccacggtggaggata
tcctacgctcccgggacatgaccacgggcattgtggagaacaagttcaccttcaaggagcttaccttcaagatggtggacgtgggcgg
gcagaggtcagaacgcaaaaagtggatccattgctttgaaggcgtcacagccatcatcttctgtgtggagctcagtggctatgacctga
agctctatgaggacaaccagacgagccggatggcggagagcctgcgcctctttgactccatctgcaacaacaactggttcatcaacacc
tcgctcatcctcttcctgaacaagaaggacctcctggcagagaagatccggcgtatcccgctcagcgtctgcttcccagagtacaagggt
cagaacacgtacgaggaagccgcggtctacatccaacgtcagttcgaggacctcaaccgcaacaaggagaccaaggagatctattcg
cacttcacttgtgccaccgacaccagtaacatccagtttgtgtttgacgcagtgacagatgtcatcatacagaacaatctcaagtacatcg
gcctttgctgaggagccgggcgcagcctgctcgcctgtggtgaaacctcgagaagcttatcgataatcaacctctggattacaaaatttg
tgaaagattgactggtattcttaactatgttgctccttttacgctatgtggatacgctgctttaatgcctttgtatcatgctattgcttcccgtat
ggctttcattttctcctccttgtataaatcctggttgctgtctctttatgaggagttgtggcccgttgtcaggcaacgtggcgtggtgtgcac
tgtgtttgctgacgcaacccccactggttggggcattgccaccacctgtcagctcctttccgggactttcgctttccccctccctattgccac
ggcggaactcatcgccgcctgccttgcccgctgctggacaggggctcggctgttgggcactgacaattccgtggtgttgtcggggaaa
tcatcgtcctttccttggctgctcgcctgtgttgccacctggattctgcgcgggacgtccttctgctacgtcccttcggccctcaatccagcg
gaccttccttcccgcggcctgctgccggctctgcggcctcttccgcgtcttcgccttcgccctcagacgagtcggatctccctttgggccg
cctccccgcatcgataccgtcgactcgctgatcagcctcgactgtgccttctagttgccagccatctgttgtttgcccctcccccgtgccttc
cttgaccctggaaggtgccactcccactgtcctttcctaataaaatgaggaaattgcatcgcattgtctgagtaggtgtcattctattctgg
ggggtggggtggggcaggacagcaagggggaggattgggaagacaatagcaggcatgctggggatgcggtgggctctatggct
tctgaggcggaaagaaccagctggggctcgactagagcatggctacgtagataagtagcatggcgggttaatcattaactacaagga
acccctagtgatggagttggccactccctctctgcgcgctcgctcgctcactgaggccgggcgaccaaaggtcgcccgacgcccgggc
tttgcccgggcggcctcagtgagcgagcgagcgcgcagagcttttgcaaaagcctaggcctccaaaaaagcctcctcactacttctgg
aatagctcagaggccgaggcggcctcggcctctgcataaataaaaaaaattagtcagccatggggcggagaatgggcggaactggg
cggagttaggggcgggatgggcggagttaggggcgggactatggttgctgactaattgagatgcatgctttgcatacttctgcctgct
ggggagcctggggactttccacacctggttgctgactaattgagatgcatgctttgcatacttctgcctgctggggagcctggggacttt
ccacaccctaactgacacacattccacagctgcattaatgaatcggccaacgcgcggggagaggcggtttgcgtattgggcgctcttcc
gcttcctcgctcactgactcgctgcgctcggtcgttcggctgcggcgagcggtatcagctcactcaaaggcggtaatacggttatccaca
gaatcaggggataacgcaggaaagaacatgtgagcaaaaggccagcaaaaggccaggaaccgtaaaaaggccgcgttgctggcgt
ttttccataggctccgccccccctgacgagcatcacaaaaatcgacgctcaagtcagaggtggcgaaacccgacaggactataaagatac
caggcgtttcccccctggaagctccctcgtgcgctctcctgttccgaccctgccgcttaccggatacctgtccgcctttctcccttcgggaag
cgtggcgctttctcatagctcacgctgtaggtatctcagttcggtgtaggtcgttcgctccaagctgggctgtgtgcacgaaccccccgtt
cagcccgaccgctgcgccttatccggtaactatcgtcttgagtccaacccggtaagacacgacttatcgccactggcagcagccactggt
aacaggattagcagagcgaggtatgtaggcggtgctacagagttcttgaagtggtggcctaactacggctacactagaagaacagtat
ttggtatctgcgctctgctgaagccagttaccttcggaaaaagagttggtagctcttgatccggcaaacaaaccaccgctggtagcggt
ggtttttttgtttgcaagcagcagattacgcgcagaaaaaaaggatctcaagaagatcctttgatcttttctacggggtctgacgctcagt
ggaacgaaaactcacgttaagggattttggtcatgagattatcaaaaaggatcttcacctagatccttttaaattaaaaatgaagttttaaa
tcaatctaaagtatatatgagtaaacttggtctgacagttaccaatgcttaatcagtgaggcacctatctcagcgatctgtctatttcgttcat
ccatagttgcctgactccccgtcgtgtagataactacgatacgggagggcttaccatctggccccagtgctgcaatgataccgcgagac
ccacgctcaccggctccagatttatcagcaataaaccagccagccggaagggccgagcgcagaagtggtcctgcaactttatccgcctc
catccagtctattaattgttgccgggaagctagagtaagtagttcgccagttaatagtttgcgcaacgttgttgccattgctacaggcatc
gtggtgtcacgctcgtcgtttggtatggcttcattcagctccggttcccaacgatcaaggcgagttacatgatcccccatgttgtgcaaaa
aagcggttagctccttcggtcctccgatcgttgtcagaagtaagttggccgcagtgttatcactcatggttatggcagcactgcataattct
cttactgtcatgccatccgtaagatgcttttctgtgactggtgagtactcaaccaagtcattctgagaatagtgtatgcggcgaccgagttg
ctcttgcccggcgtcaatacgggataataccgcgccacatagcagaactttaaaagtgctcatcattggaaaacgttcttcggggcgaaa

actctcaaggatcttaccgctgttgagatccagttcgatgtaacccactcgtgcacccaactgatcttcagcatcttttactttcaccagcgtt
tctgggtgagcaaaaacaggaaggcaaaatgccgcaaaaaagggaataagggcgacacggaaatgttgaatactcatactcttccttt
ttcaatattattgaagcatttatcagggttattgtctcatgagcggatacatatttgaatgtatttagaaaaataaacaaataggggttccgc
gcacatttccccgaaaagtgccacctgacgtctaagaaaccattattatcatgacattaacctataaaaataggcgtatcacgaggcccttt
cgtctcgcgcgtttcggtgatgacggtgaaaacctctgacacatgcagctcccggagacggtcacagcttgtctgtaagcggatgccg
ggagcagacaagcccgtcagggcgcgtcagcgggtgttggcgggtgtcggggctggcttaactatgcggcatcagagcagattgta
ctgagagtgcaccattcgacgctctcccttatgcgactcctgcattaggaagcagcccagtagtaggttgaggccgttgagcaccgccg
ccgcaaggaatggtgcatgcaaggagatggcgcccaacagtcccccggccacggggcctgccaccatacccacgccgaaacaagcg
ctcatgagcccgaagtggcgagcccgatcttccccatcggtgatgtcggcgatataggcgccagcaaccgcacctgtggcgccggtg
atgccggccacgatgcgtccggcgtagaggatctggctagcgatgaccctgctgattggttcgctgaccatttccgggtgcgggacgg
cgttaccagaaactcagaaggttcgtccaaccaaaccgactctgacggcagtttacgagagagatgatagggtctgcttcagtaagcca
gatgctacacaattaggcttgtacatattgtcgttagaacgcggctacaattaatacataaccttatgtatcatacacatacgatttaggtga
cactatagaatacacggaattaattc

**pAM/CAG-HA-G_alpha(o)-WPRE-bGHpA (pAM-HA-Gα$_o$)**

tagctgcgcgctcgctcgctcactgaggccgcccgggcaaagcccgggcgtcgggcgacctttggtcgcccggcctcagtgagcga
gcgagcgcgcagagagggagtggccaactccatcactaggggttccttgtagttaatgattaacccgccatgctacttatctacgtagc
catgctctaggtacctaatatcacaaactggaaatgtctatcaatatatagttgctctagttattaatagtaatcaattacggggtcattagtt
catagcccatatatggagttccgcgttacataacttacggtaaatggcccgcctggctgaccgcccaacgacccccgcccattgacgtca
ataatgacgtatgttcccatagtaacgccaatagggactttccattgacgtcaatgggtggactatttacggtaaactgcccacttggcag
tacatcaagtgtatcatatgccaagtacgccccctattgacgtcaatgacggtaaatggcccgcctggcattatgcccagtacatgacctt
atgggactttcctacttggcagtacatctacgtattagtcatcgctattaccatggtcgaggtgagccccacgttctgcttcactctccccat
ctccccccccctcccccacccccaattttgtatttatttatttttttaattattttgtgcagcgatgggggcgggggggggggggggcgcgcg
ccaggcggggcggggcggggcgaggggcggggcggggcgaggcggagaggtgcggcggcagccaatcagagcggcgcgct
ccgaaagtttccttttatggcgaggcggcggcggcggcccctataaaaagcgaagcgcgcggcgggcgggagtcgctgcgacg
ctgccttcgccccgtgccccgctccgccgccgcctcgcgccgcccgccccggctctgactgaccgcgttactcccacaggtgagcggg
cgggacggcccttctcctccgggctgtaattagcgcttggtttaatgacggcttgtttcttttctgtggctgcgtgaaagccttgaggggc
tccgggagggcccttttgtgcgggggggagcggctcggggctgtccgcgggggggacggctgccttcgggggggacggggcagggc
ggggttcggcttctggcgtgtgaccggcggctctagagcctctgctaaccatgttcatgccttcttcttttttcctacagctcctgggcaacg
tgctggttattgtgctgtctcatcattttggcaaagaattggatctcgagatccatgtatccgtatgatgttcctgattatgctagcctcgaat
tcatgggatgtacgctgagcgcagaggagagagccgccctcgagcggagcaaggcgattgagaaaaacctcaaagaagatggcat
cagcgccgccaaagacgtgaaattactcctgctgggggctggagaatcaggaaaaagcaccattgtgaagcagatgaagatcatcca
tgaagatggcttctctggggaagacgtgaagcagtacaagcctgtggtctacagcaacaccatccagtctctggcggccattgtccgg
gccatggacactttgggcgtggagtatggtgacaaggagaggaagacggactccaagatggtgtgtgacgtggtgagtcgtatgga
agacactgaaccgttctctgcagaacttctttctgccatgatgcgactctggggcgactcggggatccaggagtgcttcaaccgatctcg
ggagtatcagctcaatgactctgccaaatactacctggacagcctggatcggattggagccggtgactaccagcccactgagcaggac
atcctccgaaccagagtcaaaacaactggcatcgtagaaacccacttcaccttcaagaacctccacttcaggctgtttgacgtcgggggc
cagcgatctgaacgcaagaagtggatccactgctttgaggatgtcacggccatcatcttctgtgtcgcactcagcggctatgaccaggt
gctccacgaggacgaaaccacgaaccgcatgcacgagtctctcatgctcttcgactccatctgtaacaacaagtttttcattgatacctcca
tcatcctcttcctcaacaagaaagacctctttggcgagaagattaagaagtcacccttgaccatctgctttcccgaatacccaggctccaac
acctatgaagatgcagctgcctacatccaaacacagtttgaaagcaaaaaccgctcacccaacaaagaaatttactgtcacatgacttgt
gccacagacacgaataatatccaggtggtattcgacgccgtcaccgacatcatcattgccaacaatctccggggctgcggcttgtactga
aagcttatcgataatcaacctctggattacaaaatttgtgaaagattgactggtattcttaactatgttgctccttttacgctatgtggatacg
ctgctttaatgcctttgtatcatgctattgcttcccgtatggctttcattttctcctccttgtataaatcctggttgctgtctctttatgaggagttg
tggcccgttgtcaggcaacgtggcgtggtgtgcactgtgtttgctgacgcaacccccactggttggggcattgccaccacctgtcagct
cctttccgggactttcgctttcccctccctattgccacggcggaactcatcgccgcctgccttgcccgctgctggacaggggctcggctg
ttgggcactgacaattccgtggtgttgtcggggaaatcatcgtcctttccttggctgctcgcctgtgttgccacctggattctgcgcgggga
cgtccttctgctacgtcccttcggcccctcaatccagcggaccttccttcccgcggcctgctgccggctctgcggcctcttccgcgtcttcgc
cttcgccctcagacgagtcggatctcccttgggccgcctccccgcatcgataccgtcgactcgctgatcagcctcgactgtgccttctag
ttgccagccatctgttgtttgcccctcccccgtgccttccttgaccctggaaggtgccactcccactgtcctttcctaataaaatgaggaaat

tgcatcgcattgtctgagtaggtgtcattctattctgggggtggggtggggcaggacagcaaggggaggattgggaagacaata
gcaggcatgctggggatgcggtgggctctatggcttctgaggcggaaagaaccagctggggctcgactagagcatggctacgtaga
taagtagcatggcgggttaatcattaactacaaggaacccctagtgatggagttggccactccctctctgcgcgctcgctcgctcactga
ggccgggcgaccaaaggtcgcccgacgcccgggctttgcccgggcggcctcagtgagcgagcgagcgcgcagagcttttgcaaa
agcctaggcctccaaaaaagcctcctcactacttctggaatagctcagaggccgaggcggcctcggcctctgcataaataaaaaaaatt
agtcagccatggggcggagaatgggcggaactgggcggagttaggggcgggatgggcggagttaggggcgggactatggttgc
tgactaattgagatgcatgctttgcatacttctgcctgctggggagcctggggactttccacacctggttgctgactaattgagatgcatg
ctttgcatacttctgcctgctggggagcctggggactttccacaccctaactgacacacattccacagctgcattaatgaatcggccaacg
cgcggggagaggcggtttgcgtattgggcgctcttccgcttcctcgctcactgactcgctgcgctcggtcgttcggctgcggcgagcg
gtatcagctcactcaaaggcggtaatacggttatccacagaatcaggggataacgcaggaaagaacatgtgagcaaaaggccagcaa
aaggccaggaaccgtaaaaaggccgcgttgctggcgtttttccataggctccgccccccctgacgagcatcacaaaaatcgacgctcaa
gtcagaggtggcgaaacccgacaggactataaagataccaggcgtttcccccctggaagctccctcgtgcgctctcctgttccgaccctg
ccgcttaccggatacctgtccgcctttctcccttcgggaagcgtggcgctttctcatagctcacgctgtaggtatctcagttcggtgtaggt
cgttcgctccaagctgggctgtgtgcacgaaccccccgttcagcccgaccgctgcgccttatccggtaactatcgtcttgagtccaaccc
ggtaagacacgacttatcgccactggcagcagccactggtaacaggattagcagagcgaggtatgtaggcggtgctacagagttcttg
aagtggtggcctaactacggctacactagaagaacagtatttggtatctgcgctctgctgaagccagttaccttcggaaaaagagttggt
agctcttgatccggcaaacaaaccaccgctggtagcggtggtttttttgtttgcaagcagcagattacgcgcagaaaaaaaggatctcaa
gaagatcctttgatcttttctacggggtctgacgctcagtggaacgaaaactcacgttaagggattttggtcatgagattatcaaaaagga
tcttcacctagatccttttaaattaaaaatgaagttttaaatcaatctaaagtatatatgagtaaacttggtctgacagttaccaatgcttaatc
agtgaggcacctatctcagcgatctgtctatttcgttcatccatagttgcctgactccccgtcgtgtagataactacgatacgggagggctt
accatctggccccagtgctgcaatgataccgcgagacccacgctcaccggctccagatttatcagcaataaaccagccagccggaagg
gccgagcgcagaagtggtcctgcaactttatccgcctccatccagtctattaattgttgccgggaagctagagtaagtagttcgccagtta
atagtttgcgcaacgttgttgccattgctacaggcatcgtggtgtcacgctcgtcgtttggtatggcttcattcagctccggttcccaacga
tcaaggcgagttacatgatcccccatgttgtgcaaaaaagcggttagctccttcggtcctccgatcgttgtcagaagtaagttggccgca
gtgttatcactcatggttatggcagcactgcataattctcttactgtcatgccatccgtaagatgcttttctgtgactggtgagtactcaacca
agtcattctgagaatagtgtatgcggcgaccgagttgctcttgcccggcgtcaatacgggataataccgcgccacatagcagaactttaa
aagtgctcatcattggaaaacgttcttcggggcgaaaactctcaaggatcttaccgctgttgagatccagttcgatgtaacccactcgtgc
acccaactgatcttcagcatcttttactttcaccagcgtttctgggtgagcaaaaacaggaaggcaaaatgccgcaaaaaagggaataa
gggcgacacggaaatgttgaatactcatactcttccttttcaatattattgaagcatttatcagggttattgtctcatgagcggatacatatt
tgaatgtatttagaaaaataaacaaatagggttccgcgcacatttccccgaaaagtgccacctgacgtctaagaaaccattattatcatg
acattaacctataaaaataggcgtatcacgaggccctttcgtctcgcgcgtttcggtgatgacggtgaaaacctctgacacatgcagctcc
cggagacggtcacagcttgtctgtaagcggatgccgggagcagacaagcccgtcagggcgcgtcagcgggtgttggcgggtgtcg
gggctggcttaactatgcggcatcagagcagattgtactgagagtgcaccattcgacgctctcccttatgcgactcctgcattaggaagc
agcccagtagtaggttgaggccgttgagcaccgccgccgcaaggaatggtgcatgcaaggagatggcgcccaacagtcccccggcc
acggggcctgccaccatacccacgccgaaacaagcgctcatgagcccgaagtggcgagcccgatcttccccatcggtgatgtcggcg
atataggcgccagcaaccgcacctgtggcgccggtgatgccggccacgatgcgtccggcgtagaggatctggctagcgatgaccctg
ctgattggttcgctgaccatttccgggtgcgggacggcgttaccagaaactcagaaggttcgtccaaccaaaccgactctgacggcagt
ttacgagagagatgatagggtctgcttcagtaagccagatgctacacaattaggcttgtacatattgtcgttagaacgcggctacaatta
atacataaccttatgtatcatacacatacgatttaggtgacactatagaatacacggaattaattc

## 8.3 Abbreviations

| | |
|---|---|
| 2-AG | 2-arachidonyl glycerol |
| 5-$HT_{1A}$ | 5-hydroxytryptamine / Serotonin 5-$HT_{1A}$ receptor |
| 5-$HT_{2A}$ | 5-hydroxytryptamine / Serotonin 5-$HT_{2A}$ receptor |
| 7TM | Seven-transmembrane / heptahelical |
| $A_1$ | Adenosine $A_1$ receptor |
| $A_{2A}$ | Adenosine $A_{2A}$ receptor |
| AAV | Adeno-associated virus |
| ABHD4 | *N*-acyl phosphatidylethanolamine-lipase α-β hydrolase 4 |
| ABHD6 | α-β hydrolase 6 |
| ABHD12 | α-β hydrolase 12 |
| ABI2 | Abl interactor 2 |
| AC | Adenylyl cyclase |
| ADAM | A disintegrin and metalloproteinase |
| AEA | Arachidonylethanolamide / Anandamide |
| Ag | Agonist |
| Akt | Protein kinase B |
| Ant | Antagonist |
| AP | Anteroposterior |
| AP-1 | Activator protein 1 |
| Arr2 | β-arrestin 1 |
| Arr3 | β-arrestin 2 |
| ATP | Adenosine triphosphate |
| BDNF | Brain-derived neurotropic factor |
| bGHpA | Bovine growth hormone polyadenylation signal |
| BP | Biological Process |
| BRET | Bioluminescence Resonance Energy Transfer |
| BSA | Bovine serum albumin |
| $Ca^{2+}$ | Calcium |
| CalPhos | Calcium phosphate |
| cAMP | Cyclic adenosine monophosphate |
| CB1 | Cannabinoid receptor type 1 |
| CB2 | Cannabinoid receptor type 2 |

| | |
|---|---|
| CC | Cellular compartment |
| $CCK^+$ | cholecystokinin-positive |
| cDNA | complementary DNA |
| CDS | Coding sequence |
| cGMP | cyclic guanosine monophosphate |
| CHO | Chinese hamster ovary |
| CMC | Critical micellar concentration |
| CNS | Central nervous system |
| CoIP | Co-immunoprecipitation |
| COX-2 | Cyclooxygenase-2 |
| CoxIV | Cytochrome c oxidase subunit IV |
| CP | CP55,940 |
| Cre | Cre recombinase |
| CRE | cAMP response element |
| CREB | cAMP response element-binding protein |
| Crip1a | Cannabinoid receptor interacting protein 1a |
| CYFP2 | Cytoplasmic FMR1-interacting protein 2 |
| D2 | Dopamine D2 receptor |
| DAG | Diacyglycerol |
| DAGL | Diacylglycerol lipase |
| DAPI | 4',6-diamidino-2-phenylindole |
| dFISH | Double fluorescent *in situ* hybridization |
| DG | Dentate gyrus |
| DIG | Digoxigenin |
| DMEM | Dulbecco's modified Eagle's medium |
| DMSO | Dimethyl sulfoxide |
| DNA | Deoxyribonucleic acid |
| DSE | Depolarization-induced suppression of excitation |
| DSI | Depolarization-induced suppression of inhibition |
| DTT | Dithiothreitol |
| DV | Dorsoventral |
| e1 - e3 | Extracellular loops 1 – 3 |
| eCB1 | endogenous CB1 |
| eCB-LTD | Endocannabinoid-mediated long term depression |
| eCB-STD | Endocannabinoid-mediated short term depression |

| | |
|---|---|
| ECS | Endocannabinoid system |
| EDTA | Ethylenediaminetetraacetic acid |
| EGF | Epidermal growth factor |
| EGFR | Epidermal growth factor receptor |
| EMT | Endocannabinoid membrane transporter |
| ER | Endoplasmic reticulum |
| FAAH | Fatty acid amide hydrolase |
| FASP | Filter-aided sample preparation |
| FBS | Fetal bovine serum |
| FITC | Fluorescin |
| FRET | Fluorescence Resonance Energy Transfer |
| G protein | Guanine nucleotide-binding protein |
| GABA | γ-aminobutyric acid |
| GAP | GTPase activating protein |
| GASP | GPCR-associated sorting protein |
| GC | Guanylyl cyclase |
| GDE1 | Glycerophosphodiesterase 1 |
| GEF | Guanine nucleotide exchange factor |
| GFP | Green fluorescent protein |
| GIRK | G protein-activated inwardly rectifying potassium channel |
| Glu | Glutamate |
| GO | Gene Ontology |
| GPCR | G protein-coupled receptor |
| GRIN1 | G protein-regulated inducer of neurite outgrowth 1 |
| GRIN2 | G protein-regulated inducer of neurite outgrowth 2 |
| GRK | G protein-coupled receptor kinase |
| GSK3 | Glycogen synthase kinase 3 |
| GTP | Guanosine-5'-triphosphate |
| $G\alpha_{12/13}$ | Gα proteins of the $G_{12/13}$-family |
| $G\alpha_{i/o}$ | Gα proteins of the $G_{i/o}$-family |
| $G\alpha_{o}$ | G protein G(o) subunit alpha |
| $G\alpha_{q}$ | G protein G(q) subunit alpha |
| $G\alpha_{q/11}$ | Gα proteins of the $G_{q/11}$-family |
| $G\alpha_{s}$ | Gα proteins of the $G_{s}$-family |
| $G\alpha_{z}$ | G protein G(z) subunit alpha |

| | |
|---|---|
| HA | Human influenza hemagglutinin |
| HEK293 | Human embryonic kidney |
| HINT1 | Histidine triad nucleotide-binding protein 1 |
| HSP90 | Heat shock protein 90 |
| i.p. | Intraperitoneal |
| i1 - i3 | Intracellular loops 1 - 3 |
| IBMX | Isobutyl-1-methylxanthine |
| IMEM | Iscove's modified Dulbecco's medium |
| $IP_3$ | Inositol trisphosphate |
| ITR | Inverted terminal repeat |
| JNK | c-Jun N-terminal kinase |
| $K^+$ | Potassium |
| KO | Knockout |
| lyso-PLD | Lyso-phospholipase D |
| M2 | Muscarinic acetylcholine receptor $M_2$ |
| MAGL | Monoacylglycerol lipase |
| MAPK | Mitogen-activated protein kinase |
| MCL | Markov Cluster Algorithm |
| MF | Molecular function |
| mGluR | Group I metabotropic glutamate receptor |
| ML | Mediolateral |
| MS | Mass spectrometry |
| MSN | Medium spiny neuron |
| $MT_1$ | $MT_1$ melatonin receptor |
| $MT_2$ | $MT_2$ melatonin receptor |
| mTOR | Mammalian target of rapamycin |
| nanoUPLC | Nano ultra performance liquid chromatography |
| NAPE-PLD | *N*-acyl phosphatidylethanolamine-selective phospholipase D |
| NArPE | *N*-arachidonoyl phosphatidylethanolamine |
| NC | Negative control |
| NCKAP1 | Nck-associated protein 1 |
| NGS | Normal goat serum |
| NOS | Nitric oxide synthase |
| NPYR | Neuropeptide Y receptor |
| ORF | Open reading frame |

| | |
|---|---|
| $Ox_1R$ | Orexin receptor type 1 |
| PAG | Periaqueductal gray |
| PAK1 | p21-activated kinase 1 |
| PBS | Phosphate-buffered saline |
| PC12 | Pheochromocytoma |
| PCR | Polymerase chain reaction |
| PDE | Phosphodiesterase |
| PDZ | PSD95-disc large-zona occludens |
| PE | Phosphatidylethanolamine |
| PFA | Paraformaldehyde |
| PI | Phosphatidylinositol |
| PI3K | Phosphoinositide 3 kinase |
| $PIP_2$ | Phosphatidylinositol 4,5-bisphosphate |
| PKA | Protein kinase A |
| PKB | Protein kinase B |
| PLA | Proximity Ligation Assay |
| PLA2 | Phospholipase A2 |
| PLA2G4E | phospholipase A2 group IVE |
| PLC | Phospholipase C |
| PLCβ | Phospholipase Cβ |
| POD | Peroxidase |
| POI | Protein of interest |
| PP2A | Protein phosphatase 2A |
| PSD95 | Postsynaptic density protein 95 |
| PTPN22 | Protein tyrosine phosphatase, non-receptor type 22 |
| PTPRS | Receptor-type tyrosine-protein phosphatase σ |
| PTX | Pertussis toxin |
| PV | Parvalbumin |
| qPCR | quantitative PCR |
| R state | Inactive state of a GPCR |
| R* state | Active state of a GPCR |
| Rac1 | Ras-related C3 botulinum toxin substrate 1 |
| RAMP | Receptor activity modifying protein |
| RGS | Regulator of G protein signaling |
| RNA | Ribonucleic acid |

| | |
|---|---|
| RNAi | RNA interference |
| Ro 20-1724 | 4-(3-butoxy-4-methoxy-benzyl)imidazolidone |
| RT | Room temperature |
| RTK | Receptor tyrosine kinase |
| s.c. | Subcutaneous |
| SDS | Sodium dodecyl sulfate |
| SDS-PAGE | Sodium dodecyl sulfate polyacrylamide gel electrophoresis |
| SF | StrepII/FLAG |
| SHIP | SH2 domain-containing inositol 5'-phosphatase |
| SSC | Saline-sodium citrate |
| TA | Transacylase |
| TAP | Tandem affinity purification |
| TBS | Tris-buffered saline |
| TH | Tyrosine hydroxylase |
| THC | $\Delta^9$-tetrahydrocannabinol |
| TM1 - TM7 | membrane-spanning α-helices 1 - 7 |
| TNT | Tris-NaCl-Tween |
| Tris | Tris(hydroxymethyl)aminomethane |
| TRPV1 | Transient receptor potential cation channel subfamily V member 1 |
| VGAT | Vesicular GABA transporter |
| VGCC | Voltage-gated $Ca^{2+}$-channel |
| VGlut1 | Vesicular glutamate transporter 1 |
| WAVE1 | Wiskott-Aldrich syndrome protein-family verprolin-homologous protein 1 |
| WB | Western blot |
| WIN | WIN55,212-2 |
| WPRE | Woodchuck hepatitis virus posttranscriptional regulatory element |
| $\alpha_2$AR | $\alpha_2$ adrenergic receptor |
| $\beta_2$AR | $\beta_2$ adrenergic receptor |
| δ-OR | δ-opioid receptor |
| μ-OR | μ-opioid receptor |

## 8.4 List of figures

## 8.5 List of tables